Final Technical Report (FTR)
Cover Page

a. *Federal Agency*	Department of Energy	
b. *Award Number*	**DE-EE0008770**	
c. *Project Title*	**Photovoltaic Analysis and Response Support (PARS) Platform for Solar Situational Awareness and Resiliency Services**	
d. *Recipient Organization*	**North Carolina State University**	
e. *Project Period*	*Start:* **Nov. 1, 2019**	*End:* **Oct. 31, 2023**
f. *Principal Investigator (PI)*	**Ning Lu** Professor nlu2@ncsu.edu (509) 554-0678	
g. *Business Contact (BC)*	**Sherrie Settle** Director, Sponsored Programs, sesettle@ncsu.edu 919-515-4323	
h. *Certifying Official (if different from the PI or BC)*		

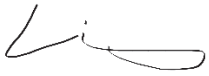

Signature of Certifying Official — *Date*: *3/28/2024*

By signing this report, I certify to the best of my knowledge and belief that the report is true, complete, and accurate. I am aware that any false, fictitious, or fraudulent information, misrepresentations, half-truths, or the omission of any material fact, may subject me to criminal, civil or administrative penalties for fraud, false statements, false claims or otherwise. (U.S. Code Title 18, Section 1001, Section 287 and Title 31, Sections 3729-3730). I further understand and agree that the information contained in this report are material to Federal agency's funding decisions and I have any ongoing responsibility to promptly update the report within the time frames stated in the terms and conditions of the above referenced Award, to ensure that my responses remain accurate and complete.

Acknowledgement

"This material is based upon work supported by the U.S. Department of Energy's Office of Energy Efficiency and Renewable Energy (EERE) Solar Energy Technologies Office (SETO) under the DE-FOA-0001987 Award Number DE-EE0008770."

Disclaimer

Executive Summary

The project's primary objective is to develop a digital-twin based Photovoltaic (PV) Analysis and Response Support (PARS) platform, which aims to provide real-time situational awareness and optimal response plans. This platform is designed to enhance the performance of hybrid PV systems, making them competitive with or even superior to conventional generation resources. The PARS platform enabled the project team to develop and evaluate an extensive suite of grid support functionalities for the hybrid PV systems to enhance grid performance, across key areas including visibility, dispatchability, security, resilience, and reliability.

Given the global push toward achieving 100% clean energy by 2035, there is a significant increase in the integration of inverter-based resources (IBRs) throughout the energy grid. Effectively managing the inherent variability and uncertainty associated with IBRs is crucial for ensuring cost-effectiveness, reliability, and security in both the main grid and islanded microgrids.

Constrained to a limited array of IEEE test systems or standard feeder models, traditional IBR modeling struggles to assimilate new field data, accurately reflect system dynamics, and adapt to the evolving energy landscape. In our project, we embraced a Digital Twin (DT) strategy for crafting the PARS platform. A digital twin acts as a precise virtual counterpart of a physical system, built on historical data and continuously honed with real-time insights. This enables the high-fidelity DT to accurately mirror current system operations and forecast future scenarios. Consequently, the PARS platform becomes an ideal environment for testing and refining monitoring, control, power, and energy management algorithms designed to boost hybrid PV system performance. The defining feature of the PARS platform, distinguishing it from other advanced simulation tools, is its exceptional adaptability. This is achieved by employing actual network topologies and utilizing real-time field data for fine-tuning and calibration, ensuring a close emulation of real-world conditions.

The project deliverables include: 1) High-fidelity IBR models and tools for real-time parameterization, utilizing real-time field measurements to refine IBR models for enhanced accuracy and performance; 2) Grid-forming and Grid-following capabilities to deliver resilience services, including blackstart, voltage and frequency support, cold-load pick-up, power reserves, and three-phase load balancing across grid-connected and microgrid settings; 3) Machine learning-based forecasting tools and methods for generating synthetic data and topologies, creating diverse and realistic simulation environments for evaluating varied operational scenarios; 4) Advanced microgrid power and energy management algorithms for optimizing the integration and operation of PV, storage, and demand response resources within both feeder and community scales.

The power grid data sets are provided by four utility companies in North Carolina and the New York Power Administration. Acting as industry advisors, our industry partners communicated stakeholder needs and regulatory standards to the research teams, aiding technology transfer by incorporating the developed methodologies into their daily operations. This collaboration ensures that the PARS platform, functioning as a power system digital twin, enhances our understanding of IBR dynamic behaviors and enables the development and evaluation of IBR control functions that match or exceed the capabilities of conventional synchronous generators.

Table of Contents

Contents

1. Background

Project overview: The objective of this project is to develop a digital-twin based *Photovoltaic (PV) Analysis and Response Support* (PARS) platform that provides real-time situational awareness and optimal response plan selection. By binding steady-state and dynamic simulation and integrating faster-than-real-time simulation into real-time simulation, the PARS operation platform can be used to emulate, monitor, and develop optimal response plans for hybrid PV systems located at transmission, distribution and behind-the-meter customer sites for both normal and emergency operations. When running off-line using historical data, PARS can also be used as a planning platform to design and test PV-based grid support functions and perform cost-benefit studies. Note that we refer to hybrid PV systems as solar farms or roof-top PV systems operated with other generation resources or distributed energy resources (DERs).

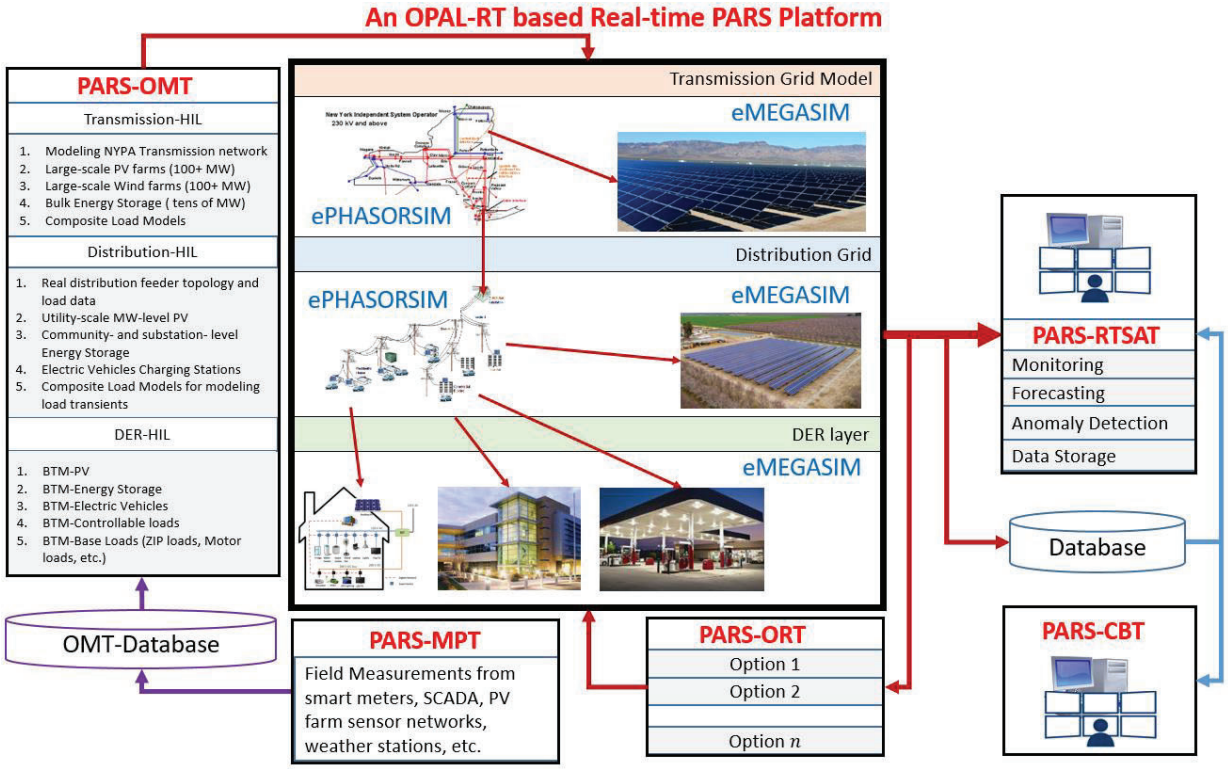

Figure 1. Configuration of the PARS platform and information flows

The configuration of the PARS platform and information exchanges between the PARS components are shown in Figure 1. The expected outcome of this project is to bring the performance of the hybrid PV systems up to par with those of flexible generation resources in the following five performance areas when providing Grid Support Functions (GSFs): visibility, dispatchability, security, reliability and resilience. To achieve this goal, five tools will be developed for the PARS platform: 1) an Operation Model Tool (PARS-OMT) that models both steady-state and dynamic behaviors of hybrid PV systems when providing GSFs in real-time, 2) a Model Parameterization Tool (PARS-MPT) that uses field measurements as inputs to derive and update the OMT parameters, 3) a real-time Situational Awareness Tool (PARS-RTSAT) that monitors hybrid PV systems, predicts the GSF capacity and performance, and detects anomalies caused by malfunctions, man-

made errors, or cyber-attacks, 4) an Optimal Response Tool (PARS-ORT) that runs parallel, faster-than-real-time simulations for best response plan selection, and 5) a Cost-Benefit Tool (PARS-CBT) that determines the value proposition for hybrid PV systems at strategic locations associated with critical infrastructure to provide GSFs for both normal and emergency operations.

Project Organization: Figure 2 shows the summary description of the overall work scope of each year. In Year 1, we developed a prototype of each of the five tools and prepared a benchmark real-time simulation test bed for running those prototype systems. In Year 2 and 3, we integrated the tools on realistic transmission and distribution models. In Year 4, we assisted ElectriCities, NYPA, and Strata Solar to tools developed into their control, simulation, and planning platforms. The end results of each task by performance periods are listed in the figure.

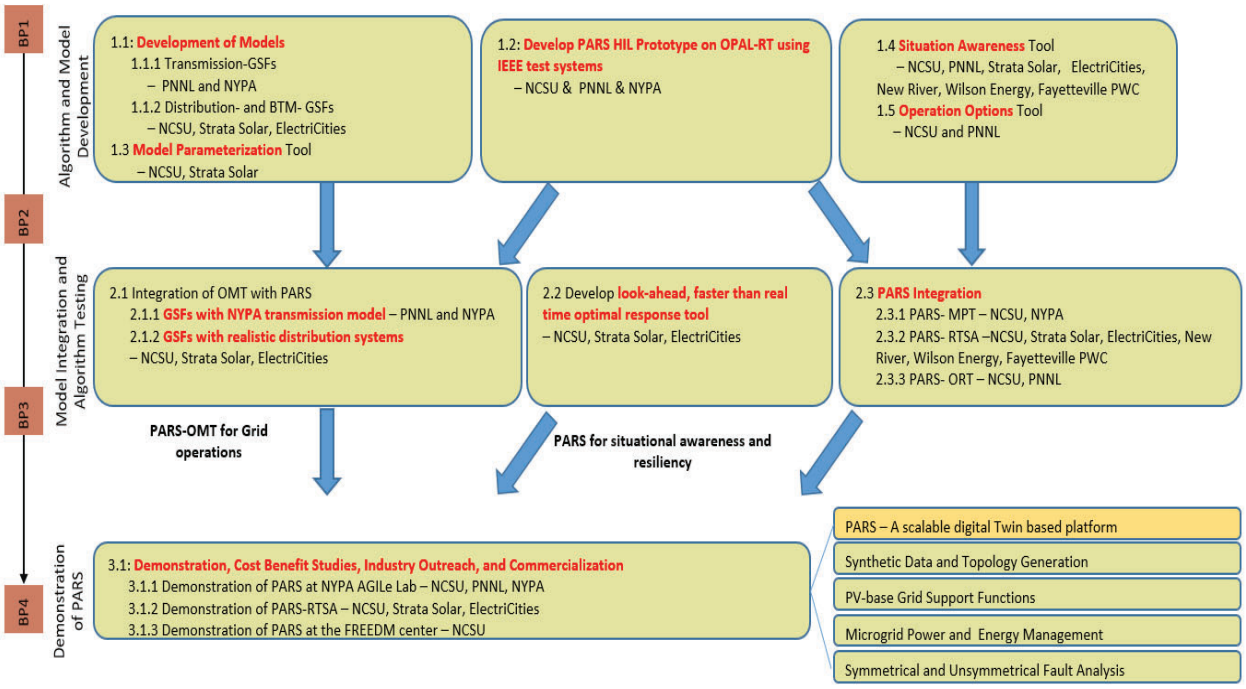

Figure. 2: Project tasks for each budget year and primary focuses

Motivation: The transition towards a net-zero carbon economy by 2050 is critically dependent on the integration of grid-scale and distributed photovoltaic (PV) systems. As these systems evolve from auxiliary power sources to primary generators, their ability to deliver grid-stability functions (GSFs) comparable to or better than traditional synchronous generators becomes essential. This is particularly vital in regions where PV penetration surpasses 20%, posing unique challenges and opportunities for energy systems.

Recent research has shed light on the capabilities of hybrid PV systems in which flexible generation resources such as hydro power plants, combined heat and power units, battery energy storage systems (BESS), and dynamically controllable loads can be used to regulate the real and reactive power output of PV systems. These systems can then be controlled for providing services traditionally provided by synchronous

generators, for instance, power reserves, volt-var support, and rapid frequency response to name a few. Moreover, the strategic positioning of distributed PV resources, especially rooftop installations, minimizes the need for fuel storage or transportation, offering an economical solution to energy sustainability and resilience.

In the context of microgrids, integrating distributed PVs with diesel generators, BESS (either stationary or mobile), and controllable loads can create resilient power ecosystems. These microgrids are designed to withstand extended blackouts, supplying reliable power for prolonged periods. Thus, enhancing the GSF capabilities of PV systems for grid-forming activities like black-start, cold-load pickup, and localized ancillary services becomes imperative, especially in scenarios where reconnecting to the main grid may take an extended duration.

Furthermore, the increasing amalgamation of DERs calls for a unified approach to Transmission and Distribution (T&D) monitoring and control. Traditional models, which treat T&D systems separately, are becoming insufficient. An integrated T&D operational framework is essential for reflecting real-time grid conditions and evaluating the outcomes of potential control strategies accurately. This integration is crucial for maintaining grid reliability, security, and resilience across both transmission and distribution levels, particularly in light of the challenges posed by faults at the transmission level that affect the operation of IBRs across the grid.

Innovations: As shown in Figure 3, the PARS platform advanced grid simulation technology across three major research domains.

- First, we developed an integrated T&D digital twin that can serve as a real-time HIL simulation platform. This tool dramatically improves upon traditional static models by dynamically modeling PV outputs and adjusting parameters in real-time based on actual field measurements (see Figure 4 and Table 1). Such adaptability allows for precise representation of PV farm performance, enabling the power and energy management system to be tested in a realistic system setting considering system dynamic responses. The digital twin not only accurately forecasts PV farm behavior but also swiftly identifies and corrects parameter deviations or estimation errors, a significant leap over conventional, non-adaptive power system models.
- Secondly, our suite of situation awareness tools employs cutting-edge machine learning techniques, originally developed for speech recognition, image processing, and natural language processing, to tackle unique challenges in the power system domain. These tools enhance load and PV forecasting, load disaggregation, synthetic scenario generation, load model parameterization, anomaly detection, and cyber-attack mitigation. By leveraging advanced analytics, we can predict and respond to complex grid dynamics more effectively, enhancing reliability and security.
- Finally, we developed optimal response strategies for hybrid PV farms to provide black-start support, provide voltage and frequency regulation, and enable microgrid operations down to the feeder and community levels. We developed control methods for providing power reserve margins, coping with cold-load pickup effects, and correcting 3-phase load imbalances.

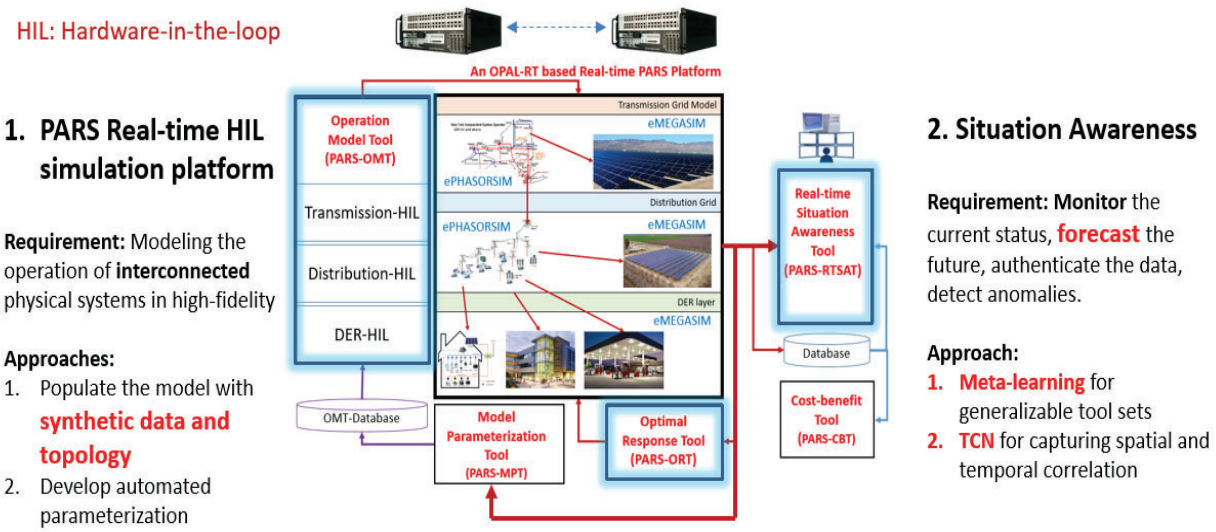

Figure 3: Unique features of the integrated T&D power system digital twin

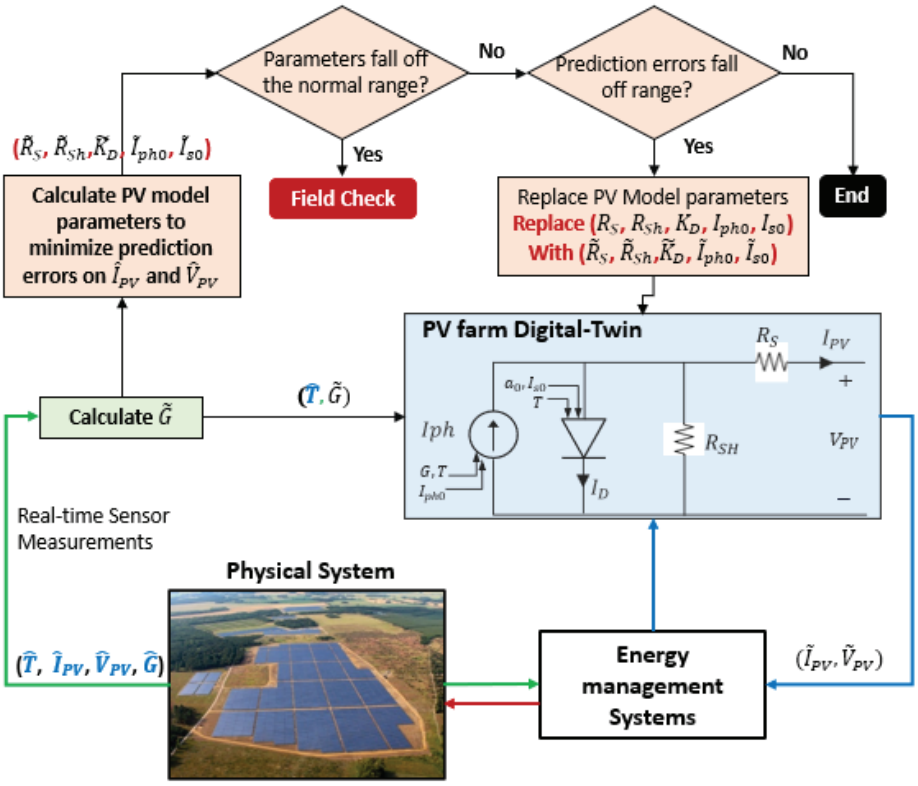

Figure 4: An overview of the PVDT parameterization process

Table 1: Digital-twin based approach versus conventional approaches

Reference	Modeling Considerations	Synchronization	Communication
[1]	Electromagnetic transients + phasor model	Yes	N/A
[2]	Electromagnetic transients + phasor model	Yes	N/A
[3]	Phasor model	Yes	Wireless communication simulator
[4]	Electromagnetic transients + hardware	Asynchronous	N/A
[5]	Phasor model + hardware	Asynchronous	JSON-link over Ethernet
Digital-twin based PARS Platform [6-12]	Electromagnetic transients + phasor model + hardware **+ Parameter Updates+ Communication Links+ Forecast the Model Evolutions+ Energy/Power Management Systems**	Asynchronous	Modbus + File-shared over Ethernet + VPN connections required for implementation of multi-area networked digital twins

In Section 2, we presented a comprehensive list of deliverables categorized by tasks and technical categories. In Section 3, we supplemented this information by including references that highlight recent advancements in technologies relevant to each deliverable outlined in Section 2. Additionally, within Section 3, we provided concise technical discussions and performance comparisons to elucidate the distinctions between our work and the state-of-the-art, showcasing the extent to which we improve upon the existing state-of-the-art.

2. Project Objectives:

The objective of this project is to develop a digital-twin based PARS platform that improves the real-time visibility, dispatchability, security, and reliability of hybrid PV systems when providing grid services in both normal and emergency operations. When running off-line using historical data, the PARS platform can also be used as a planning platform to test, develop, and validate the performance of hybrid PV systems when providing GSFs.

As shown in Fig. 1, the PARS platform consists of five tools: OMT, MPT, RTSAT, OPT, and CBT. The technology advancements that make the PARS platform transformative are summarized as follows:

- Development of operation models of hybrid PV systems that bind steady-state simulation together with dynamic response modeling on a real-time HIL simulation platform that co-simulates multi-rate, multi-scale control systems considering communication protocols.
- Development of data-driven, machine-learning based model parameterization algorithms that allow control and model parameters of the OMT to be updated close to real-time using field measurements from multiple sensor networks for real-time situational awareness.
- Development of physics-based anomaly detection algorithms by characterizing signatures of key data streams required for decision making and comparing the signatures predicted by the high-fidelity real-time HIL simulations with those of the field measurements to detect bad/fake/tampered data streams from malfunctions or cyber-attacks.
- Development of a transformational modeling mechanism that allows faster-than-real-time scenario simulations to be conducted in parallel within the main real-time simulation thread for preparing emergency operation and selecting optimal response and restoration plans on the fly over the entire event horizon. This technology is essential when prompt actions to fast changing operating conditions are required.
- Development of a performance based cost-benefit assessment tool for capturing the benefit of PV-based GSFs in typical operation scenarios. This cost-benefit assessment tool will use the actual field data to estimate the economic benefits for the services provided under both normal and emergency conditions. The goal is to estimate the economic value in integrating PV systems with other resources for providing grid services.

The scientific principle, relevance to the goals of the FOA, feasibility, innovation and impacts of each of the five technology will be discussed in the following subsections in Section 3.

The Go/No Go deliverables are summarized in Table 1. The outcome of this project enables the development of coordinative operation schemes across distribution and transmission systems for reliably orchestrating the operations of thousands of interconnected DERs in achieving system wide benefits. Technical descriptions of each deliverable can be found in the Appendix.

Table 2: The Go/No-Go deliverables per tasks and per functionalities.

	Functions Tested and Validated		HIL Test System		Situation Awareness	Cost-benefit and Demo
	Transmission	**Distribution**	**Transmission**	**Distribution**		
Teams	**PNNL, NYPA**	**NCSU, ElectriCities, Strata Clean Energy, Roanoke, New River, Fayetteville PWC, Wilson Energy**	**PNNL, NYPA**	**NCSU, ElectriCities, Strata Clean Energy**	**NCSU, ElectriCities, New River, Fayetteville PWC**	**NCSU, ElectriCities, New River, Fayetteville PWC**
Tasks	**A (1.1, 2.1, 3.1)**	**B (1.1, 1.5, 2.1, 2.2, 2.5, 3.1)**	**C (1.2, 1.3, 2.4, 3.1)**	**D (1.2, 1.3, 2.1, 2.3,2.4, 3.1)**	**E (1.4, 2.4, 3.1)**	**F (3.2)**
Deliverables	**Developed** Two main grid support functions: Volt-var control (A1) and Black-start (A2) **Benchmarked** on the IEEE 118-bus test system **Tested and validated** on the NYISO system	**Developed** energy scheduling and power dispatch for residential and commercial roof-top PV systems and MW-level utility-scale PV farms supported by battery storage systems **Developed** Use Cases 1-3 to demonstrate the developed grid support functions with forecasting errors considering cold-load pick-up and black-start sequence **Developed** use cases 4, 5, and 6: considering combinations of PV systems in a multi-feeder systems for optimal response tool development (B1&B2&B3) **Developed** load control strategies to increase the flexibility in microgrid operation (B1) **Developed** reinforcement-learning based localized controller (model-free, adaptable) (B4) **Developed** dynamic VAR compensation schemes (B5)	**Developed** 100 MW+ PV farm and energy storage system models **Benchmarked** blackstart sequence control on the NYISO network model on OPAL-RT (A1&A2)	**Developed** PV (roof-top & PV farm), Diesel Generator, Battery, load, cold-load pickup model with Grid-forming and Grid-following functions and communication protocols and b**enchmarked** on the IEEE-123 bus test system with actual smart meter data and PV farm data 24-hour real-time simulation for the 3 use cases for different event days (48 hour simulation) (D1&D2&D3) **Developed** cold load pick up and motor start-up models (B1&D1) **Developed** under-frequency load shedding schemes (D4) **Developed** faults modeling for IBR impact analysis (D5) **Developed** cyber-attack scenarios (D6) **Developed** encoding method for mitigating unreliable communication links (D7) **Developed** PV parameterization methods (D8)	**Developed** a general-purpose forecasting tool: meta-learning based load forecast for EMS at different load aggregation levels: multiple-look out windows, different load aggregation levels, variable forecasting horizons (E1) **Developed** short-term PV forecasting tool for forecasting sudden PV output changes (E2) **Developed** GAN-based method to convert low-resolution meter data to high-resolution data for the HIL test system to parameterize its load profiles (E3) **Developed** Synthetic data generation for modeling different operation conditions (E4) **Developed** smart meter anomaly detection schemes (E5)	**Developed** demand response baseline identification tools (F1&F2) **Developed** Load disaggregation Baseline estimation algorithms (F3&F4) **Demonstrated** the algorithms and assist utilities to adapt the technologies developed for optimizing the operation of their DERs **Assessed** the performance improvement of each GSF on different reliability and resiliency metrics **Assessed** the additional cost for mitigating communication network errors and cyber attacks

3. Project Results and Discussion

The key technologies developed in this project can be summarized into five categories:

- **Transmission-level PV grid support functions**
  - PV-based volt/var control function
  - PV-based black start function
- **Microgrid Power and Energy Management:** managing PV, storage, and demand response resources at both the feeder and community levels accounting for feeder reconfiguration, 3-phase balancing, and cold-load pickup requirements for multi-day off-grid operation.
  - Feeder-level microgrid
  - Community level microgrid
  - Mobile storage powered microgrid
  - A localized reinforcement learning based PV controller for coordinative volt/var control on a feeder with multiple PV farms
  - Dynamic VAR compensation schemes
- **An integrated T&D Simulation Platform**
  - High Fidelity DT Models: IBRs (PV farms, roof-top PV systems, energy storage devices), distributed generators, and controllable/non-controllable loads
  - Grid-Forming and Grid-Following Functions: providing power reserves, tracking load balance signals, cold-load pick-up, balancing 3-phase loads, and offering adaptive voltage and frequency supports in grid-connected and microgrid operation modes.
  - Real-time Parameterization: Using real-time field measurements to parameterize and fine-tune the IBR DTs.
- **Situation Awareness Tools**
  - Forecasting:
    - Meta learning based load forecasting
    - TCN-based PV forecasting
  - Smart Meter Data Analysis:
    - Smart meter data analysis for meter-transformer pairing, behind-the-meter PV and EV detection, and customer segmentation
    - Demand response baseline derivation
  - Cyber Attacks: data-injection based cyber-attack and mitigation mechanisms
  - Synthetic Data and Topology Generation: Creating highly realistic and diversified DT simulation environments.
- **Scale-up Technologies**
  - An integrated T&D simulation via VPN based connections
    - Use case 1: symmetrical and unsymmetrical transmission fault impact on distributed IBRs
  - An integrated T&D simulation via file sharing
    - Use case 2: volt/var control coordination
  - Integrated communication and power distribution network modeling
    - Use case 3: cyber-attack on grid forming battery energy storage units.

3.1 General Modeling Approach

3.2.1 Test Systems: We employed two distinct types of test systems: one based on IEEE test systems (as shown in Figure 5(a)) and the other on actual utility network models (depicted in Figure 5(b)). The IEEE test systems serve as the foundation for developing core technologies. To verify

their efficacy, we perform validations on real utility network models, utilizing data from various operational conditions to ensure the results are broadly applicable. The IEEE-118 system is used by PNNL for transmission level GSF development. NYPA actual transmission level model is used for testing the Transmission-level PV grid support functions, including PV-based volt/var control and black start functions. The IEEE-123 system is used by NCSU for distribution level function development. Two utility feeders with five 5-MW PV farms are used for testing.

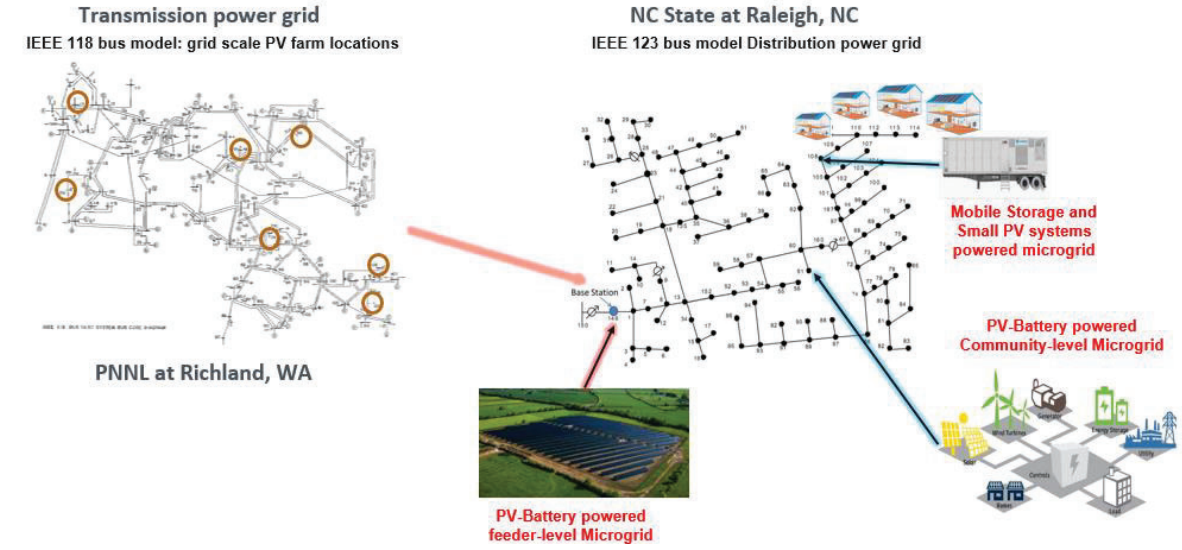

(a)

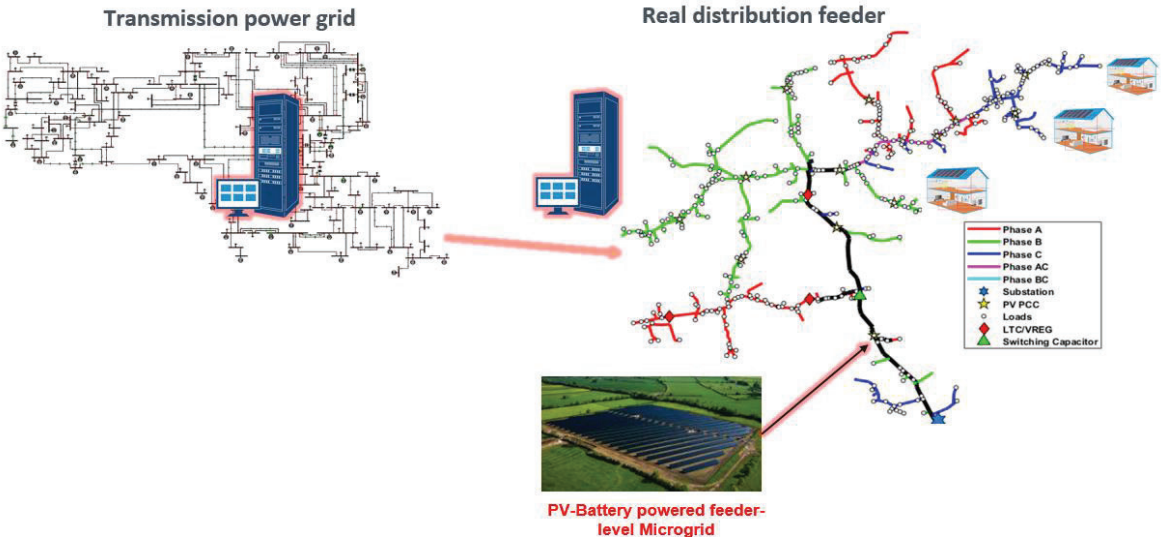

(b)

Figure 5. Network Models developed on the PARS platform. (a) IEEE test systems, and (b) Actually utility network models.

3.2.2 Data Sources: To construct a realistic simulation environment, we purchased PECAN Street Data Sets and obtained smart meter data collected from 8,720 customers served by 1,410 transformers on 23 actual power distribution feeders from 2017 to 2020 in a city at North Carolina. There are 8650 residential loads (including single family house and apartment buildings) and 70 small commercial and industrial loads. The network topology model comprises links from substations to distribution transformers and end customers to each transformer. A significant advantage of this method is the spatial and temporal

synchronization of the 8000 load profiles, guaranteeing a realistic emulation of consumer electricity usage patterns at the household, transformer, feeder, and city scales.

Additionally, we devised a Generative Adversarial Network (GAN)-based technique to create clusters of synthetic data sets for assigning load profiles. This innovation allows other researchers to replicate our findings.

The data sets used in this project can be summarized as:

- Topology Data
    - PNNL IEEE-118 System: Specifically used for the development of transmission-level Grid Support Functions, providing a detailed framework for high-voltage network analysis.
    - NYPA Transmission Level Model: Employed for testing transmission-level PV grid support functions, including volt/var control and black start capabilities, using an actual transmission network model.
    - NCSU IEEE-123 System: Dedicated to the development of distribution-level functions, focusing on the integration and management of distributed energy resources within lower voltage networks.
    - Utility Feeders with PV Farms: Comprising a utility feeders equipped with five 5-MW PV farms each, these setups are instrumental in assessing the performance of PV integration and grid support functionalities at the distribution level. For this feeder, we have load and PV power profiles for two years (2022 and 2023) with 1-hour resolution. Additionally, we obtained 4-day load and PV power profiles with 1-minute resolution for investigating extreme operation conditions, i.e., high PV-load ratio.
- Smart Meter Data
    - PECAN Street Data Sets (with sub-metered data for major appliances and roof-top PV)
    - A few EV charging station data
    - 15-minute actual smart data sets from more than 8000 customers for 3 years from New River Light and Power
    - 15-minute actual smart data sets from 100 residential, 100 commercial, and 100 industrial loads from Wilson Power.
- Transmission level data
    - NYPA black start procedure
    - NYPA generator models and load data
- SCADA Data
    - 5-minute SCADA data from New Reviver and Fayetteville PWC for 5 feeders
    - SCADA data at feeder head for the three feeders with five PV farms
    - Demand response data
    - Conservation voltage reduction data for year 2019 and 2020
- PV Plant Sensor Data
    - 1 year 5-minute PV output data for 100 utility-scale PV farms from Strata Solar
    - 1-second, 2-weeks inverter level data from 1 PV farm
- Microgrid Device Data
    - Devices: Battery, PV Panel, Diesel Generators
    - Data sources: Factory data sheets, field test results, field measurements, default model data from the Simulink
- Synthetic Load Profiles: Generated using a GAN-based method, these synthetic data sets simulate customer electricity consumption behaviors across different levels

(household, transformer, feeder, city) to ensure comprehensive and lifelike testing scenarios.

- Method: see deliverable E3&E4 described in Appendix 8.18 and 8.19.
- Inputs: PECAN Street data & New River Data
- Resolution: from low-resolution (15-minute) to high resolution (1-minute)
- Amount: unlimited. Generated as a group of load supplied by one transformer.
- Accessible online at Github

3.2.3 Data flows: The data flows among different PARS platform modules are highlighted in Figure 6. There are four primary types of data exchanges within the PARS platform's real-time simulation environment:

- From *Actual Power Grids* to the *Model Parameterization Tool*: This flow is essential for the calibration of digital twin models, where real-world grid data is utilized to accurately parameterize these virtual models, ensuring they reflect the current state and dynamics of the physical grids.
- From *Actual Power Grids* to the *Real-Time Situation Awareness Tool*: This data flow is critical for anomaly detection and forecasting within the power grid. By analyzing real-time data from the actual grids, the tool can identify deviations from normal operations and predict future grid conditions.
- From *the Digital Twin* to *the Real-Time Situation Awareness Tool*: This involves the transfer of generated virtual sensor measurements from the digital twin. These simulated data points are used to augment the Situation Awareness tool's ability to monitor and forecast grid conditions, especially when testing scenarios that cannot be safely or practically executed on the actual grid, as shown in Figure 7(a).
- From *the Real-Time Situation Awareness Tool* to *the Optimal Response Selection Tool*: This data flow provides vital inputs for decision-making by delivering forecasts related to resource availability, output levels, grid flexibility, and control needs. Such information is crucial for selecting the most appropriate response strategies to maintain or restore grid stability and efficiency.

These data exchanges facilitate an integrated approach for managing and simulating grid operations, ensuring that the PARS platform work in synergy with the actual world in order to serve as a high-fidelity virtual environment.

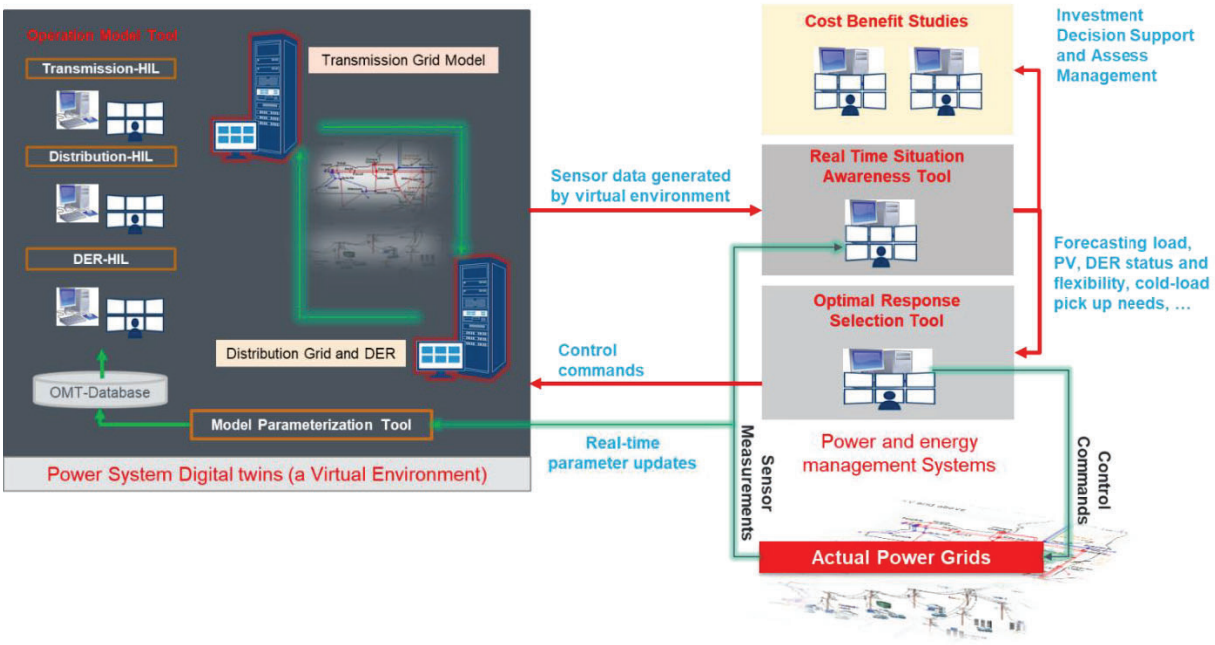

Figure 6. Data flows in the PARS platform.

The PARS platform can have two control command flows:

- From the *Optimal Response Selection Tool* to the *Digital Twin*: This flow is designed for evaluating the outcomes of control strategies in a simulated environment. The digital twin serves as a virtual replica of the power grid, allowing for a safe and efficient assessment of how control commands would perform under real-world conditions, as shown in Figure 7(b).
- From *the Optimal Response Selection Tool* to *Actual Power Grids*: Through this communication link, control commands can be directly executed on the physical power grids. In practical this command flow in real-time operations is crucial for actual grid management and response strategies.

Due to the high costs and operational challenges (e.g., reliability, security, and safety) of executing field experiments, particularly for assessing resilience measures like black start capabilities at the transmission level and microgrid control functionalities at the distribution level, this project leveraged the PARS platform for conducting simulations based on digital twins as substitutes for actual field tests. This also demonstrates that the PARS can provide a high-fidelity virtual environment for validating the effectiveness and safety of control strategies before their deployment in actual grid scenarios, thus serving a key role in bridging the gap between theoretical development and practical application.

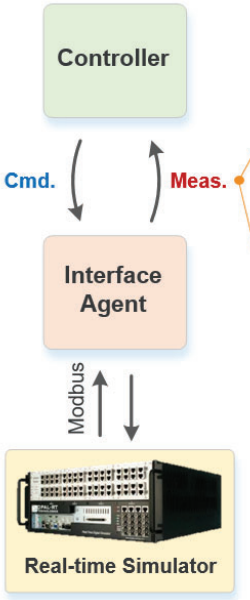

Measurements	Description	Dim
Simulation time	Time of real-time simulation	1
Node voltage	Node voltage of IEEE 123 bus system	266
Load power	Real and reactive power of loads in phase	190
Tap position	Tap position of the voltage regulators	9
Shunt capacitor status	Shunt capacitors ON and OFF	6
Breaker status	Breaker ON and OFF	6
PV power	P/Q of PV system for each phase	6
ES power	P/Q of energy storage system for in phase	6
Diesel generator power	P/Q of diesel generator for each phase	6
Battery measurements	SoC, voltage and current of battery system	3

(a)

Control Commands	Target devices	Description	Dim
Topology management	Breaker	Manage the topology of the microgrid through the breakers	18
Load control	Breaker & Load	Cold load pickup, load shedding	95
Voltage regulation	Voltage regulator	Adjust the load side voltage by tap position	9
Q regulation	Shunt capacitor	Volt-var control support	6
PCC voltage control	ES inverter	Adjust the voltage set point at the point of common coupling (PCC)	1
Diesel generator	Diesel generator	Support the critical load if ES and PV are not able to support.	1

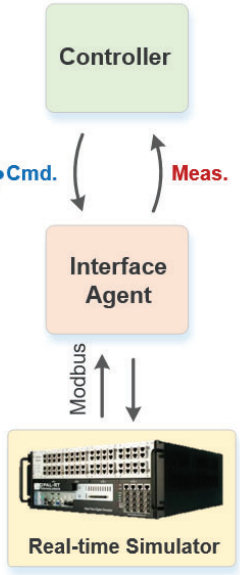

(b)

Figure 7. Data Transfer between HIL and EMS applications. (a) Example of the Measurement List, (b) Example of the Commands List.

3.2.4 Time Coordination: Data transfer among applications and the corresponding simulation time coordination inside the HIL test bed and between HIL test systems and EMS algorithms are illustrated in Figure 8.

As shown in Figure 8(a) and (b), the data exchanges between the *Optimal Response Selection*, *Real-Time Situation Awareness*, and *Digital Twins* modules are asynchronous. While the Optimal Response Tool's energy management functions generate operation schedules ranging from day-ahead to 5-minute intervals, the digital twins simulate the dynamic responses of power grids in real-time demands much quicker simulation steps (every 100 ms or 50μs). Consequently, as shown in Figure 8(c), control commands issued from the energy management functions are sent to the digital twins via different communication protocol every 5 minutes. Within these intervals, device-level controllers residing in the digital twin models act to balance generation and load, thereby maintaining voltage and frequency stability.

Uniqueness of the PARS platform is that it models the full sequence of grid operation including energy management, power balance, frequency and voltage regulation. It can thus captures the device-level and system-level controller interactions via realistic communication protocols, models both fast and slow transients between state transitions, and enables the modeling of communication delays, errors, cyber-attacks on controlling distributed energy resources.

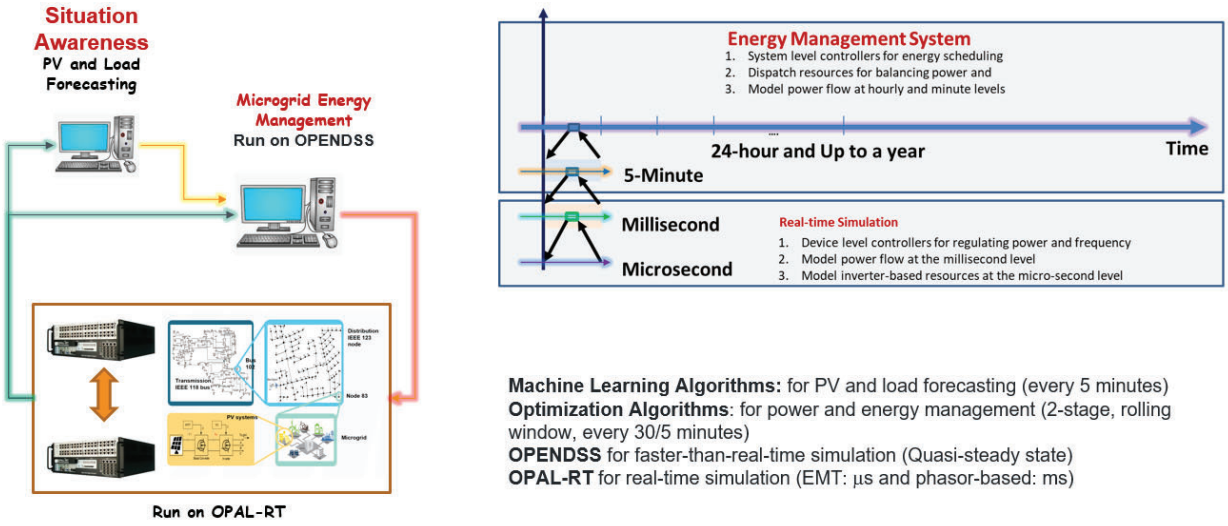

(a)

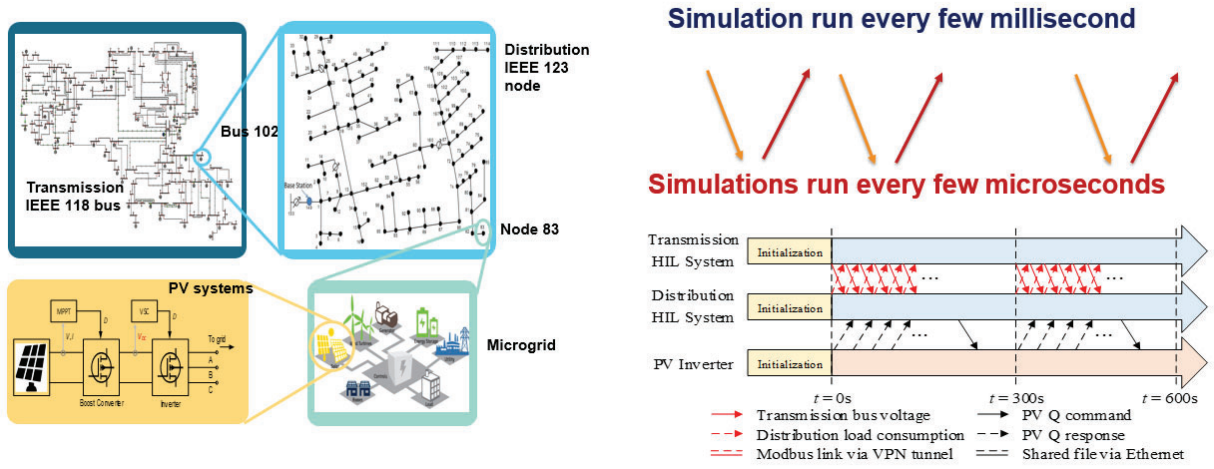

(b)

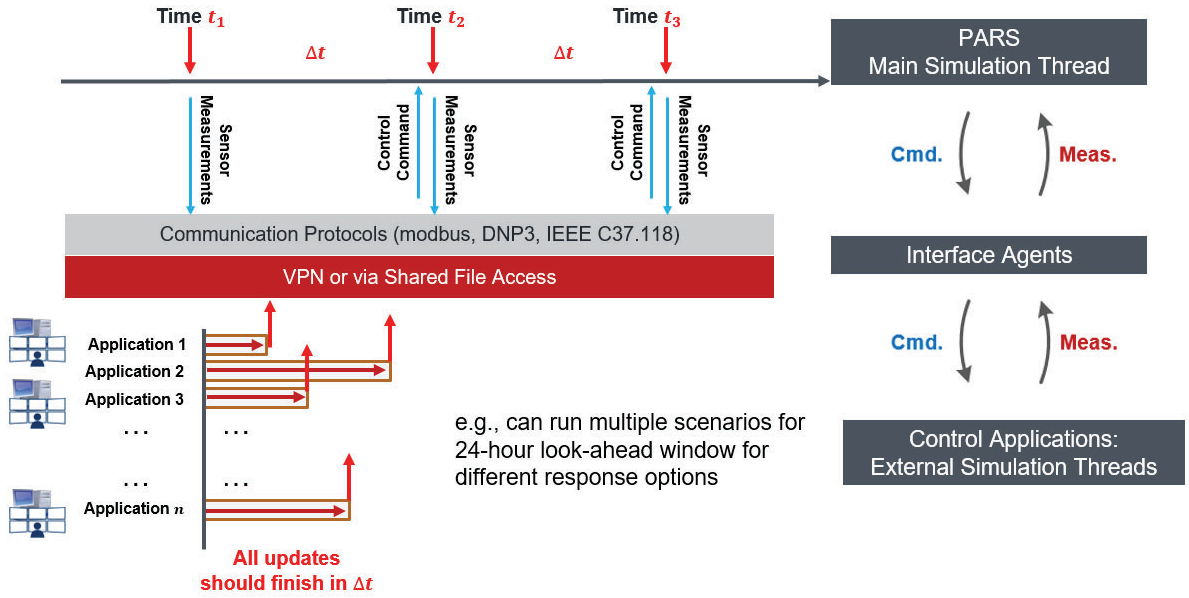

(c)

Figure 8. Data Transfer and Simulation Time Coordination. (a) Between HIL and EMS, (b) Inside HIL among different HIL systems, (c) Time coordination among Energy and Power management systems and device level controllers

3.2 Model Parameterization Tool

Conventional power system simulation test beds are typically established through two primary methods. The first method entails crafting a fictitious system characterized by a standard network topology and populated with typical parameters, such as the IEEE test systems [16]-[18]. The second method involves directly capturing a snapshot of an existing physical power system to generate a static replica, essentially freezing a moment in time for analysis and simulation purposes. For example, a Dispatch Training Simulator (DTS) is a perfect replication of a real power grid that is initialized from a real time and historian snapshot [19]-[21].

The core difference between a conventional power system test bed and a DT lies in the dynamic nature of the latter. To act as a real-time replica of an actual system in the virtual realm, the PSDT need to closely emulate the physical system behavior when the system evolves in real-time. If a significant deviation from the real system behavior is detected, the DT parameters need to be adjusted using real-time or near-real-time field measurements without causing abrupt disruptions in simulation results.

To date, although there are extensive publication on power system test bed development, there has been relatively limited research on real-time parameterization for Power System Digital Twins (PSDTs). Thus, in this project, the parameterization tool (See Figure 4) has two DT parameterization functions: offline- and online- parameterization.

- The *off-line parameterization tool* uses field test results and factory data sheets as inputs. Optimization based methods are used to find an optimal set of model parameters for minimizing the mismatch between the simulation results and field measurements for a prolonged period, for example, an entire day, week, or month, as illustrated in Figure 9 (a) and (b). The developed offline parameterization methods for the battery energy storage systems [6], combined heat and power systems [13], diesel generators [14], and loads [15] have been published in IEEE Transactions on Smart Grid.
- The *real-time model parametrization tool* uses real-time SCADA data as inputs, as shown in Figure 6. To achieve higher accuracy for real-time control applications, we developed a novel two-stage optimization-based method for real-time, online parameterization of a photovoltaic digital twin (see Figure 4) will use *real-time*, *1-second field measurements* as inputs. As shown in Figure 10, the PV model parameters are adjusted in real-time for matching field measurements and minimizing perdition errors. The method for parameterizing a PV farm digital twin is introduced in detail in Appendix 9.15 D8.

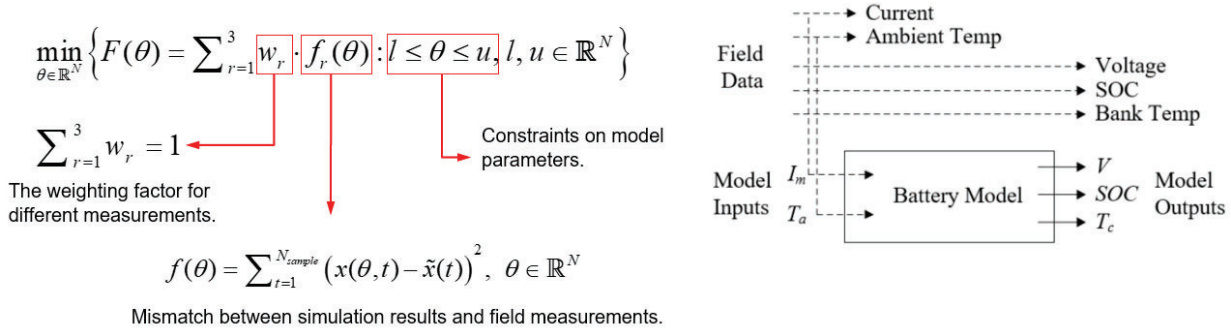

(a)

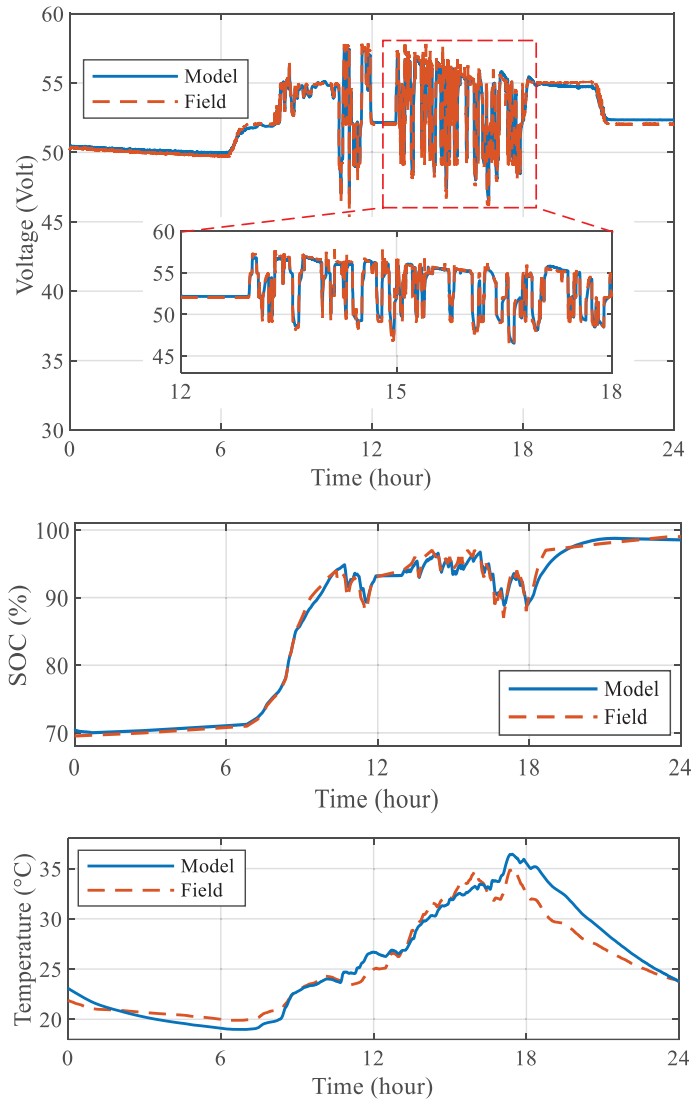

(b)

Figure 9. (a) An example of optimization objective function, and (b) Modeled Outputs and Field Measurements (battery voltage, state-of-charge, and cell temperature)

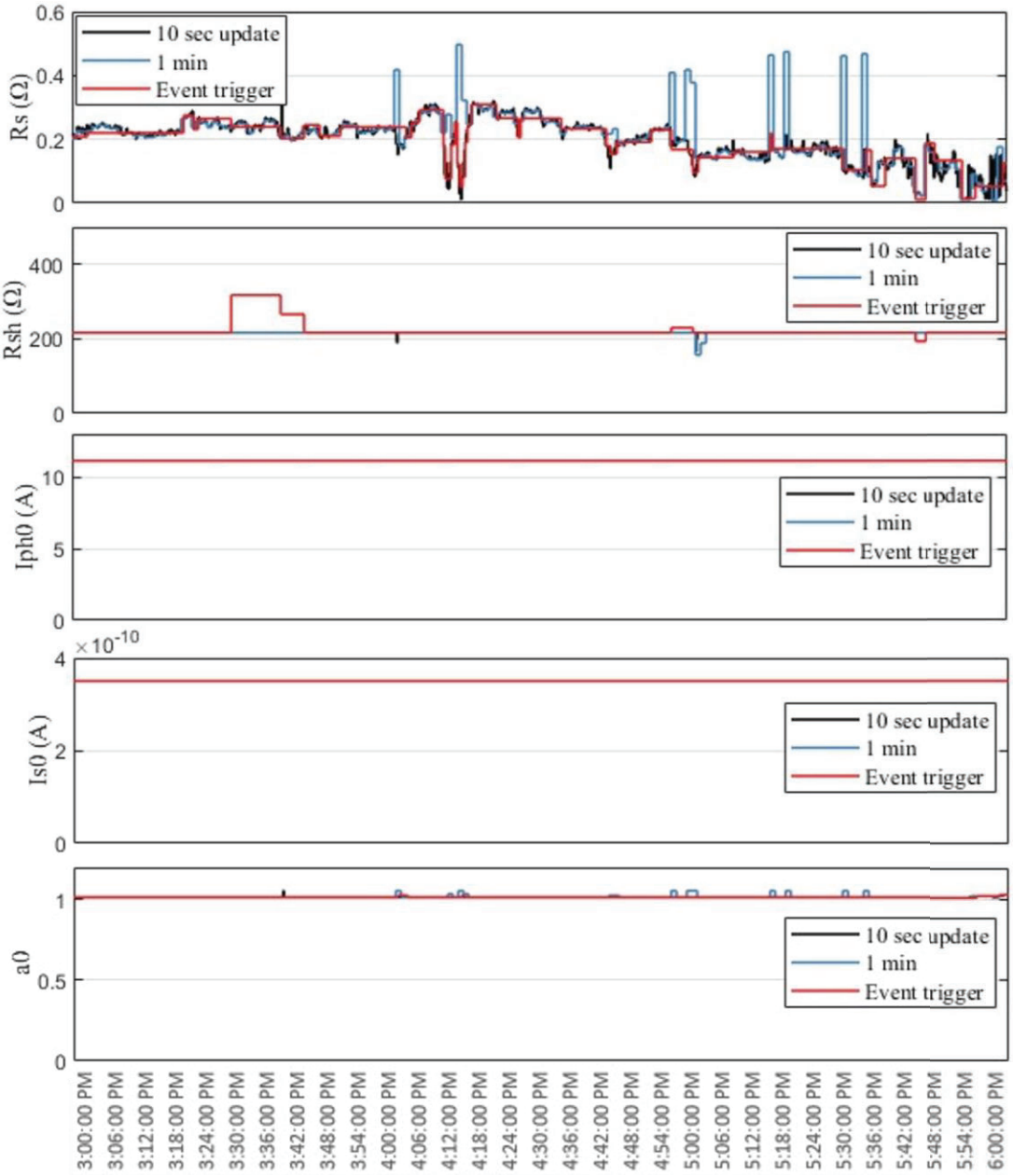

Fig. 10. Changes in 5 model parameters according to update criteria (3-hours)

3.3 Operation Model Tool

In this section, we will provide an overview of the modeling considerations and validation methods. For a comprehensive understanding of the technical approaches, problem formulations, and simulation results, please refer to Appendix 9.1-9.7 (Deliverables A1-2 and B1-B5) and our published papers.

3.3.1 Modeling Considerations

This section outlines the key models incorporated into the operation model tools, which include:

- PV farms equipped with grid-following capabilities, ranging from large-scale models for 100MW and above (developed by PNNL) to 5-50 MW PV farms and rooftop PV systems (both developed by NCSU). The grid-following functionalities of these PV models are detailed in Table 3 and illustrated in Figure 11.
- Diesel generators, with their modeled functions listed in Table 4.
- Battery systems, where Figure 12 presents battery inverter modeling considerations, and Table 5 outlines battery modeling details.
- Various load models such as the ZIP model, motor load model, and cold-load-pick-up models, with Table 6 discussing the load modeling considerations and Figure 13 displaying the cold load pick up modeling outcomes.

Table 3: Grid following Functions for a roof-top PV system

Module	Functionality	Requirements
Rooftop PV	**Active power curtailment**	Follow power curtailment setpoints.
	Disturbance ride-through	Trip in accordance with default settings from IEEE 1547-2018
	Reactive power control modes	Provide all reactive power control modes established for Category II-B DER from IEEE 1547-2018.
	Frequency-watt droop	Provide f-watt droop to support the grid.
	Voltage-active power droop	Curtail output power if the grid voltage increases (optional mode)
	Code-based model	Implemented in a code-based environment to provide an alternative model without block diagrams (reducing model)

Table 4: Diesel generator modeling considerations

Module	Functionality	Requirement
Diesel Generator	Ramping Capability	Regulate its output power ramping to a pre-specified p.u./s for improving system robustness.
	Grid Synchronization	Adjust its voltage magnitude and phase for a smooth grid synchronization.
	Fuel Consumption Estimation	Calculate the fuel consumption.
	Mode switching capability – grid forming / grid-following	Operate in grid-forming or grid-following modes.
	Power factor control	Follow active power setpoint and a given power factor.

	Disturbance ride-through	Trip in accordance with PRC-024-2 (NERC)

Table 5: Battery modeling considerations

Module	Operation mode	Functionality	Requirement
Battery Energy Storage Model	Grid-forming	Voltage and frequency regulation	It's responsible for regulating PCC voltage and setting the system frequency.
		Three-phase imbalance control	If the distribution grid is imbalanced, ES should quickly readjust its output voltage to maintain voltage balance.
		Current limiting control	The inverters must be protected from overcurrent of the semiconductor devices in overload and fault cases.
		Coordinated voltage regulation with multiple ES units	If there are multiple ES units are connected into the distribution grid and worked as grid-forming mode, PCC voltage can be regulated using the centralized secondary control.
		Resynchronization	To connect the MG to the grid, the phase and amplitude voltage between the grid and the MG will be regulated as an equal value using the synchronization control loop.
	Grid-following	Real and reactive power dispatch	In grid-tied or grid-following mode, the model should make the output power of the inverter follow the reference values and maintain the voltage reference tracking.
		Disturbance ride-through	When working in the grid-following mode, the machine will trip if the grid's voltage or frequency goes beyond the specified limits.

Table 6: Load modeling considerations

	Functionality	Requirement
Load Model	Realistic load profile synthesis	Generate node load profile from smart meter data actual load data. Use Super–Resolution algorithms for increased data resolution
	Modeling demand response (pay-back and cold load effects): HVAC load modeling	Model the behavior of HVAC load regarding house scale and appliance parameters
	Load model parameterization	Estimate the parameters of the state-space model based on actual HVAC load profile
	Real-time Cold Load Pickup (CLPU) profile generation	Generate real-time cold-load-pickup response according to the commands from EMS system

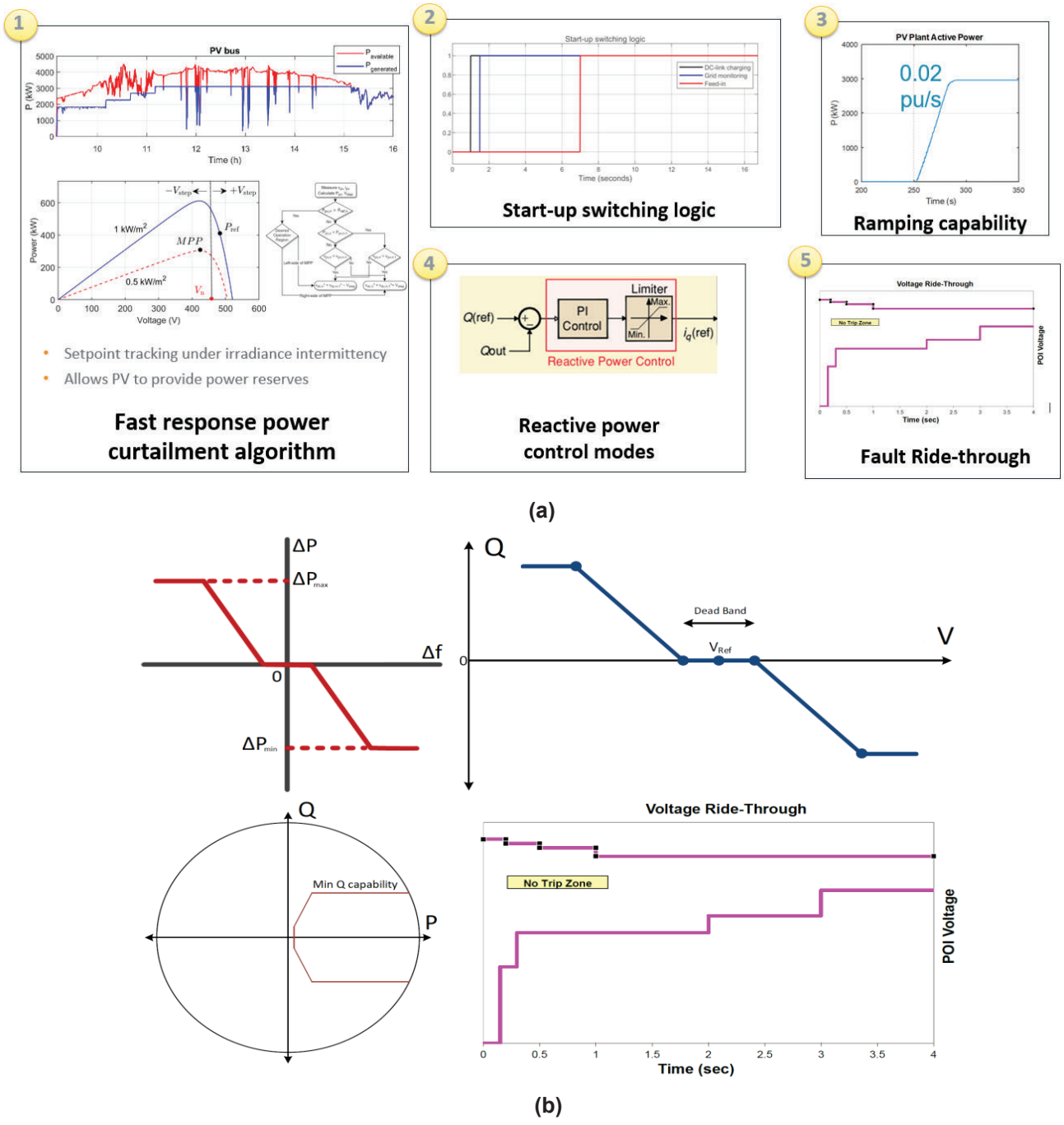

Figure 11. PV model development considerations. (a) Functions developed for MW-level PV farm, and (b) Grid-following functions developed for roof-top PV systems (Includes IEEE 1547-2018 Category II-B DER requirements)

	Three Single-Phase Inverter Model	Three-phase Inverter Model
Characteristic	Separate circuit and controllers for each phase.	Integrated circuit and controller.
Application	Mostly used in the residential applications and for running lower power loads.	Mostly used in large industries and for high power applications.
Grid-forming mode	BESS power limitation for unbalance regulation: $\lvert P_a\rvert, \lvert P_b\rvert, \lvert P_c\rvert \le P_{rated}$	BESS power limitation for unbalance regulation: 1) power unbalance factor* ≤ 0.6; 2) $\lvert P_a\rvert, \lvert P_b\rvert, \lvert P_c\rvert \le 0.95\ P_{rated}$
Grid-following mode	Output power for each phase is controllable.	Output power can't be controlled per phase

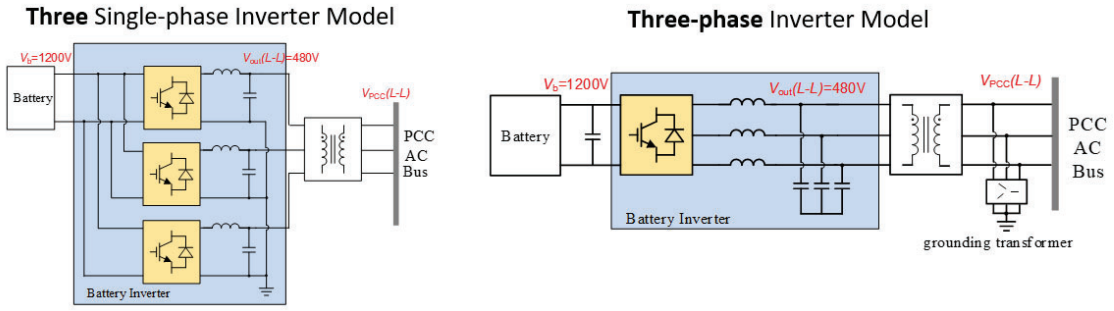

Figure 12. BESS Inverter models (single-phase versus three-phase)

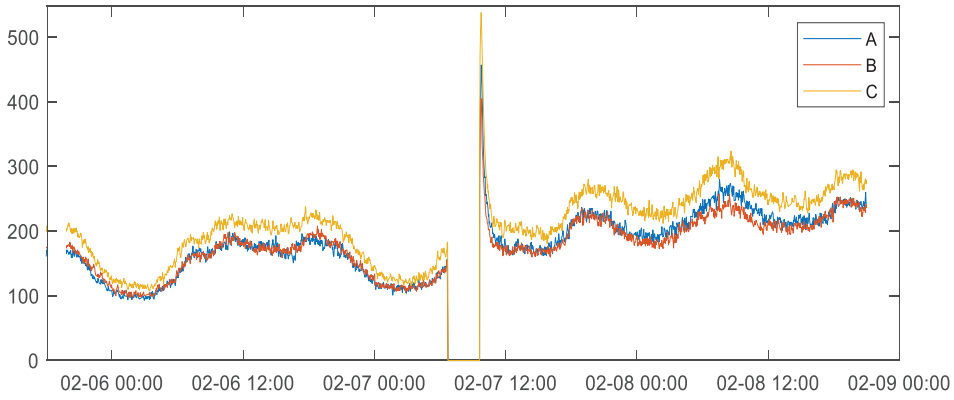

Figure 13. Cold load pick up model

3.3.2 Model validation: The PARS platform co-simulates Electromagnetic Transient and Transient Stability (EMT-TS) models, as demonstrated in Figure 14(a). Grid-forming units are modeled in the EMT domain and the distribution network along with grid-following units are modeled in the phasor domain. This strategy provides a viable computational approach for grids heavily populated with Inverter-Based Resources. Microsecond-level EMT simulations run concurrently with millisecond-level phasor simulations, transferring data between the two every 100 ms, as depicted in Figure 8(b). This time lag may introduce discrepancies in the TS simulation results due to the EMT simulation's faster execution rate. The following benchmark tests have been conducted for model validation purposes.

Benchmark Method 1: Base cases for distribution models are typically created using CYME or OPENDSS, while PSSE is preferred for transmission models. Consequently, once the real-time simulation models on OPAL-RT are developed, our initial step involves comparing the results from OPAL-RT with those derived from CYME/OPENDSS or PSSE.

Benchmark Method 2: To validate the data-driven model performance, we compared the simulation results with the field measurements.

Benchmark Method 3: Next, we assess our performance against established methods. As shown in Figure 15, when developing the PV tracking models, we compare the results with the

Benchmark Method 4: The performance of this hybrid EMT-TS framework is also compared with that of a solely EMT-based simulation framework. As indicated in Figure 14, the hybrid system delivers a performance comparable to the full EMT model but requires significantly less computational effort, showcasing the architecture's ability to strike a balance between accuracy and computational efficiency.

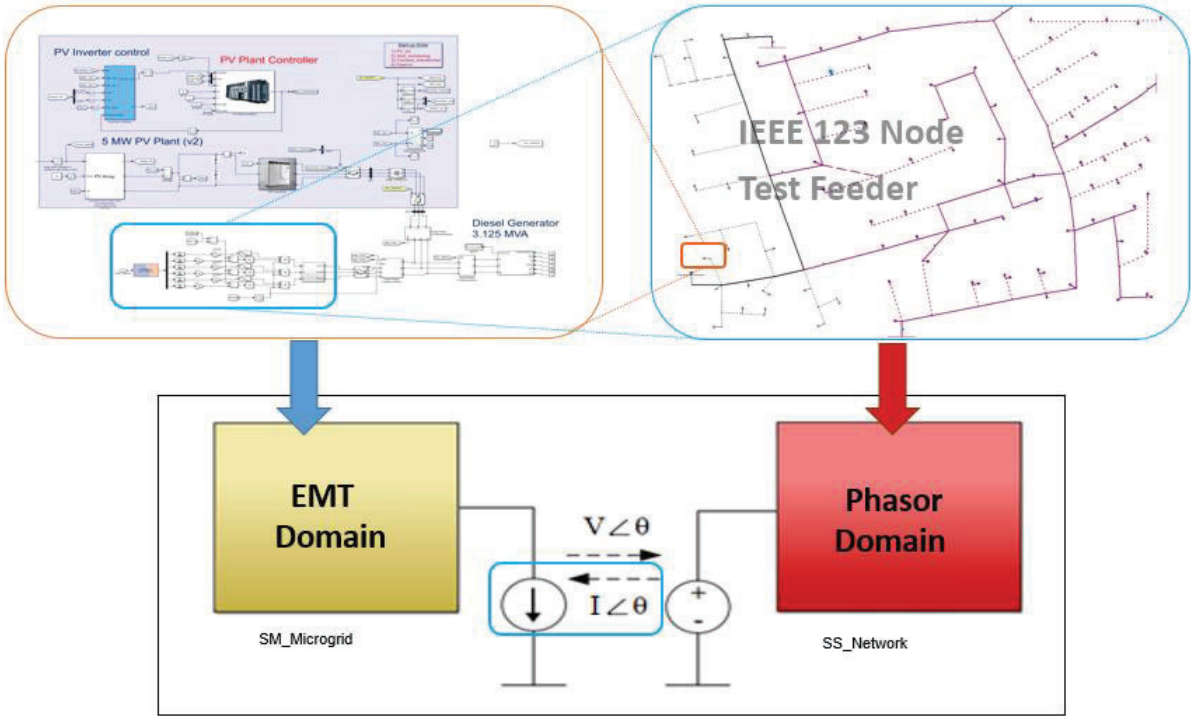

(a)

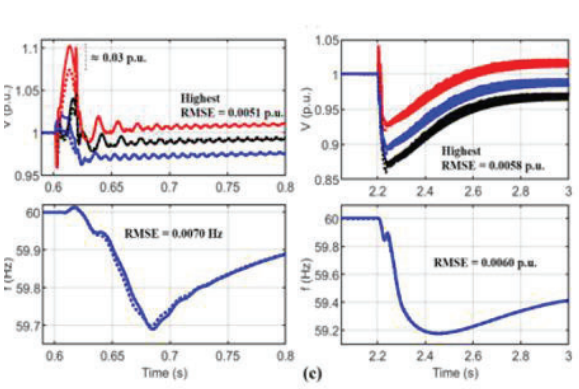

1) Transient response: EMT-TS versus the full EMT testbed when a step load change happens.

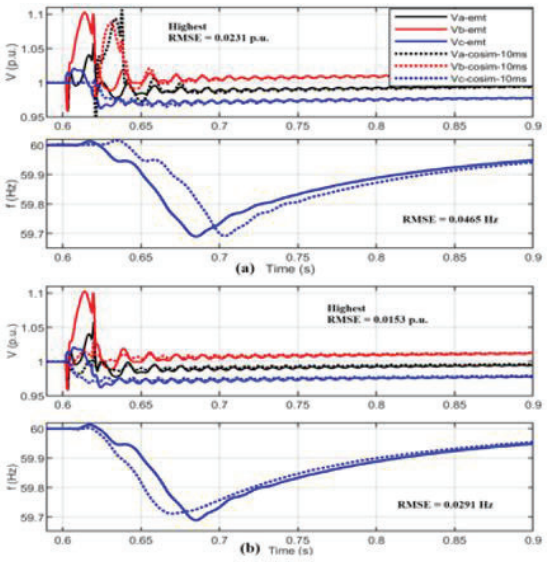

2) (a) increasing the communication delay between EMT and phasor domains; (b) utilizing the time interpolation coupling technique

(b)

Figure 14. EMT-TS versus EMT simulation (Appendix 9.9: D2) (a) Configuration of the Co-simulation test system, and (b) Comparison of EMT-TS results with EMT results

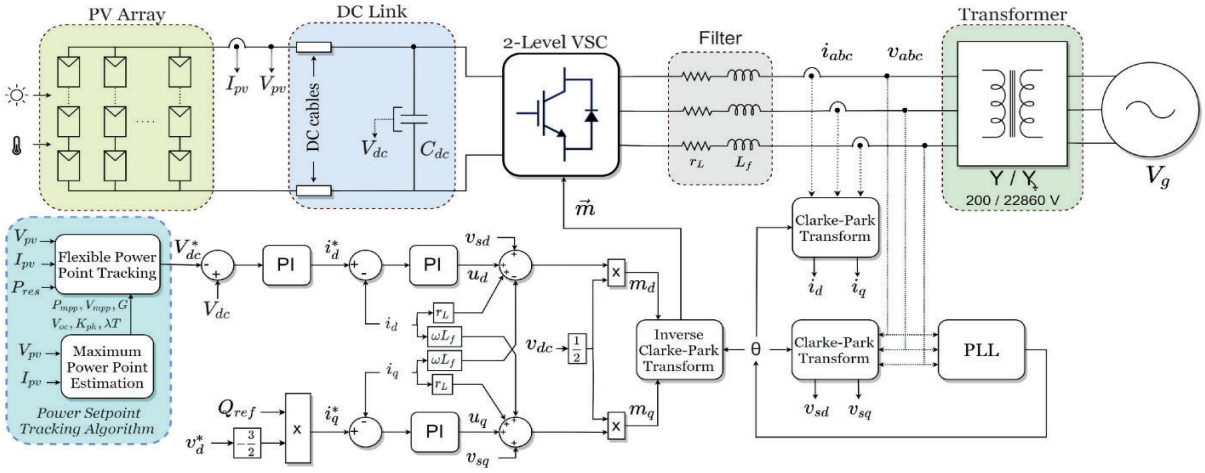

(a)

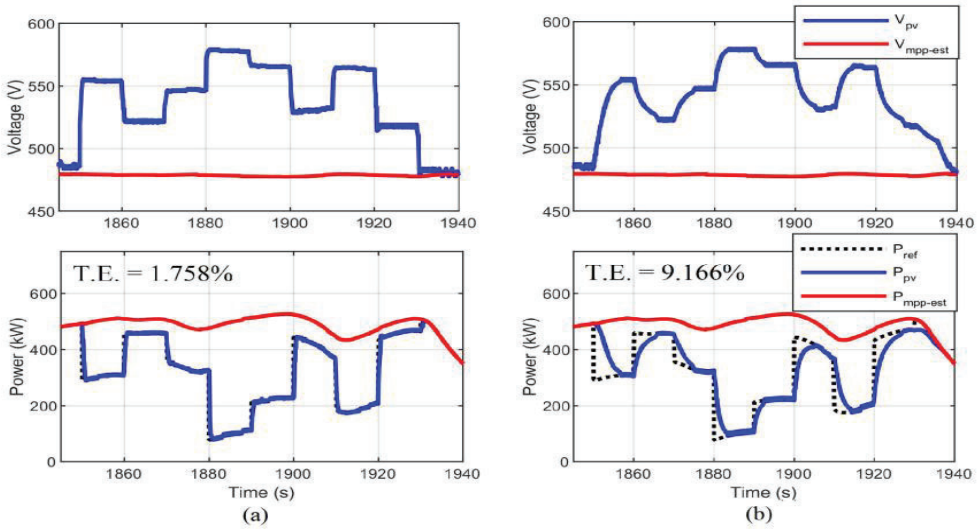

Figure 15. (a) Circuit and control system block diagrams of a utility-scale PV system (b) Comparison of the power setpoint tracking performance under irradiance intermittency between the proposed RST method (left-side figures) and the state-of-the-art adaptive FPPT (right-side figures).

3.3.3 Scale-up studies

Scale-up studies were executed by orchestrating co-simulation scenarios across various institutions, as depicted in Figures 16 (a) and (b). These studies utilized two primary connectivity methods: file-transfer and VPN connections, with delays capped at 1 second for file transfers and 50 milliseconds for VPNs. Regardless of the method, multiple smaller simulation systems were operated concurrently to emulate a comprehensive hardware-in-the-loop, integrated Transmission and Distribution (T&D) model.

These scale-up studies were conducted with the co-simulation configurations detailed below:

- Collaborations among PNNL, UT Austin, and NCSU focused on integrated volt/var support across transmission and distribution systems (see Figure 16(b)).
- Partnerships between NCSU and Clemson to analyze the effects of transmission faults on distributed inverter-based resources, facilitated by a CAPER project with funding from Duke Energy and Dominion Power.
- Within the North Carolina university system, for simulating cyber-attacks on DERs, a shared Google file was created, granting North Carolina universities access to real-time simulation results from the PARS platform.

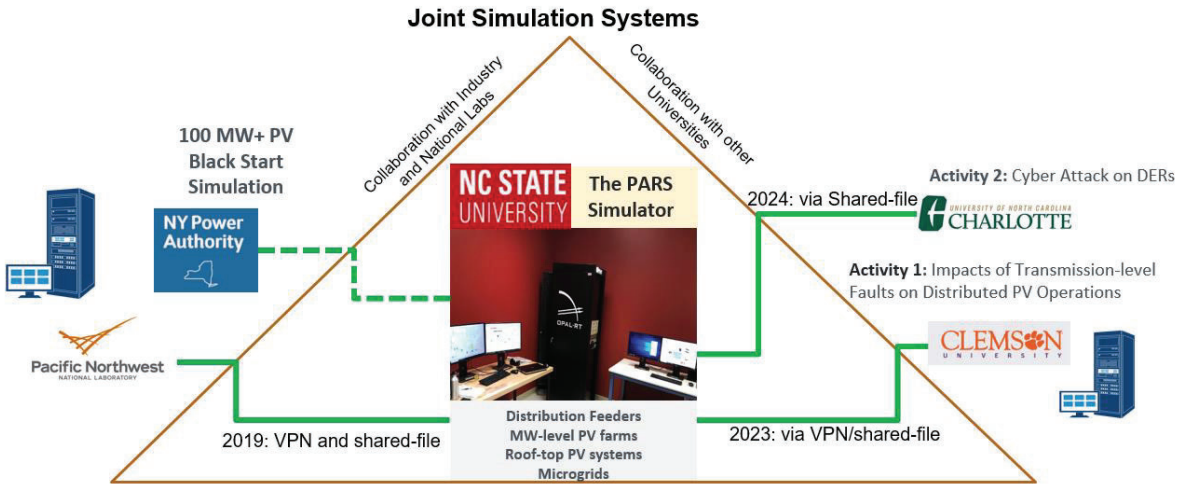

(a)

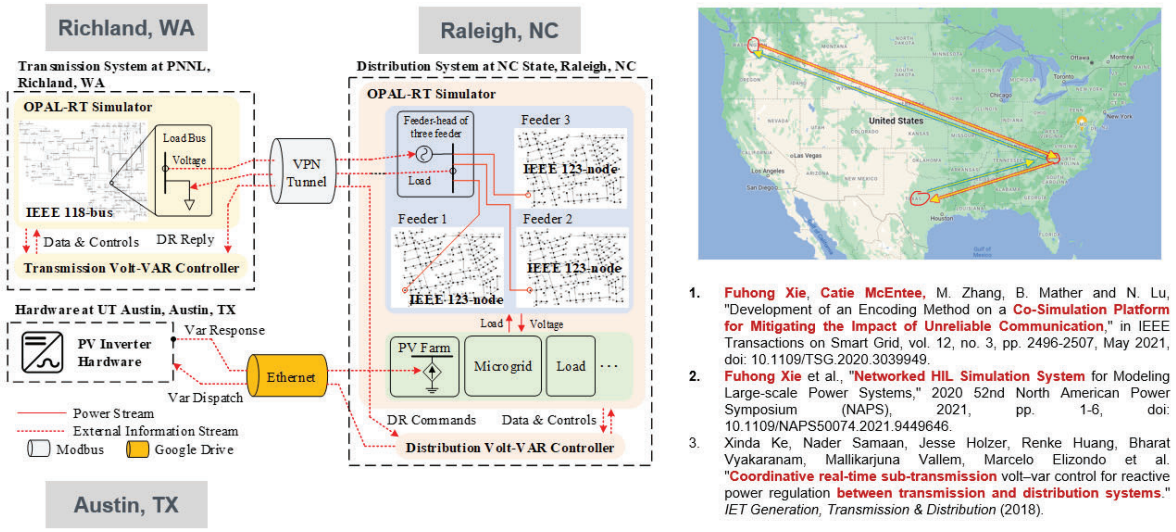

1. **Fuhong Xie**, **Catie McEntee**, M. Zhang, B. Mather and N. Lu, "Development of an Encoding Method on a **Co-Simulation Platform for Mitigating the Impact of Unreliable Communication**," in IEEE Transactions on Smart Grid, vol. 12, no. 3, pp. 2496-2507, May 2021, doi: 10.1109/TSG.2020.3039949.
2. **Fuhong Xie** et al., "**Networked HIL Simulation System** for Modeling Large-scale Power Systems," 2020 52nd North American Power Symposium (NAPS), 2021, pp. 1-6, doi: 10.1109/NAPS50074.2021.9449646.
3. Xinda Ke, Nader Samaan, Jesse Holzer, Renke Huang, Bharat Vyakaranam, Mallikarjuna Vallem, Marcelo Elizondo et al. "**Coordinative real-time sub-transmission** volt–var control for reactive power regulation **between transmission and distribution systems**." *IET Generation, Transmission & Distribution* (2018).

(b)

Figure 16. Co-Simulation test cases conducted. (a) Co-simulation cases conducted and (b) Simulation setup of one simulation between PNNL, NCSU, and UT Austin.

3.4 Situation Awareness Tool

Figure 17 shows that the PARS Situation Awareness tool accepts either field measurement data or digital twin simulated data. When using field data, we initially identify and discard any incorrect segments using state estimation based bad data detection. Then, we fill in and align missing data using regression-based or generative learning based methods (i.e., GAN-based and BERT-based). If field measurements fall short for data-driven applications like machine learning-based load disaggregation, we can create synthetic data to supplement the field data. Those tools are highly flexible and can facilitate various downstream tasks such as PV and load forecasting, real-time volt/var control, model parameterization, power dispatch, energy scheduling, cybersecurity, and cost-benefit analyses.

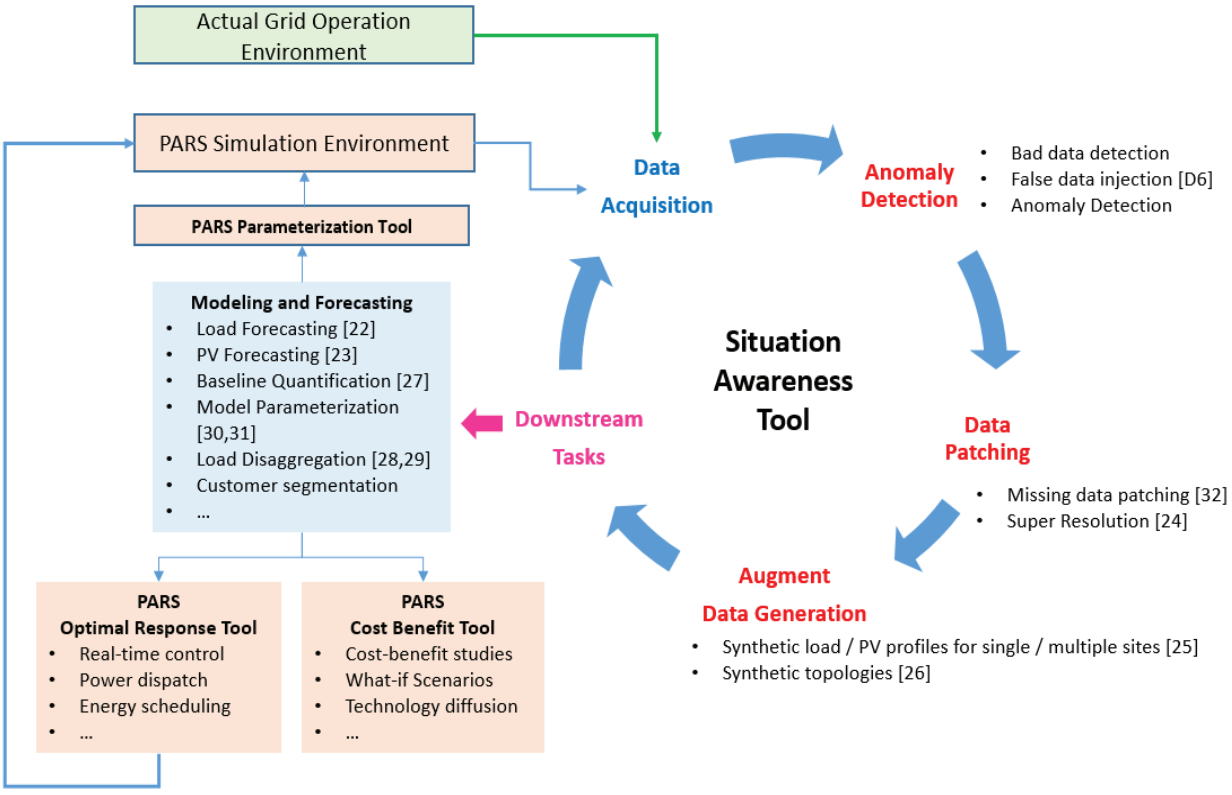

Figure 17. The work flow of the Real-time Situation Awareness tool.

3.5.1 Delayed Stealth False Data Injection Attack Tool (Appendix 9.13: D6)

The development of a deep reinforcement learning (DRL)-based scheme for delayed stealth false data injection attacks (SFDIAs) against Battery Energy Management Systems (BEMS) represents a sophisticated approach to compromising the operational integrity of Battery Energy Storage Systems (BESSs) within Advanced Distribution Networks (ADNs). We leverage a DRL framework to generate falsified battery voltage and current measurements capable of evading traditional and cross-validation Bad Data Detection (BDD) checks, thereby inducing targeted SoC errors with highly stealthy. As shown in Figure 18, the attacker can disrupt BESS operations at any predetermined future intervals without detection by the BDD mechanisms. The results demonstrate that by misleading the BEMS about the stored energy levels, we can cause premature system shutdowns or accelerated BESS degradation through over-discharging. This approach not only showcases the effectiveness of DRL in crafting stealthy and temporally precise cyber-attacks but

also highlights the critical need for advanced security measures in safeguarding energy management systems from such sophisticated threats.

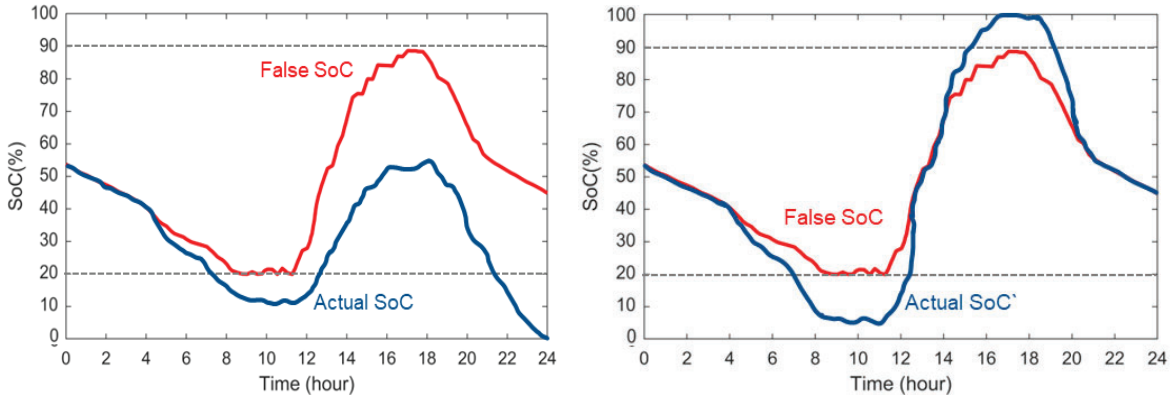

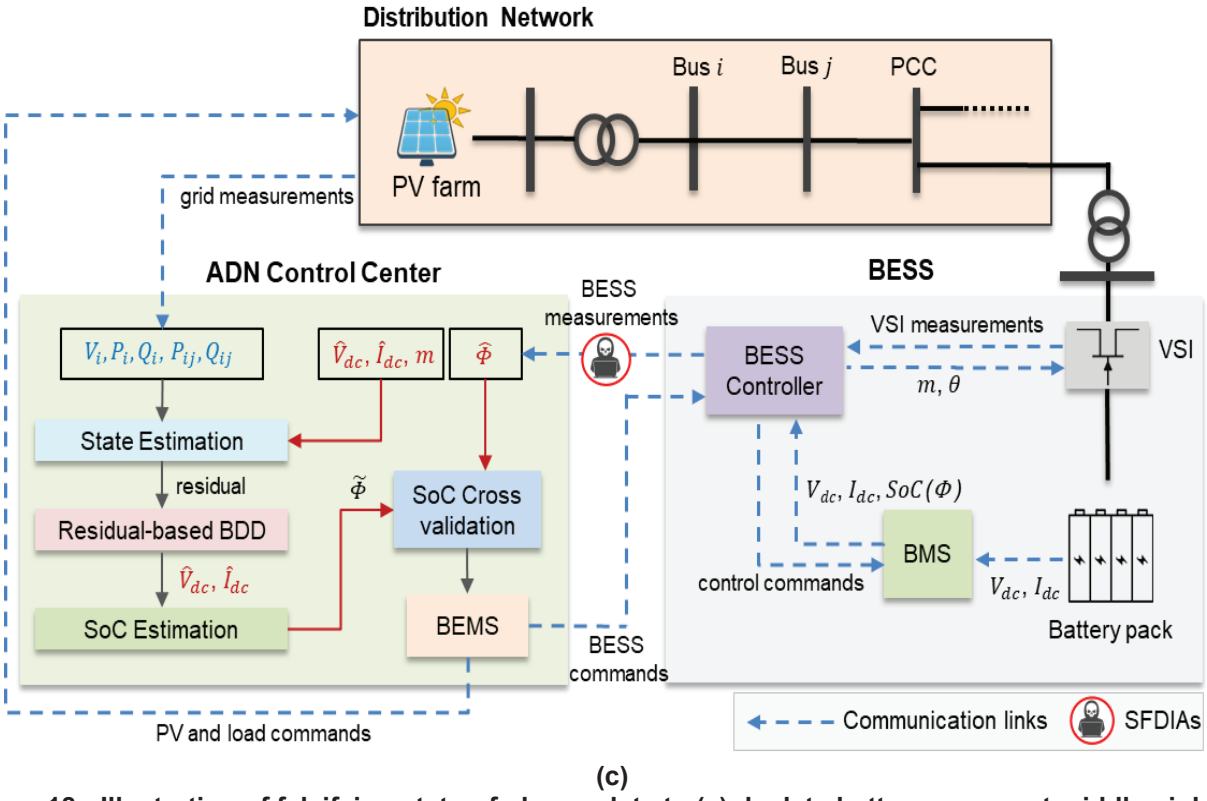

Figure 18. Illustration of falsifying state-of-charge data to (a) deplete battery energy at middle night, (b) run battery outside it allowable storage range, and (c) An illustration of the attacking scenarios

3.5.2 Topology and Meter Phase Mislabeling Detection Tool (Appendix 9.20: E5)

The Power-Band based Data Segmentation (PBDS) method introduces an innovative approach for meter topology identification, specifically in customer phase identification and transformer-meter pairing. Tested on thirteen real feeders in North Carolina, this method surpasses existing techniques by significantly enhancing accuracy while maintaining low computational complexity. The PBDS method stands out in its ability to efficiently utilize data through segmentation, facilitating the identification process without the need for extensive additional data or equipment, unlike other methods which may require signal injections, PMU data, or suffer from data inefficiency and interpretability issues. The proposed approach is characterized by its simplicity, accuracy, and the use of readily available AMI data, achieving notable improvements in phase identification accuracy and a substantial reduction in the false positive rate for transformer-meter pairing. This demonstrates the PBDS method's effectiveness in automating the identification of smart meter phase and transformer-meter relationships, offering a significant contribution to the field of meter topology identification.

3.5.3 Missing Data Restoration Tool (Appendix 9.22: F2)

The Load Profile Inpainting Network (Load-PIN), based on Generative Adversarial Nets (GAN), introduces a novel approach for restoring missing load data and estimating demand response event baselines. Unlike traditional methods that struggle with variable-length data segments, Load-PIN excels in handling varying durations of missing data and differing lengths of available measurements, overcoming the limitations of fixed input-output formats required by existing generative methods. This flexibility is achieved through a two-stage generator process involving initial estimation and fine-tuning, paired with a deep convolutional discriminator optimized with specially designed loss functions. Load-PIN's capability to adapt to variable data resolutions and durations sets it apart, demonstrating superior accuracy and a notable 15-30% improvement over other models in restoring high-resolution load data segments. However, its performance is less pronounced at lower data resolutions, highlighting its optimized use for high-resolution data to uncover detailed load shape information. This advancement in missing data restoration and baseline estimation represents a significant leap forward in the accuracy and applicability of data-driven methods for load profile inpainting. We also developed a BERT based method [33] that can generate an ensemble of missing data restoration options (see Figure 19) where the restored data segments can be ranked by the likelihood of occurrence.

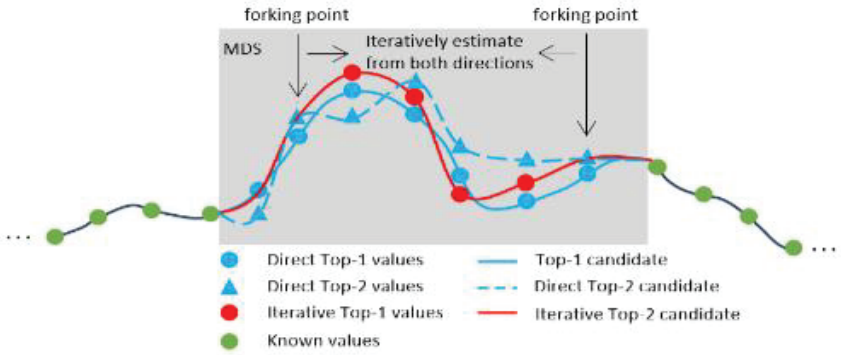

Figure 19. Illustration of missing data restoration.

3.5.4 An Data Encoding Tool for Mitigating the Impact of Unreliable Communication (Appendix 9.14: D7)

The encoding tool aimed to mitigate the impact of unreliable communication between distributed energy resources (DERs) and central controllers in a power distribution network. Utilizing a

hardware-in-the-loop (HIL) co-simulation environment, which includes a real-time simulation on OPAL-RT and a simulated communication network, we develop an encoding algorithm for counteracting communication noise, errors, and missing data. The proposed mitigation method, formulated as a matrix recovery problem, optimizes LTE communication data and error estimations, demonstrating its efficacy through simulations that replicate system dynamics and communication challenges in a controlled lab setting. Simulation results highlighted the effectiveness of centralized volt-var control (CVVC) strategies under perfect and interrupted communication scenarios, showing how appropriate voltage margins can eliminate voltage violations without causing excessive control actions. This innovative approach enhances the reliability of DER management and voltage control in the face of communication uncertainties, offering a significant advancement in the development and testing of algorithms for distribution system analysis.

3.5.5 Super-resolution Tool (Appendix 9.18: E3)

This task introduces ProfileSR-GAN, a GAN-based super-resolution method designed to enhance low-resolution load profiles (e.g., 30-minute) into high-resolution (e.g., 15-, 5- and 1-minute), as shown in Figure 20. This tool offers a significant advancement in the field of data-driven applications where high-resolution load data is increasingly crucial. Traditional methods, categorized into model-based and deep learning-based approaches, often struggle with introducing unrealistic details or causing over-smoothing. ProfileSR-GAN addresses these issues by a two-stage process. First, we apply a GAN-based model to restore high-frequency components. Next, we refine the generated high-resolution profiles using a polishing network consisting of deep convolution layers, residual blocks, and batch normalization that can eliminate unrealistic power fluctuations. Simulation results validated ProfileSR-GAN's superior performance, showing 36%-62% improvements in shape-related metrics over baseline methods. Additionally, a case study on Non-Intrusive Load Monitoring methods showcases the framework's potential to significantly enhance appliance-level activity recognition. This further demonstrates that ProfileSR-GAN can improve the quality and utility of load data for various downstream tasks.

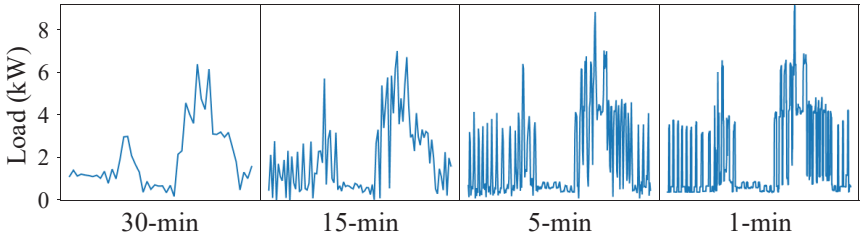

Figure 20. Illustration of missing data restoration.

3.5.6 Synthetic Data Generation Tool (Appendix 9.19: E4)

This task introduces the Multi-load Generative Adversarial Network (MultiLoad-GAN), a pioneering deep-learning framework designed to generate synthetic load profiles (SLPs) for groups of loads served by the same distribution transformer, capturing their spatial-temporal correlations. As shown in Figure 21, unlike traditional methods that generate SLPs individually, MultiLoad-GAN innovatively produces multiple correlated SLPs simultaneously, addressing a gap in existing generative approaches. It leverages a generator and discriminator network to create realistic load profiles in large quantities, essential for microgrid and distribution system planning. The framework's effectiveness is demonstrated through comparisons with original load data using statistical and deep-learning metrics, showing its superiority in capturing group-level characteristics and benefiting from an Automatic Data Augmentation (ADA) process. This process prevents overfitting, ensuring the generation of diversified, realistic SLPs that closely resemble real-world data, thus offering a significant advancement in the field of load profile generation.

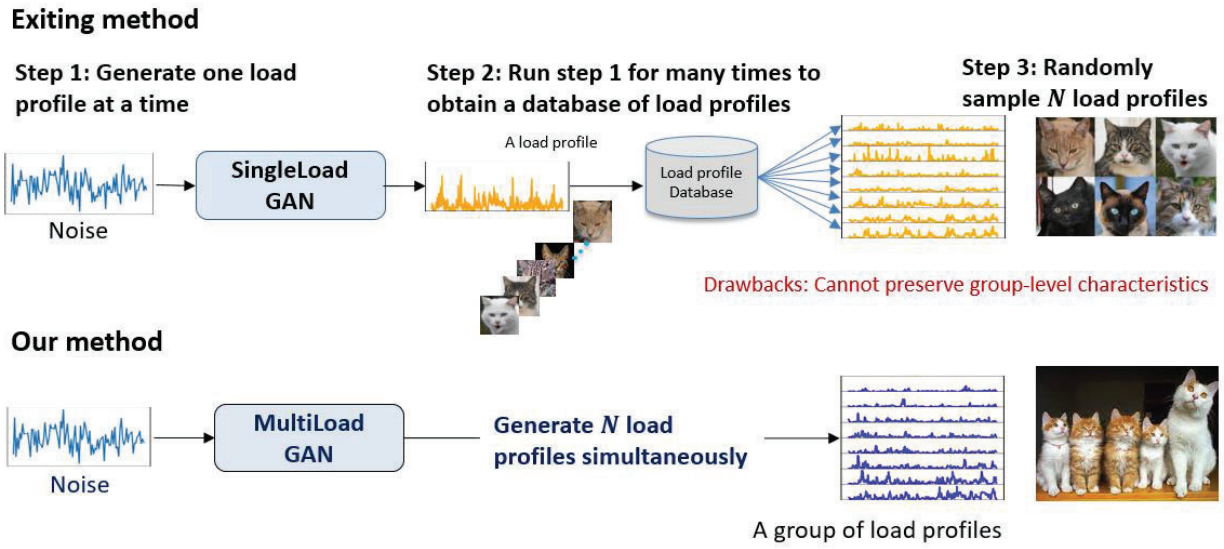

Figure 21. Illustration of single and group synthetic load profiles generation.

3.5.7 The meta-learning based load forecasting tool (Appendix 9.16: E1)

This tool is developed as an innovative model selection framework for load forecasting in power systems, addressing the variability in forecasting requirements and data availability. It compares knowledge-based expert systems and machine-learning methods. The meta-learning based framework automates and extends model selection by evaluating candidate models on specific tasks and using task features (see Figure 22) to train a meta-learner. This approach provides a general purpose forecasting tool for identifying top-performing models and thereby reducing forecasting errors.

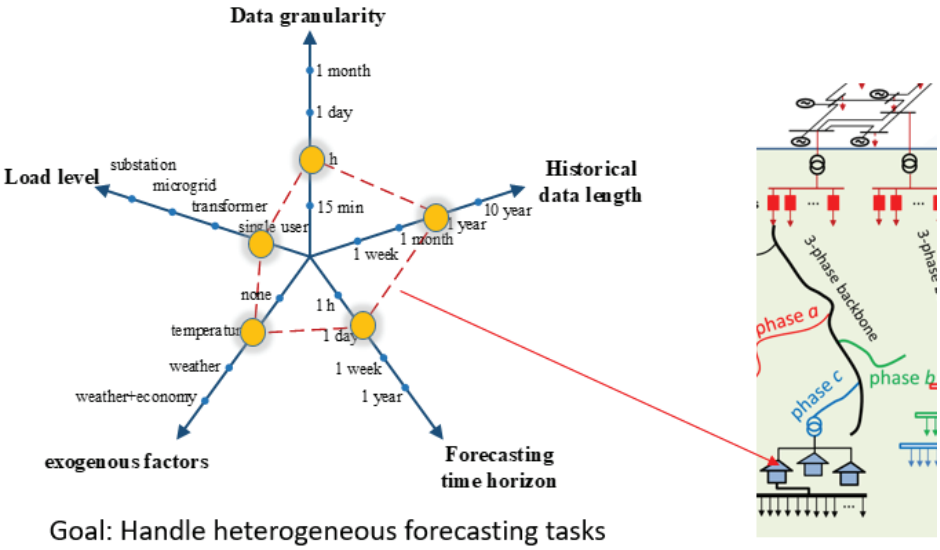

Figure 22. Illustration of high-level features for selecting the forecasting models.

3.5.8 The TCN-based PV forecasting tool (Appendix 9.17: E2)

The TCN-based hybrid forecasting framework (See Figure 23) tailored for hours-ahead forecasting in utility-scale PV farms, merging the strengths of both physics-based and data-driven models.

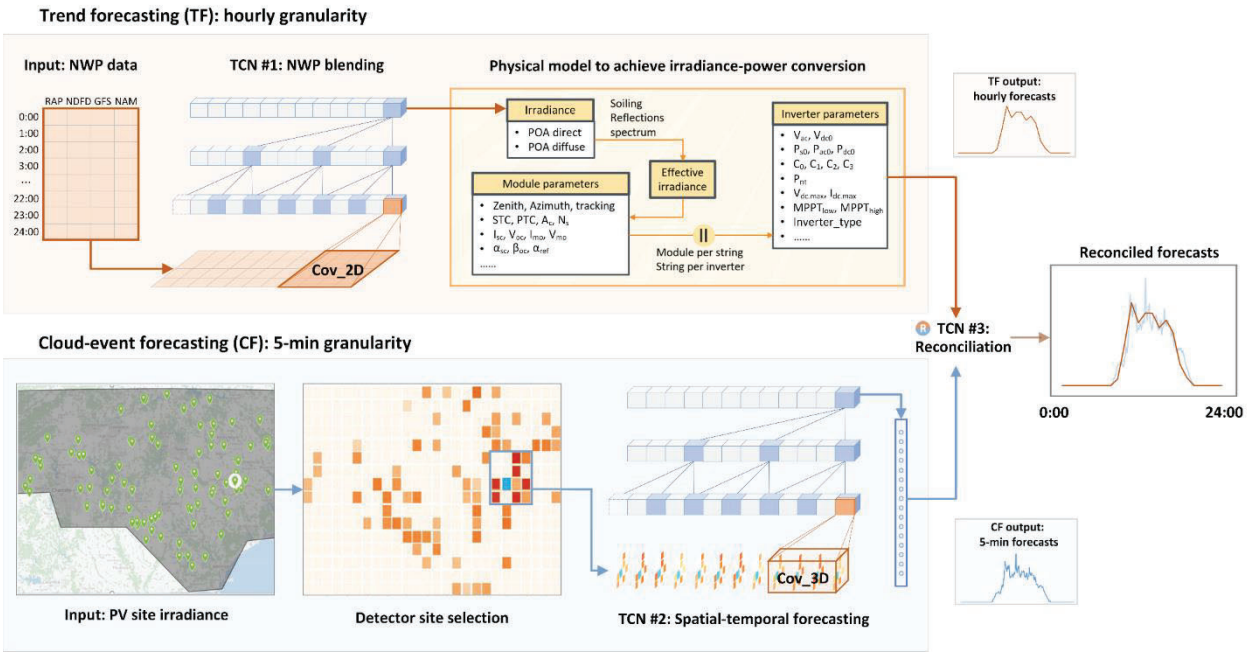

Figure 23. An illustration of using TCN and the selection of neighboring sites for improving the short-term PV forecast accuracy

Traditional models, while beneficial, either depend on historical data or are limited by the accuracy of Numerical Weather Prediction (NWP) results, lacking a method to integrate these approaches for enhanced accuracy. This framework introduces a novel solution that not only combines the predictive power of physics-based and data-driven models but also incorporates spatial-temporal correlations from neighboring sites to refine forecasts. It employs a TCN network

for trend forecasting by converting NWP results to power outputs, another TCN for capturing intra-hour fluctuations through spatial-temporal correlations, and a third for reconciling these forecasts into a final prediction. A unique neighboring site selection algorithm automatically identifies the most effective neighboring networks, significantly improving forecasting accuracy. Tested across 95 PV farms in North Carolina, this hybrid method demonstrated a 30% increase in forecasting accuracy for 6-hour ahead predictions, outperforming benchmark models with its innovative approach and efficient training time.

3.5.9 CVR Baseline Detection Tool (Appendix 9.21: F1)

The Iterative Bidirectional Gradient Boosting (IBi-GBM) method presents a novel approach for Conservation Voltage Reduction (CVR) baseline estimation. The method combines a hybrid similar day selection technique with a bi-directional gradient boosting framework to assess CVR's load reduction efficacy. Figure 24 presents examples of the restored CVR baselines.

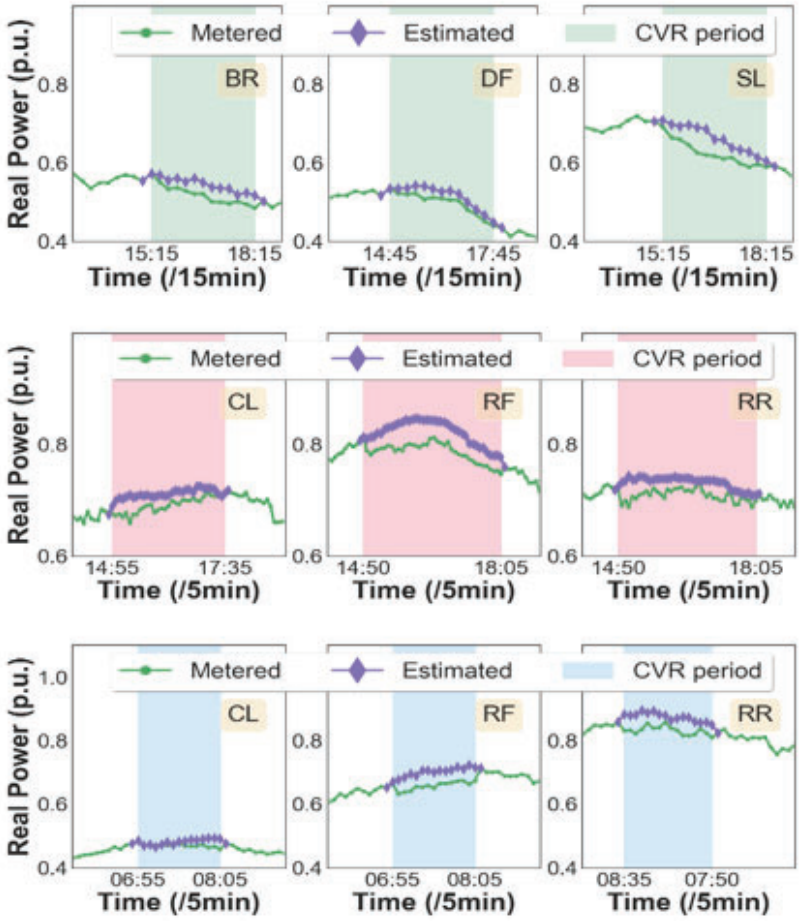

Figure 24. An illustration of the CVR baseline recovery results from three utility substations

This method is highly adaptable across different data resolutions, types, and seasonal variations, showing significant improvement in accuracy over existing models without adding considerable computational complexity. Unlike traditional methods that are either uni-directional, non-iterative, or demand large volumes of training data, IBi-GBM offers a streamlined, interpretable solution capable of capturing nonlinear load behaviors with minimal training data. Through rigorous testing on real-world datasets, IBi-GBM not only demonstrates robust performance across various conditions but also achieves a notable reduction in normalized Root Mean Square Error, thereby enhancing the accuracy and reliability of CVR performance evaluations. This innovative approach

marks a significant advancement in the field of demand response program assessment, providing utilities with a precise and efficient tool for CVR baseline estimation.

3.5.10 Load Disaggregation Tools (Appendix 9.23&24: F3&F4)

Load disaggregation is an important step for load model parameterization and for assessing demand response potentials. As shown in Figure 25, load disaggregation can be at different levels, for example, regional, feeder, and building levels. The methods can separate PV, electric vehicle charging loads, water heater loads, and the heat, ventilation and air conditioning (HVAC) loads from the total loads.

We developed two load disaggregation methods as follows:

- Method 1 (F3) utilizes an optimization-based algorithm for HVAC load disaggregation from smart meter data at various resolutions, notably without requiring detailed sub-meter data. This method's strength lies in its minimal reliance on extensive labeled datasets, employing daily temperature and load profiles alongside a base load dictionary to isolate HVAC consumption efficiently.
- Method 2 (F4) employs a Sequence-to-Point (S2P) algorithm, adept at processing low-resolution smart meter data, incorporating ambient temperature and load profiles, and utilizing transfer learning for enhanced adaptability across different locales. Demonstrating superior performance in accuracy and generalization in Austin, Texas, this method proves highly effective for dynamic response (DR) initiatives, enabling precise HVAC system utilization.

Both approaches present scalable and efficient solutions for load disaggregation, marking a considerable leap forward for utility engineers and service providers in enhancing energy consumption and operational efficiency. Evaluated using data from Pecan Street Inc. across various states, these models surpassed traditional benchmark techniques in accuracy and consistency, evidenced by reduced mean square errors and standard deviations. Moreover, they exhibited strong performance across diverse levels of customer aggregation. These methods signify a major breakthrough in the field of load disaggregation, enabling more precise customer segmentation and rate recommendation, thereby improving accuracy and broadening applicability.

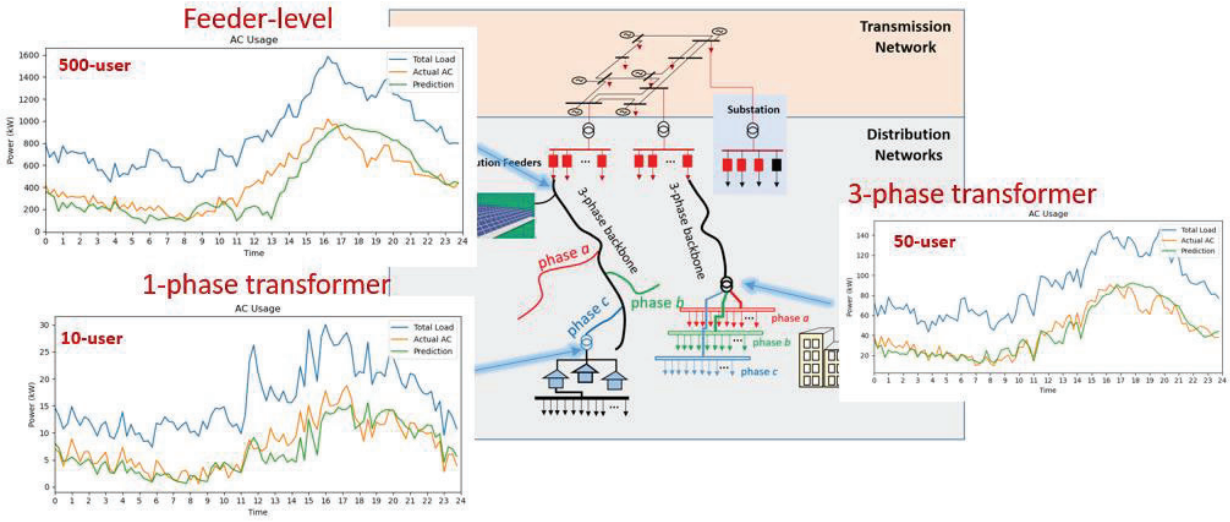

(a)

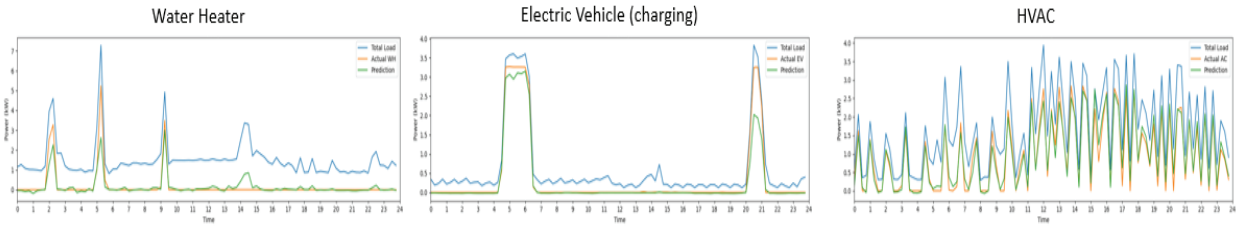

(b)

Figure 25. An illustration of the load disaggregation process (a) Load disaggregation levels, and (b) Load categories

3.5 Optimal Response Selection Tool

The optimal response Selection tool for resilience improvement using solar generation resources can be divided into two level functions: transmission and distribution level. At the transmission level, PV hybrid systems provide volt/var support and black-start functions, as shown in Figure 26. At the distribution level, PV hybrid systems provide microgrid, volt/var support, and demand response functions, as shown in Figure 27. The following subsections summarize the grid support functions developed at each levels.

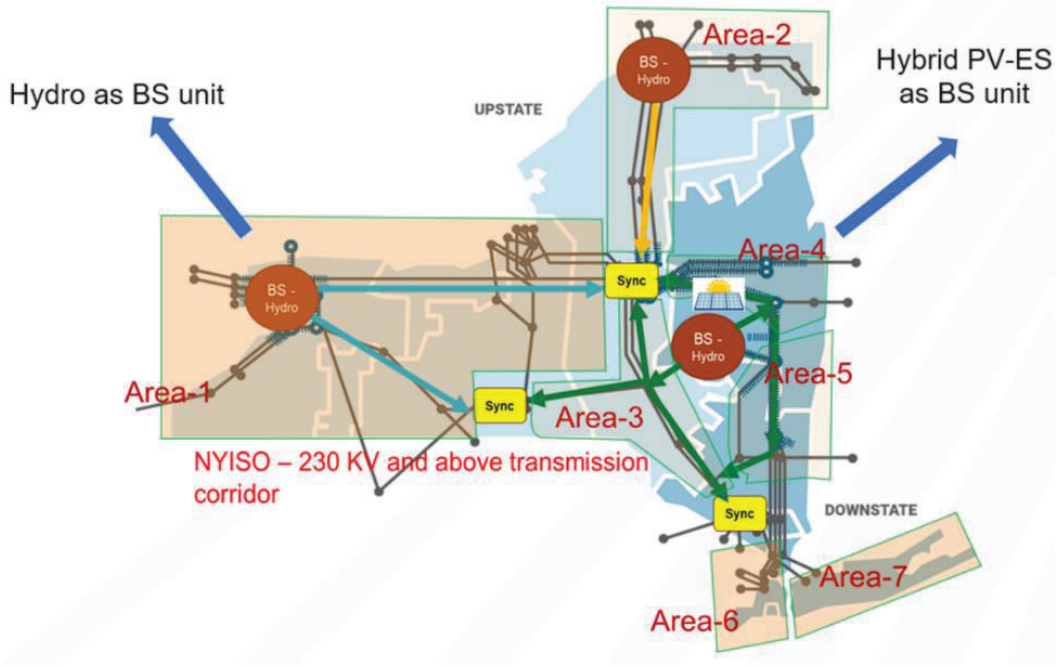

Figure 26. NYPA power system and 7 sub-areas

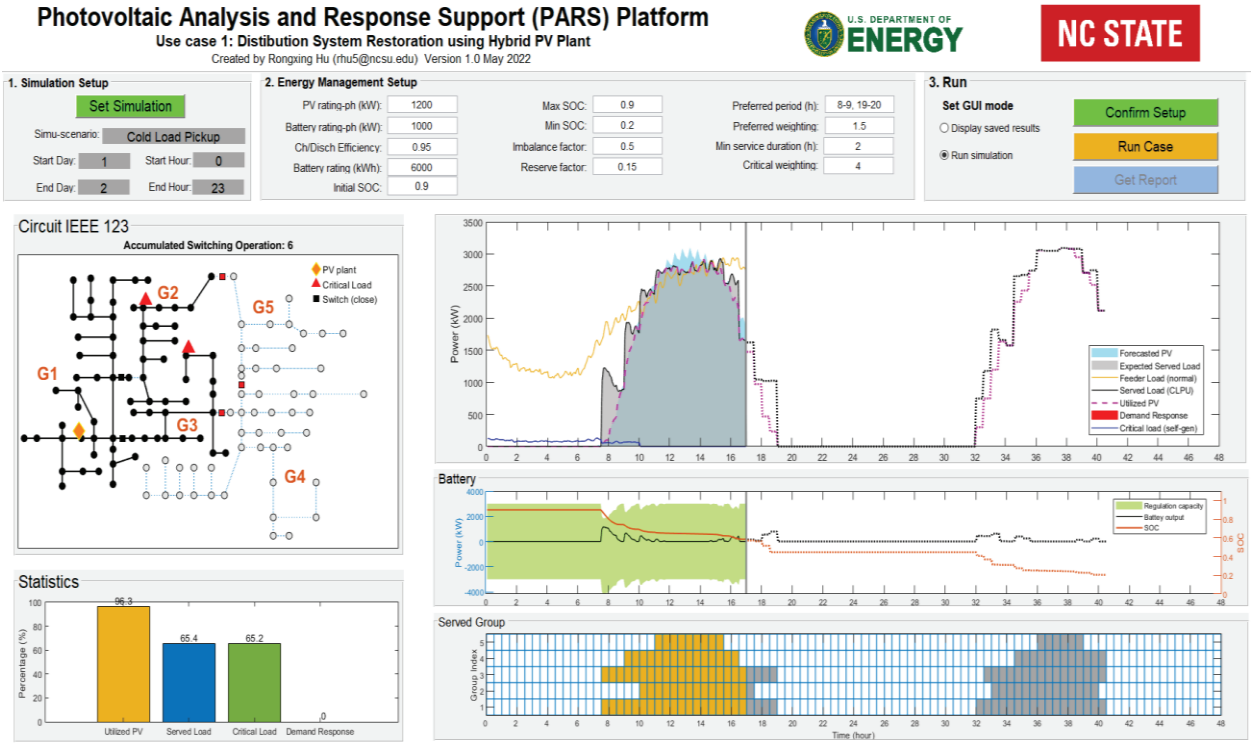

Figure 27. An illustration of the Microgrid energy management system

3.5.1 Transmission GSF 1: A Solar-assisted Voltage Optimization Method (Appendix 19.1: A1)

The voltage optimization function is developed by PNNL. A security-constrained optimal power flow (SCOPF)-based volt-var control algorithm is developed and validated using the New York Power Authority (NYPA) transmission system model and data. Aiming to stabilize voltage fluctuations under various scenarios, this method integrates solar power with minimal post-contingency adjustments across a 500-bus network, utilizing the NYPA energy management system data collected from 06/03/2014 to 09/10/2015. The two-stage volt-var SCOPF algorithm demonstrated significant effectiveness in eliminating voltage violations for both base and contingency scenarios, highlighted by a detailed comparison of bus voltage profiles and power outputs before and after algorithm application. Despite challenges in comparing with existing methods due to scale and complexity differences, the approach leverages real system topology and optimization-assisted procedures for a robust demonstration, underscoring the potential of solar resources in providing volt-var support services.

3.5.2 Transmission GSF 2: Solar-assisted Blackstart Method (Appendix 19.2: A2)

The solar-assisted black-start process are developed and demonstrated using two sub-areas of the New York Power Authority (NYPA) system on the HYPERsim electromagnetic-transient (EMT) real-time simulation test system. A hybrid solar-storage power plant with grid-forming (GFM) capability is used as a novel black-start resource alongside traditional hydro power plants. The results demonstrate the optimality of the black-start sequencing and generator dispatch. The tests also verify the stability in voltage and frequency regulation in the presence of transformer inrush currents and when long transmission lines are energized in sequence. The approach contrasts with existing methods by incorporating both ac-side and dc-side dynamics, employing industry-approved GFM control for comprehensive dynamic modeling, and demonstrating autonomous coordination between solar and storage. Despite the complexity and effort required for

implementation in HYPERsim, this method shows effective stabilization and operational feasibility of the black-start process, as evidenced by the close alignment of actual system behaviors with numerical predictions and the maintenance of system stability across multiple areas.

3.5.3 Distribution GSF 1: Feeder-level Microgrid EMS (Appendix 19.3: B1)

The function enhances feeder-level microgrid operation using utility-scale MW-level PV systems and grid-forming battery energy storage systems for improving resilience during extended outages. It contrasts existing methods by prioritizing the integration of renewable energy sources and introducing an adaptive model for cold load pickup (CLPU), addressing the shortcomings of fixed CLPU parameters that often lead to significant estimation errors. The developed energy management system (EMS) for a feeder-level microgrid incorporates an adaptive CLPU model to optimize the day-ahead energy scheduling and intra-hour power dispatch, considering the dynamic impacts of temperature and scheduled outage durations. This approach not only maximizes load service while maintaining customer comfort but also minimizes the CLPU effect more accurately than traditional models. The EMS demonstrates superior performance in energy service, critical load support, baseload maintenance, and PV utilization, significantly outperforming systems that rely on fixed or no CLPU estimation models. This advancement indicates a promising direction for microgrid resilience services, particularly in scenarios involving long-duration outages and the integration of renewable energy resources.

3.5.3 Distribution GSF 2: Community Microgrid EMS (Appendix 19.4: B2)

The function enhances community-level microgrid operation using a novel Secure and Adaptive Three-Stage Hierarchical Multi-Timescale (SA-HMTS) framework for the energy management of community microgrids (CMGs) with hybrid PV systems, aimed at enhancing power distribution resilience during prolonged outages. Unlike previous strategies, this comprehensive approach focuses on proactive scheduling and real-time dispatch of CMGs, integrating uncertainty mitigation to handle the volatility of high impact low frequency (HILF) events, and prioritizing critical loads, resource optimization, demand response, cold-load pick-up, and support expansion to neighboring grids. The framework operates across three hierarchical stages: stochastic extended duration scheduling, near-real-time scheduling, and real-time dispatch, incorporating a novel delayed recourse concept for improved decision robustness against forecast inaccuracies. Validated through OpenDSS and hardware-in-loop simulations, the SA-HMTS framework outperforms traditional deterministic, stochastic, and robust optimization methods in critical load supply, PV utilization, energy storage management, and operational duration of CMGs, showcasing its effectiveness in uncertainty-aware decision-making for community-level dynamic microgrid energy management.

3.5.4 Distribution GSF 3: EMS for Managing Mobile Battery and Rooftop PV Powered Microgrids (Appendix 19.5: B3)

The function enhances microgrid operation using a two-stage hierarchical energy management strategy tailored for managing mobile battery storage units for operating small microgrids powered by high penetration of distributed rooftop PV systems and diesel generators. This approach uses sequential rolling optimization for resource scheduling and real-time dispatch adjustments to effectively mitigate the uncertainties inherent to residential PV systems. It addresses the limitations of existing methods that fail to account for realistic operational conditions and prolonged outages, offering solutions like multi-day fuel rationing, learning-based forecast correction, and dynamic reserve management to enhance microgrid operation. Simulation results highlight the proposed scheme's superiority in improving critical and non-critical load service, PV utilization, and

minimizing disruptions during extended restoration periods, showcasing its effectiveness in overcoming significant forecast errors and leveraging limited microgrid resources under challenging conditions.

3.5.5 Distribution GSF 4: Reinforcement-Learning based Volt-var Control (Appendix 19.6: B4)

This function uses a reinforcement learning (RL)-based Volt/Var Control (VVC) strategy for regulating nodal voltages in a distribution feeder to be within the preferred operation range. A novel two-stage progressive training approach to enhance the speed and convergence of the training process. Unlike traditional rule-based and optimization-based VVC methods, which either lack adaptability or require complex computational resources and accurate network models, the proposed RL approach is highly adaptive to changing operation conditions and network topology and parameters.

As shown in Figure 28, the first stage training concentrates on teaching each PV control agent on learning under which operation condition it should generate, absorb, or take no action. In the second stage training, the learning focus shifts to collaborative training across agents to optimize the allocation of reactive power regulation responsibilities among various PV farms. This strategy not only shortens the training duration but also enhances the system's robustness and flexibility, facilitating adjustments in real-time. Simulation outcomes reveal that policies implemented in the second phase surpass traditional decentralized VVC approaches by markedly diminishing the cumulative duration of voltage violations, thus demonstrating superior voltage regulation capabilities amidst uncertainties in load demands, PV generation, and variations in network configurations or parameters. This forward-thinking method shows significant potential for efficient VVC management within power distribution networks characterized by high PV farm density.

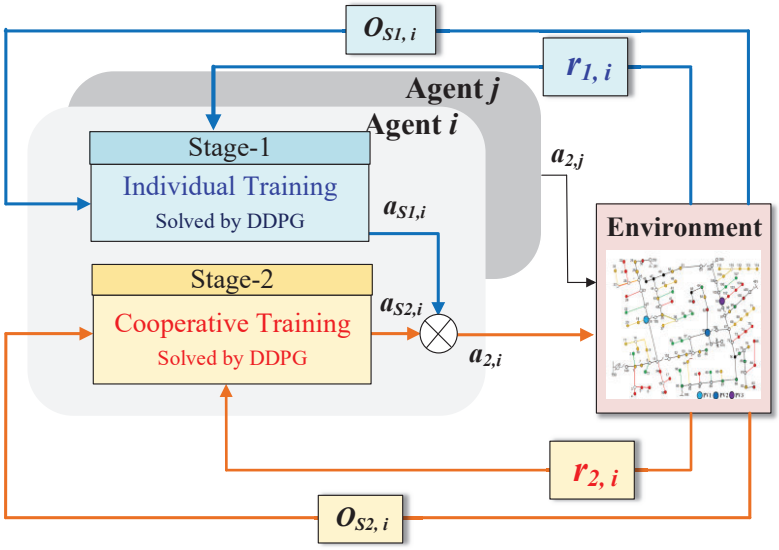

Figure 28. An illustration of the two-stage training process

3.5.6 Distribution GSF 5: Dynamic Volt-var Control (Appendix 19.7: B5)

The function introduces a dynamic VAR compensator (DVC) strategy, employing a novel two-stage hierarchical optimization and control framework to mitigate the impacts of high solar penetration on unbalanced distribution systems. By analyzing existing methods for DVC placement and control, the study identifies gaps in addressing prolonged reactive power deficiencies, system

unbalance, and the need for practical dispatch schemes capable of handling distribution system communication limitations. The proposed method emphasizes optimal DVC dispatch, placement, and control to minimize voltage variations and regulator operations, tailored for unbalanced three-phase systems. It introduces a multi-objective optimization framework and two supervisory control strategies for dynamic Volt/VAR curve adjustment, ensuring alignment with optimal reactive power trajectories. Simulation results validate the approach, showing significant improvements in voltage stability and reduction in regulator operations, particularly with a 120-minute update frequency for the Volt/VAR curve, highlighting the method's efficiency in enhancing power distribution resilience against solar-induced volatility.

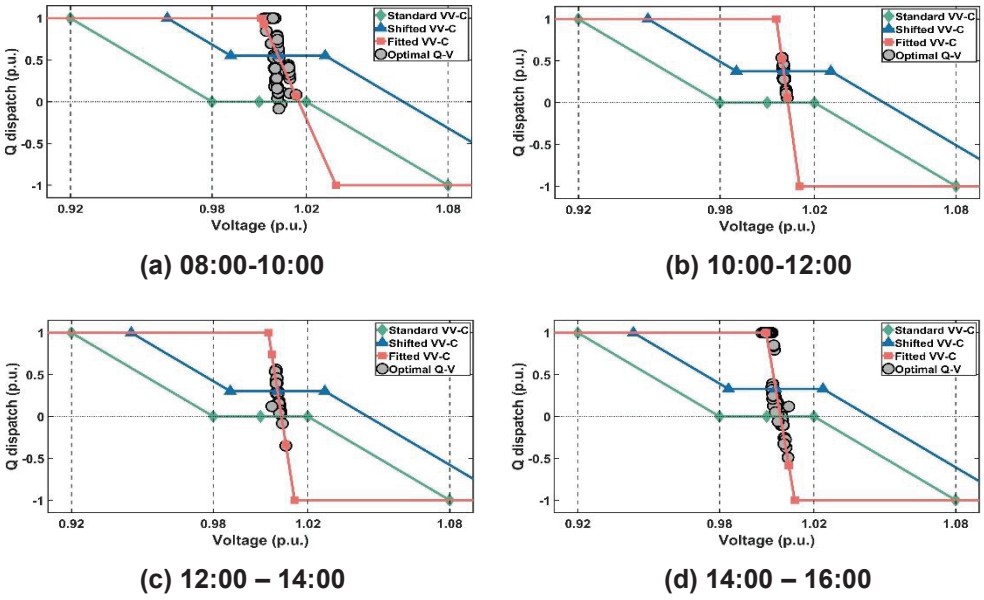

Figure 29. Optimal Q dispatch of the DVC at Phase C in winter and local control schemes.

3.5.6 Distribution GSF 6: PV Power Tracking for Providing Power Reserves and Fast Frequency Response (Appendix 19.8: D1)

The function merges a modified robust perturb-and-observe (P&O) flexible power point tracking (FPPT) technique with a real-time curve-fitting-based maximum power point estimation (MPPE) for enhanced performance in both power curtailment and MPPE within single-stage and two-stage PV system topologies. This combined approach facilitates fast tracking of power-reference changes, aiding in frequency stabilization during grid disturbances, particularly beneficial for low-inertia microgrids. As renewable energy integration into the grid increases, this method allows utility-scale PV farms to offer frequency support and maintain power reserves efficiently and cost-effectively, akin to battery-energy-storage systems. The algorithm demonstrates rapid convergence to new setpoints, significantly reducing tracking error and improving frequency response during load pickups in distribution grids. This advancement in PV power tracking presents a promising solution for managing power reserves and providing fast frequency response, showcasing superior performance in maintaining grid stability and supporting renewable energy integration.

3.5.6 Distribution GSF 6: Grid-forming Voltage Control Strategy for Supplying Unbalanced Microgrid Loads using Inverter-based Resources (Appendix 19.10: D3)

The task introduces a grid-forming (GFM) voltage control strategy tailored for battery energy storage systems, aiming to maintain balanced three-phase output voltages amidst unbalanced loads in microgrids. As shown in Figure 30, utilizing a stationary αβ reference frame for regulating positive and negative sequence voltages and incorporating a grounding transformer for zero-sequence voltage mitigation, this approach offers a sophisticated solution to voltage unbalance issues. The strategy is distinctive for its direct regulation of sequence components without decomposing them, simplifying the control process while effectively addressing unbalance. Simulation results underscore the strategy's efficacy, particularly with the αβ-based control scheme demonstrating superior dynamic performance. The use of a grounding transformer alongside a Y-Yg output transformer significantly improves the system's ability to handle unbalanced loads, maintaining Voltage Unbalance Factor (VUF) within 3% for a Power Unbalance Factor (PUF) of up to 55%, showcasing a notable advancement over traditional dq-based and αβ-based control methods in supplying balanced voltages to unbalanced microgrid loads.

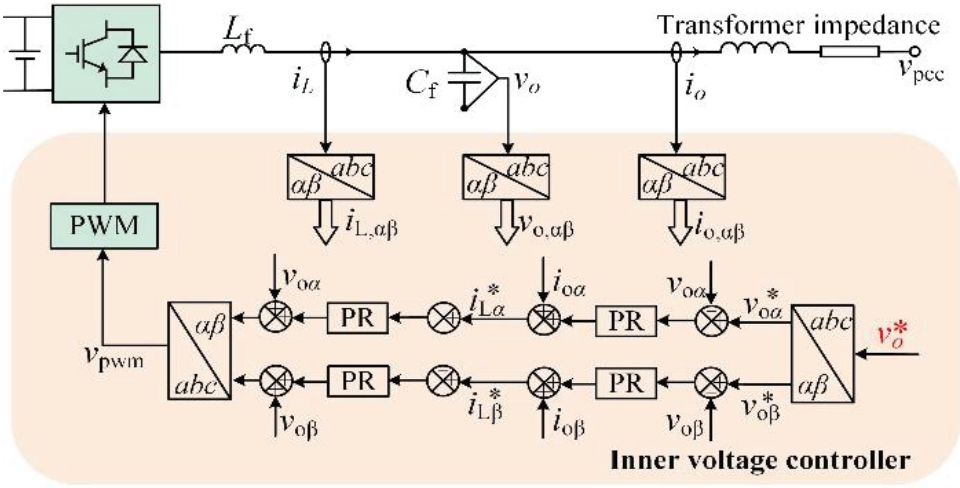

Figure 30. Control diagram of the αβ SRF-based inner voltage controller.

3.5.6 Distribution GSF 6: Under-frequency Load Shedding for Power Reserve Management in Islanded Microgrids (Appendix 19.11: D4)

The function features an innovative under-frequency load shedding (UFLS) scheme designed for islanded microgrids (MGs) with a single grid-forming (GFM) resource, aiming to manage power reserves effectively during conditions where power demand exceeds supply, triggering frequency reductions to enact load shedding at various levels. Unlike traditional UFLS methods that act as emergency measures to prevent frequency collapse, this scheme focuses on maintaining power reserve margins during normal MG operations, incorporating smart technologies like sectionalizers, smart meters, and controllable appliances for autonomous operation. This allows for efficient power reserve replenishment and mitigation of three-phase imbalances without relying on extensive communication networks. Simulation results demonstrate the scheme's capability in managing power reserves more dynamically, offering gradual, appliance-based load shedding for enhanced phase balance and sustained power output, distinguishing it significantly from conventional approaches by supporting more loads with improved three-phase voltage.

3.6 Cost Benefit Studies

Published papers have detailed the cost benefits of utilizing hybrid PV systems for frequency and voltage regulation, blackstart capabilities, and microgrid management. This report highlights several critical factors, previously under examined, that we discovered can significantly influence the outcomes of cost-benefit analyses.

Control Coordination and Communication Cost: Figure 31 shows the control architecture for using hybrid energy systems to provide aggregated transmission-level functions. Coordinating device-level controllers with system-level controllers via communication networks incurs additional costs compared to services delivered by generator units. This is attributed to the need for tens or hundreds of hybrid energy systems to match the service capacity of a single generator. However, most cost-benefit study failed to account for the cost of communication when coordinating many DERs.

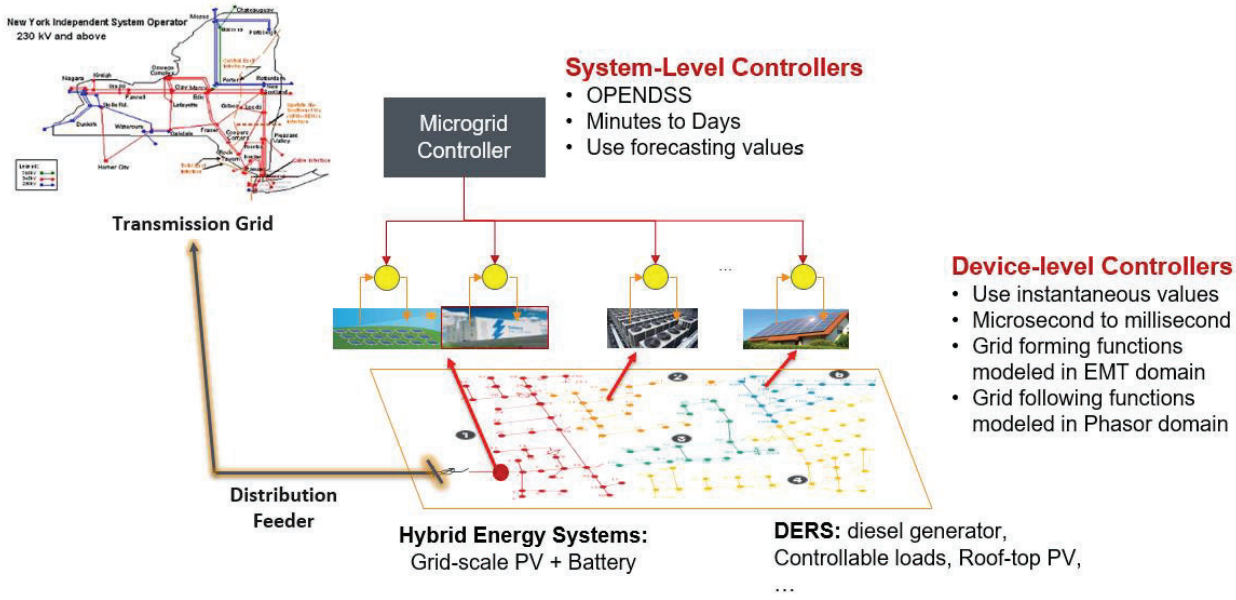

Figure 31. Control Coordination.

DER Availability Considering Fault-ride Through: In addition, the availability of hybrid energy systems can be affected by faults. We have conducted an assessment of transmission-level fault impacts on distribution DER operation (Appendix 19.12: D5). We delve into the effects of transmission-level faults on the operation of inverter-based resources (IBRs) in distribution networks, leveraging a real-time transmission and distribution (T&D) co-simulation platform. Recognizing the gap in existing research, particularly the lack of detailed analysis on the impact of such faults on high-penetration IBR systems, the study simulates symmetrical and unsymmetrical faults within an equivalent transmission network to assess their influence on distribution IBR tripping. The methodology encompasses modeling both 3-phase and 1-phase IBRs using EMT and phasor domains to accurately capture their behavior during fault conditions.

Simulation results reveal that higher power-to-load ratios tend to reduce IBR tripping by improving voltage levels along the feeder. However, point of common coupling faults notably degrade voltage, increasing IBR tripping instances. The study also finds that 3-phase IBRs are more affected by transmission-level faults than 1-phase IBRs, and unsymmetrical faults can lead

to the tripping of IBRs on non-faulty phases, causing significant power and voltage unbalance in systems with high PLRs. This analysis reveals that while the hybrid system can improve resilience, it is essential to establish robust fault response strategies. These strategies ensure that IBRs remain operational during transient faults, maintaining their availability and contributing to system stability. However, most cost-benefit study failed to account for the availabilities of IBRs when switching events occur.

Cost of Demand Response for Maintaining Power and Energy Reserves: Our study indicates that insufficient power reserves and three-phase imbalances can notably diminish the capacity of hybrid energy systems to sustain microgrid operations. Consequently, it is crucial to employ demand response strategies, including under-frequency load shedding during standard microgrid functioning, to preserve power and energy reserve margins and ensure three-phase load balance. However, most cost-benefit study when considering microgrid functions failed to account for the cost for establishing such services.

4. Significant Accomplishments and Conclusions

In the PARS project, we demonstrated the feasibility and benefits of using high-fidelity digital twins for grid support functions, offering a safer, cost-effective, and scalable alternative to traditional testing methods. We utilized machine learning-based approaches to enhance automation, efficiency, adaptability, and consistency in power system applications. This includes tasks such as load and PV forecasting, anomaly detection, model parameterization, and reinforcement learning-based DER control. Our collaboration with utilities and vendors has been instrumental in accessing the substantial real data needed for developing these tools. This includes realistic network topologies, extensive real-time operational data sets, and field validation, all of which have been crucial to our success.

Our accomplishments are summarized as follows:

- **Grid Support Functions (see Table 2 for details)**
- **Grid Intelligence**
  - Developed meta-learning based method for load forecasting model selection and TCN-based methods for enhancing forecasting large PV short-term output drops
  - Developed reinforcement learning-based volt-var control and cyber- attack strategies
  - Developed GAN-based synthetic data generation methods
  - Developed BERT, GAN, and gradient boost methods for demand response baseline identification
  - Developed a suit of load disaggregation methods using contextual based methods, vision-transformer, and GPT based generative methods.
  - Developed super-resolution methods for enhancing load profile resolutions
- **Power System Digital Twins**
  - Real-time parameterization for PV-farm digital twins
  - Co-simulation platforms for scaling up the models
  - Encoding messages to mitigate unreliable communication in enhancing reliability of grid operations and cybersecurity
  - Using synthetic data and network models to enrich modeling scenarios
- **Microgrid power management**
  - Considered reconfiguration when there are multiple grid-forming resources in one microgrids
  - Considered cold-load pickup for maintaining microgrid reserves
  - Added demand response budget for meeting cold-load pickup needs
  - Managed mobile energy storage for enhancing rooftop PV powered community microgrid
  - Microgrid hierarchical management for merging smaller microgrids into a large one or dissolve a large microgrid into a few smaller microgrids
- **Reliability and Resiliency:** Coordination with grid-forming BESS and controllable loads, the use of PV systems for blackstart, voltage regulation, precise power tracking, and microgrid operation significantly enhances the overall efficiency and reliability of distribution power system operations.

5. Path Forward

Future research directions:

- Collaborate with ElectriCities and NCEMC to integrate the machine-learning-driven data analytics tools into the existing data analytic tools used at municipal and co-op utilities.

- Create automated tools for model parameterization to streamline the development of real-time power system digital twins.
- Construct integrated Transmission and Distribution (T&D) power system digital twins and seamlessly integrate these digital twins with conventional utility operation and planning tools, thereby improving overall system efficiency and performance.

Funding generated by the PARS project:

Beyond the PARS project, we have the following ongoing synergy activities:

- Sponsored by *the National Science Foundation (NSF)* on the development of a machine learning-based model reduction method for integrated Transmission and Distribution (T&D) models.
- Sponsored by *CAPER* for IBR (Integrated Bulk and Retail) fault analysis and composite load model parameterization, enabling us to assess the impacts on distributed PV (Photovoltaic) farms.
- Sponsored by *the North Carolina University Systems* to establish a multi-university co-simulation testbed for cybersecurity analysis

Completed synergy activities as listed as follows:

- Sponsored by **GismoPower (finished in BP3).** American-Made Solar Prize, Round 5. Use the PARS platform and tools to study the impact of adopting solar panel powered EV chargers on distribution grid operation.
- Sponsored by **ElectriCities** and their municipal utility members **(BP2-BP3Q8)**
    - Utility sponsors: **New River Light&Power (NRLP) and Fayetteville PWC**
    - Transformer overloading and lifetime studies
    - Meter-phase and meter-transformer pairing studies
    - Demand response baseline derivation
    - Load disaggregation studies
    - Behind-the-meter EV and PV identification
- Sponsored by **Pacific Northwest National Lab (BP2-BP3Q4)**
    - Utility sponsors: NRLP and Fayetteville PWC
    - Goal: Benefit and potential for energy storage applications
    - Coordinative energy management for demand charge mitigation
    - Load disaggregation (identify demand response resources)
    - CVR and Demand response baseline identification
- Sponsored by **CAPER (on going)**
    - Utility sponsors: **Duke Energy and Dominion Power**
    - Project 1: Grid Observatory. Connect the PARS with utility EMS to model the distribution grid with high PV in detail (with a focus on studying fault propagation from transmission to distribution)
    - Project 2: Machine learning based load model parameterization. Integrate composite load models to PARS platform

6. Products

In this section, we highlight the significant accomplishments and explain why they are significant. The PARS sites include:

- GitHub repository for sharing data, models, and algorithms: https://github.com/SyntheticDataGenerationAndSharing/SDG_Algorithms-Data.
- PARS platform site: https://sites.google.com/a/ncsu.edu/ninglu/pars-platform?authuser=0

6.1 Major Presentations

	Links to the Presentation recordings/documents
Overviews of the PARS Platform	1. An overview of the PARS platform by Dr. Ning Lu at the MIT Seminar series 2. An Overview of the PARS Platform by Dr. Ning Lu at the DOE workshop. 3. Bigdata Seminar about the machine learning based methods used to develop the PARS platform: https://www.public.asu.edu/~kghosh10/Tutorial5/56_talk_lu_li_song.html
PNNL HIL Team	1. Quan Nguyen, 'Control & Simulation of a Grid-Forming Inverter for Hybrid PV-ES Plants in BlackStart', 21PESGM2143, 2021 IEEE PES General Meeting. 2. Quan Nguyen, 'Demonstration of Black Start On New York Power System In EMT Real-time Simulator HYPERsim', at the FREEDM seminar series., April 2022.
PARS Energy Management Systems Team	1. Energy management systems by Ashwin Shirsat, Valliappan Muthukaruppan, Rongxing Hu. at the FREEDM seminar series. 2. Rongxing Hu: MW microgrid: https://youtu.be/1kIBTnE8V24; Demo link 2: A recording of one complete run: https://youtu.be/b5sv8SozFSk 3. Valliappan Muthukaruppan: Presentation Link: https://youtu.be/Sr-OC075gZo; Demo link: https://youtu.be/I885azl3hpU 4. Ashwin Shirsat: https://youtu.be/z1D5T1R9abI
PARS HIL Team	1. Fuhong Xie: Battery Parameterization at FREEDM Tech Seminar Series 2. Victor Paduani: Maximum Power Reference Tracking Algorithm for Power Curtailment of PV Systems, 21PESGM0055 - Best paper session 3. Jiyu Wang: "A data-driven Pivot-point-based Time-series Feeder Load Disaggregation Method", 21PESGM0790
PARS Situation Awareness Team	1. FeederGan presentation: https://www.youtube.com/watch?v=r8cmSDyxIJ8. By Dr. Ming Liang at PES General meeting 2. ProfileSR-GAN: https://www.youtube.com/watch?v=nBkwTqHplh8&t=30s. By Lidong Song at the FREEDM seminar series. 3. Meta-learning based load forecasting tool. by Dr. Yiyan Li at the FREEDM seminar series.

6.2 Publications in Machine-learning and Data Analytics

The publications related with the machine learning applications are listed as follows:

1. Kai Ye, Hyeonjin Kim, Yi Hu, Ning Lu, Di Wu, and P. J. Rehm. "A Modified Sequence-to-point HVAC Load Disaggregation Algorithm." In 2023 IEEE Power & Energy Society General Meeting (PESGM), pp. 1-5. IEEE, 2023.
2. Kim, Hyeonjin, Kai Ye, Duehee Lee, and Ning Lu. "A Contextually Supervised Optimization-Based HVAC Load Disaggregation Methodology." IEEE Transactions on Smart Grid (2024).
3. Yi Hu, Yiyan Li, Lidong Song, Han Pyo Lee, PJ Rehm, Mattew Makdad, Edmond Miller, and Ning Lu, "MultiLoad-GAN: A GAN-Based Synthetic Load Group Generation Method Considering Spatial-Temporal Correlations," in IEEE Transactions on Smart Grid, vol. 15, no. 2, pp. 2309-2320, Mar. 2024, doi: 10.1109/TSG.2023.3302192. (Youtube video: https://youtu.be/DFPjr2flxwg)
4. Yiyan Li, Lidong Song, Yi Hu, Hanpyo Lee, Di Wu, PJ Rehm, Ning Lu, "Load Profile Inpainting for Missing Load Data Restoration and Baseline Estimation," in IEEE Transactions on Smart Grid, vol. 15, no. 2, pp. 2251-2260, Mar. 2024, doi: 10.1109/TSG.2023.3293188.
5. Ming Liang, Y. Meng, J. Wang, D. Lubkeman and N. Lu, "FeederGAN: Synthetic Feeder Generation via Deep Graph Adversarial Nets," in IEEE Transactions on Smart Grid, doi: 10.1109/TSG.2020.3025259.
6. Lidong Song, Yiyan Li, and Ning Lu. "ProfileSR-GAN: A GAN based Super-Resolution Method for Generating High-Resolution Load Profiles," http://arxiv.org/abs/2107.09523, Youtube video.
7. Yiyan Li, Lidong Song, Si Zhang, Laura Kraus, Taylor Adcox, Roger Willardson, Abhishek Komandur, and Ning Lu, "TCN-based Spatial-Temporal PV Forecasting Framework with Automated Detector Network Selection," submitted to IEEE Trans. Sustainable Energy. https://arxiv.org/abs/2111.08809.
8. Si Zhang, Mingzhi Zhang, Rongxing Hu, David Lubkeman, Yunan Liu, and Ning Lu, "A Two-stage Training Strategy for Reinforcement Learning based Volt-Var Control," submitted to 2022 PES General Meeting. https://arxiv.org/abs/2111.11987
9. Mingzhi Zhang, Xiangqi Zhu, and Ning Lu, "A Data-driven Probabilistic-based Flexibility Region Estimation Method for Aggregated Distributed Energy Resources," Submitted to IEEE Trans. Smart Grid. https://arxiv.org/abs/2110.07406.
10. Hanpyo Lee, Han Pyo Lee, Mingzhi Zhang,Mesut Baran, Ning Lu, PJ Rehm, Edmond Miller, Matthew Makdad P.E., "A Novel Data Segmentation Method for Data-driven Phase Identification," submitted to 2022 PES General Meeting. http://arxiv.org/abs/2111.10500
11. Hyeonjin Kim, Kai Ye, Han Pyo Lee, Rongxing Hu, Di Wu, PJ Rehm, and Ning LU, "An ICA-Based HVAC Load Disaggregation Method Using Smart Meter Data" submitted to 2023 ISGT. Available online at: https://arxiv.org/abs/2209.09165
12. Wang, Jiyu, Xiangqi Zhu, Ming Liang, Yao Meng, Andrew Kling, David L. Lubkeman, and Ning Lu. "A Data-Driven Pivot-Point-Based Time-Series Feeder Load Disaggregation Method." IEEE Transactions on Smart Grid 11, no. 6 (2020): 5396-5406.
13. Ming Liang, Jiyu Wang, Yao Meng, Ning LU, David Lubkeman, and Andrew Kling. "A Sequential Energy Disaggregation Method using Low-resolution Smart Meter Data, " Proc. of IEEE Innovative Smart Grid Technologies, Washington DC, 2019.
14. Yao Meng, Ming Liang, and Ning LU. "Design of Energy Storage Friendly Regulation Signals using Empirical Mode Decomposition," Proc. of the 2019 IEEE Power & Energy Society General Meeting, Atlanta, GA, Aug. 2019.
15. Yao Meng, Z. Yu, N. Lu and D. Shi, "Time Series Classification for Locating Forced Oscillation Sources," in IEEE Transactions on Smart Grid, vol. 12, no. 2, pp. 1712-1721, March 2021, doi: 10.1109/TSG.2020.3028188.
16. Hyeonjin Kim, Yi Hu, Kai Ye, Ning Lu. "A Novel Vision Transformer based Load Profile Analysis using Load Images as Inputs". Accepted by 2024 IEEE PES General Meeting. 24PESGM0338-T2YicBQXD.

6.3 Publications in PARS Hardware-in-the-loop Platform Development

The publications related with the HIL platform development are listed as follows:

1. X. Ke, A. Tbaileh, Q. Nguyen, T. Becejac, M. R. Vallem and N. Samaan, "A Solar-assisted Voltage Optimization Method for Transmission Solar Network Power System," *2022 IEEE Power & Energy*

Society General Meeting (PESGM), Denver, CO, USA, 2022, pp. 1-5, doi: 10.1109/PESGM48719.2022.9917048.

2. A. Tbaileh *et al*., "Optimal Power System Black start using Inverter-Based Generation," *2021 IEEE Power & Energy Society General Meeting (PESGM)*, Washington, DC, USA, 2021, pp. 1-5, doi: 10.1109/PESGM46819.2021.9638043.
3. Q. Nguyen, M. R. Vallem, B. Vyakaranam, A. Tbaileh, X. Ke and N. Samaan, "Control and Simulation of a Grid-Forming Inverter for Hybrid PV-Battery Plants in Power System Black Start," *2021 IEEE Power & Energy Society General Meeting (PESGM)*, Washington, DC, USA, 2021, pp. 1-5, doi: 10.1109/PESGM46819.2021.9637882.
4. Q. Nguyen, A. Tbaileh , Laura A. Ward, X. Ke, M. R. Vallem, B. Vyakaranam, and N. Samaan, "Real-Time Demonstration of Black-Start using a Grid-Forming Hybrid Solar-Energy Storage Power Plant," *IEEE Transaction on Industrial Applications (in preparation)*.
5. Q. Long, H. Yu, F. Xie, N. Lu and D. Lubkeman, "Diesel Generator Model Parameterization for Microgrid Simulation Using Hybrid Box-Constrained Levenberg-Marquardt Algorithm," in IEEE Transactions on Smart Grid, doi: 10.1109/TSG.2020.3026617.
6. F. Xie, H. Yu, Q. Long, W. Zeng and N. Lu, "Battery Model Parameterization Using Manufacturer Datasheet and Field Measurement for Real-Time HIL Applications," in IEEE Transactions on Smart Grid, vol. 11, no. 3, pp. 2396-2406, May 2020, doi: 10.1109/TSG.2019.2953718.
7. F. Xie, C. McEntee, M. Zhang, B. Mather and N. Lu, "Development of an Encoding Method on a Co-Simulation Platform for Mitigating the Impact of Unreliable Communication," in IEEE Transactions on Smart Grid, vol. 12, no. 3, pp. 2496-2507, May 2021, doi: 10.1109/TSG.2020.3039949. Videos related with the paper: https://www.youtube.com/watch?v=SdibDKEpw60
8. F. Xie et al., "Networked HIL Simulation System for Modeling Large-scale Power Systems," 2020 52nd North American Power Symposium (NAPS), 2021, pp. 1-6, doi: 10.1109/NAPS50074.2021.9449646.
9. F. Xie, C. McEntee, M. Zhang and N. Lu, "An Asynchronous Real-time Co-simulation Platform for Modeling Interaction between Microgrids and Power Distribution Systems," Proc. of 2019 IEEE Power & Energy Society General Meeting (PESGM), Atlanta, GA, USA, 2019, pp. 1-5, doi: 10.1109/PESGM40551.2019.8973802.
10. Victor Paduani, Bei Xu, David Lubkeman, Ning Lu, “Novel Real-Time EMT-TS Modeling Architecture for Feeder Blackstart Simulations,” submitted to 2022 IEEE PESGM. https://arxiv.org/pdf/2111.10031.pdf
11. Victor Paduani, Lidong Song, Bei Xu, Dr. Ning Lu, "Maximum Power Reference Tracking Algorithm for Power Curtailment of Photovoltaic Systems", Proc. of IEEE PES 2021 General Meeting. 2021. arXiv preprint arXiv:2011.09555.
12. Bei Xu, Victor Paduani, David Lubkeman, and Ning Lu, “A Novel Grid-forming Voltage Control Strategy for Supplying Unbalanced Microgrid Loads Using Inverter-based Resources,” submitted to 2022 PES General meeting. https://arxiv.org/pdf/2111.09464.pdf
13. Long Qian, Hui Yu, Fuhong Xie, Wenti Zeng, Srdjan Lukic, Ning Lu, and David Lubkeman., "Microgrid Power Flow Control with Integrated Battery Management Functions," Proc. of 2020 IEEE Power & Energy Society General Meeting (PESGM), Montreal, QC, 2020, pp. 1-5, doi: 10.1109/PESGM41954.2020.9281437.
14. Nguyen, Quan, Jim Ogle, Xiaoyuan Fan, Xinda Ke, Mallikarjuna R. Vallem, Nader Samaan, and Ning Lu. "EMS and DMS Integration of the Coordinative Real-time Sub-Transmission Volt-Var Control Tool under High DER Penetration." arXiv preprint arXiv:2103.10511 (2021).
15. Qi Xiao, et al., "Assessment of Transmission-level Fault Impacts on 3-phase and 1-phase Distribution IBR Operation," Accepted by 2024 IEEE PES General Meeting, Available online: https://arxiv.org/abs/2311.11339. 24PESGM1188-ZZQ781QL7

6.4 Publications in Power and Energy Management Algorithms

The publications related with the power and energy management algorithms are listed as follows:

1. Wu, Di, Xu Ma, Tao Fu, Zhangshuan Hou, P. J. Rehm, and Ning Lu. "Design of a Battery Energy Management System for Capacity Charge Reduction." IEEE Open Access Journal of Power and Energy 9 (2022): 351-360.
2. Han Pyo Lee, Keith DSouza, Ke Chen, Ning Lu, and Mesut Baran, "Adopting Dynamic VAR Compensators to Mitigate PV Impacts on Unbalanced Distribution Systems," submitted to IEEE Access (2023). Accepted. Available online at: Available online at: http://arxiv.org/abs/2309.06098
3. Shirsat, Ashwin, Valliappan Muthukaruppan, Rongxing Hu, Victor Paduani, Bei Xu, Lidong Song, Yiyan Li et al. "A Secure and Adaptive Hierarchical Multi-timescale Framework for Resilient Load Restoration Using a Community Microgrid." IEEE Transactions on Sustainable Energy (2023).
4. Rongxing Hu, Ashwin Shirsat, Valliappan Muthukaruppan, Wenyuan Tang, Mesut Baran, Ning Lu. "Adaptive Cold-Load Pickup Considerations in 2-Stage Microgrid Unit Commitment for Enhancing Microgrid Resilience ." submitted to Applied Energy. Available online at:
5. Lu, Ning. "Load Control: A new era of intelligent automation." IEEE Electrification Magazine 9, no. 3 (2021): 18-28.
6. Si Zhang, Mingzhi Zhang, Rongxing Hu, David Lubkeman, Yunan Liu, and Ning Lu, "A Two-stage Training Strategy for Reinforcement Learning based Volt-Var Control," 22PESGM3454, Proc. of 2022 PES General Meeting. http://arxiv.org/abs/2111.11987
7. Rongxing Hu, Yiyan Li, Si zhang, Valliappan Muthukaruppan, Ashwin Shirsat, Mesut Baran, Wenyuan Tang, David Lubkeman, Ning Lu, "A Load Switching Group based Feeder-level Microgrid Energy Management Algorithm for Service Restoration in Power Distribution System", Proc. of IEEE PES 2021 General Meeting. 2021. Available online at:https://arxiv.org/abs/2011.08735
8. Ashwin Shirsat, Valliappan Muthukaruppan, Rongxing Hu, Ning Lu, Mesut Baran, David Lubkeman, Wenyuan Tang, "Hierarchical Multi-timescale Framework for Operation of Dynamic Community Microgrid", Proc. of IEEE PES 2021 General Meeting. 2021. https://arxiv.org/abs/2011.10087
9. V. Muthukaruppan, A. Shirsat, et. al., "Feeder Microgrid Management on an Active Distribution System during a Severe Outage", submitted to IEEE Trans. on Power System, 2022 (available: arXiv:2208.10712).
10. J. Wang, S. Huang, D. Wu and N. Lu, "Operating a Commercial Building HVAC Load as a Virtual Battery Through Airflow Control," in IEEE Transactions on Sustainable Energy, vol. 12, no. 1, pp. 158-168, Jan. 2021, doi: 10.1109/TSTE.2020.2988513.
11. Nguyen, Quan, Jim Ogle, Xiaoyuan Fan, Xinda Ke, Mallikarjuna R. Vallem, Nader Samaan, and Ning Lu. "EMS and DMS Integration of the Coordinative Real-time Sub-Transmission Volt-Var Control Tool under High DER Penetration." arXiv preprint arXiv:2103.10511 (2021).
12. C. McEntee, D. Mulcahy, J. Wang, X. Zhu and N. Lu, "A VSM-Based DER Dispatch MINLP for Volt-VAR Control in Unbalanced Power Distribution Systems," Proc. of 2019 IEEE Power & Energy Society General Meeting (PESGM), 2019, pp. 1-5, doi: 10.1109/PESGM40551.2019.8973721
13. Asmaa Alrushoud, Catie McEntee, and Ning Lu, "A Zonal Volt/VAR Control Mechanism for High PV Penetration Distribution Systems", Proc. of IEEE PES 2021 General Meeting. 2021. Available online at: https://arxiv.org/abs/2101.00106.
14. Rongxing Hu, Kai Ye, Hyeonjin Kim, Hanpyo Lee, Di Wu, P.J. Rehm, Ning Lu "Coordinative Demand Charge Mitigation Strategies," Proc. of 2023 IEEE PES General Meeting, Available online at: https://arxiv.org/abs/2212.08535. 23PESGM1367
15. Han Pyo Lee, Keith DSouza, Ke Chen, Ning Lu, and Mesut Baran, "Adopting Dynamic VAR Compensators to Mitigate PV Impacts on Unbalanced Distribution Systems," submitted to IEEE Access (2023). Accepted. Available online at: Available online at: http://arxiv.org/abs/2309.06098
16. Han Pyo Lee, Lidong Song, Yiyan Li, Ning Lu, Di Wu, PJ Rehm, Matthew Makdad, Edmond Miller, "An Iterative Bidirectional Gradient Boosting Algorithm for CVR Baseline Estimation" 23PESGM0022, Proc. of 2023 IEEE PES General Meeting, Available online at: http://arxiv.org/abs/2211.03733. 23PESGM0022.

7. Project Team and Roles:

Table 1: Lead Institute: North Carolina State University Participants

Name	Role	Contribution
Ning Lu	PI	Manage the overall project and modeling team
David Lubkeman	Co-PI	Manage the HIL team
Mesut Baran	Co-PI	Supervise PhD students for EMS algorithm development
Wenyuan Tang	Co-PI	Supervise PhD students for EMS algorithm development
Srdjan Lukic	Co-PI	Supervise PhD students for HIL testbed development

Table 2: North Carolina State University Student Participants
GRA: Graduate research assistant; URA: undergraduate research assistant

Name		Start Date	End Date	Role	Contribution
Students in the HIL Team					
Jongha Woo	PhD	Fall 2022	Fall 2023	GRA	PV parameterization
Charles Kelly	PhD	Fall 2021	Fall 2023	GRA	PV modeling
Qi Xiao	PhD	Fall 2021	Fall 2023	GRA	Feed Reduction and Cyber attack
Lidong Song	PhD	Spring 2020	Fall 2022	GRA	Super resolution and Cyber attack
Bei Xu	PhD	Spring 2020	Fall 2023	GRA	Battery modeling
Victor Paduani	PhD	Fall 2020	Spr. 2022	GRA	PV farm GSF development
Fuhong Xie	PhD	Spring 2020	Fall 2020	GRA	Battery GSF development
Long Qian	PhD	Spring 2020	Fall 2020	GRA	Diesel generator GSF
Hui Yu	PhD	Spring 2020	Fall 2020	GRA	Battery GSF development
Students in the Modeling Team					
Rongxing Hu	PhD	Spring 2020	Fall 2023	GRA	Feeder-level microgrid EMS
Ashwin Shirsat	PhD	Spring 2020	Fall 2022	GRA	Community microgrid EMS
Valliappan Muthukaruppan	PhD	Spring 2020	Fall 2022	GRA	Mobile storage EMS
Asmaa Alrushoud	PhD	Fall 2020	Fall 2021	GRA	Volt/var control
Jiyu Wang	PhD	Spring 2020	Spr. 2020	GRA	Load disaggregation
Postdoc/Students in the SA Team					
Yiyan Li	**Post doc**	Spring 2020	Fall 2022	GRA	Load and PV forecasting Synthetic Data generation
Si Zhang	PhD	Spring 2020	Spr. 2023	GRA	RL-based Volt/var control
Hanpyo Lee	PhD	Spring 2020	Fall 2023	GRA	Smart meter analysis CVR baseline detection
Yi HU	PhD	Fall 2021	Fall 2023	GRA	Synthetic generation DR baseline detection
Kai Ye	PhD	Spr. 2021	Fall 2023	GRA	Load disaggregation and behind-the-meter DER Detection
Hyeonjin Kim	PhD	Fall 2021	Fall 2023	GRA	
Master/Under graduate students					
Ignacio Aguilar	BS	Spring 2023		URA	PV modeling
Jakob Triemstra	BS	Spring 2023		URA	PV modeling
Charlie Averett	BS	Summer 2021		URA	PV forecasting
Luna Zhu	BS	Summer	Spr. 2021	URA	PV forecasting
Eli Hubble	BS	Spr. 2020	Spr. 2020	URA	PV forecasting
Issac Little	MS	Summer 2021		GRA	PV forecasting
Jacob Triemstra	BS	Spring 2023	Fall 2023	URA	PV forecasting

Table 3: Collaboration Organization 1: Pacific Northwest National Lab (requested DOE funding)

Name	Role	Contribution
Xinda Ke	team lead	Steady state optimization model development for volt-var control function, project management
Quan Nguyen	participant	Demonstration of black start in two sub-areas of NYPA system in OPAL-RT Hyper-SIM model
Ahmad Tbaileh	participant	Steady state optimization based black start path model development
Mallikarjuna Vallem	participant	Project management, Opal-RT Ephasor-Sim model development, industry outreach, technical support
Samaan, Nader A	advisor	Advisor of the project
Tamara Becejac	participant	Explore the NYPA system in Opal-RT Hyper-sim model
Laura A. Ward	participant	Demonstration of black start in two sub-areas of NYPA system in OPAL-RT Hyper-SIM model

Table 4: Collaboration Organization 2: Industry Teams and Advisors (in-kind cost-share)

Name	Company	Contribution
Xia Jiang	NYPA	Provided NYPA blackstart procedure and network models. Provide technical support for developing the PV farm models and verify performance of the volt/var control scheme and the black start sequences using PV farm as a major black start resource.
George Stefopoulos		
Victor Paduani		
PJ Rehm	ElectriCities	Coordinating with municipal utilities and provide data support. Disseminate results to municipal utilities.
Andy Fusco		
Greg Flinn		
Laura Kraus	Strata Solar	Providing 1-second PV farm data for parameterizing PV farm digital twin models and anomaly detection. Provided 100 PV farm data for short term PV large power drop forecast.
Roger Willardson		
Keary Dosier		
Taylor Adcox		
Abhishek Komandur		
Roger Willardson		
Matt Makdad	New River	Providing SCDA, smart meter data for CVR performance assessment and behind the meter PV and EV and identification
Edmond Miller		
Timothy Stankiewicz	Fayetteville PWC	Providing SCDA data for CVR and demand response program performance assessment and baseline derivation
Marshall Cherry	Roanoke Electric Co-op	Industry advisor
Daniel Gillen	Wilson Energy	Providing smart meter (residential, commercial, and industrial loads) and PV data for synthetic data generation and digital twin parameterization
Paul Darden		

8. Reference

1. Plumier, Frédéric, et al. "Co-simulation of electromagnetic transients and phasor models: A relaxation approach." IEEE Transactions on Power Delivery 31.5 (2016): 2360-2369.
2. Palmintier, Bryan, et al. "Design of the HELICS highperformance transmission-distribution-communication-market co-simulation framework." Proc. 2017 Workshop on Modeling and Simulation of Cyber-Physical Energy Systems, Pittsburgh, PA. 2017.
3. Godfrey, Tim, et al. "Modeling smart grid applications with cosimulation.“ Smart Grid Communications (SmartGridComm), 2010 First IEEE International Conference on. IEEE, 2010.
4. Godfrey, Tim, et al. "Modeling smart grid applications with cosimulation.“ Smart Grid Communications (SmartGridComm), 2010 First IEEE International Conference on. IEEE, 2010.
5. Palmintier, Bryan, et al. "A power hardware-in-the-loop platform with remote distribution circuit cosimulation." IEEE Transactions on Industrial Electronics 62.4 (2015): 2236-2245.
6. F. Xie, H. Yu, Q. Long, W. Zeng and N. Lu, "Battery Model Parameterization Using Manufacturer Datasheet and Field Measurement for Real-Time HIL Applications," in IEEE Transactions on Smart Grid, vol. 11, no. 3, pp. 2396-2406, May 2020, doi: 10.1109/TSG.2019.2953718.
7. F. Xie, C. McEntee, M. Zhang, B. Mather and N. Lu, "Development of an Encoding Method on a Co-Simulation Platform for Mitigating the Impact of Unreliable Communication," in IEEE Transactions on Smart Grid, vol. 12, no. 3, pp. 2496-2507, May 2021, doi: 10.1109/TSG.2020.3039949. Videos related with the paper: https://www.youtube.com/watch?v=SdibDKEpw60.
8. F. Xie et al., "Networked HIL Simulation System for Modeling Large-scale Power Systems," 2020 52nd North American Power Symposium (NAPS), 2021, pp. 1-6, doi: 10.1109/NAPS50074.2021.9449646.
9. Bei Xu, Victor Paduani, David Lubkeman, and Ning Lu, “A Novel Grid-forming Voltage Control Strategy for Supplying Unbalanced Microgrid Loads Using Inverter-based Resources,” 22PESGM1399, submitted to 2022 PES General meeting. Available online at: https://arxiv.org/pdf/2111.09464.pdf
10. Victor Paduani, Bei Xu, David Lubkeman, Ning Lu, “Novel Real-Time EMT-TS Modeling Architecture for Feeder Blackstart Simulations,” 22PESGM1449, submitted to 2022 IEEE PESGM. Available online at: https://arxiv.org/pdf/2111.10031.pdf
11. Victor Paduani, Qi Xiao, Bei Xu, David Lubkeman, and Ning Lu. "Optimal Control Design for Operating a Hybrid PV Plant with Robust Power Reserves for Fast Frequency Regulation Services", submitted to IEEE Transactions on power systems. https://arxiv.org/abs/2212.03803 A
12. Bei Xu, Victor Daldegan Paduani, Qi Xiao, Lidong Song, David Lubkeman, and Ning Lu. "Under-frequency Load Shedding for Power Reserve Management in Islanded Microgrids", https://arxiv.org/abs/2309.01278v2
13. Sun, Tiankui, Jian Lu, Zhimin Li, David Lubkeman, and Ning Lu. "Modeling Combined Heat and Power Systems for Microgrid Applications." IEEE Transactions on Smart Grid, Jan. 2017.
14. Q. Long, H. Yu, F. Xie, N. Lu and D. Lubkeman, "Diesel Generator Model Parameterization for Microgrid Simulation Using Hybrid Box-Constrained Levenberg-

Marquardt Algorithm," in IEEE Transactions on Smart Grid, doi: 10.1109/TSG.2020.3026617.
15. Wang, Jiyu, Xiangqi Zhu, Ming Liang, Yao Meng, Andrew Kling, David L. Lubkeman, and Ning Lu, A Data-Driven Pivot-Point-Based Time-Series Feeder Load Disaggregation Method., IEEE Transactions on Smart Grid.
16. S. Gallardo-Saaverdra, and B. Karlsson, "Simulation, validation and analysis of shading effects on a PV system," Solar Energy, vol. 170, pp. 820-39, Aug. 2018.
17. R. Ahmad, A. F. Murtaza, H. A. Sher, U. T. Shami, and S. Olalekan, "An analytical approach to study partial shading effects on PV array supported by literature," Renewable and Sustainable Energy Reviews, vol. 74, pp.721-32, Jul. 2017.
18. C. Saiprakash, A. Mohapatra, B. Nayak, and S. R. Ghatak, "Analysis of partial shading effect on energy output of different solar PV array configurations," Materials Today: Proceedings, vol. 39, no. 5, pp.1905-09, 2021.
19. D. Yousri, T. S. Babu, E. Beshr, M. B. Eteiba, and D. Allam, "A Robust Strategy Based on Marine Predators Algorithm for Large Scale Photovoltaic Array Reconfiguration to Mitigate the Partial Shading Effect on the Performance of PV System," IEEE ACCESS, vol. 8, pp. 112407-26, Jun. 2020.
20. M. J. Hossain, T. K. Saha, N. Mithulananthan, and H. R. Pota, "Robust control strategy for PV system integration in distribution systems," Applied Energy, vol. 99, pp. 355-62, Nov. 2012.
21. T. Stetz, F. Marten, and M. Braun, "Improved Low Voltage Grid-Integration of Photovoltaic Systems in Germany," IEEE Transactions on Sustainable Energy, vol. 4, no. 2, pp. 534-42 Apr. 2013.
22. Yiyan Li, Lidong Song, Si Zhang, Laura Kraus, Taylor Adcox, Roger Willardson, Abhishek Komandur, and Ning Lu, “TCN-based Spatial-Temporal PV Forecasting Framework with Automated Detector Network Selection,” submitted to IEEE Trans. Sustainable Energy. https://arxiv.org/abs/2111.08809.
23. Li, Yiyan, Si Zhang, Rongxing Hu, and Ning Lu. "A meta-learning based distribution system load forecasting model selection framework." Applied Energy 294 (2021): 116991.
24. Lidong Song, Yiyan Li, and Ning Lu. "ProfileSR-GAN: A GAN based Super-Resolution Method for Generating High-Resolution Load Profiles," http://arxiv.org/abs/2107.09523, Youtube video.
25. Yi Hu, Yiyan Li, Lidong Song, Han Pyo Lee, PJ Rehm, Matthew Makdad, Edmond Miller, and Ning Lu, "MultiLoad-GAN: A GAN-Based Synthetic Load Group Generation Method Considering Spatial-Temporal Correlations," accepted by IEEE Transactions on Smart Grid (2022). Available online at: https://arxiv.org/abs/2210.01167. Github code sharing: https://github.com/SyntheticDataGenerationAndSharing/SDG_Algorithms-Data
26. Ming Liang, Y. Meng, J. Wang, D. Lubkeman and N. Lu, "FeederGAN: Synthetic Feeder Generation via Deep Graph Adversarial Nets," in IEEE Transactions on Smart Grid, doi: 10.1109/TSG.2020.3025259.
27. Han Pyo Lee, Lidong Song, Yiyan Li, Ning Lu, Di Wu, PJ Rehm, Matthew Makdad, Edmond Miller, "An Iterative Bidirectional Gradient Boosting Algorithm for CVR Baseline Estimation" 23PESGM0022, Proc. of 2023 IEEE PES General Meeting, Available online at: http://arxiv.org/abs/2211.03733. 23PESGM0022
28. Kai Ye, Hyeonjin Kim, Di Wu, PJ Rehm, and Ning Lu, "A Modified Sequence-to-point HVAC Load Disaggregation Algorithm," Proc. of 2023 IEEE PES General Meeting, Available online at: https://arxiv.org/abs/2212.04886. 23PESGM1248

29. Hyeonjin Kim, Kai Ye, Han Pyo Lee, Rongxing Hu, Di Wu, PJ Rehm, and Ning LU, “An ICA-Based HVAC Load Disaggregation Method Using Smart Meter Data” submitted to 2023 ISGT. Available online at: https://arxiv.org/abs/2209.09165
30. Wang, Jiyu, Xiangqi Zhu, Ming Liang, Yao Meng, Andrew Kling, David L. Lubkeman, and Ning Lu. "A Data-Driven Pivot-Point-Based Time-Series Feeder Load Disaggregation Method." IEEE Transactions on Smart Grid 11, no. 6 (2020): 5396-5406.
31. Ming Liang, Jiyu Wang, Yao Meng, Ning LU, David Lubkeman, and Andrew Kling. "A Sequential Energy Disaggregation Method using Low-resolution Smart Meter Data, " Proc. of IEEE Innovative Smart Grid Technologies, Washington DC, 2019.
32. Li, Yiyan, Lidong Song, Yi Hu, Hanpyo Lee, Di Wu, P. J. Rehm, and Ning Lu. "Load Profile Inpainting for Missing Load Data Restoration and Baseline Estimation." accepted by IEEE Transactions on Smart Grid. arXiv preprint arXiv:2211.16332 (2022). Github code sharing: https://github.com/SyntheticDataGenerationAndSharing/SDG_Algorithms-Data
33. Hu, Yi, Kai Ye, Hyeonjin Kim, and Ning Lu. "BERT-PIN: A BERT-based Framework for Recovering Missing Data Segments in Time-series Load Profiles." arXiv preprint arXiv:2310.17742 (2023).

9. Appendix

9.1 Task A.1 Transmission GSF 1: Demonstration of a Solar-assisted Voltage Optimization Method in NYPA Transmission System by PNNL

Background: This task aims to demonstrate and validate a security-constrained optimal power flow (SCOPF)-based volt-var control algorithm within the New York Power Authority (NYPA) transmission system. The objective is to enhance the stability of voltage fluctuations in transmission networks under both base case and contingency scenarios. This is achieved by integrating a bulk solar power plant with a minimal number of post-contingency corrections in a 500-bus NYPA network. The algorithm utilizes EMS data spanning from 06/03/2014 to 09/10/2015 from NYPA as inputs. Simulation results indicate that the proposed two-stage volt-var ACOPF algorithm effectively eliminates voltage violations in both base case and contingency scenarios.

TABLE I: Comparison of the Developed Volt/Var control Algorithm and Existing Related Works

	Advantages	Disadvantages
[1]-[5]	- Focus on security-constrained optimal power flow (SCOPF) based volt-var control algorithm with significantly reduced problem scale	- Cannot remove every volt-var violations from all N-1 contingency scenarios
[3]-[5]	- Use the preventive security-constrained optimal power flow (PSCOPF) problems to handle volt-var violations for all contingency scenarios	- Very large-scale power flow problems and are hard to solve directly
[6]	- Use the corrective security constraint optimal power flow (CSCOPF) to handle volt-var violations for all contingency scenarios	- The model requires additional decision variables and solution actions with respect to different contingency scenarios
[8]	- Use GFM-based wind for black start	- Do not focus on a full sequence of black-start process - Focus on wind instead of solar and storage as generation resources
[9]-[10]	- Use GFM inverters as black start unit - Conduct a real-time simulation with multiple steps with autonomous actions of circuit breakers	- Do not model the dc-side dynamics
Approach developed by PNNL [11, 12]	- Use real system topology and parameters and optimization-assisted black-start procedure - Full demonstration with 25 steps in Area 1 and 17 steps in Area 4. - Detailed dynamic model at the dc side and autonomous coordination between solar and storage - Use the only industry-approved GFM control model with current limiting and P-Q capability limit	- The demonstration and control implementation in HYPERsim requires greater effort compared other EMT simulation tools

Task Objectives:

- Develop the equivalent NYISO power flow cases from the NYPA EMS state estimator data.
- Run contingency analysis for major contingencies. Identify voltage violations. Baseline will be obtained.
- Apply the proposed Preventive volt/var control algorithms to reduce voltage violations.

Methodology Overview: The probability density function representing the voltage magnitude extracted from the NYISO system over a span of 15 months is depicted in Fig. 1 below. On the x-axis, the voltage magnitude is presented in per unit (p.u.), while the y-axis illustrates the probability of various voltage magnitudes throughout the entire year's dataset. The figure reveals that, for the majority of the time, the voltages in the NYISO area range between 0.9 and 1.1 p.u. Nonetheless, there are instances where the system experiences both under-voltage and over-voltage issues.

Simulation Results: The proposed volt-var ACOPF voltage control algorithm was implemented in the NYPA for a full day, and the simulation results are compared for the following two cases:

- Case 1: Base case with no control on solar inverter
- Case 2: Proposed volt-var ACOPF algorithm.

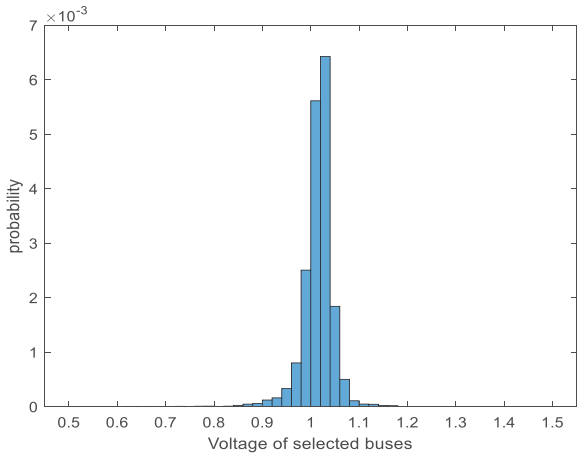

Figure 1. Probability density function of voltage magnitude in NYISO area.

Figure 2(a) illustrates the bus voltage comparison between Case 1 and Case 2, specifically focusing on the selected solar bus 782 during a 1-day simulation period (24 hours) on 7/25/2014. Noticeable under-voltage issues can be seen at the selected bus 782 after 3 p.m., coinciding with a decrease in system load. In contrast, the volt/var ACOPF algorithm maintains the voltage level within its scheduled range of 0.95 p.u to 1.05 p.u, showcasing the effectiveness of the proposed algorithm. Figure 2(b) presents the real and reactive power output of the utility-scale PV plant at bus 782. The reactive power output of each solar unit is constrained by the apparent power limits of the solar inverter. Additionally, the solar units actively generate reactive power for the grid, particularly post 3 p.m., contributing to volt-var support services. These results underscore the effective utilization of solar resources for providing volt-var support services.

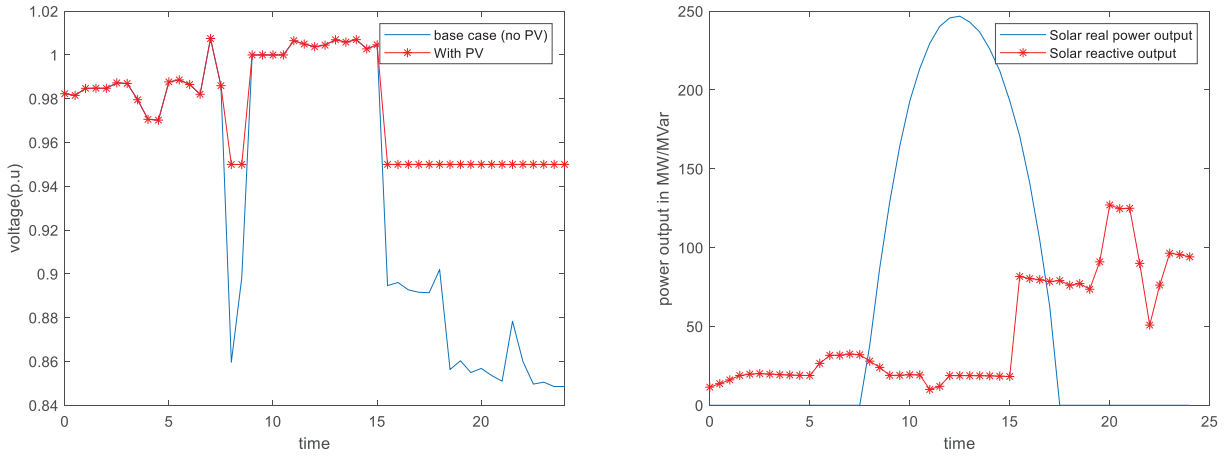

Figure 2. (a) Comparison of voltage profile on a selected solar bus 782. (b)The power output of utility-scale PV plant located at bus 782.

Figure 3 illustrates the cumulative comparison of bus voltage violations in p.u. between Case 2 and Case 3 across all contingency scenarios during a 1-day simulation period (24 hours). As depicted in Fig. 3, the second stage security constraint volt/var ACOPF effectively eradicates all voltage violations in contingency scenarios. This affirms that the proposed two-stage volt-var ACOPF algorithm is capable of eliminating voltage violations in both base case and contingency scenarios.

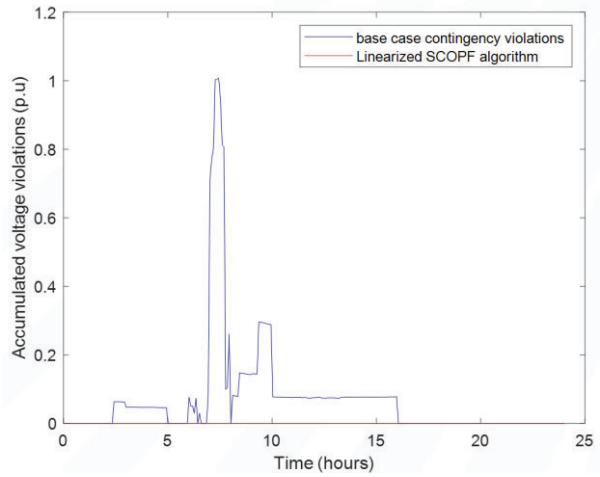

Figure 3. Comparison of accumulated voltage violations on all contingency cases.

References

[1] X. Ke, A. Tbaileh, Q. Nguyen, T. Becejac, M. R. Vallem and N. Samaan, "A Solar-assisted Voltage Optimization Method for Transmission Solar Network Power System," 2022 IEEE Power & Energy Society General Meeting (PESGM), Denver, CO, USA, 2022, pp. 1-5, doi: 10.1109/PESGM48719.2022.9917048.

[2] X. Ke et al., "A three-stage enhanced reactive power and voltage optimization method for high penetration of solar," 2017 IEEE Power & Energy Society General Meeting, Chicago, IL, 2017, pp. 1-5.

[3] W. Sun, C. -C. Liu and L. Zhang, "Optimal generator start-up strategy for bulk power system restoration," 2012 IEEE Power and Energy Society General Meeting, San Diego, CA, USA, 2012, pp. 1-1, doi: 10.1109/PESGM.2012.6345502.

[4] A. Marano-Marcolini, F. Capitanescu, J. L. Martinez-Ramos and L. Wehenkel, "Exploiting the Use of DC SCOPF Approximation to Improve Iterative AC SCOPF Algorithms," in IEEE Transactions on Power Systems, vol. 27, no. 3, pp. 1459-1466, Aug. 2012.

[5] F. Capitanescu, M. Glavic, D. Ernst, and L. Wehenkel, “Contingency filtering techniques for preventive security-constrained optimal power flow,” IEEE Trans. Power Syst., vol. 22, no. 4, pp. 1690–1697, 2007.

[6] F. Bouffard, F. D. Galiana, and J. M. Arroyo, “Umbrella contingencies in security constrained optimal power flow,” in 15th Power Systems Computation Conference (PSCC 05), Li`ege, Belgium, Aug 2005.

[7] D. Phan and J. Kalagnanam, "Some Efficient Optimization Methods for Solving the Security-Constrained Optimal Power Flow Problem," in IEEE Transactions on Power Systems, vol. 29, pp. 863-872, March 2014.

[8] M. Lu, G.-S. Seo, M. Sinha, F. Rodriguez, S. Dhople, and B. Johnson, “Adaptation of commercial current-controlled inverters for operation with virtual oscillator control,” in 2019 IEEE Applied Power Electronics Conference and Exposition (APEC), pp. 3427–3432, IEEE, 2019.

[9] H. Jain, G. Seo, E. Lockhart, V. Gevorgian, and B. D. Kroposki, “Blackstart of power grids with inverter-based resources,” tech. rep., National Renewable Energy Lab.(NREL), Golden, CO (United States), 2020.

[10] W. Sun, C.-C. Liu, and L. Zhang, “Optimal generator start-up strategy for bulk power system restoration,” IEEE Transactions on Power Systems, vol. 26, no. 3, pp. 1357–1366, 2010.

[11] Tbaileh, Ahmad, et al. "Optimal Power System Black start using Inverter-Based Generation." 2021 IEEE Power & Energy Society General Meeting (PESGM). IEEE, 2021.

[12] Nguyen, Quan, et al. "Control and simulation of a grid-forming inverter for hybrid PV-battery plants in power system black start." 2021 IEEE power & energy society general meeting (PESGM). IEEE, 2021.

9.2 Task A.2 Demonstration of black-start process using two sub-areas of NYPA system in EMT real-time simulation tool HYPERsim

Background:

This task demonstrates transient stability and validates the effectiveness of the numerical optimization-based black-start function within the New York Power Authority (NYPA) transmission system, utilizing the electromagnetic-transient (EMT) real-time simulation tool, HYPERsim. The EMT demonstration involves the creation of a high-fidelity hybrid solar-storage power plant with grid-forming (GFM) capability, positioning it as a potential black-start resource alongside existing hydroelectric power plants in the NYPA system. By employing the optimal black-start sequence and generator dispatch obtained from the numerical solution as inputs, the EMT real-time demonstration not only closely aligns all steady-state parameters with those in the numerical solution but also showcases the NYPA system's capability to maintain voltage and frequency stability. Furthermore, it demonstrates the system's resilience in overcoming practical dynamic black-start challenges, such as transformers' inrush current and the energization of long transmission lines.

TABLE I: Comparison of the Developed Black-Start and Existing Related Works

	Advantages	Disadvantages
[1]-[5]	- Focus on optimal blackstart with multiple steps	- Only focus on steady-state analysis, and cannot capture system dynamics during black-start
[3]-[6]	- Use the only industry-approved GFM control model with current limiting and P-Q capability limit	- Only model the ac-side dynamic - Do not focus on black-start
[7]	- Use an autonomous coordination between solar and storage	- Only focus on grid-following control - Do not focus on black-start
[8]	- Use GFM-based wind for black start	- Do not focus on a full sequence of black-start process - Focus on wind instead of solar and storage as generation resources
[9]-[11]	- Use GFM inverters as black start unit - Conduct a real-time simulation with multiple steps with autonomous actions of circuit breakers	- Do not model the dc-side dynamics
Approach developed by PNNL [12, 13]	- Use real system topology and parameters and optimization-assisted black-start procedure - Full demonstration with 25 steps in Area 1 and 17 steps in Area 4. - Detailed dynamic model at the dc side and autonomous coordination between solar and storage - Use the only industry-approved GFM control model at the ac side with current limiting and P-Q capability limit	- The demonstration and control implementation in HYPERsim requires greater effort compared other EMT simulation tools

Task Objectives:

- Develop a high-fidelity hybrid dc-coupled solar-storage power plant model with grid-forming capability and autonomous power sharing between solar and storage.
- Demonstrate system stability and characterize dynamic behaviors of a black-start process for 2 sub-areas in the NYPA system with input from the numerical optimization solution via a developed automated co-simulation framework.

Methodology Overview: As depicted in Figure 1, we have developed a comprehensive model for the hybrid solar-storage plant, incorporating both ac-side and dc-side control strategies. The ac-side control employs an industry-approved droop-based Grid-Forming Mode (GFM) control strategy, regulating terminal voltage and voltage control based on P-f and Q-V droop characteristics. On the other hand, the dc-side control autonomously coordinates solar generation at the maximum power point and manages bidirectional storage dispatch in response to the required ac-side demand.

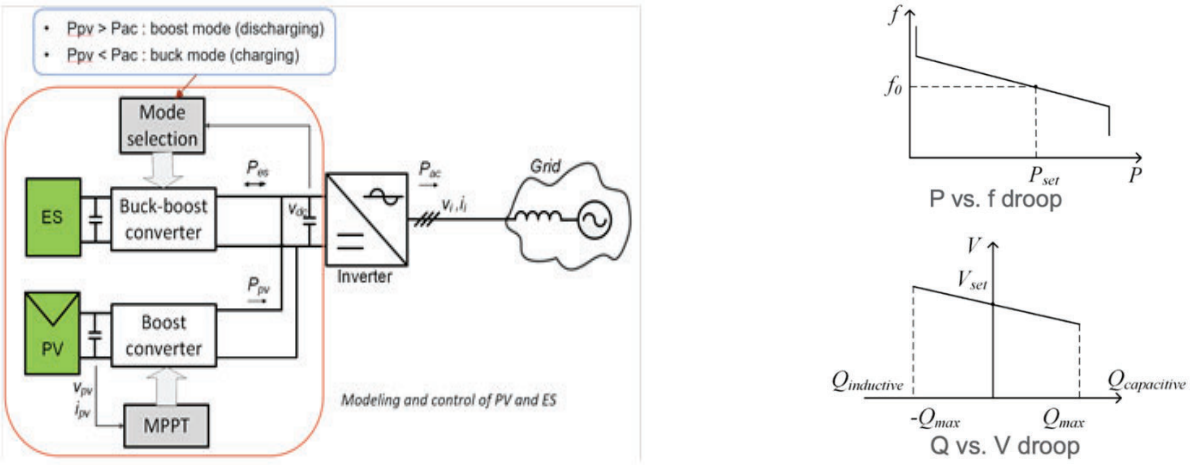

Figure. 1 Modeling and control of a hybrid solar-storage plant with droop-based GFM capability

Figure 2 illustrates the EMT real-time demonstration within HYPERsim, conducted separately for Area 1 and Area 4 in the NYPA system, as shown in Figure 3. Area 1 utilizes a hydro plant as a black-start resource, while Area 4 leverages the developed hybrid solar-storage plant. To facilitate this, we have established a communication-based co-simulation framework. This framework automatically collects real-time measurement data of system states, identifies when the system reaches steady-state after each switching event, and determines readiness for the subsequent step in the black-start process. Additionally, it transmits the optimal line and transformer energizing sequence, along with reference dispatch information for the hydro and hybrid storage plants.

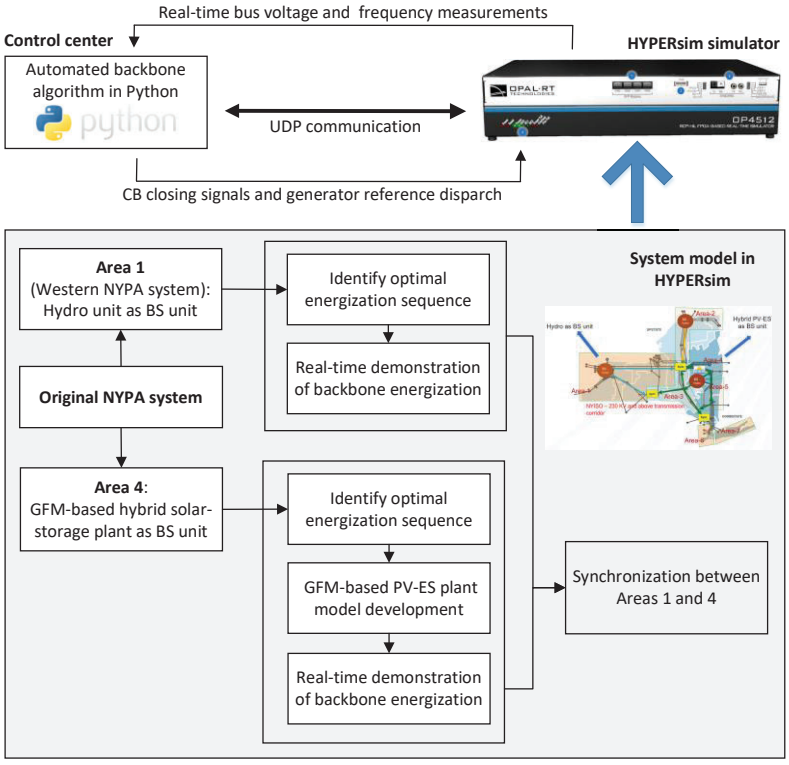

Figure 2. Framework of demonstrating an automated blackstart process in 2 sub-areas in NYPA system in HYPERsim

Simulation Results: Simulation results corresponding to the blackstart in Area 4 are shown as examples. Figure 4(a) shows the optimal energizing sequence, With the GFM control, Figures 4(b) and 4(e) show the stable voltage magnitudes at different locations and instantaneous terminal voltage of the hybrid plant during entire process. While Figure 4(c) shows the total hybrid plant generation, Figure 4(d) shows the break-down of individual solar and storage generations to demonstrate the developed coordinative at the dc side.

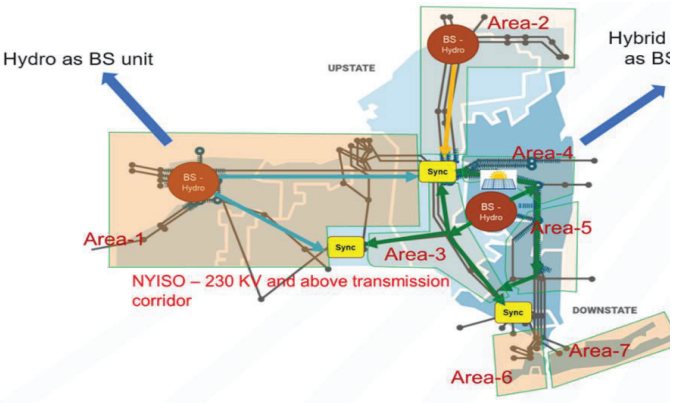

Figure 3. NYPA power system and 7 sub-areas

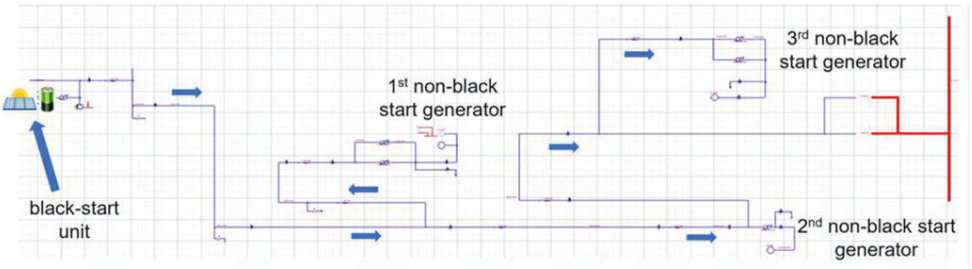

(a) Backbone and energizing sequence in Area 4

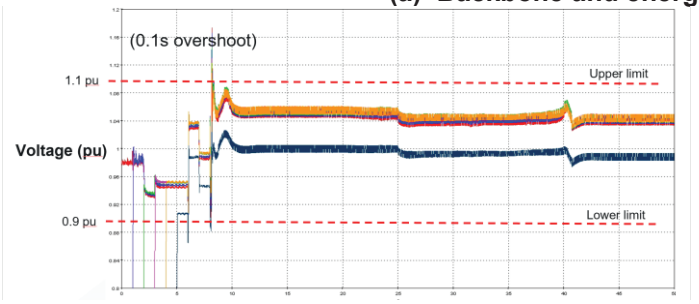

(b) Bus voltages during blackstart process

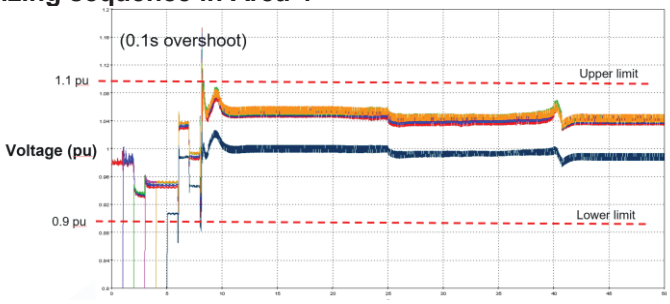

(c) Bus voltages during blackstart process

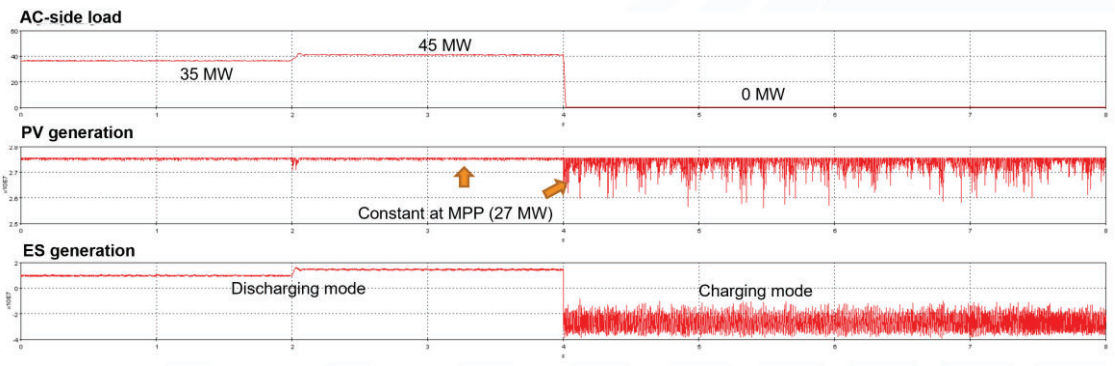

(d) Power generation from solar and storage with varying ac-side load.

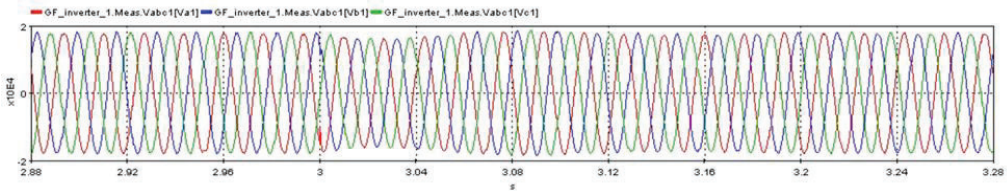

(e) Instantaneous terminal voltage of the GFM-based hybrid solar-storage power plant

Figure 4. Simulation results of the demonstrated black-start process in Area 4.

References

[1] A. Tbaileh et al., "Optimal Power System Black start using Inverter-Based Generation," 2021 IEEE Power & Energy Society General Meeting (PESGM), Washington, DC, USA, 2021, pp. 1-5, doi: 10.1109/PESGM46819.2021.9638043.
[2] W. Sun, C. -C. Liu and L. Zhang, "Optimal generator start-up strategy for bulk power system restoration," 2012 IEEE Power and Energy Society General Meeting, San Diego, CA, USA, 2012, pp. 1-1, doi: 10.1109/PESGM.2012.6345502.
[3] W. Du, R. H. Lasseter and A. S. Khalsa, "Survivability of Autonomous Microgrid During Overload Events," in IEEE Transactions on Smart Grid, vol. 10, no. 4, pp. 3515-3524, July 2019
[4] W. Du, Q. Nguyen, Y. Liu and S. M. Mohiuddin, "A Current Limiting Control Strategy for Single-Loop Droop-Controlled Grid-Forming Inverters Under Balanced and Unbalanced Faults," 2022 IEEE Energy Conversion Congress and Exposition (ECCE), 2022
[5] S. Konstantinopoulos, D. Ramasubramanian, E. Farantatos and V. Singhvi, "Blackstart and Restoration of 100% Renewable Power Systems with Grid Forming Converters," 2022 IEEE Power & Energy Society General Meeting (PESGM), Denver, CO, USA, 2022, pp. 1-5, doi: 10.1109/PESGM48719.2022.9916718.
[6] Jain, Himanshu, Gab-Su Seo, Eric Lockhart, Vahan Gevorgian, and Benjamin Kroposki. 2020. Blackstart of Power Grids with Inverter-Based Resources: Preprint. Golden, CO: National Renewable Energy Laboratory. NREL/CP-5D00-75327.
[7] M. Z. Daud, A. Mohamed, M. Z. Che Wanik and M. A. Hannan, "Performance evaluation of grid-connected photovoltaic system with battery energy storage," 2012 IEEE International Conference on Power and Energy (PECon), Kota Kinabalu, Malaysia, 2012, pp. 337-342
[8] H. N. Villegas Pico and V. Gevorgian, "Blackstart Capability and Survivability of Wind Turbines With Fully Rated Converters," in IEEE Transactions on Energy Conversion, vol. 37, no. 4, pp. 2482-2497, Dec. 2022, doi: 10.1109/TEC.2022.3173903.
[9] A. Banerjee et al., "Autonomous Microgrid Restoration Using Grid-Forming Inverters and Smart Circuit Breakers," 2022 IEEE Power & Energy Society General Meeting (PESGM), Denver, CO, USA, 2022, pp. 1-5, doi: 10.1109/PESGM48719.2022.9916679.
[10] Coughlin, Abdulrahman Alassi, Zhiwang Feng, Khaled Ahmed, Mazheruddin Syed, Agusti Egea-Alvarez, Colin Foote, “Grid-forming VSM control for black-start applications with experimental PHiL validation”, International Journal of Electrical Power & Energy Systems, Volume 151, 2023,
[11] H. Burroughs, C. Klauber, C. -C. Sun and M. Culler, "Black Start with Inverter-Based Resources: Hardware Testing," 2023 IEEE Power & Energy Society General Meeting (PESGM), Orlando, FL, USA, 2023, pp. 1-5
[12] Q. Nguyen, M. R. Vallem, B. Vyakaranam, A. Tbaileh, X. Ke and N. Samaan, "Control and Simulation of a Grid-Forming Inverter for Hybrid PV-Battery Plants in Power System Black Start," 2021 IEEE Power & Energy Society General Meeting (PESGM), Washington, DC, USA, 2021, pp. 1-5, doi: 10.1109/PESGM46819.2021.9637882.
[13] Q. Nguyen, A. Tbaileh , Laura A. Ward, X. Ke, M. R. Vallem, B. Vyakaranam, and N. Samaan, "Real-Time Demonstration of Black-Start using a Grid-Forming Hybrid Solar-Energy Storage Power Plant," IEEE Transaction on Industrial Applications (in preparation).

9.3 Task B.1 Feeder-level Microgrid Energy Management

Background: This task focuses on developing grid support functions for utility-scale MW-level PV systems, specifically tailored for extended outages. The aim is to achieve optimal resilience service performance and regulate the operation of the formed microgrid. Table I provides a summary of the state-of-the-art works in this area, revealing key observations: 1) Few studies concentrate on extreme outages lasting multiple days; 2) Existing approaches often rely on dispatchable distributed resources, which can be costly and unavailable for most distribution feeders. In contrast, renewables, expected to be prevalent in most distribution systems in the near future, are not extensively explored; 3) Limited consideration is given to cold load pickup (CLPU), a crucial factor impacting microgrid operation. While some models use fixed CLPU parameters based on assumed temperature and outage duration, this approach introduces significant CLPU estimation errors. Alternatively, candidate-based methods generate CLPU curves for all events, allowing the microgrid to select optimal CLPU scheduling. However, this becomes impractical during long outages due to the extensive candidate set.

TABLE I: Comparison of STATE-OF-THE-ART Algorithms for Microgrid Resilience Service

Ref.	Microgrid Operation Setup			Microgrid Unit Commitment Algorithm Setup						Verified dynamic responses§
	3-phase unbalanced system	Outage duration	Main energy source*	Optimization stages	Rolling horizon	Forecast error	CLPU			
							Y/N	CLPU events	CLPU model	
[1]		< 1 hour	DG	RT	✓		✓	one	fixed	no real-time CLPU simulation
[2]		up to days	DG	DA		✓	✓	one	fixed	
[3]	✓	up to days	DG + BESS	DA		✓	✓	one	fixed	
[4]	✓	several hours	DG	RT		✓	✓	one	candidate	
[5]		several hours	DG	RT		✓	✓	one	candidate	
[6]		several hours	DG	DA		✓		multiple		
[7]		< 1 day	DG	DA+RT		✓		multiple		
[8]	✓	< 1 hour	DG	RT				one		
[9]	✓	up to days	DG	DA				multiple		no CLPU
[10]	✓	< 1 day	DG + BESS	DA	✓			multiple		
[11]	✓	several hours	DG + BESS	RT				multiple		
[12]		multi-days	BESS + PV	DA				multiple		
Our Method	✓	**multi-days**	**BESS + PV**	**DA+RT**	✓	✓	✓	**multiple**	**adaptive**	**verified by real-time CLPU simulation**

*DG denotes dispatchable distributed generations; § Using openDSS, gridLAB or HIL simulation

Task Objectives:

- Develop an energy management system (EMS) for a hybrid PV plant to power a feeder-level microgrid
- Maximize the total serve load considering customer comfort and minimize the CLPU effect by using an adaptive CLPU model to accurately capture the CLPU consumption accounting for impacts of time-varying ambient temperature and uncertainties in scheduled outage duration.

Approach: Figure 1 illustrates the framework of the two-stage feeder-level microgrid EMS and provides a conceptual comparison of CLPU models. The EMS effectively coordinates day-ahead energy scheduling and intra-hour power dispatch. Notably, the adaptive CLPU model, in contrast to the fixed CLPU model, accurately considers the influences of temperature and interruptions in each time step. This precision aids the microgrid in mitigating energy and power deficits attributed to CLPU, ultimately facilitating optimal operation.

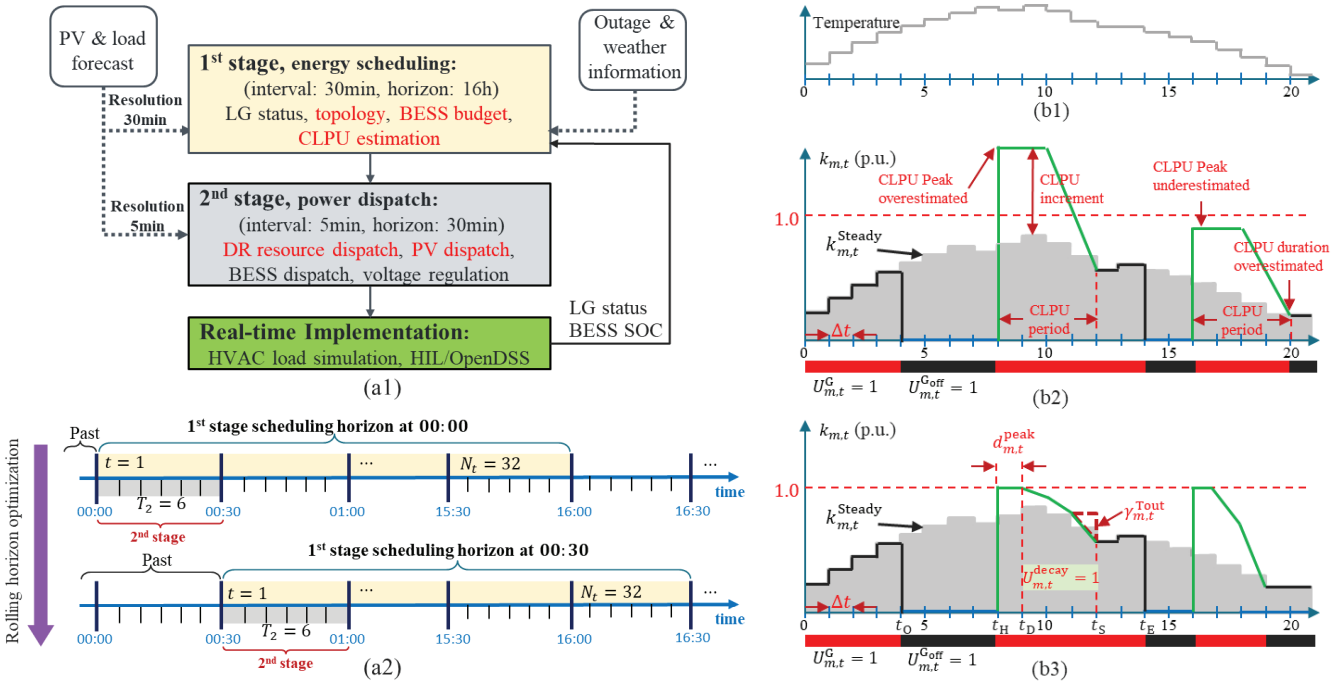

Figure 1. Two-stage EMS: (a1) Flowchart of the 2-Stage MGUC, (a2) Scheduling Horizons and Intervals; Conceptual comparison of the CLPU models: (b1) Temperature; (b2) the fixed CLPU model, (b3) the adaptive CLPU model, grey shaded areas are the HVACs' normal electricity consumption when there is no interruption.

Project Results and Discussions: In Fig. 2, it is evident that the adaptive CLPU model accurately captures CLPU dynamics. As presented in Table I, the EMS utilizing the adaptive CLPU model (AdaptCLPU) demonstrates the best overall performance, excelling in terms of served energy, critical load, baseload, and PV utilization. In contrast, the EMS employing the Fixed CLPU (FixCLPU) model provides the least served energy, primarily due to higher PV curtailment. The EMS without CLPU estimation (NoCLPU) results in the highest CLPU consumption [13].

TABLE II: Comparison of Microgrid Performance with and Without CLPU Estimation

Case	Served load (kWh)	Served load in preferred periods (kWh)		Served critical load (kWh)	Served baseload (kWh)	Curtailed PV (kWh)	CLPU (kWh)	Estimated CLPU (kWh)
		total	CLPU part					
NoCLPU	54493	**10196**	1757	4734	21438	2999	7697	-
FixCLPU [12]	50737	7445	540	4814	20464	5877	**5893**	12885
AdaptCLPU	**55173**	7771	667	**4857**	**22210**	**2591**	6835	5565

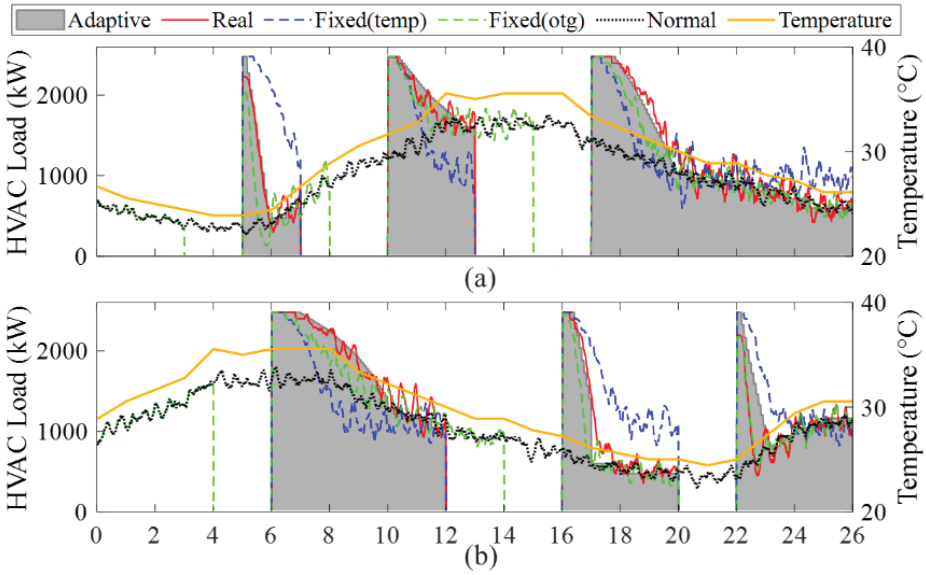

Figure 2. Two-stage EMS: Comparing various CLPU models, high temperature during: (a) hours 12-16; (b) hours 4-8.

References

[1] Chen B, Chen C, Wang J, Butler-Purry KL. “Multi-time step service restoration for advanced distribution systems and Microgrids”, IEEE Transactions on Smart Grid 2018;9:6793–805. doi:10.1109/tsg.2017.2723798.

[2] Arif A, Ma S, Wang Z, Wang J, Ryan SM, Chen C. “Optimizing service restoration in distribution systems with uncertain repair time and demand”, IEEE Transactions on Power Systems 2018;33:6828–38. doi:10.1109/tpwrs.2018.2855102.

[3] Arif A, Wang Z, Chen C, Wang J. “Repair and resource scheduling in unbalanced distribution systems using neighborhood search”, IEEE Transactions on Smart Grid 2020;11:673–85. doi:10.1109/tsg.2019.2927739.

[4] Song M, nejad RR, Sun W. “Robust distribution system load restoration with time-dependent cold load pickup”, IEEE Transactions on Power Systems 2021;36:3204–15. doi:10.1109/tpwrs.2020.3048036.

[5] Li YL, Sun W, Yin W, Lei S, Hou Y. “Restoration strategy for active distribution systems considering endogenous uncertainty in cold load pickup”, IEEE Transactions on Smart Grid 2022;13:2690–702. doi:10.1109/tsg.2021.3120555.

[6] Arif A, Wang Z. “Networked microgrids for service restoration in resilient distribution systems”, IET Generation, Transmission & Distribution 2017;11:3612–9. doi:10.1049/iet-gtd.2017.0380.

[7] Mousavizadeh S, Haghifam M-R, Shariatkhah M-H. “A linear two-stage method for resiliency analysis in distribution systems considering renewable energy and Demand Response Resources”, Applied Energy 2018;211:443–60. doi:10.1016/j.apenergy.2017.11.067.

[8] Chen B, Chen C, Wang J, Butler-Purry KL. “Sequential Service Restoration for unbalanced distribution systems and microgrids”, IEEE Transactions on Power Systems 2018;33:1507–20. doi:10.1109/tpwrs.2017.2720122.

[9] Xu Y, Liu C-C, Schneider KP, Tuffner FK, Ton DT. “Microgrids for service restoration to critical load in a resilient distribution system”, IEEE Transactions on Smart Grid 2018;9:426–37. doi:10.1109/tsg.2016.2591531.

[10] Fobes DM, Nagarajan H, Bent R. Optimal microgrid networking for maximal load delivery in phase unbalanced distribution grids: A declarative modeling approach. IEEE Transactions on Smart Grid 2023;14:1682–91. doi:10.1109/tsg.2022.3208508.

[11] Wang Z, Wang J, Chen C. “A three-phase microgrid restoration model considering unbalanced operation of distributed generation. “IEEE Transactions on Smart Grid”, 2018;9:3594–604. doi:10.1109/tsg.2016.2621412.

[12] Hu R, Li Y, Zhang S, Shirsat A, Muthukaruppan V, Tang W, et al. “A load switching group based feeder-level Microgrid Energy Management Algorithm for service restoration in Power Distribution System”, 2021 IEEE Power & Energy Society General Meeting (PESGM) 2021. doi:10.1109/pesgm46819.2021.9638231.

[13] Hu, R, Shirsat A, Muthukaruppan V, et al. “Adaptive cold-load pickup considerations in 2-stage microgrid unit commitment for enhancing microgrid resilience”, Applied Energy, 2024: 356, 122424.

9.4 Task B.2 Community-level Dynamic Microgrid Energy Management

Background: This task introduces a comprehensive and adaptive three-stage hierarchical multi-timescale (SA-HMTS) framework designed for scheduling and real-time dispatch of community microgrids (CMGs) equipped with hybrid PV systems. The primary goal is to restore loads during prolonged outages when transmission network support is unavailable, thereby enhancing the resilience of power distribution systems. Numerous strategies leveraging microgrids for load restoration have been proposed in the literature, as outlined in Table I. However, a holistic and computationally efficient approach for proactive scheduling and dispatch of distribution network-integrated CMGs during extended emergencies, with a focus on real-time uncertainty mitigation, prioritizing critical loads, optimizing resource allocation for self-sustained continuous operation, incorporating demand response, modeling cold-load pick-up, and expanding CMG support to the neighboring grid, remains unexplored.

Table I: Comparison of state-of-the-art methods against proposed SA-HMTS framework.

Reference	Framework specifics						Numerical simulation specifics		
	Load maximization	Stages	Rolling horizon	Dynamic MG formation	Uncertainty aware	RT dispatch frequency	Digital twin validation*	Forecast error analysis	Temporal generalizability
[1]	✓	1	x	✓	x	N/A	✓	x	x
[2]	x	2	✓	x	x	15 minutes	x	x	x
[3]	x	1	x	x	✓	N/A	✓	x	x
[4]	x	3	✓	x	✓	5 minutes	x	x	x
[5]	✓	1	✓	✓	✓	1 hour	x	x	x
[6]	✓	1	x	x	x	N/A	✓	x	x
[7]	✓	1	x	x	✓	1 hour	x	x	✓
[8]	x	1	✓	x	x	1 hour	x	x	x
[9]	x	3	✓	x	✓	15 minutes	x	x	x
[10], [11]	x	2	✓	x	✓	5 minutes	x	x	x
[12]	✓	1	x	✓	x	N/A	x	x	x
[13]	x	1	✓	✓	✓	1 hour	✓	x	✓
SA-HMTS	✓	3	✓	✓	✓	5 minutes	✓	✓	✓

* Using OpenDSS or HIL simulations.

Task Objectives:

- Develop an optimal decision-making framework that will enable CMGs to securely restore loads during extended duration outages caused by high impact low frequency (HILF) events.
- Incorporate uncertainty mitigation mechanisms within the optimal decision-making framework for bolstering against the extreme volatility inherent to HILF events.

Methodology Overview:

The proposed optimal decision-making framework is depicted in Fig. 1. The Secure and Adaptive Three-Stage Hierarchical Multi-Timescale (SA-HMTS) framework consists of three hierarchical stages, each operating on a distinct timescale. The initial stage tackles a stochastic extended duration scheduling (EDS) problem, establishing reference plans for optimal resource allocation and determining the extent to which the Community Microgrid (CMG) can restore neighboring loads. The intermediate near-real-time (NRT) scheduling stage refines the EDS schedule closer to the dispatch time using newly obtained forecasts, followed by the Real-Time (RT) dispatch stage.

To enhance decision robustness against forecast errors, a novel concept called delayed recourse is introduced. The framework encompasses decision-making for various load types and distributed energy resources, including energy storage (ES) systems, MW-scale PV generators,

and rooftop PV generators. It takes into account uncertainties in load demand, solar irradiance, and outage duration. The framework is validated using OpenDSS software and hardware-in-loop simulations.

Project Results and Discussions: Table II presents the outcomes of the proposed approach in contrast to traditionally employed deterministic, stochastic, and robust optimization approaches, each utilizing a commonly employed two-stage approach. The objective of this comparison is to underscore the effectiveness of the proposed approach in the context of uncertainty-aware decision-making, as reflected in the resiliency metrics detailed in the table. Definitions of these metrics can be found in [16]. Across all compared scenarios, the proposed Secure and Adaptive Three-Stage Hierarchical Multi-Timescale (SA-HMTS) framework consistently demonstrates superior results in critical load supply, PV utilization, availability of adequate reserved limits with grid-forming Energy Storage (ES) systems, and CMG operational duration.

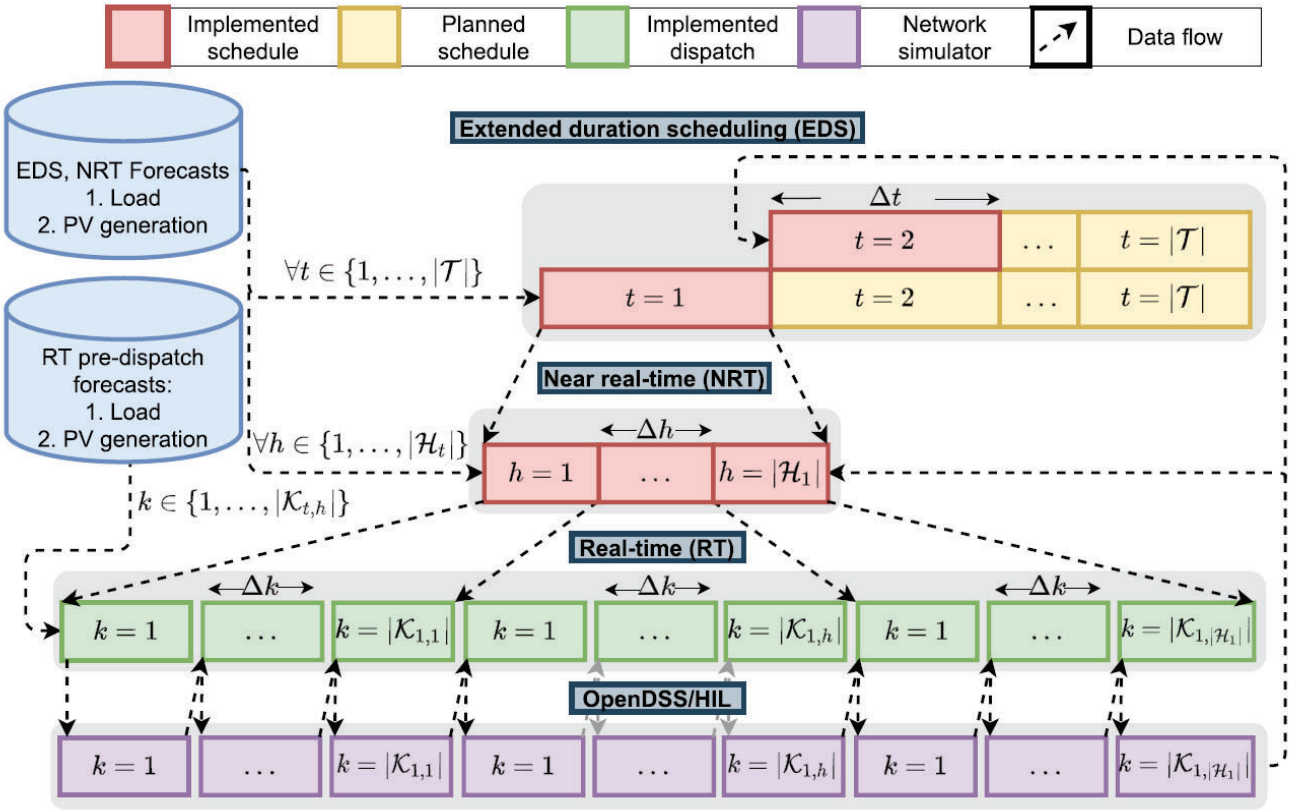

Figure 1. Schematic layout of the proposed framework.

Table II: Comparative analysis with existing approaches.

Metric	SA-HMTS	Deterministic	Stochastic	Robust
P^{NCL} (%)	62.83	71.25	68.12	54.33
P^{CL} (%)	100	86.79	87.34	54.33
$P^{\text{PV, Total}}$ (%)	86.34	85.13	87.12	79.11
$T^{\text{RL,ES}}$ (%)	4.12	39.58	27.23	21.12
$T^{\text{CMG,OFF}}$ (hours)	0	9	5	4

References

[1] Y. Xu, C. Liu, K. P. Schneider, F. K. Tuffner, and D. T. Ton, “Microgrids for service restoration to critical load in a resilient distribution system,” IEEE Transactions on Smart Grid, vol. 9, no. 1, pp. 426–437, 2018.
[2] W. Gu, Z. Wang, Z. Wu, Z. Luo, Y. Tang, and J. Wang, “An online optimal dispatch schedule for cchp microgrids based on model predictive control,” IEEE Transactions on Smart Grid, vol. 8, no. 5, pp. 2332–2342, 2017.
[3] A. Gholami, T. Shekari, and S. Grijalva, “Proactive management of microgrids for resiliency enhancement: An adaptive robust approach,” IEEE Transactions on Sustainable Energy, vol. 10, no. 1, 2019.
[4] H. Qiu, W. Gu, Y. Xu, and B. Zhao, “Multi-time-scale rolling optimal dispatch for AC/DC hybrid microgrids with day-ahead distributionally robust scheduling,” IEEE Transactions on Sustainable Energy, vol. 10, no. 4, pp. 1653–1663, 2019.
[5] Z. Wang and J. Wang, “Self-healing resilient distribution systems based on sectionalization into microgrids,” IEEE Transactions on Power Systems, vol. 30, no. 6, pp. 3139–3149, 2015.
[6] M. H. Amirioun, F. Aminifar, and H. Lesani, “Towards proactive scheduling of microgrids against extreme floods,” IEEE Transactions on Smart Grid, vol. 9, no. 4, pp. 3900–3902, 2018.
[7] K. Balasubramaniam, P. Saraf, R. Hadidi, and E. B. Makram, “Energy management system for enhanced resiliency of microgrids during islanded operation,” Electric Power Systems Research, vol. 137, pp. 133–141, 2016.
[8] J. Silvente, G. M. Kopanos, E. N. Pistikopoulos, and A. Espu˜na, “A rolling horizon optimization framework for the simultaneous energy supply and demand planning in microgrids,” Applied Energy, vol. 155, pp. 485–501, 2015.
[9] Y. Tian, L. Fan, Y. Tang, K. Wang, G. Li, and H. Wang, “A coordinated multi-time scale robust scheduling framework for isolated power system with esu under high res penetration,” IEEE Access, vol. 6, pp. 9774–9784, 2018.
[10] Z. Bao, Q. Zhou, Z. Yang, Q. Yang, L. Xu, and T. Wu, “A multi time-scale and multi energy-type coordinated microgrid scheduling solution—part i: Model and methodology,” IEEE Transactions on Power Systems, vol. 30, no. 5, pp. 2257–2266, 2015.
[11] Z. Bao, Q. Zhou, Z. Yang, Q. Yang, L. Xu, and T. Wu, “A multi time-scale and multi energy-type coordinated microgrid scheduling solution—part ii: Optimization algorithm and case studies,” IEEE Transactions on Power Systems, vol. 30, no. 5, pp. 2267–2277, 2015.
[12] B. Chen, Z. Ye, C. Chen, and J. Wang, “Toward a milp modeling framework for distribution system restoration,” IEEE Transactions on Power Systems, vol. 34, no. 3, pp. 1749–1760, 2019.
[13] W. Liu and F. Ding, “Hierarchical distribution system adaptive restoration with diverse distributed energy resources,” IEEE Transactions on Sustainable Energy, vol. 12, no. 2, pp. 1347–1359, 2021.
[14] C. M. Colson and M. H. Nehrir, “Comprehensive real-time microgrid power management and control with distributed agents,” IEEE Transactions on Smart Grid, vol. 4, no. 1, pp. 617–627, 2013.
[15] A. Shirsat et al., "Hierarchical Multi-timescale Framework For Operation of Dynamic Community Microgrid," 2021 IEEE Power & Energy Society General Meeting (PESGM), Washington, DC, USA, 2021, pp. 1-5, doi: 10.1109/PESGM46819.2021.9638104. (Conference publication from this subtask)
[16] A. Shirsat et al., "A Secure and Adaptive Hierarchical Multi-Timescale Framework for Resilient Load Restoration Using a Community Microgrid," in IEEE Transactions on Sustainable Energy, vol. 14, no. 2, pp. 1057-1075, April 2023, doi: 10.1109/TSTE.2023.3251099. (Journal publication from this subtask)

9.5 Task B.3 Mobile Storage powered Microgrid Energy Management

Background: This task introduces a two-stage hierarchical energy management approach designed to securely manage feeder-level microgrids within a distribution system experiencing severe outages and a high presence of distributed rooftop residential PV. This approach solves a sequential rolling optimization problem to schedule main resources and adopts a dispatching scheme for real-time adjustments. It incorporates novel elements to effectively handle the considerable uncertainty associated with residential PV systems and optimize the utilization of microgrid resources. Table I provides a summary of the pros and cons of current state-of-the-art methods. As indicated in the table, existing methods have so far overlooked realistic operational conditions for the restoration of distribution systems during prolonged outages. The current distribution systems exhibit low controllability (limited controllable switches) and observability (behind-the-meter PV, uncertainty in forecasts, etc.), posing considerable challenges in securely operating feeder-level microgrids.

TABLE I : Comparison of STATE-OF-THE-ART power system restoration strategies

		Description	Advantages	Disadvantages
Short-term Restoration [1]-[4]		During extreme events, outages last over multiple days. Existing approaches only consider a short restoration time scale ranging from 6-24 hours.	Short-term restoration enables uninterrupted service to load even with limited microgrid resources.	Proposed EMS must be able to ration the microgrid resources over multiple days to provide service to loads and better utilize the distributed residential PV.
Realistic Distribution System	High Controllability [5]	Distribution systems have a limited number of controllable switches which splits the systems into load zones. But existing works consider direct control on loads.	Direct control over loads helps to better prioritize and provide uninterrupted service to critical loads.	Without this consideration most of the proposed approaches in literature are not implementable in current distribution systems.
	High Observability [6]-[7]	High penetration of residential PV is an untapped resource during outages but most of these PV net-metered and hence are not observable in the distribution system. But existing consider full observability and direct control on the PV systems.	High observability leads to better forecasts and hence better utilization of PV systems and management of microgrid resources.	Lack of observability of high PV leads to challenges in secure operation of the microgrid which can in turn lead to devastating failure in the system.

Task Objectives:

- Develop a two-stage hierarchical energy management approach for securely operating feeder-level microgrids within a distribution system facing severe outages and high distributed rooftop residential PV penetration.
- Introduce innovative elements to effectively manage uncertainty associated with residential PV systems and address the oversight in existing methods regarding realistic operational conditions during extended outages in distribution systems.
- Extend the proposed scheme to multi-feeder cases to improve utilization of resources and provide better service to loads [8].

Methodology Overview: In the proposed 2-stage hierarchical energy management framework, stage-1 schedules the microgrid for the next period (such as ½ or 1 hour) by taking into account future load and PV forecast. Stage-2 is the short term dispatching stage which determines the proper dispatch levels for the microgrid resources. The major issue with BTM PV is lack of real-time data. Being net metered, dis-aggregating PV from load and forecasting just PV components becomes challenging and leads to significant forecast error as highlighted in Fig. 1. The low

accuracy in forecasting individual house PV and load leads to really large forecast errors at the feeder-level (as high as 2MW on a 3.5MW circuit). Handling such forecast errors becomes challenging since with limited microgrid resources. To securely operate the microgrid under such challenging conditions three innovative strategies are proposed:

- Multi-Day Fuel Rationing
- Learning-based Forecast Correction
- Dynamic Reserve Management

Details of these strategies are explained in [9].

Simulation Results: As shown in Table II, both on day-1 and day-3 we see that the proposed scheme with all the innovative forecast error management strategies performs better than the base scheme. There is significant service to critical and non-critical loads, better utilization of PV, reduction in scheduled and unscheduled shutdown of the microgrid and minimum disruption to critical loads even up to 3 days of restoration.

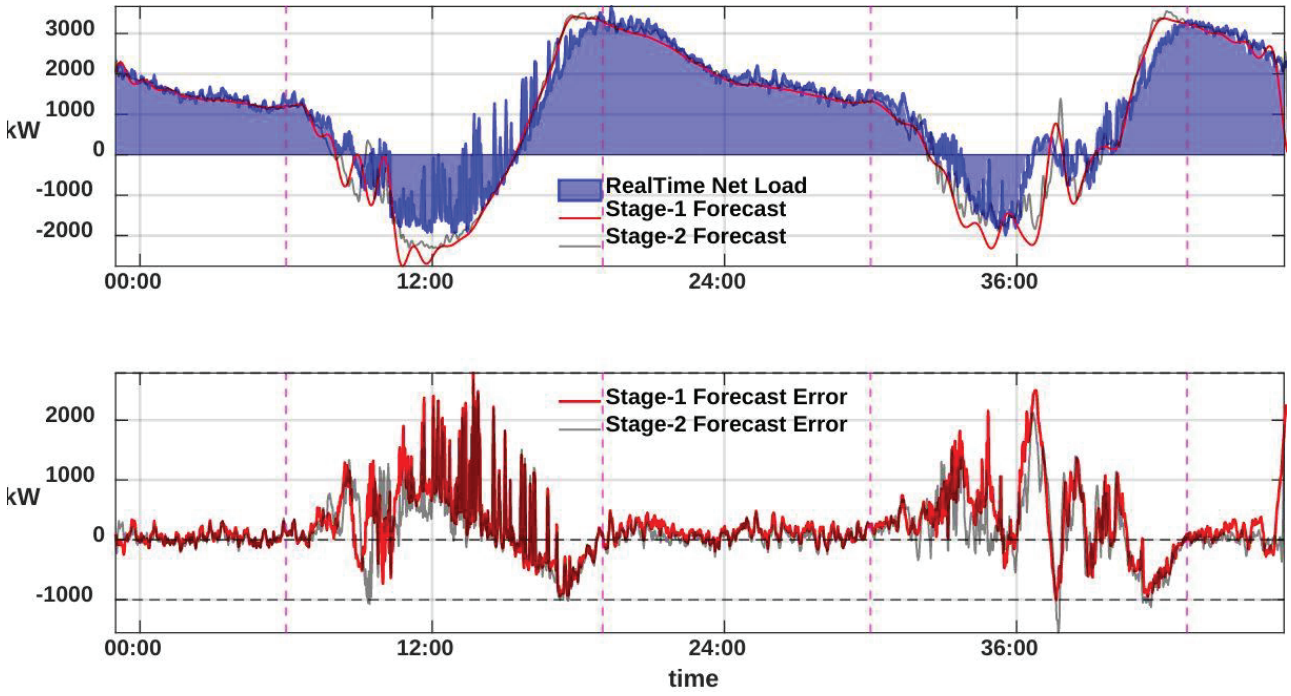

Figure 1. High forecast error in short-term and day-ahead forecast of aggregated BTM PV. (top) Real-time net load measurement, stage-1, and stage-2 forecast. (bottom) Total net load forecast error in stage-1 and stage-2 forecast. Zoomed plot shows stage-2 forecast is more accurate than stage-1 forecast during no PV duration and error is close to zero.

TABLE II: Performance on day-1 and day-3 of proposed scheme against a base scheme with basic energy management without any forecast error correction strategies over multi-day restoration.

Metric	Day-1		Day-2	
	Base Case	Proposed Scheme	Base Case	Proposed Scheme
% of Critical Load (CL) Served	72.73%	**79.2%**	71.69%	**76.44%**
% of Non-Critical Load (NCL) Served	71.1%	**75.244%**	67.76%	**71.38%**
% of PV utilized	78.33%	**86.92%**	81.88%	**90.35%**
Avg served duration of CL	37h 15m	**39h 20m**	34h 45m	**3h 30m**
No. of interruptions in serving CL	8	**9**	10	**7**
Total scheduled shutdown duration of microgrid	2h 40m	**2h 30m**	4h 5m	**3h 30m**
Total unscheduled shutdown duration of microgrid	1h	**0**	1h 30m	**30m**

References

[1] H. Momen, A. Abessi, S. Jadid, M. Shafie-khah, and J. P. S. Catalao, ˜ "Load restoration and energy management of a microgrid with distributed energy resources and electric vehicles participation under a twostage stochastic framework," International Journal of Electrical Power & Energy Systems, vol. 133, p. 107320, Dec. 2021.

[2] S. Poudel and A. Dubey, "Critical Load Restoration Using Distributed Energy Resources for Resilient Power Distribution System," IEEE Transactions on Power Systems, vol. 34, no. 1, pp. 52–63, Jan. 2019.

[3] W. Liu and F. Ding, "Collaborative Distribution System Restoration Planning and Real-Time Dispatch Considering Behind-the-Meter DERS," IEEE Transactions on Power Systems, vol. 36, no. 4, pp. 3629– 3644, Jul. 2021.

[4] W. Liu and F. Ding, "Hierarchical Distribution System Adaptive Restoration With Diverse Distributed Energy Resources," IEEE Transactions on Sustainable Energy, vol. 12, no. 2, pp. 1347–1359, Apr. 2021.

[5] M. R. Kleinberg, K. Miu, and H.-D. Chiang, "Improving Service Restoration of Power Distribution Systems Through Load Curtailment of In-Service Customers," IEEE Transactions on Power Systems, vol. 26, no. 3, pp. 1110–1117, Aug. 2011.

[6] N. C. Koutsoukis, P. S. Georgilakis, and N. D. Hatziargyriou, "Service restoration of active distribution systems with increasing penetration of renewable distributed generation," IET Generation, Transmission & Distribution, vol. 13, no. 14, pp. 3177–3187, 2019.

[7] M.-G. Choi, J.-H. Choi, S.-Y. Yun, and S.-J. Ahn, "MILP-Based Service Restoration Method Utilizing Both Existing Infrastructure and DERs in Active Distribution Networks," IEEE Access, vol. 10, pp. 36 477–36 489, 2022.

[8] Valliappan Muthukaruppan, Rongxing Hu, Ashwin Shirsat, Mesut Baran, Ning Lu, Wenyuan Tang, David Lubkeman, "Multi-Feeder Restoration using Multi-Microgrid Formation and Management," submitted to 2024 IEEE PES General Meeting, Available online at: https://arxiv.org/abs/2311.15351.

[9] Valliappan Muthukaruppan, Ashwin Shirsat, Rongxing Hu, Victor Paduani, Bei Xu, Yiyan Li, Mesut Baran, Ning Lu, David Lubkeman, Wenyuan Tang, "Feeder Microgrid Management on an Active Distribution System during a Severe Outage," Available online at: https://arxiv.org/abs/2208.10712

9.6 Task B.4 Reinforcement Learning-based Volt-Var Control for Distribution System

Background: This task presents a reinforcement learning (RL) approach to solve a cooperative, multi-agent Volt-Var Control(VVC) problem for high solar penetration distribution systems. The ingenuity of our RL method lies in a novel two-stage progressive training strategy that can effectively improve training speed and convergence of the machine learning algorithm. In general, there are three popular VVC approaches: rule-based, optimization-based, and more recently, machine learning-based. Although rule-based approaches are widely used in the field due to the ease of implementation, they lack the ability to adapt to fast-changing operational conditions. The major drawbacks of optimization-based approaches are their strict requirement of accurate network models and complex computational platforms for implementation. Furthermore, the computational complexity increases exponentially as the system scale (e.g. number of controllable devices) increases.

TABLE I: Comparison of STATE-OF-THE-ART missing data restoration methods

		Description	Advantages	Disadvantages
Rule-based System		Widely used in current power system operation	Fast and stable	The optimality cannot be guaranteed
Optimization-base system [1]-[2]		With accurate system modeling, minimize the cost and loss while satisfying operation constraint	provide a stable and optimal command after the optimization Optimal solution if system models are known	Highly rely on the model accuracy and huge joint search space would cause scalability issue Suboptimal solutions when model is not accurate
Machine Learning methods	Multi-Agent Reinforcement Learning [5]-[7]	Reinforcement Learning base approach under the centralized training, decentralized execution.	Easy to implement, similar to single agent setting. Better performance in the cooperative setting	The agents cannot learn directly from the decentralized environment. Cannot self-correct in field deploy. Can reach suboptimal solutions.
	Muti-Agent Morkov Game[11]-[11]	Model the process as Markov Game which training in decentralized environment	Learn from a decentralized environment and can infer other agents' behaviors in the training. Robust in decentralized in cooperative setting	Inferring other agents' intention increases the computational burden. The model complexity prevents be multi-agents be scaled up. Can reach suboptimal solutions
	The proposed approach	Separate the training process in 2 stages. Stage-1 is individual training. Stage-2 is centralized cooperation training	Training objectives explainable and trackable. Less training time, more robust and adaptive, allow for fine-tuning in real-time	Require system models for more effective first stage training. Can reach suboptimal solutions.

Task Objectives:

- Develop a novel two-stage, progressive training strategy.
- Propose a novel reward design and allocation mechanism to account for the contributions of all agents.

Methodology Overview: The 2-stage progressive training framework and the system model are illustrated in the left and right figures in Fig. 1, respectively. Stage 1 is individual training, in which each agent learns to take three basic control actions: "generate-Q", "consume-Q", and "do-nothing", assuming all other agents are inert. Stage 2 is cooperative training, where the training focus on learning to generate the "optimal" magnitude of Q in the presence of the other agents. In

the second stage, we assume that all agents have gained understanding of when to “generate-Q”, “consume-Q”, and “do-nothing”.

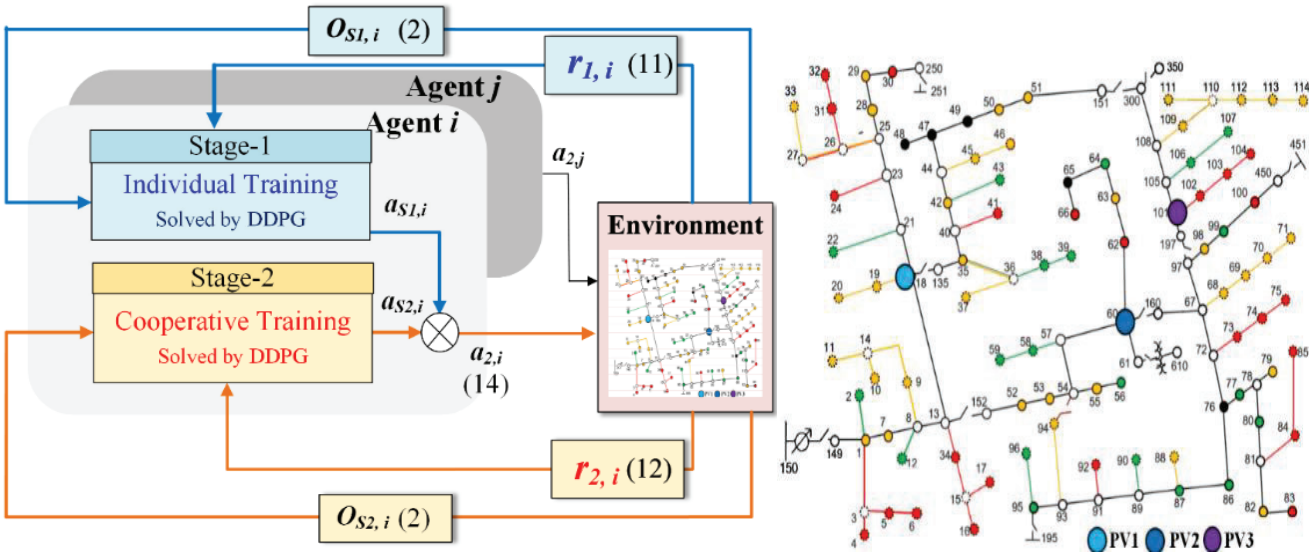

Fig. 1. The proposed 2-stage progressive training framework. “O” refers to observation, “r” refers to reward, “a” refers to action (Q command), and “DDPG” refers to Deep Deterministic Policy Gradient. The environment on the left is based on modified IEEE 123bus system.

Simulation Results: As shown in Table I, the conventional decentralized VVC takes the least number of actions, which is measured by the cumulative Q consumption, $\sum Q$. However, it receives the lowest Voltage score, showing an inferior voltage regulation performance. Stage-1 policy does not consider coordination. Thus, PV1 always generates Q, causing more V^{hlim} violations. Stage-2 policy has the highest voltage score, showing superior VVC control performance. By coordinating with other agents, ∑Q is significantly reduced in stage-2.

If some nodal voltages fall outside of the designated interval $[V^{llim}, V^{hlim}]$ in a control interval, we consider this interval to be a voltage violation event. Then, we compare the duration of such voltage events in four use cases: base case, conventional, stage-1 policy, and stage-2 policy in the summer season. Table II summarizes the statistics of the durations of all voltage violation events in the three summer testing days. Conventional VVC is effective in reducing longer voltage violations while leading to many shorter voltage violations. This results in a large number of cumulative violations. Overall, the stage-2 policy exhibits optimal performance in terms of reducing the total voltage violation duration.

TABLE II: VVC PERFORMANCE COMPARISON (THE SUMMER CASE) EVALUATION

Algorithm	Voltage Score	$Q_{total}(KVAR)$	$Q_{pv1}(p.u.)$	$Q_{pv2}(p.u.)$	$Q_{pv3}(p.u.)$
Base Case	0.98756	-	-	-	-
Conventional	0.98995	93.859	0.01688	0.07611	0.09242
Our method Stage1	0.99286	452.43	0.41250	0.12527	0.04583
Our method Stage2	0.99556	144.03	0.01660	0.14361	0.11305

TABLE III: STATISTICS OF THE VOLTAGE EVENT

Statistics	Base	Conventional	Our method Stage 1	Our method Stage 2
Count	4031	30219	4831	3314
Mean	6.74	1.16	2.64	2.08
Standard deviations	15.83	1.075	4.16	2.86
25 percentile	1	1	1	1
50 percentile	2	1	1	1
75 percentile	4	1	2	2
Max Duration	95	43	47	44
Nodes of Max Duration	2	5	1	2
Integration Sum	27176	34940	12759	6914

References

[1]] A. Abessi, V. Vahidinasab, and M. S. Ghazizadeh, “Centralized support distributed voltage control by using end-users as reactive power support,” *IEEE Trans. Smart Grid*, vol. 7, no. 1, pp. 178–188, Jan. 2016

[2] M. Chamana and B. H. Chowdhury, “Optimal voltage regulation of distribution networks with cascaded voltage regulators in the presence of high PV penetration,” *IEEE Trans. Sustain. Energy*, vol. 9, no. 3, pp. 1427–1436, Jul. 2018

[3] Y. Zhang, X. Wang, J. Wang, and Y. Zhang, “Deep reinforcement learning based volt-var optimization in smart distribution systems,” IEEE Transactions on Smart Grid, vol. 12, no. 1, pp. 361–371, Jan. 2021.

[4] X. Sun and J. Qiu, “Two-stage volt/var control in active distribution networks with multi-agent deep reinforcement learning method,” IEEE
Transactions on Smart Grid, vol. 12, no. 4, pp. 2903–2912, Jul. 2021.

[5] S. Wang, J. Duan, D. Shi, C. Xu, H. Li, R. Diao, and Z. Wang, “A data- driven multi-agent autonomous voltage control framework using deep
reinforcement learning,” IEEE Transactions on Power Systems, vol. 35, no. 6, pp. 4644–4654, Nov. 2020.

[6] R. Lowe, Y. Wu, A. Tamar, J. Harb, P. Abbeel, and I. Mordatch, “Multi-agent actor-critic for mixed cooperative-competitive environ-
ments,” arXiv:1706.02275 [cs], Mar. 2020, arXiv: 1706.02275.

[7] V. Mnih, A. P. Badia, M. Mirza, A. Graves, T. P. Lillicrap, T. Harley, D. Silver, and K. Kavukcuoglu, “Asynchronous methods for deep
reinforcement learning,” arXiv:1602.01783 [cs], Jun. 2016, arXiv: 1602.01783.

[8] T. P. Lillicrap, J. J. Hunt, A. Pritzel, N. Heess, T. Erez, Y. Tassa, D. Silver, and D. Wierstra, “Continuous control with deep reinforcement learning,” arXiv:1509.02971 [cs, stat], Jul. 2019, arXiv: 1509.02971.

[9] S. Zhang, M. Zhang, R. Hu, D. Lubkeman, Y. Liu, N. Lu, “Reinforcement Learning for Volt- Var Control: A Novel Two-stage Progressive Training Strategy”, 2022 IEEE Power & Energy Society General Meeting (PESGM)

9.7 Task B.5 Adopting Dynamic VAR Compensators (DVCs) to Mitigate PV Impacts on Unbalanced Distribution Systems

Background: Table 1 presents a comprehensive overview of existing methods for addressing the optimal placement and control schemes for DVCs, along with a comparison of their strengths and weaknesses in relation to the proposed approach.

Table I: A Review of Existing Methods and Our Contributions

Category	Methodology	Descriptions	Strength	Weakness
Device	DVR [1-2]	Add the missing voltage during a voltage sag	Injects a voltage in series with the system voltage	Can inject a voltage for a short time Unsuitable for systems with prolonged reactive power deficiencies
	D-STATCOM [3-4]	Compensate the bus voltage so as to provide improved power factor and reactive power control	Generate the rated current at any network voltage Use of a relatively small capacitor on the DC bus Harmonic current compensation Load balancing	Generating the harmonics distortion Designed for FIDVR mitigation
Placement	Analytical [5-7]	Analytical method to determine the optimal location for placing DGs	Easy to implement	Only consider balanced systems A detailed 3-phase distribution system model is necessary
	Meta-heuristic [8-9]	Application of particle swarm optimization for optimal DGs allocation and sizing	Simple to implement Less computational effort	
	Combination [10-11]	Combining genetic algorithms with particle swarm optimization to determine the optimal location and sizing of DGs	Superior to the individual method in terms of solution quality and number of iterations	
Control scheme	IEEE 1547 [12]	Include the functionality of local regulation of voltages through inverter VVC	Simple design Easy implementation	Non-adaptability Not taking all the benefits of DVC
	Delayed VVC [13]	Actively adjusts its VAR output as a function of local bus voltage	Control stability	Cannot maintain a feasible voltage profile under certain circumstances
	Scaled VVC [14]	Feedback-based VVC strategy by means of a diagonality scaled gradient projection method	Control stability Set-point tracking	Requires full centralized topology information Theoretical analysis only builds on 1-phase
	Adaptive VVC [15]	Achieves both low steady state error and control stability, and makes control parameters self-adaptive to external disturbances	Achieve high set-point tracking accuracy and control stability Self-adaptive parameter selection	Considers the node voltage where the inverter is located, not the voltage profile of the entire system
	Our method [16]	**Optimal dispatch, placement and control scheme for DVCs to minimize voltage variations and voltage regulator operations**	**Consider unbalanced 3-phase systems Practical dispatch scheme that overcomes the limitations of communication in distribution systems Consider the voltage variation of the entire system**	**Require short-term load and solar PV forecasting**

Task Objectives:

- Establish a multi-objective optimization framework to identify the optimal dispatch strategy and suitable placement for the DVC.
- Introduce two supervisory control strategies to determine the appropriate instances for adjusting the Volt/VAR Curve (VV-C) when the operating condition changes.

Methodology Overview: Determine the optimal dispatch and suitable placement of the DVC to minimize voltage variations and voltage regulator operations. Next, consider two schemes for updating the VV-C for the DVC. The first scheme, referred to as the shifted VV-C (Fig. 1(b)), involves shifting the midpoint of the standard VV-C (Fig. 1(a)) to align with the average Q-V point obtained from the optimal Q-V trajectory. In the second approach, known as the fitted VV-C (Fig. 1(c)), we employ linear regression to determine the slope that best fits the VV-C, ensuring it closely matches the optimal Q-V trajectory.

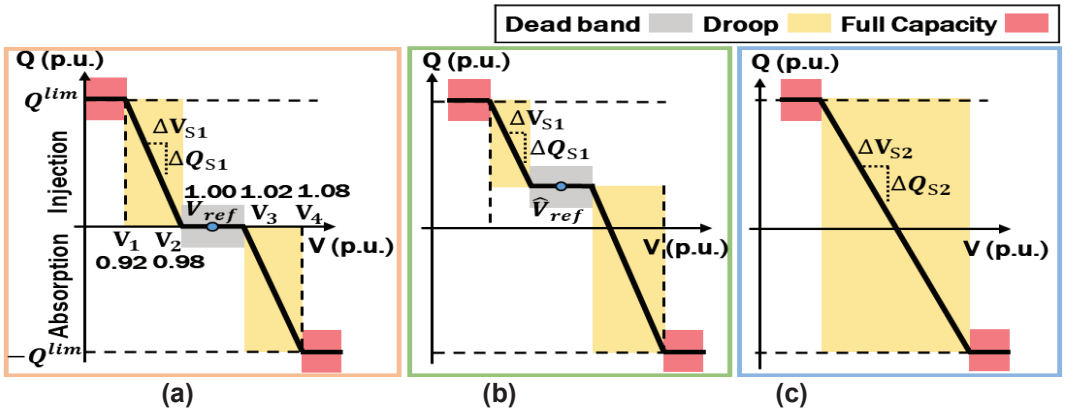

Figure. 1. Volt/VAR Curves (VV-Cs) for (a) the standard VV-C, (b) a shifted VV-C with the midpoint adjustment, and (c) a fitted VV-C without a deadband, featuring only the new slope that best fits with the optimal Q-V trajectories of the DVC.

Simulation Results: Tables II and III show the statistics for voltage variation and voltage regulator operation for different cases: base case, standard VV-C, shifted VV-C, and fitted VV-C, respectively. These results demonstrate a substantial reduction in voltage variations compared to the standard VV-C when using the revised curves. To investigate the impact of different VV-C update frequencies on the DVC, tests were performed with update rates set at 30-, 60-, 120-, and 240-min. The test results reveal that the optimal performance is attained with a 120-minute update frequency. As shown in Tables II and III, the proposed fitted VV-C can achieve a 0.3% reduction in voltage violations and a 12.7% decrease in voltage regulator operations compared to the standard VV-C. Figure 2 presents a sample of the optimal Q-V trajectories and the VV-Cs fitted using the two proposed approaches: shifted VV-C and fitted VV-C.

TABLE II: Voltage Violation by Different VV-C

VV-C		V_{out}^{lower} (1)	V_{in} (2)	V_{out}^{upper} (3)	Out of limits (%) ((1)+(3))/(T)
Base		3,744	1,100,393	445,303	28.98
Standard		3,462	1,102,683	443,295	28.83
Shifted	30-min	3,535	1,099,059	446,846	29.07
	60-min	3,670	1,108,645	437,125	28.45
	120-min	4,198	1,111,648	433,594	28.25
	240-min	4,536	1,096,431	448,473	29.24
Fitted	30-min	3,413	1,084,852	461,175	29.98
	60-min	3,456	1,099,197	446,787	29.06
	120-min	3,483	1,107,690	438,267	28.51
	240-min	4,399	1,105,347	439,694	28.66

*T: the total number of voltage points monitored during the scheduling period (1,549,440)

TABLE III: LTC and LVR Tap Changes by Different VV-C

VV-C		LTC	LVR						Total
		3-ph	Ph-A	Ph-A	Ph-C	Ph-A	Ph-B	Ph-C	
		150R	9R	25R	25R	160R	160R	160R	
Base		20	6	93	46	45	35	14	259
Standard		20	6	90	47	45	34	14	256
Shifted	30-min	29	4	86	46	46	49	16	276
	60-min	24	4	85	44	43	37	15	252
	120-min	19	5	84	42	42	37	12	241
	240-min	23	7	81	47	45	32	14	249
Fitted	30-min	33	6	82	44	43	37	14	259
	60-min	24	6	83	42	40	38	14	247
	120-min	20	4	78	40	42	29	13	226
	240-min	21	5	79	41	45	32	15	238

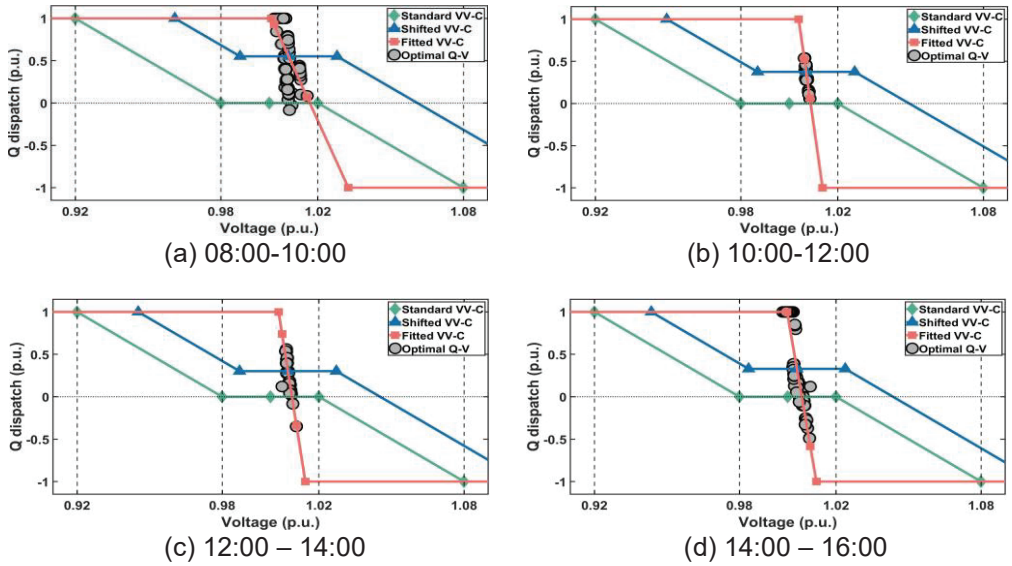

Figure. 2. Optimal Q dispatch of the DVC at Phase C in winter and local control schemes.

References

[10] Sadigh, A. Khoshkbar, and K. M. Smedley. "Review of voltage compensation methods in dynamic voltage restorer (DVR)." 2012 IEEE Power and Energy Society General Meeting. IEEE, 2012.
[11] Monti, Antonello, et al. Converter-based dynamics and control of modern power systems. Academic Press, 2020.
[12] Singh, Bhim, and Sabha Raj Arya. "Design and control of a DSTATCOM for power quality improvement using cross correlation function approach." International Journal of Engineering, Science and Technology 4.1 (2012): 74-86.
[13] Kumar, Chandan, and Mahesh K. Mishra. "A voltage-controlled DSTATCOM for power-quality improvement." IEEE transactions on power delivery 29.3 (2014): 1499-1507.
[14] Wang, Caisheng, and M. Hashem Nehrir. "Analytical approaches for optimal placement of distributed generation sources in power systems." IEEE Transactions on Power systems 19.4 (2004): 2068-2076.
[15] Keane, Andrew, and Mark O'malley. "Optimal allocation of embedded generation on distribution networks." IEEE Transactions on Power Systems 20.3 (2005): 1640-1646.
[16] Gözel, Tuba, and M. Hakan Hocaoglu. "An analytical method for the sizing and siting of distributed generators in radial systems." Electric power systems research 79.6 (2009): 912-918.
[17] Soroudi, Alireza, and Mozhgan Afrasiab. "Binary PSO-based dynamic multi-objective model for distributed generation planning under uncertainty." IET renewable power generation 6.2 (2012): 67-78.
[18] Abdi, Sh, and K. Afshar. "Application of IPSO-Monte Carlo for optimal distributed generation allocation and sizing." International Journal of Electrical Power & Energy Systems 44.1 (2013): 786-797.
[19] Moradi, Mohammad Hasan, and M. Abedini. "A combination of genetic algorithm and particle swarm optimization for optimal DG location and sizing in distribution systems." International Journal of Electrical Power & Energy Systems 34.1 (2012): 66-74.
[20] Tan, Wen Shan, et al. "Multi-distributed generation planning using hybrid particle swarm optimisation-gravitational search algorithm including voltage rise issue." IET Generation, Transmission & Distribution 7.9 (2013): 929-942.
[21] Photovoltaics, Distributed Generation, and Energy Storage. "IEEE standard for interconnection and interoperability of distributed energy resources with associated electric power systems interfaces." IEEE Std 1547 (2018): 1547-2018.
[22] Jahangiri, Pedram, and Dionysios C. Aliprantis. "Distributed Volt/VAr control by PV inverters." IEEE Transactions on power systems 28.3 (2013): 3429-3439.
[23] Zhu, Hao, and Hao Jan Liu. "Fast local voltage control under limited reactive power: Optimality and stability analysis." IEEE Transactions on Power Systems 31.5 (2015): 3794-3803.
[24] Singhal, Ankit, et al. "Real-time local volt/var control under external disturbances with high PV penetration." IEEE Transactions on Smart Grid 10.4 (2018): 3849-3859.
[25] Lee, Han Pyo, et al. "Adopting Dynamic VAR Compensators to Mitigate PV Impacts on Unbalanced Distribution Systems." IEEE Access (2023). Available online at: https://ieeexplore.ieee.org/

9.8 Task D.1 PV Power Tracking for Providing Power Reserves and Fast Frequency Response

Background: There are several PV power curtailment and PV maximum power point estimation (MPPE) techniques proposed in the literature; however, not much work has been done to combine power curtailment and MPPE methods to achieve a better performance for both algorithms. In this task, we developed an algorithm that combines a modified robust perturb-and-observe (P&O) flexible power point tracking (FPPT) technique with a real-time curve-fitting-based MPPE that can be applied to both single-stage and two-stage PV system topologies. The algorithm was first introduced in the literature in our published paper [1]. By leveraging information provided by the MPPE, we were able to create a fast convergence technique for tracking power-reference changes within three steps of the FPPT, which can be used to help reduce frequency drops during grid disturbances. This is especially useful when operating the PV farm in low-inertia weak grids such as microgrids. In addition, as the U.S. energy policies move towards more renewable energy integration, this method can be utilized to allow utility-scale PV farms to provide frequency support while maintaining power reserves as if they were composed by battery-energy-storage systems, with the advantage of being much cheaper.

Table I summarizes the advantages and disadvantages of the state-of-the-art methods. As can be seen in the table, up till now, all existing generative methods require the format of the input and output to be fixed. However, in practice, the duration of missing data (model output) varies from minutes to several hours, and the length and number of available measurements (model input) also vary case by case. To cope with the varying-length cases, traditional methods need either increase the output window to cover the longest event or train separate models for different scenarios.

TABLE I : Comparison of STATE-OF-THE-ART ON PV Power Curtailment and MPPE Methods

	Description	Advantages	Disadvantages
Adaptive FPPT Method [13]	Use physical system models to simulate responses to external disturbances in hope of restoring missing data segments.	Robust and superior transient performance when compared to conventional P&O methods.	Does not provide fast convergence or maximum power point estimation for maintaining power reserves for grid support.
Use a subset of PV Inverters as MPP References [16]-[17]	By operating a few pilot inverters at MPP, they could be used as references for estimating the total power available in a farm.	Easy to implement.. Ideal for large farms with identical arrays. Can utilize conventional power setpoint tracking methods.	Only applicable to large farms with identical arrays. Cannot provide fast frequency response. Can suffer performance if pilot arrays are not rotated regularly (as proposed in [16]).
Real-time curve-fitting technique from [18]-[19]	Utilize real-time curve fitting for finding incident irradiance and temperature at the panel with higher accuracy and without need for sensors.	Can provide very accurate MPPE without need for sensors (cheaper implementation), based on conventional PI controllers.	Requires an external ripple for proper convergence. Cannot provide fast and robust power-setpoint tracking due to trade-offs between speed and robustness in PI controller performance.
Combined power curtailment and MPPE method introduced in [20]-[21]	Methods that proposed the combination of power curtailment and MPPE methods for improved performance of both algorithms.	Can quickly provide MPPE without the need for sensors while providing conventional tracking capability.	Only applicable to two-stage PV system that operates on left side of the MPP. Does not provide fast frequency response support.

Task Objectives:

- Develop a PV system power setpoint tracking algorithm capable of maintaining power reserves that can be used as back-up power for dealing with uncertainties and PV intermittency during the distribution grid blackstart process.
- Develop a fast frequency response capability that is especially helpful when operating in weak grids with low inertia which can help maintain frequency above load shedding during disturbances.

Methodology Overview: The circuit and control block diagram of a utility-scale PV system is shown in Fig. 1. A hierarchical control structure composed of a dc-link voltage controller cascaded with a current controller is used to generate the inverter modulation signal '*m*'. More details regarding the generation of the modulation signal and the PV array model are given in one of our papers [13]. The main novel functionalities developed in this task are related to the power setpoint tracking algorithm highlighted in the bottom left side of the figure. By utilizing information from an MPPE algorithm, the FPPT method can quickly find what should be the voltage reference for the dc-link (V_{dc}*) to achieve the desired power injected into the grid.

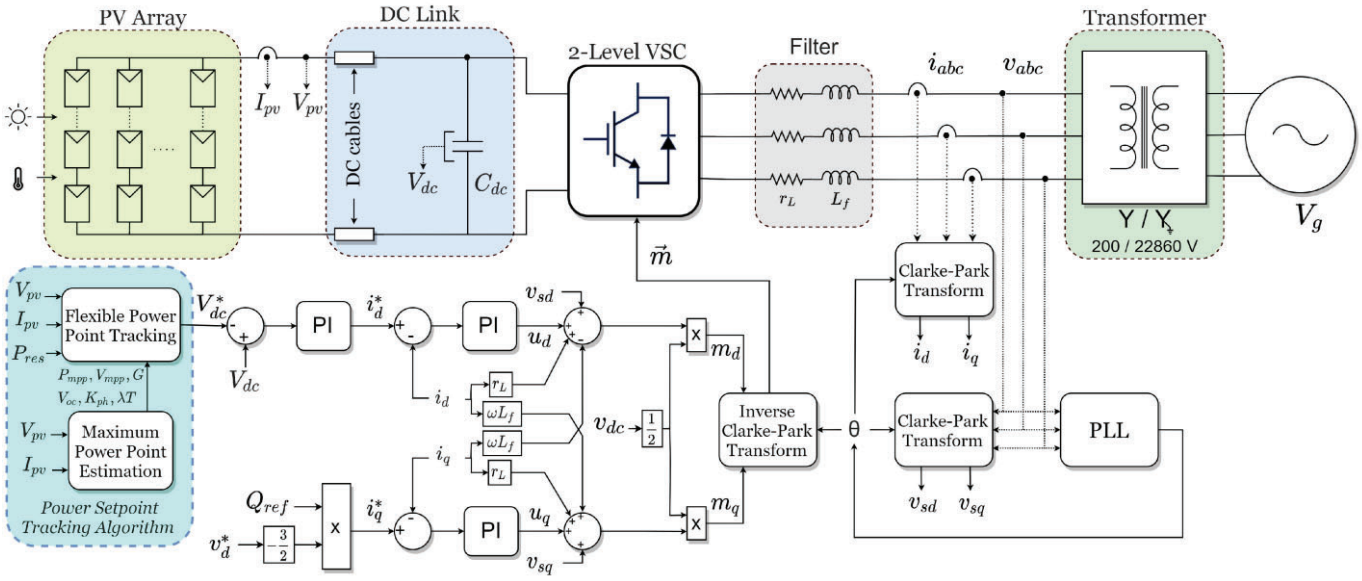

Fig. 1. Circuit and control system block diagrams of a utility-scale PV system.

Simulation Results: Figure 2 demonstrates a comparison between one of the state-of-the-art power curtailment algorithms (from [12]) and the algorithm we present [1], which includes a fast convergence technique. Due to the fast convergence capability, the algorithm is able to quickly achieve new setpoints, reducing the overall tracking error (T.E.) from 9.166% to 1.758%. In Fig. 3, we setup a scenario in which a 2 MVA utility-scale PV plant and a 3.125 MVA diesel generator are used to pick-up cold-loads from a distribution grid in steps of 0.5 MVA. Fig. 4 demonstrates the microgrid frequency under one of the cold-load pick-ups. As shown in Fig. 16, the proposed method outperforms the state-of-the-art method from [12] by reducing the frequency nadir during the cold-load pickup thanks to its faster power setpoint tracking convergence capability.

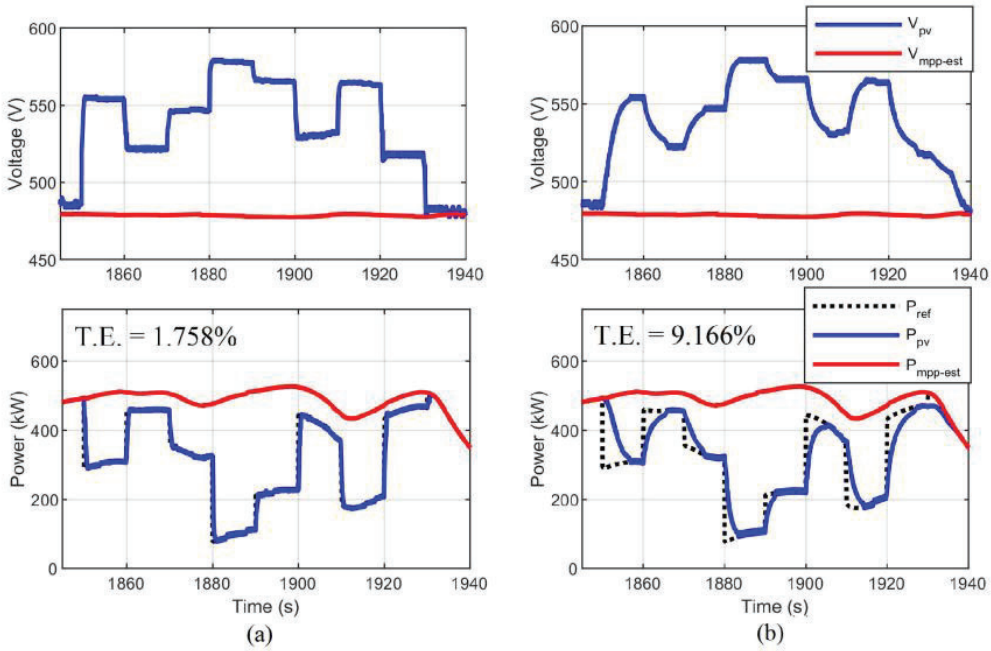

Fig. 2. Comparison of the power setpoint tracking performance under irradiance intermittency between (a) the proposed RST method and (b) the adaptive FPPT (state-of-the-art).

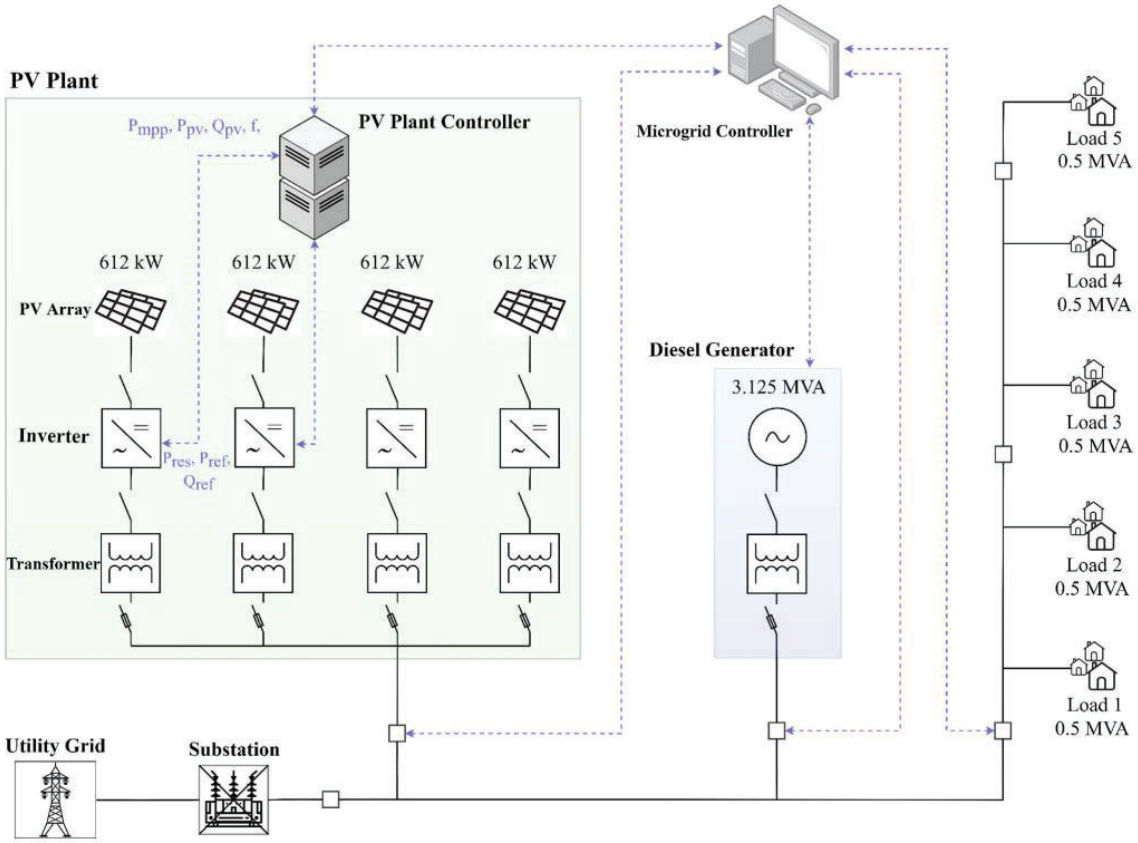

Fig. 3. Configuration of a feeder-level microgrid.

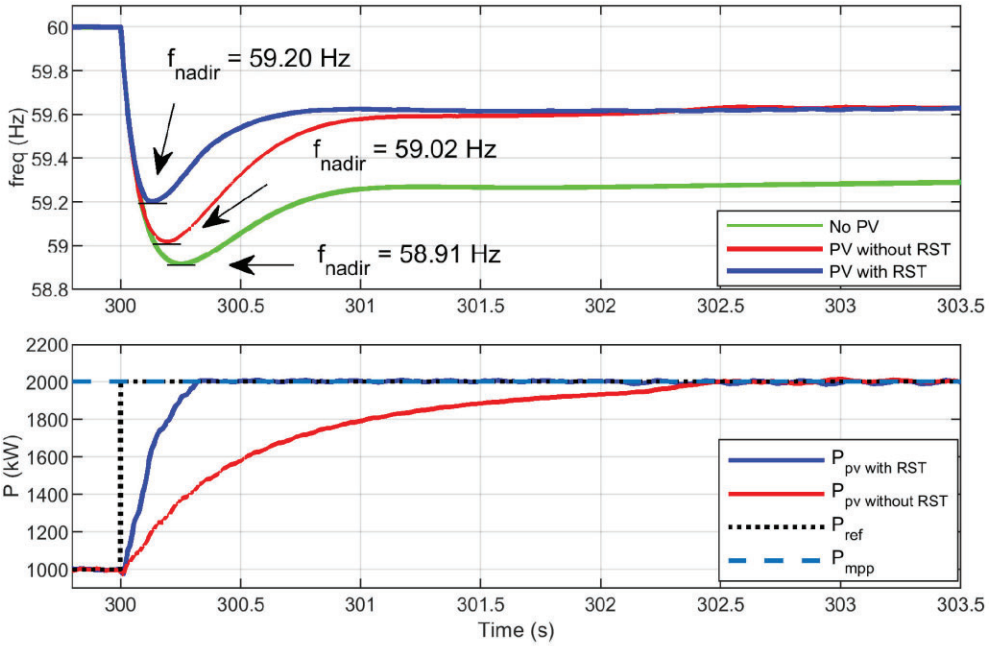

Fig. 4. Frequency and voltage plots during microgrid cold-load pickup

References

[1] V. D. Paduani, H. Yu, B. Xu and N. Lu, "A Unified Power-Setpoint Tracking Algorithm for Utility-Scale PV Systems With Power Reserves and Fast Frequency Response Capabilities," in *IEEE Transactions on Sustainable Energy*, vol. 13, no. 1, pp. 479-490, Jan. 2022, doi: 10.1109/TSTE.2021.3117688.

[2] Standard for Interconnection and Interoperability of Distributed Energy Resources With Associated Electric Power Systems Interfaces, IEEE Std. 1547-2018, I. S. Association et al., 2018.

[3] Pacific Gas and Electric Company (PG&E). “Electric rule no.21 generating facility interconnections.” [Online]. Available: https://www.pge.com/ tariffs/assets/pdf/tariffbook/ELEC_RULES_21.pdf.

[4] K. Ishaque, Z. Salam, M. Amjad, and S. Mekhilef, “An improved particle swarm optimization (PSO)-based MPPT for PV with reduced steady-state oscillation,” IEEE Trans. Power Electron., vol. 27, no. 8, pp. 3627–3638, Aug. 2012.

[5] A. Hoke and D. Maksimovi´c, “Active power control of photovoltaic power systems,” in Proc. 1st IEEE Conf. Technol. Sustainability, 2013, pp. 70–77.

[6] A. F. Hoke, M. Shirazi, S. Chakraborty, E. Muljadi, and D. Maksimovic, “Rapid active power control of photovoltaic systems for grid frequency support,” IEEE Trans. Emerg. Sel. Top. Power Electron., vol. 5, no. 3, pp. 1154–1163, Sep. 2017.A. F. Hoke, M. Shirazi, S. Chakraborty, E. Muljadi, and D. Maksimovic, “Rapid active power control of photovoltaic systems for grid frequency support,” IEEE Trans. Emerg. Sel. Top. Power Electron., vol. 5, no. 3, pp. 1154–1163, Sep. 2017.

[7] J. M. Blanes, F. J. Toledo, S. Montero, and A. Garrigós, “In-site realtime photovoltaic I-V curves and maximum power point estimator,” IEEE Trans. Power Electron., vol. 28, no. 3, pp. 1234–1240, Mar. 2013.Han Pyo Lee, Lidong Song, Yiyan Li, Ning Lu, Di Wu, PJ Rehm, Matthew Makdad, Edmond Miller, "An Iterative Bidirectional Gradient Boosting Algorithm for CVR Baseline Estimation" 23PESGM0022, submitted to 2023 IEEE PES General Meeting, Available online at: http://arxiv.org/abs/2211.03733. . (An alternative approach: Conference publication from another subtask)

[8]] M. A. G. De Brito, L. Galotto, L. P. Sampaio, G. D. A. e Melo, and C. A. Canesin, “Evaluation of the main MPPT techniques for photovoltaic applications,” IEEE Trans. Ind. Electron., vol. 60, no. 3, pp. 1156–1167, Mar. 2013.Oyedokun, James, et al. "Customer baseline load estimation for incentive-based demand response using long short-term memory recurrent neural network." 2019 IEEE PES Innovative Smart Grid Technologies Europe (ISGT-Europe). IEEE, 2019.

[9] T. K. Soon and S. Mekhilef, “A fast-converging MPPT technique for photovoltaic system under fast-varying solar irradiation and load resistance,” IEEE Trans. Ind. Informat., vol. 11, no. 1, pp. 176–186, Feb. 2015.

[10] J. Ahmed and Z. Salam, “An enhanced adaptive P&O MPPT for fast and efficient tracking under varying environmental conditions,” IEEE Trans. Sustain. Energy, vol. 9, no. 3, pp. 1487–1496, Jul. 2018.
[11] A. Sangwongwanich, Y. Yang, F. Blaabjerg, and H. Wang, “Benchmarking of constant power generation strategies for single-phase grid-connected photovoltaic systems,” IEEE Trans. Ind. Appl., vol. 54, no. 1, pp. 447–457, Jan./Feb. 2018.
[12] H. D. Tafti et al., “Extended functionalities of photovoltaic systems with flexible power point tracking: Recent advances,” IEEE Trans. Power Electron., vol. 35, no. 9, pp. 9342–9356, Sep. 2020.
[13] H. D. Tafti, A. Sangwongwanich, Y. Yang, J. Pou, G. Konstantinou, and F. Blaabjerg, “An adaptive control scheme for flexible power point tracking in photovoltaic systems,” IEEE Trans. Power Electron., vol. 34, no. 6, pp. 5451–5463, Jun. 2019.
[14] V. Paduani, L. Song, B. Xu, and N. Lu, “Maximum power reference tracking algorithm for power curtailment of photovoltaic systems,” in IEEE Power Energy Soc. Gen. Meeting, 2021, pp. 1–5.
[15] V. Gevorgian and B. O’Neill, “Advanced grid-friendly controls demonstration project for utility-scale PV power plants,” National Renewable Energy Laboratory(NREL), Golden, CO, USA, Tech. Rep. NREL/TP5D00-65368, Jan. 2016, pp. 30–57.
[16] A. Sangwongwanich, Y. Yang, F. Blaabjerg, and D. Sera, “Delta power control strategy for multistring grid-connected PV inverters,” IEEE Trans. Ind. Appl., vol. 53, no. 4, pp. 3862–3870, Jul./Aug. 2017.
[17] V. Gevorgian, “Highly accurate method for real-time active power reserve estimation for utility-scale photovoltaic power plants,” National Renewable Energy Laboratory (NREL), Golden, CO, USA, Tech. Rep. NREL/TP-5D00-73207, Feb. 2019, pp. 1–24.
[18] E. I. Batzelis, G. E. Kampitsis, and S. A. Papathanassiou, “Power reserves control for PV systems with real-time mpp estimation via curve fitting,” IEEE Trans. Sustain. Energy, vol. 8, no. 3, pp. 1269–1280, Jul. 2017.
[19] E. I. Batzelis, A. Junyent-Ferre, and B. C. Pal, “MPP estimation of PV systems keeping power reserves under fast irradiance changes,” in Proc. IEEE Power Energy Soc. Gen. Meeting, 2020, pp. 1–5.
[20] Y. Zhu, H. Wen, G. Chu, Y. Hu, X. Li, and J. Ma, “High-performance photovoltaic constant power generation control with rapid maximum power point estimation,” IEEE Trans. Ind. Appl., vol. 57, no. 1, pp. 714–729, Jan./Feb. 2021.
[21] X. Li, H. Wen, Y. Zhu, L. Jiang, Y. Hu, and W. Xiao, “A novel sensorless photovoltaic power reserve control with simple real-time MPP estimation,” IEEE Trans. Power Electron., vol. 34, no. 8, pp. 7521–7531, Aug. 2019.

9.9 Task D.2 A Real-Time EMT-TS Modeling Architecture for Feeder Blackstart Simulations

Background: In this task, we developed and assessed an innovative real-time architecture for Electromagnetic Transient and Transient Stability (EMT-TS) modeling, specifically designed for distribution feeder restoration studies. Notably, we established, for the first time in the literature, a real-time EMT-TS testbed. This testbed features a grid-forming unit simulated in the EMT domain, operating as the slack bus of the phasor domain during the restoration process of a distribution feeder, even under unbalanced voltage conditions. While EMT tools offer in-depth analysis across a broad frequency range (compared to TS), their computational cost becomes impractical for simulating larger grids with numerous components. To address this, we integrated EMT-modeled power electronic systems into the TS-modeled distribution network. This co-simulation approach proves computationally feasible and provides an effective method for simulating grids under high penetration of Inverter-Based Resources (IBRs), such as Battery Energy Storage Systems (BESS).

Task Objectives:

- Introduce a new method to model a real-time EMT-TS testbed in which the grid-forming unit is modeled in EMT domain, operating as the slack bus of the phasor domain including unbalanced voltage conditions.
- Present a coupling method for multiple coupling points between the EMT and phasor domains for moving devices across the feeder into the EMT domain as desired.

Methodology Overview: Figure 1 displays the EMT-TS testbed, which consists of a microgrid connected to a distribution feeder via a point of common coupling (PCC). The components are split into two subsystems. The first includes DERs such as BESS, diesel generators, and PV systems, and a grounding transformer, which is needed to provide grounding when the feeder is disconnected from the substation. This subsystem is simulated at microsecond level in eMEGASIM, whereas the second is simulated in ePHASORSIM at the millisecond level, including distributed rooftop PVs, shunt capacitor banks, voltage regulators, ZIP load models, and the distribution feeder. Due to the parallel operation of the subsystems in real-time, there is a delay for events to propagate from one to another.

Simulation Results: We apply load steps both to the proposed EMT-TS co-simulation architecture, and to a full EMT simulation of the exact same system to compare performance, with the full EMT being the benchmark. Two different types of grid-forming units are analyzed: a 2 MVA BESS (parameters from [14]), and a 3.125 MVA diesel generator (parameters from [15]). The voltage and frequency dynamic responses are shown in Fig. 2 for a step of 1978 kVA. The RMS error (RMSE) between the EMT and EMT-TS curves is included in the figure of each test, with the highest RMSE value corresponding to the phase with the largest deviation. A maximum voltage RMSE of 0.03 p.u. is observed for the BESS; however, note this is an extreme scenario and thus, represents the upper bound of the modeling error. A comprehensive list of test results is demonstrated in [1], showing that the EMT-TS testbed can greatly match its EMT counterpart, with the advantage of requiring only one tenth of the EMT testbed computational effort.

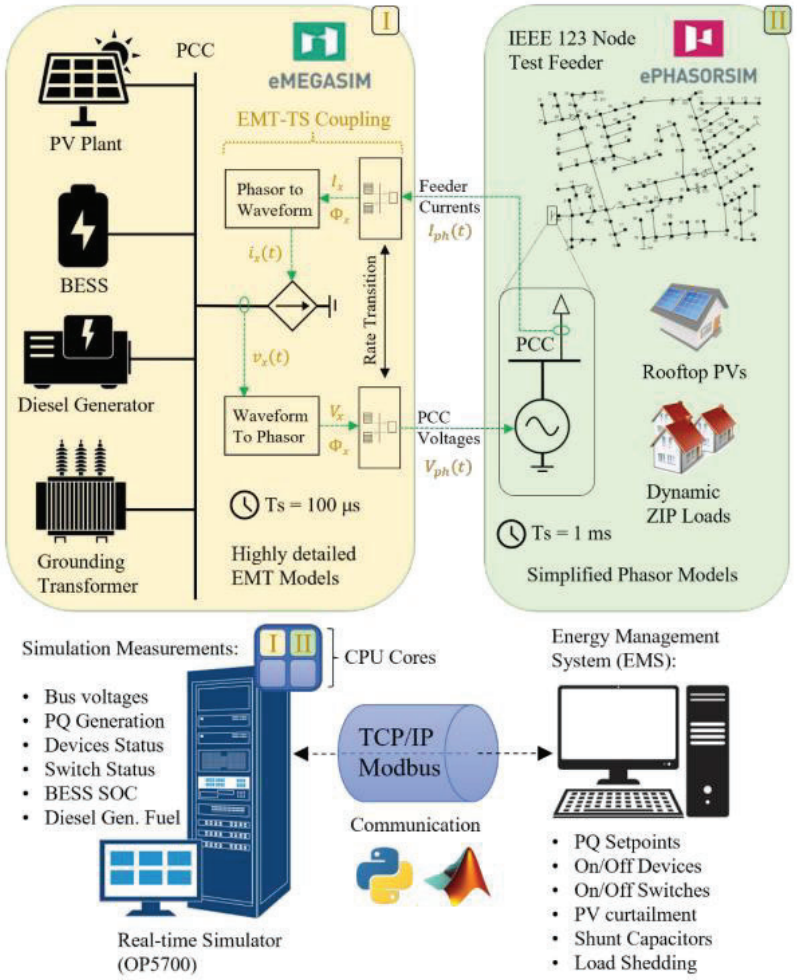

Fig. 1. Proposed EMT-TS co-simulation testbed framework.

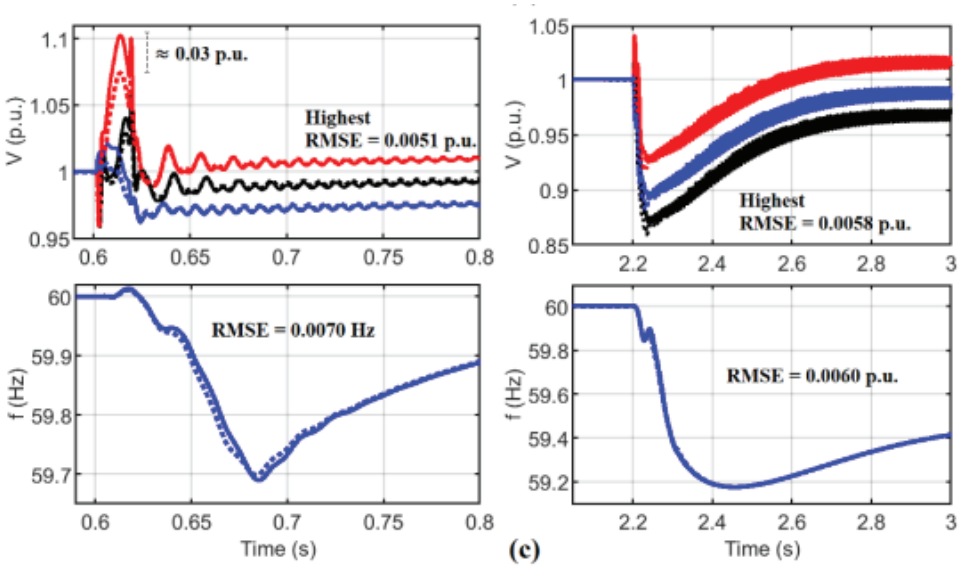

Fig. 2. Transient response comparison between an EMT-TS and a full EMT testbed.

References

[1] V. Paduani, B. Xu, D. Lubkeman and N. Lu, "Novel Real- Time EMT- TS Modeling Architecture for Feeder Blackstart Simulations," *2022 IEEE Power & Energy Society General Meeting (PESGM)*, Denver, CO, USA, 2022, pp. 1-5, doi: 10.1109/PESGM48719.2022.9917086..

[2] V. Paduani, L. Song, B. Xu, and N. Lu, “Maximum power reference tracking algorithm for power curtailment of photovoltaic systems,” in 2021 IEEE Power & Energy Society General Meeting (PESGM). IEEE, 2021, pp. 1–5.

[3] V. Paduani and N. Lu, “Implementation of a two-stage PV system testbed with power reserves for grid-support applications,” in 2021 North American Power Symposium, 2021, pp. 1–6.

[4] H. Jain, B. A. Bhatti, T. Wu, B. Mather, and R. Broadwater, “Integrated transmission-and-distribution system modeling of power systems: Stateof-the-art and future research directions,” Energies, vol. 14, no. 1, p. 12, 2021.

[5] D. Shu, X. Xie, Q. Jiang, Q. Huang, and C. Zhang, “A novel interfacing technique for distributed hybrid simulations combining emt and transient stability models,” IEEE Transactions on Power Delivery, vol. 33, no. 1, pp. 130–140, 2017.

[6] A. Shirsat, V. Muthukaruppan, R. Hu, N. Lu, M. Baran, D. Lubkeman, and W. Tang, “Hierarchical multi-timescale framework for operation of dynamic community microgrid,” arXiv preprint arXiv:2011.10087, 2020.

[7] R. S. Mongrain, Z. Yu, and R. Ayyanar, “A real-time simulation testbed for hierarchical control of a renewable energy-based microgrid,” in 2019 IEEE Texas Power and Energy Conference (TPEC). IEEE, 2019, pp. 1–6.

[8] D. Athaide, J. Qin, and Y. Zou, “Matlab/simulink-based electromagnetic transient-transient stability hybrid simulation for electric power systems with converter interfaced generation,” in 2019 IEEE Texas Power and Energy Conference (TPEC). IEEE, 2019, pp. 1–6.

[9] H. Konara Mudiyanselage, “Interfacing a transient stability model to a real-time electromagnetic transient simulation using dynamic phasors,” 2020.

[10] X. Song, H. Cai, T. Jiang, T. Sennewald, J. Kircheis, S. Schlegel, L. N. Martinez, Y. Benzetta, and D. Westermann, “Research on performance of real-time simulation based on inverter-dominated power grid,” IEEE Access, vol. 9, pp. 1137–1153, 2020.

[11] IEEE 123 Node Test Feeder. [Online]. Available: http://sites.ieee.org/ pes-testfeeders/resources/.

[12] F. Plumier, P. Aristidou, C. Geuzaine, and T. Van Cutsem, “Cosimulation of electromagnetic transients and phasor models: A relaxation approach,” IEEE Transactions on Power Delivery, vol. 31, no. 5, pp. 2360–2369, 2016.

[13] C. Dufour, J. Mahseredjian, and J. Belanger, “A combined state-space ´ nodal method for the simulation of power system transients,” IEEE Transactions on Power Delivery, vol. 26, no. 2, pp. 928–935, 2010.

[14] B. Xu, V. Paduani, D. Lubkeman, and N. Lu, “A novel grid-forming voltage control strategy for supplying unbalanced microgrid loads using inverter-based resources,” arXiv preprint arXiv:2111.09464, 2021.

[15] V. Paduani, H. Yu, B. Xu, and N. Lu, “A Unified Power-Setpoint Tracking Algorithm for Utility-Scale PV systems with Power Reserves and Fast Frequency Response Capabilities,” IEEE Transactions on Sustainable Energy, pp. 1–12, 2021.

[16] F. Xie, C. McEntee, M. Zhang, and N. Lu, “An asynchronous real-time co-simulation platform for modeling interaction between microgrids and power distribution systems,” in 2019 IEEE Power & Energy Society General Meeting (PESGM). IEEE, 2019, pp. 1–5.

9.10 Task D.3 A Grid-forming Voltage Control Strategy for Supplying Unbalanced Microgrid Loads using Inverter-based Resources

Background: This task introduces a grid-forming (GFM) voltage control strategy designed for a battery energy storage system to uphold balanced three-phase output voltages while serving unbalanced loads. The proposed control scheme operates in a stationary reference frame (αβ) and regulates positive-sequence (PS) and negative-sequence (NS) voltages. Additionally, a grounding transformer (GT) is employed to mitigate the zero-sequence (ZS) voltage. The advantages and disadvantages of existing unbalance control methods are summarized in Table I [1]-[6].

Based on the outcomes, a power-voltage unbalance curve is derived for various output transformer configurations, establishing the relationship between the power unbalance factor (PUF) and the voltage unbalance factor (VUF) for microgrid power scheduling.

TABLE I. Comparison of STATE-OF-THE-ART unbalance voltage control methods

Method	Description	Advantages	Disadvantages
dq-based control scheme [1]-[5]	Use two pairs of PI controllers, which situate in two reference frames while rotating in the opposite directions.	Reliable, easy to implement	Need band-stop filters, introduce filter delay and slow down regulation speed.
αβ-based control scheme [11]-[11]	Require one pair of PR controllers for voltage regulation in AC domain.	Better unbalance regulation performance, simplified computational burden	Hard to find the good control gains.

Task Objectives:

- Developed a grid-forming voltage control strategy to maintain balanced three-phase output voltages when serving unbalanced loads.
- Derived the relationship between power and voltage unbalance and introduce a performance metric for regulating power unbalance to meet inverter voltage unbalance requirements.

Methodology Overview: The topology and control scheme are illustrated in Fig. 1. The voltage reference of the inner voltage controller, v_o^*, is generated using the conventional droop and secondary control methods [8]-[9]. Notably, there is no requirement for decomposing the positive-sequence (PS) and negative-sequence (NS) components. The inner voltage control operates on an αβ-based controller, successfully achieving NS regulation without the need for an unbalance compensator, as depicted in Fig. 2. Furthermore, a grounding transformer (GT) has been incorporated into the circuit to alleviate the impact of zero-sequence (ZS) currents on voltage regulation, ensuring balanced Point of Common Coupling (PCC) voltage [10].

Simulation Results: As depicted in Fig. 3, when the data granularity is set at 5-min and 15-min intervals, the steady-state values of Point of Common Coupling (PCC) voltage and current remain consistent in both cases. This suggests that both control schemes exhibit commendable current tracking performance in steady-state conditions. However, the dynamic performance of the αβ-based control scheme stands out significantly. Additionally, as illustrated in Fig. 4, when employing a Y-Yg output transformer, Voltage Unbalance Factor (VUF) [11]-[14] can be regulated within 3% only when Power Unbalance Factor (PUF) [7] is 30% or less. The introduction of a Grounding

Transformer (GT) to the Y-Yg output transformer enhances the system's capability to supply unbalanced loads, regulating VUF within 3% even when PUF is 55% or less, marking a substantial improvement.

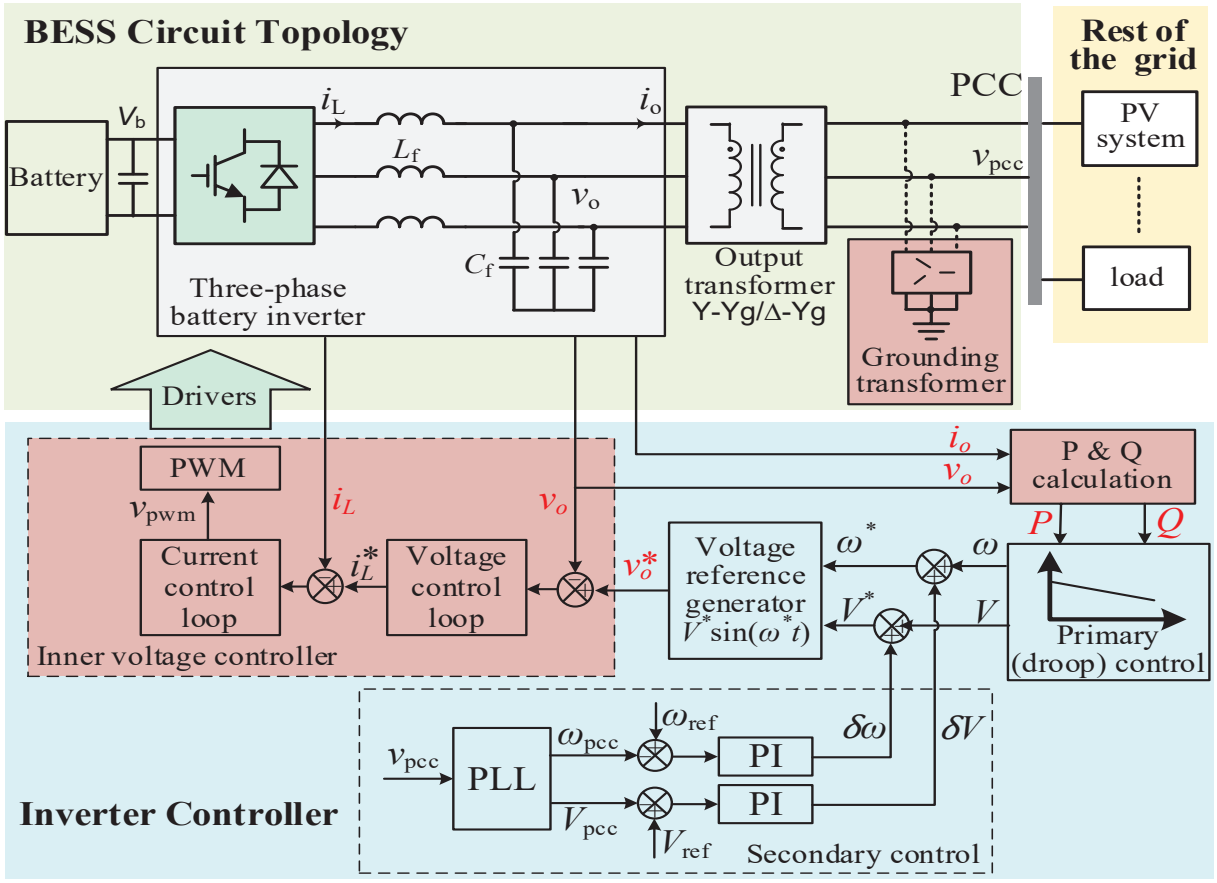

Figure 1. Topology and control structure of a three-phase grid-forming BESS.

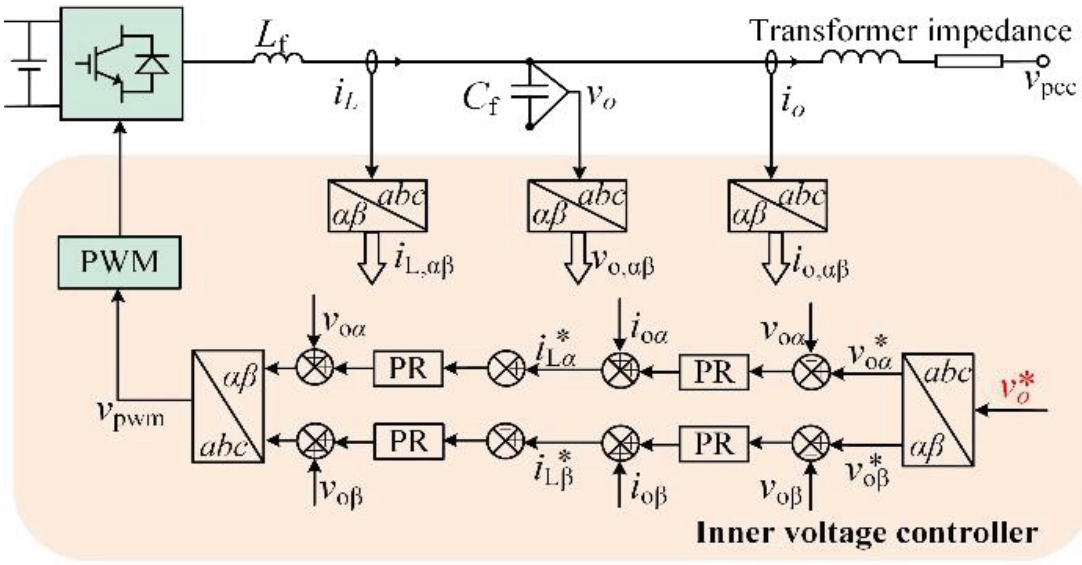

Figure 2. Control diagram of the αβ SRF-based inner voltage controller.

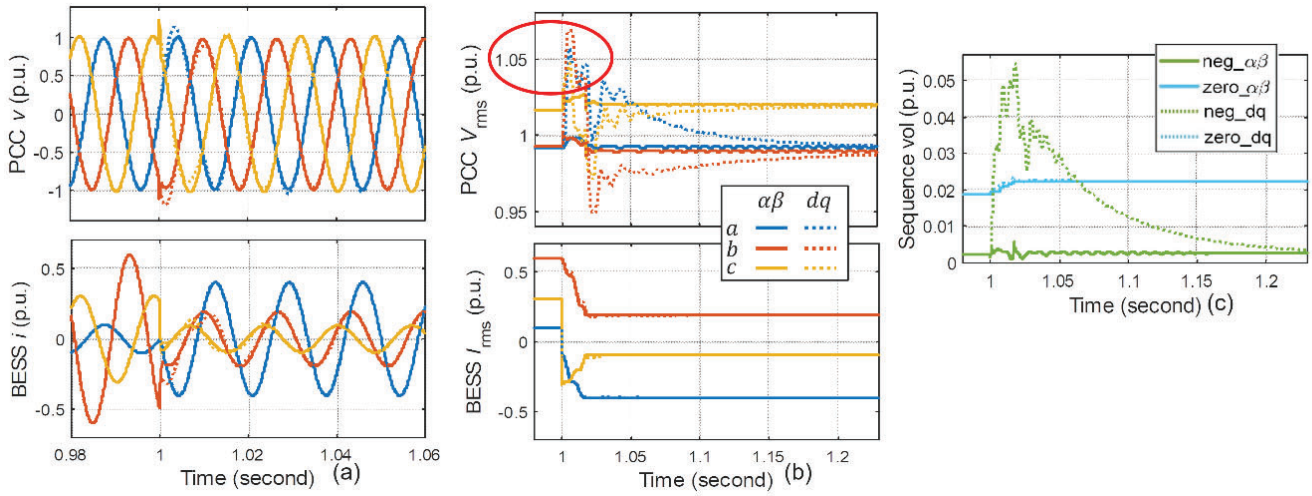

Fig. 3. Performance comparison of αβ-based and dq-based control methods. (a) Time-series waveforms of PCC voltage and current; (b) RMS profiles of PCC voltage and BESS current; (c) NS and ZS PCC voltage.

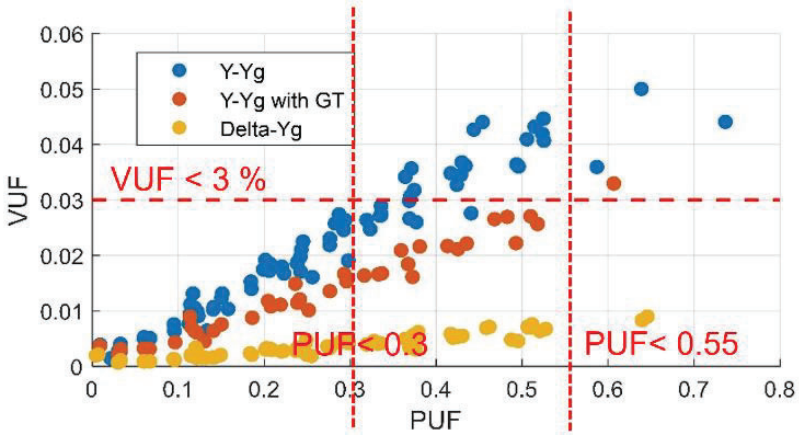

Fig. 4. PUF versus VUF for different transformer configurations.

References

[1] I. Vechiu, O. Curea, and H. Camblong, “Transient operation of a four-leg inverter for autonomous applications with unbalanced load,” IEEE Transactions on Power Electronics, vol. 25, no. 2, pp. 399–407, 2009.
[2] X. Zhang and J. Wang, “Research on phase-locked control strategy for three-phase combined inverters,” in 2009 Third International Conference on Genetic and Evolutionary Computing. IEEE, 2009, pp. 260–263.
[3] N. Tleis, Power systems modelling and fault analysis: theory and practice. Elsevier, 2007.
[4] H. Cai, P. Zhang, H. Zhao, J. Shi, W. Yao, and X. He, “Controller design for three-phase inverter with power unbalanced loads applied in microgrids,” in 2015 IEEE Energy Conversion Congress and Exposition (ECCE). IEEE, 2015, pp. 4588–4593.
[5] M. Savaghebi, A. Jalilian, J. C. Vasquez, and J. M. Guerrero, “Autonomous voltage unbalance compensation in an islanded droop-controlled microgrid,” IEEE Transactions on Industrial Electronics, vol. 60, no. 4, pp. 1390–1402, 2012.
[6] X. Zhao, X. Wu, L. Meng, J. M. Guerrero, and J. C. Vasquez, “A direct voltage unbalance compensation strategy for islanded microgrids,” in 2015 IEEE Applied Power Electronics Conference and Exposition (APEC). IEEE, 2015, pp. 3252–3259.
[7] B. Xu, V. Paduani, H. Yu, D. Lubkeman, and N. Lu. "A novel grid-forming voltage control strategy for supplying unbalanced microgrid loads using inverter-based resources." In 2022 IEEE Power & Energy Society General Meeting (PESGM), pp. 1-5. IEEE, 2022.
[8] J. M. Guerrero, J. C. Vasquez, J. Matas, L. G. De Vicuna, and ˜ M. Castilla, “Hierarchical control of droop-controlled ac and dc microgrids—a general approach toward standardization,” IEEE Transactions on industrial electronics, vol. 58, no. 1, pp. 158–172, 2010.
[9] R. Aboelsaud, A. Ibrahim, and A. G. Garganeev, “Review of three-phase inverters control for unbalanced load compensation,” International Journal of Power Electronics and Drive Systems, vol. 10, no. 1, p. 242, 2019.
[10] A. Vukojevic and S. Lukic, “Microgrid protection and control schemes for seamless transition to island and grid synchronization,” IEEE Transactions on Smart Grid, vol. 11, no. 4, pp. 2845–2855, 2020.
[11] “IEEE draft recommended practice for establishing methods and procedures that provide supplemental support for implementation strategies for expanded use of ieee standard 1547,” IEEE P1547.8/D8, July 2014, pp. 1–176, 2014.
[12] “IEEE recommended practice for monitoring electric power quality,” IEEE Std 1159-2009 (Revision of IEEE Std 1159-1995), pp. 1–94, 2009.
[13] “Motors and generators,” NEMA Standard MG1-1993, NEMA Std., 1993.
[14] F. Shahnia, P. J. Wolfs, and A. Ghosh, “Voltage unbalance reduction in low voltage feeders by dynamic switching of residential customers among three phases,” IEEE Transactions on Smart Grid, vol. 5, no. 3, pp. 1318–1327, 2014.

9.11 Task D.4 Under-frequency Load Shedding for Power Reserve Management in Islanded Microgrids

Background: This task introduces under-frequency load shedding (UFLS) schemes specifically tailored to meet power reserve requirements in islanded microgrids (MGs) featuring only one grid-forming (GFM) resource for frequency regulation. In instances where MG power consumption exceeds a predefined threshold, the MG frequency is gradually lowered to various setpoints, triggering UFLS for varying levels of load reduction. A detailed comparison between conventional UFLS and the proposed UFLS is provided in Table I.

Traditionally, UFLS serves as an emergency response mechanism to avert frequency collapse in large-scale power systems [1][2]. In contrast, the proposed UFLS method prioritizes preserving power reserves in an islanded MG during regular operation to fulfill the power reserve requirement (PRR).

TABLE 1: COMPARISON OF EXISTING AND PROPOSED UNDER-FREQUENCY LOAD SHEDDING SCHEMES

Method	Object	Operation Condition	Triggered by	UFLS Execution	Control Mechanism	3-Phase Imbalance	Power Surge
Traditional UFLS method	Recover system frequency	Emergency response	Large frequency drops due to outages	UFLS relays [3]-[5]	Autonomous [3]-[5]	No	No
				Controllable loads [6]-[9]	Centralized [6]-[8] Decentralized [9]		
Developed UFLS method [10]	Keep power reserve margin	Normal operation	Low power reserve	Sectionalizers	Autonomous	No	Yes
				Smart meters; Controllable appliances		Yes	

Task Objectives:

- Develop the UFLS scheme capable of providing power reserve for the GFM device to maintain sufficient power regulation headroom. The scheme can operate an isolated microgrid autonomously for extended durations during outages without dependence on robust communication networks.
- Implement a per-phase UFLS strategy to efficiently manage and mitigate three-phase imbalances within the grid.

Methodology Overview: As depicted in Fig. 1, in an islanded MG, three controllable devices can be used to implement UFLS: sectionalizers (e.g., S1-S6), which can turn on/off an entire load group (LG); smart meters (e.g., SM1-SM6), capable of turning on/off an entire building/house; and controllable appliances (e.g., APP1 and APP2). In this task, we assume that there is only one GFM BESS in the islanded MG. This allows us to use the simplified frequency control structure depicted in Fig. 2 to modulate the system frequency as the UFLS control signal [11]-[13]. A UFLS device is characterized by four vital control parameters [14] [15]: the triggering frequency threshold (f_{TH}), the tripping delay (τ_1), fixed recovery delay (τ_2), and the random recovery delay (τ_{rand}), as depicted in Fig. 3.

Simulation Results: Simulation results confirm the effectiveness of the proposed methods in replenishing power reserves and sustaining phase power balance. In the context of appliance-based UFLS, the power output of the BESS gradually diminishes and subsequently recovers while meeting PRR (see Fig. 4(b)). This contrasts with the sectionalizer-based scenario (see Fig. 4(a)),

where an abrupt drop or immediate rebound is observed. Moreover, the appliance-based UFLS enables a more precise per-phase load shedding in a gradual fashion, contributing to better-balanced three-phase voltage and the ability to serve more loads.

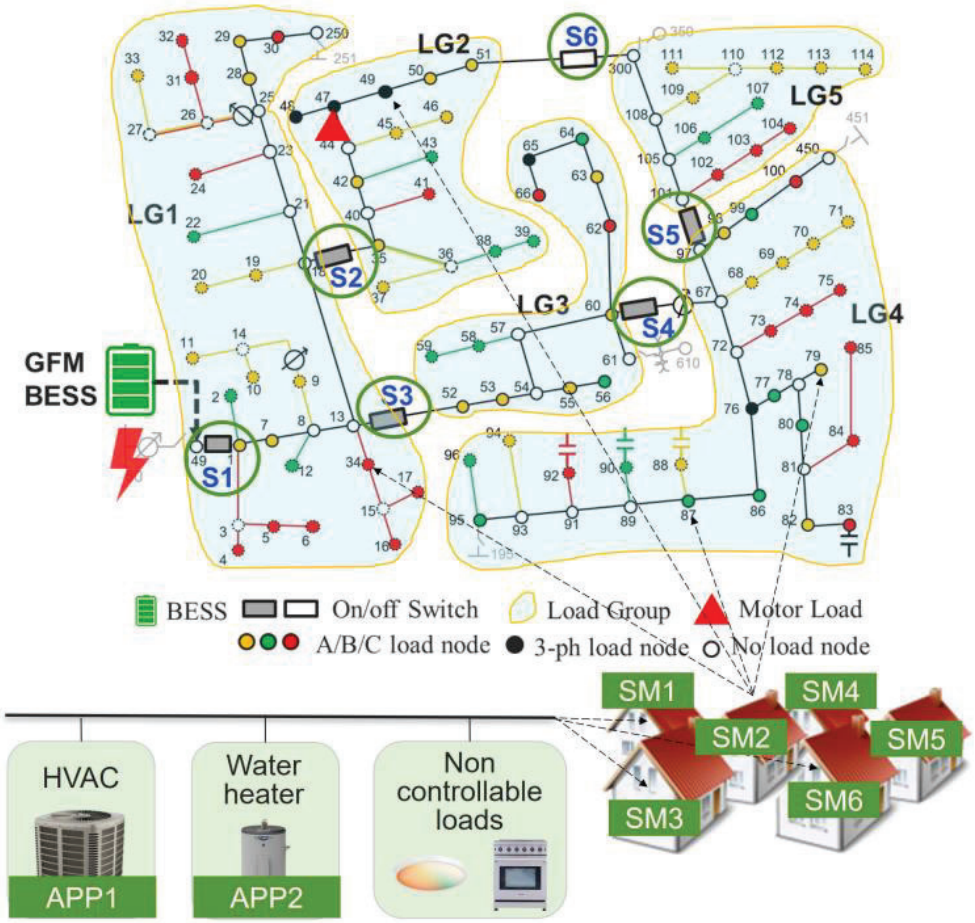

Fig. 1. Configuration of an islanded MG powered by a single GFM BESS.

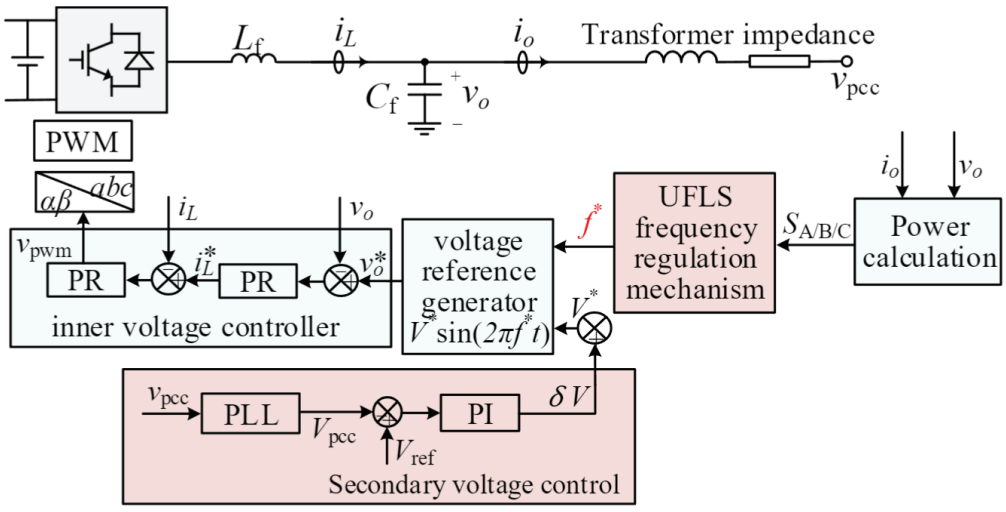

Fig. 2. The proposed, simplified BESS control structure.

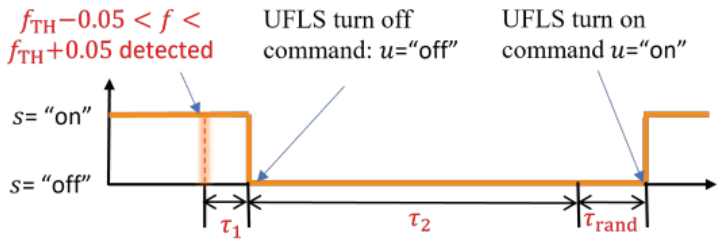

Fig. 3. An illustration of the UFLS response time delay, fixed recovery time, and random recovery delay during an UFLS event.

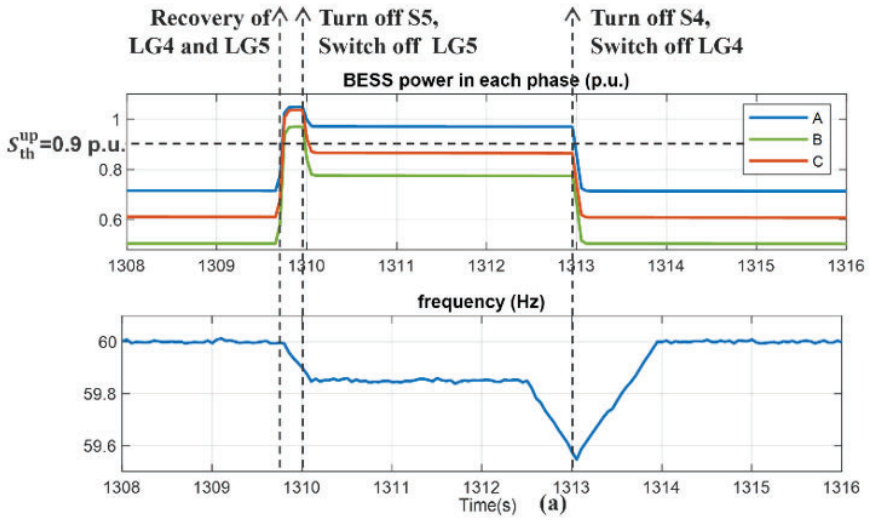

(a)

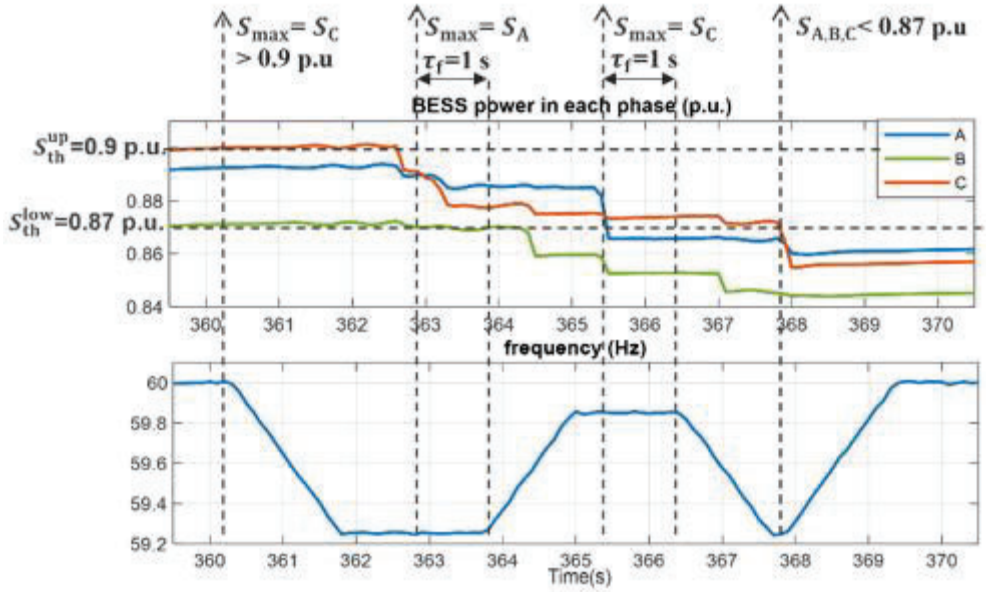

(b)

Fig. 4. Simulation results of an UFLS event. (a) with sectionalizer-based UFLS; (b) with appliance-level UFLS.

References

[1] Y. Wen, C. Chung, and X. Ye, “Enhancing frequency stability of asynchronous grids interconnected with hvdc links,” IEEE Transactions on Power Systems, vol. 33, no. 2, pp. 1800–1810, 2017.
[2] P. Ferraro, E. Crisostomi, R. Shorten, and F. Milano, “Stochastic frequency control of grid-connected microgrids,” IEEE Transactions on Power Systems, vol. 33, no. 5, pp. 5704–5713, 2018.
[3] B. Potel, V. Debusschere, F. Cadoux, and L. de Alvaro Garcia, “Under-frequency load shedding schemes characteristics and performance criteria,” in 2017 IEEE Manchester PowerTech. IEEE, 2017, pp. 1–6.
[4] S. Gordon, C. McGarry, J. Tait, and K. Bell, “Impact of low inertia and high distributed generation on the effectiveness of under frequency load shedding schemes,” IEEE Transactions on Power Delivery, vol. 37, no. 5, pp. 3752–3761, 2021.
[5] S. S. Banijamali and T. Amraee, “Semi-adaptive setting of under frequency load shedding relays considering credible generation outage scenarios,” IEEE Transactions on Power Delivery, vol. 34, no. 3, pp.
[6] M. Karimi, P. Wall, H. Mokhlis, and V. Terzija, “A new centralized adaptive underfrequency load shedding controller for microgrids based on a distribution state estimator,” IEEE Transactions on Power Delivery, vol. 32, no. 1, pp. 370–380, 2016.
[7] Q. Zhou, Z. Li, Q. Wu, and M. Shahidehpour, “Two-stage load shedding for secondary control in hierarchical operation of islanded microgrids,” IEEE Transactions on Smart Grid, vol. 10, no. 3, pp. 3103–3111, 2018.
[8] C. Li, Y. Wu, Y. Sun, H. Zhang, Y. Liu, Y. Liu, and V. Terzija, “Continuous under-frequency load shedding scheme for power system adaptive frequency control,” IEEE Transactions on Power Systems, vol. 35, no. 2, pp. 950–961, 2019.
[9] W. Gu, W. Liu, J. Zhu, B. Zhao, Z. Wu, Z. Luo, and J. Yu, “Adaptive decentralized under-frequency load shedding for islanded smart distribution networks,” IEEE Transactions on Sustainable Energy, vol. 5, no. 3, pp. 886–895, 2014.
[10] Bei Xu, Victor Daldegan Paduani, Qi Xiao, Lidong Song, David Lubkeman, and Ning Lu. "Under-frequency Load Shedding for Power Reserve Management in Islanded Microgrids", submitted to IEEEE Transactions on Smart Grid. Available online at: https://arxiv.org/abs/2309.01278v2.
[11] Matsukawa, Shun, et al. "Stable segment method for multiple linear regression on baseline estimation for smart grid fast automated demand response." 2019 IEEE Innovative Smart Grid Technologies-Asia (ISGT Asia). IEEE, 2019
[12] X. Ke, N. Lu, and C. Jin, “Control and size energy storage systems for managing energy imbalance of variable generation resources,” IEEE Transactions on Sustainable Energy, vol. 6, no. 1, pp. 70–78, 2014.
[13] J. Chang, Y. Du, E. G. Lim, H. Wen, X. Li, and L. Jiang, “Coordinated frequency regulation using solar forecasting based virtual inertia control for islanded microgrids,” IEEE Transactions on Sustainable Energy, vol. 12, no. 4, pp. 2393–2403, 2021.
[14] X. Li, D. Hui, and X. Lai, “Battery energy storage station (bess)-based smoothing control of photovoltaic (pv) and wind power generation fluctuations,” IEEE transactions on sustainable energy, vol. 4, no. 2, pp. 464–473, 2013.
[15] U. R. Nair, M. Sandelic, A. Sangwongwanich, T. Dragicevi ˇ c, R. Costa´Castello, and F. Blaabjerg, “An analysis of multi objective energy scheduling in pv-bess system under prediction uncertainty,” IEEE Transactions on Energy Conversion, vol. 36, no. 3, pp. 2276–2286, 2021.
[16] M. Rezkallah, S. Singh, B. Singh, A. Chandra, H. Ibrahim, and M. Ghandour, “Implementation of two-level coordinated control for seamless transfer in standalone microgrid,” IEEE Transactions on Industry Applications, vol. 57, no. 1, pp. 1057–1068, 2020.

9.12 Task D.5 Assessment of Transmission-level Fault Impacts on Distribution IBR Operation

Background: This task presents a comprehensive analysis of the impact of transmission-level faults on distribution IBR operation by using a real-time transmission and distribution (T&D) co-simulation platform. Currently, there are different T&D co-simulation platforms proposed for the integration study of a large amount of IBRs, and fewer of the work analyzed the impact of transmission-level on distribution IBRs. Table I summarizes the advantages and disadvantages of the state-of-the-art platforms and work. As can be seen in the table, most research focused on the power flow algorithm for the T&D co-simulation, the impact of IBRs on stability of the joint system. The system model is commonly built in phasor domain, especially the IBRs, which cannot accurately reflect the negative and zero sequence components contributed by IBRs under various operational conditions for fault assessments.

TABLE I: Comparison of STATE-OF-THE-ART T&D Co-simulation Studies

	Tran. Simulator	Dist. Simulator	Description	Advantages	Disadvantages
[1], [2]	MATLAB	MATLAB	Model the entire network (transmission and distribution) using dynamic phasors [1], proposed a coordinated T&D AC optimal power flow [2].	Simple and easy to implement. Provide a mathematical model for T&D co-simulation power flow.	Static models and verified only for simple networks without IBRs. Phasor domain model only Non-real-time modeling
[3]	OPAL-RT ePHASO Rsim	OPAL-RT ePHASO Rsim	Both transmission and distribution network are modeled in phasor domain on the real-time platform.	Can run in real time.	Can only model in phasor domain and provide fewer modeling details. Didn't consider the modeling of IBRs
[4]	MATLAB /SIMULIN K	MATLAB /SIMULI NK	Study the impact of aggregate DERs on dynamic stability for load changes and balanced/unbalanced faults using small test networks.	Simple and easy to implement.	Didn't include the modeling of high-penetration IBRs. Non-real time.
[5]-[8]	MATLAB	OPEND SS	Focus on different coupled load flow algorithms to facilitate T&D co-simulation.	Provide a mathematical model for T&D co-simulation power flow.	Didn't model a large T&D network with high-penetration IBRs. Non-real time.
[9]	InterPSS	OPEND SS	Consider a simplified transmission model (in phasor domain) to simulate various transmission-level faults on IBR tripping in the distribution systems (modeled in phasor domain).	Can run in real-time. Consider the modeling of high-penetration IBRs. Consider different kinds of transmission faults on distribution IBR operation.	Phasor domain models cannot model the responses of IBRs accurately No IBR grounding considerations
Our model [10]	**OPAL-RT eMEGAsi m**	**OPAL-RT eMEGAs im ePHASO Rsim**	**Consider an equivalent transmission network (in EMT domain) to simulate both symmetrical and unsymmetrical transmission faults on IBR operation in distribution (in EMT and phasor domain).**	**Real-time simulation Consider both symmetrical and unsymmetrical faults**	**EMT-domain modeling requires higher computational cost.**

Task Objectives:

- Developed a T&D co-simulation platform that can model high-penetration IBR penetration distribution systems under symmetrical and unsymmetrical fault scenarios.
- Assess the impact of transmission-level faults on distribution IBR operation.

Methodology Overview: Using a real-time transmission and distribution (T&D) co-simulation platform, as shown in Fig. 1, we simulate both symmetrical and unsymmetrical faults at increasing electrical distances within the transmission system while evaluating IBR tripping across various phases and locations at the distribution level. The distribution includes three 3-phase IBRs (MW-level) and 86 1-phase rooftop PVs, which are all equipped with fault ride-through (FRT) [11]. The 1-phase IBRs are evenly throughout the feeder and across a, b, c phases. All 1-phase PVs are modeled in phasor domain using ePHASORSIM OPAL-RT platform, and 3-phase IBRs are modeled in EMT domain [12] using eMEGASIM. This configuration enables us to examine the effects of transmission-level faults on both 3-phase and 1-phase IBRs across various feeder locations and across different phases.

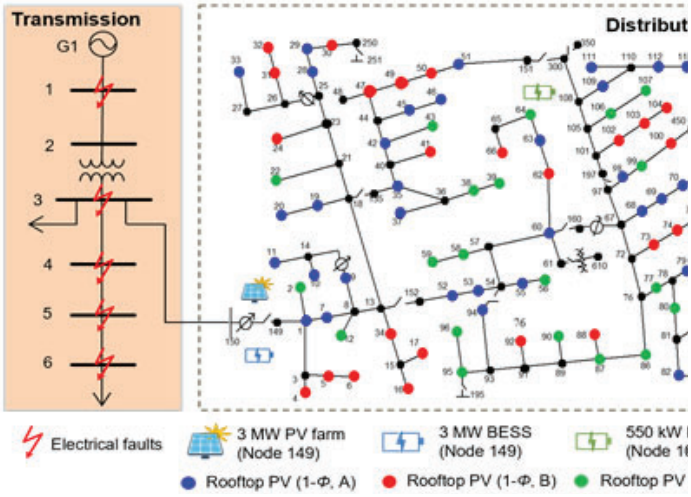

Fig. 1. Layout of the integrated T&D co-simulation testbed.

Simulation Results: Table II summarizes the percentage of IBRs tripped offline for all four fault types, where different IBR power-to-load ratios (PLRs) and the impact of voltage regulation (50%VR) are considered. It can be observed that:1) An increased PLR generally results in less IBR tripping as the combined fault current injections from distributed IBRs help raise the voltage levels along the distribution feeder; 2) The PCC fault results in the most pronounced voltage decline and leads to more instances of IBR tripping, as shown in Fig. 2; 3) 3-phase IBRs are more susceptible to transmission level faults, compared to 1-phase IBRs; 4) IBRs at non-faulty phases can also be tripped off due to the over voltage caused by unsymmetrical faults; 5) The unsymmetrical tripping of 1-phase IBRs will cause severe power and voltage unbalance at high PLRs.

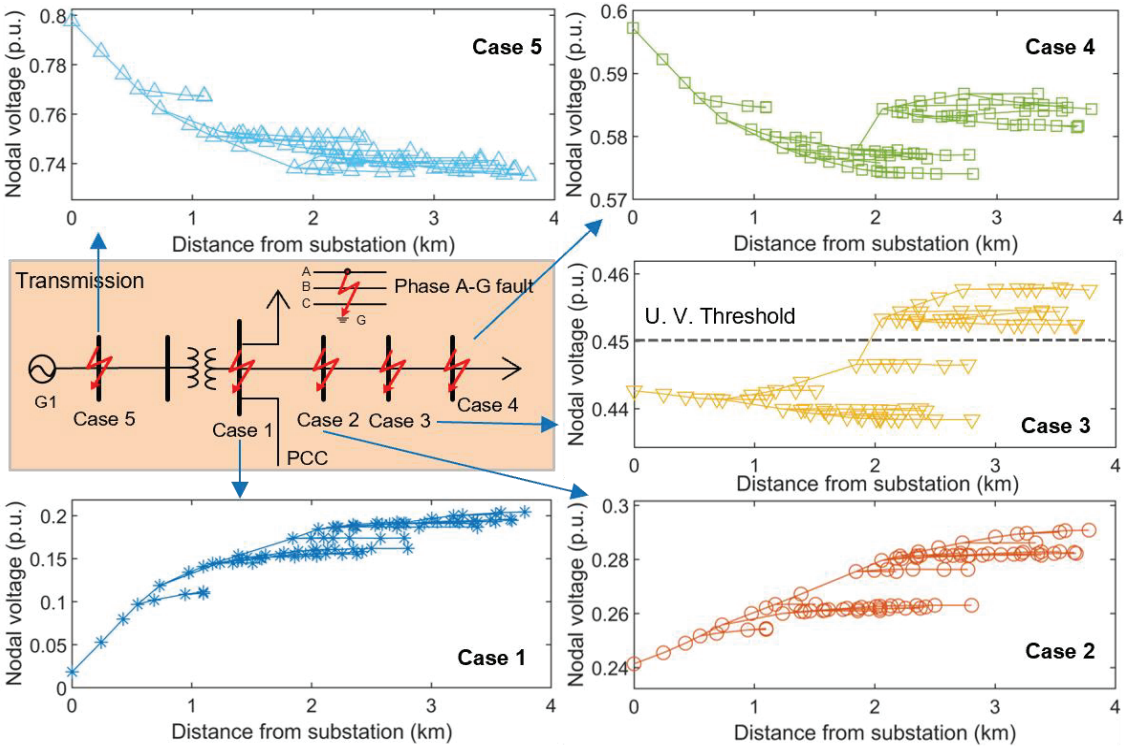

Fig. 2 Nodal voltage on Phase a for the SL2G fault at 50% PLR at different fault locations.

Table II: Trip Percentage of Distributed IBRs Under Different Transmission Faults (Ibr PLRs: 50%, 50%VR, 100%, 300%)

The numbers in the cell represent results for 50%, 50%VR, 100%, and 300% PV PLRs, respectively.

Case	Fault Loc.	Single Line-to-Ground Fault (A-G Fault)				Double Line-to-Ground Fault (A-B-G Fault)				Line-to-Line Fault (A-B Fault)				Three Phase-to-Ground Fault (A-B-C-G Fault)			
		3-ϕ (%)	ϕ-A (%)	ϕ-B (%)	ϕ-C (%)	3-ϕ (%)	ϕ-A (%)	ϕ-B (%)	ϕ-C (%)	3-ϕ (%)	ϕ-A (%)	ϕ-B (%)	ϕ-C (%)	3-ϕ (%)	ϕ-A (%)	ϕ-B (%)	ϕ-C (%)
1	PCC	100	100 100 100 62	0 0 0 68	0	100	100 100 100 57	100 100 100 55	0 0 0 41	0	0	0	0	100	100 100 100 57	100 100 100 50	100 100 100 63
2	Down stream SHORT	100	100 100 100 57	0 0 0 59	0	100	100 100 57 54	100 100 100 41	0 0 0 48	0	0	0	0	100	100 100 100 57	100 100 100 41	100 100 100 52
3	Down stream MEDIUM	0	0	0	0	100	97 57 14 0	100	0	0	0	0	0	100	100	100 100 100 41	100
4	Down stream FAR	0	0	0	0	0	0	0	0	0	0	0	0	33 33 0 0	95 35 3 0	59 47 0 0	89 0 0 0
5	GTF	0	0	0	0	100	0	100 100 100 82	0	100	0	100 100 100 59	0	100	100	100	100

References

[1] J. Gao and Y. Xu, "Co-Simulation of Power Transmission and Distribution Networks Using Dynamic Phasors," 2019 IEEE 9th Annual International Conference on CYBER Technology in Automation, Control, and Intelligent Systems (CYBER), Suzhou, China, 2019, pp. 1646-1651, doi: 10.1109/CYBER46603.2019.9066463.
[2] Z. Li, Q. Guo, H. Sun, and J. Wang, “Coordinated transmission and distribution AC optimal power flow,” IEEE Trans. Smart Grid, vol. 9, no. 2, pp. 1228–1240, Mar. 2018.
[3] G. R. Bharati, S. Chakraborty, C. Duan, and T. Nishikawa, ‘‘An integrated transmission-distribution modeling for phasor-domain dynamic analysis in real-time,’’ in Proc. IEEE Power Energy Soc. Innov. Smart Grid Technol. Conf. (ISGT), Washington, DC, USA, Feb. 2020, pp. 1–5, doi: 10.1109/ISGT45199.2020.9087705.
[4] X. Lu, J. Wang, Z. Li, and M. Yue, ‘‘Dynamic stability assessment for integrated transmission-distribution system considering distributed energy resources,’’ in Proc. Int. Conf. Smart Energy Syst. Technol. (SEST), Porto, Portugal, Sep. 2019, pp. 1–6, doi: 10.1109/SEST.2019.8849037.
[5] Z. Li, Q. Guo, H. Sun, and J. Wang, “Coordinated transmission and distribution AC optimal power flow,” IEEE Trans. Smart Grid, vol. 9, no. 2, pp. 1228–1240, Mar. 2018.
[6] M. M. Rezvani, S. Mehraeen, J. R. Ramamurthy, and T. Field, ‘‘Dynamic interaction of distribution-connected DER_A with transmission system via co-simulation analysis,’’ IEEE Trans. Ind. Appl., vol. 58, no. 2, pp. 1502–1511, Mar. 2022, doi: 10.1109/TIA.2021. 3137087.
[7] G. Krishnamoorthy and A. Dubey, “Transmission—Distribution cosimulation: Analytical methods for iterative coupling,” IEEE Syst. J., vol. 14, no. 2, pp. 2633–2642, Jun. 2020.
[8] R. Sadnan, G. Krishnamoorthy, and A. Dubey, “Transmission and distribution (T&D) quasi-static co-simulation: Analysis and comparison of T&D coupling strength,” IEEE Access, vol. 8, pp. 124007–124019, 2020.
[9] S. Thakar, V. Vittal, R. Ayyanar and C. Rojas, "The Impact of Detailed Distribution System Representation in Dynamic Sub-Transmission-Distribution Co-Simulation," in IEEE Open Access Journal of Power and Energy, vol. 10, pp. 490-502, 2023.
[10] Qi Xiao, Jongha Woo, Lidong Song, Bei Xu, David Lubkeman, Ning Lu, et.al, “Assessment of Transmission-level Fault Impacts on 3-phase and 1-phase Distribution IBR Operation,” 24PESGM1188, submitted to 2023 IEEE PES General Meeting, Available online at: https://arxiv.org/abs/2311.11339.
[11] IEEE Standards Association, “IEEE Standard for Interconnection and Interoperability of Distributed Energy Resources with Associated Electric Power Systems Interfaces,” IEEE Std 1547-2018 - Redline, pp. 1–227, April 2018.

9.13 Task D.6 Design of Delayed Stealth False Data Injection Attacks Against Battery Energy Management System

Background: This task developed a deep reinforcement learning (DRL)-based delayed stealth false data injection attack (SFDIA) scheme that targets Battery Energy Management Systems (BEMS). Battery Energy Storage Systems (BESSs) are crucial components in an Advanced Distribution Network (ADN), providing both grid-following and grid-forming functions [12] in grid-connected or microgrid operation modes. Given their significance, BESSs become a prominent target for False Data Injection Attacks (FDIAs). In TABLE I, we provide a comprehensive literature review on existing research pertaining to FDIAs against BESSs. Much of the previous work has focused on the impact of FDIAs on power grid stability, primarily employing persistent and repetitive attacks, as illustrated in Table I with scenario-based FDIAs. While these attacks are straightforward, they lack stealth and can be easily detected by certain Bad Data Detection (BDD) mechanisms, such as personnel observations or residual-based BDD. Other SFDIAs face challenges like high computational burden for real-time applications, compromised system accuracy, or insufficient stealth.

TABLE I: Comparison of state-of-the-art FDIAs targeting the BESS

Type	Approach	Attack Objectives	Falsified Data	BDD	Implementation	Advantage	Disadvantage
Scenario-based (Non-stealthy)	Persistent and repetitive attacks [13]	Power control	Active power setpoints	No	Inject bias within the operation range to active power setpoints of BESS to cause power imbalance in an islanded microgrid	Conscious manipulation Easy to implement	1. Non-stealthy 2. Easy to be detected by personnel observations or BDD
	Persistent attacks [14]	Mode control	Mode command, etc.		Falsify the mode command to disrupt the mode conversion from PQ to V_f to fail the microgrid		
	Persistent attacks [15]	ON/OFF control	ON/OFF command		Falsify the ON/OFF command to deteriorate power quality or destabilize the power system		
	Persistent attacks [16]	SoC estimation	BESS voltage		Different voltage bias is selected within the operation range to disrupt the SoC estimation		
Optimization-based (Stealthy)	Instantaneous and delayed attacks [17]	SoC estimation	BESS status	Yes	Maximize the SoC estimation error with SE-based BDD considered to cause overcharging or over discharging	Highly stealthy Maximize the SoC estimation error	System info is required, long runtime, not robust in real-time applications
Machine learning-based (Stealthy)	ANN-based attacks via MitM [18],[19]	BESS operation status	BESS status, commands and PCC meter	No	Utilize ANN to replicate the normal behavior of BESS for enhanced stealth, and take the control of the authentic BESS by employing MitM techniques	Medium stealthy Conscious manipulation	Need to attack a large amount of data and easy to be detected by residual-based BDD
	DRL-based delayed persistent and repetitive attacks [20]	SoC estimation	BESS measurements	Yes	Novel DRL-based target SoC error attacking scheme to introduce a target SoC error at the desired time by only injecting battery voltage and current bias	High stealthy and accuracy in real-time applications by conscious manipulation of SoC estimation errors. Attacks can be launched repeatitively.	System info is required and off-line training is required

Task Objectives:

- Design a delayed, highly stealthy SFDIAs against BEMS for real-time applications.

- Investigate the possible attacks against BEMS and apply the proposed attack scheme to the PARS platform.

Methodology Overview: We developed a delayed SFDIA scheme targeting the SoC estimation in BESS, aiming to disrupt the operation of the BEMS within a specified future time range. As shown in Fig. 1, the system comprises the distribution grid, an ADN control center, and a BESS, including battery packs, a voltage-source inverter, a local battery energy management system, and a BESS controller. The ADN control center employs two BDD mechanisms: residual-based BDD and cross-validation of SoC. To attack SoC estimation, the V_{dc} and I_{dc} measurements of the battery must be falsified. Then, the altered values must be able to evade detection by the two BDD mechanisms. We frame the stealthy attack as a DRL problem. Through interactions with the grid and ADN control center environment and a carefully designed reward function, an agent, represented by a deep neural network, can be offline trained to generate attack measurement bias capable of passing BDD, inducing a target SoC error at desired times. The proposed DRL framework is depicted in Fig. 2.

Simulation Results: We implemented the proposed DRL-based delayed SFDIA scheme in the BEMS of PV Plant Restoration use case. Within the BEMS, the PV plant serves to supply loads and charge BESS during the day, while the BESS sustains the system during the night. The SoC of the BESS is regulated within 20%~90%. In this context, we introduced two attack schemes. The first involves altering SoC to mislead the BEMS, causing it to believe there is enough energy stored in BESS. As illustrated in Fig. 3(a), the Delayed SFDIAs inject false data, gradually increasing the SoC error. Consequently, the BESS stops charging when the actual SoC is at 60%, resulting in a system shutdown when the attack concludes, with the actual SoC falling below the critical threshold of 20%. The second attack focuses on accelerating BESS degradation through over-discharging. In Fig. 3(b), a falsely elevated SoC is introduced to convince the BEMS that the BESS has sufficient energy to release. When the false SoC is around 20%, the actual SoC drops to approximately 5%. This deep discharge can significantly degrade the lifespan of the BESS. Additionally, for repeated launch of degradation attacks, it is crucial for the attack to remain stealthy even after it concludes. Thus, the false SoC must closely match the actual SoC at the end of the attack.

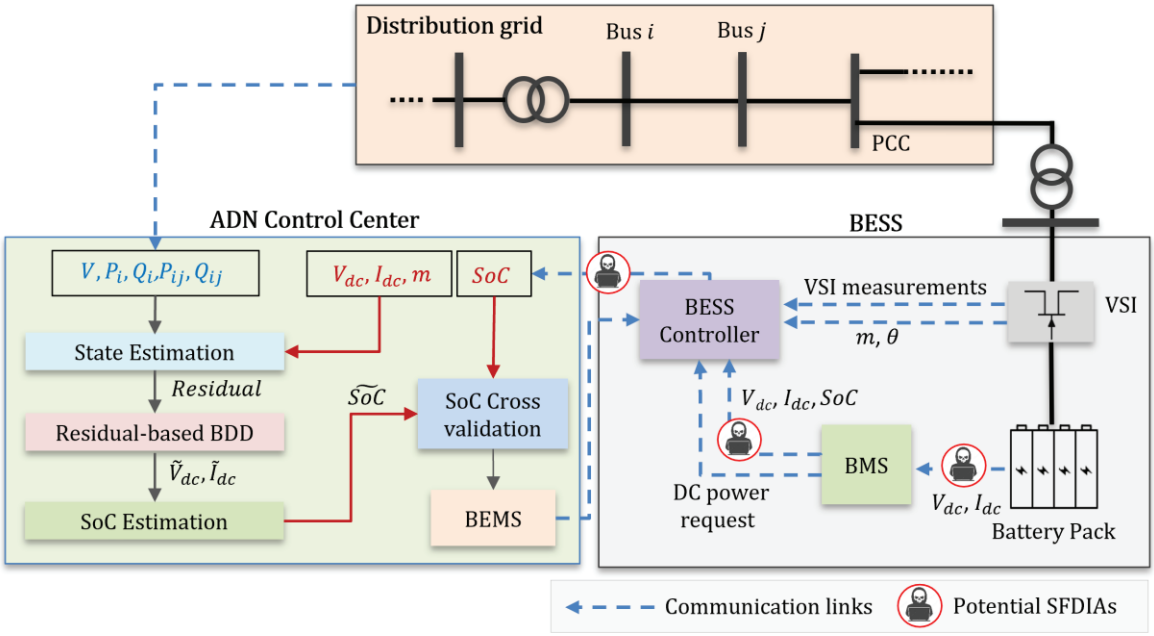

Figure 1. Layout of the integrated T&D co-simulation testbed.

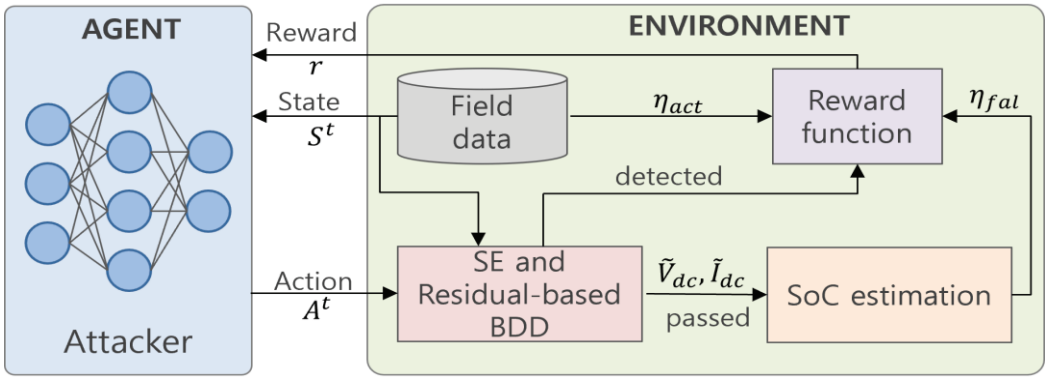

Figure 2 Proposed DRL framework for delayed SFDIAs against SoC estimation.

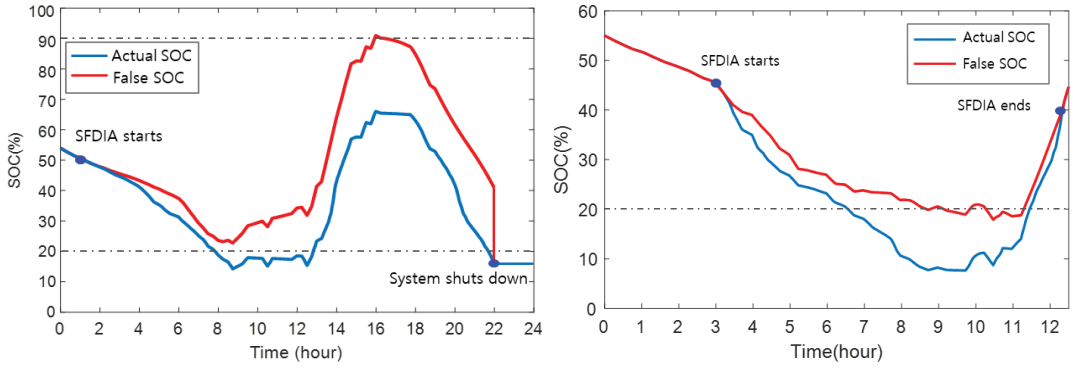

(a) **(b)**

Figure 3. SoC profile of the test case (a) with SFDIAs against microgrid reliability, and (b) with SFDIAs for deep discharge of BESS

References

[1] B. Xu, V. Paduani, Q. Xiao, L. Song, D. Lubkeman, and N. Lu, “Under-frequency Load Shedding for Power Reserve Management in Islanded Microgrids.” arXiv preprint arXiv:2309.01278, 2023.
[2] M. Chlela, G. Joos, M. Kassouf and Y. Brissette, "Real-time testing platform for microgrid controllers against false data injection cybersecurity attacks," 2016 IEEE Power and Energy Society General Meeting (PESGM), Boston, MA, USA, 2016, pp. 1-5.
[3] X. Liu, M. Shahidehpour, Y. Cao, L. Wu, W. Wei, and X. Liu, “Microgrid risk analysis considering the impact of cyber attacks on solar PV and ESS control systems,” IEEE Trans. Smart Grid, vol. 8, no. 3, pp. 1330–1339, May 2017.
[4] S. Ghosh, M. H. Ali and D. Dasgupta, "Effects of Cyber-Attacks on the Energy Storage in a Hybrid Power System," 2018 IEEE Power & Energy Society General Meeting (PESGM), Portland, OR, USA, 2018, pp. 1-5.
[5] V. Obrien, R. D. Trevizan and V. S. Rao, "Detecting False Data Injection Attacks to Battery State Estimation Using Cumulative Sum Algorithm," 2021 North American Power Symposium (NAPS), College Station, TX, USA, 2021, pp. 01-06.
[6] P. Zhuang and H. Liang, "False data injection attacks against state-of-charge estimation of battery energy storage systems in smart distribution networks," IEEE Transactions on Smart Grid, vol. 12, no. 3, pp. 2566-2577, 2020.
[7] M. Pasetti et al., "Artificial Neural Network-Based Stealthy Attack on Battery Energy Storage Systems," in IEEE Transactions on Smart Grid, vol. 12, no. 6, pp. 5310-5321, Nov. 2021.
[8] A. O. De Sá, L. M. De Souza Bento, M. L. Flavio, M. Pasetti, P. Ferrari and E. Sisinni, "ANN-Based Stealthy Attack to Battery Energy Storage Systems by Using a Low-Cost Device," 2022 IEEE International Workshop on Metrology for Industry 4.0 & IoT (MetroInd4.0&IoT), Trento, Italy, 2022, pp. 201-206.
[9] Qi Xiao, Lidong Song, Ning Lu, et.al, “Invisible Manipulation: Deep Reinforcement Learning-Enhanced Stealthy Attacks on Battery Energy Management Systems”, in preparing and will submit to IEEE Trans. Smart Grid.

9.14 Task D.7 Development of an Encoding Method on a Co-Simulation Platform for Mitigating the Impact of Unreliable Communication

Background: This task focuses on 1) the development of an encoding method to mitigate the effects of unreliable communication links, and 2) create a hardware-in-the-loop co-simulation platform to assess the performance of the algorithm. The power distribution network and distributed energy resources are simulated on an OPAL-RT-based real-time simulation environment, interconnected with energy management systems through a simulated communication network. We have conducted a thorough analysis of the pros and cons of current state-of-the-art approaches in comparison to our proposed methodology, and the findings are summarized comprehensively in Table I.

TABLE I: State-of-the-art comparison of parameterization methods

	Testbed Modeling	Communication Issue	Mitigation Method
[1]	Phasor domain distribution feeder model	Link outage	N/A
[2]	HIL based model + FPGA controller	Communication latency	N/A
[3]	Electromagnetic transients model + network simulator	Communication latency	N/A
[4], [6]	HIL based model + network simulator	Communication latency and packet drop	N/A
[5]	HIL based model + actual network link	Corrupted data	N/A
[7]	Phasor domain model + FPGA controller	Corrupted data	An ALM-based method.
Proposed [8]	Hybrid HIL based model + network simulator	Communication latency, corrupted data and packet drop	An enhanced ALM-based method.

Task Objectives:

- Model the unreliable communication links between DERs and the central controller.
- Test mitigation method for the impact of communication noise, errors, and missing data on distribution feeder nodal voltage control.

Methodology Overview: The configuration of the asynchronous HIL co-simulation platform is shown in Fig. 1. The transmission network and distribution feeder are modeled with ePHASORSIM at the millisecond-level and the DERs are modeled using eMEGASIM so that their dynamic responses can be modeled with the microsecond-level. Two communication connections are set up to model the communication between the device level controller and the centralized controller.

We assume that each feeder node is equipped with one user equipment (UE) for communicating with the base station (BS) tower and an LTE simulator is used to model wireless communication network between UEs and BS considering different communication interruptions. The configuration is shown in Fig. 2.

The proposed mitigation method can be formulated as a matrix recovery problem [8]:

$$\min_{\mathbf{L},\,\mathbf{G}} \left(\|\mathbf{L}\|_* + \lambda \left\| P_{\Omega}[\mathbf{G}] \right\|_1 \right) \tag{1a}$$

s.t.

$$\mathbf{M} = \mathbf{L} + \mathbf{G} \tag{1b}$$

$$P_{\bar{\Omega}}[\mathbf{G}] = -P_{\bar{\Omega}}[\mathbf{L}] \tag{1c}$$

where $||\cdot||_*$ is the nuclear norm of a matrix (the sum of its singular values), $||\cdot||_1$ is the sum of the absolute value of matrix entries while λ is a positive weighting factor.

By solving (1), the optimal estimations for LTE communication data and communication errors can be obtained, where $\mathbf{L} \in \mathbb{R}_s^{m\times n}$ and $\mathbf{G} \in \mathbb{R}_s^{m\times n}$. **M** is the accrual received data via the LTE link which may contain missing data and corrupted data. $P_\Omega[\cdot]$: $\mathbb{R}_s^{m\times n} \rightarrow \mathbb{R}_s^{m\times n}$ is a linear operator that keeps the entries in Ω unchanged and sets those outside Ω (e.g., $\bar{\Omega}$) to zeros.

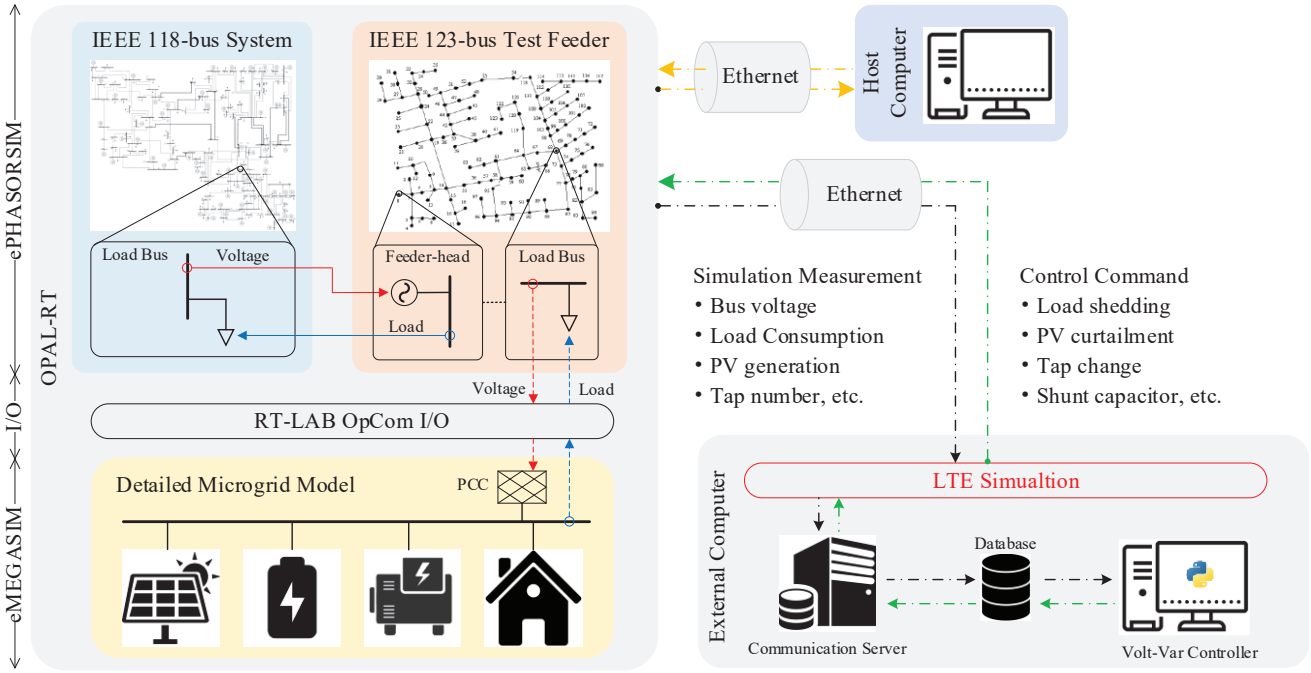

Figure 1. Architecture of the asynchronous HIL co-simulation platform.

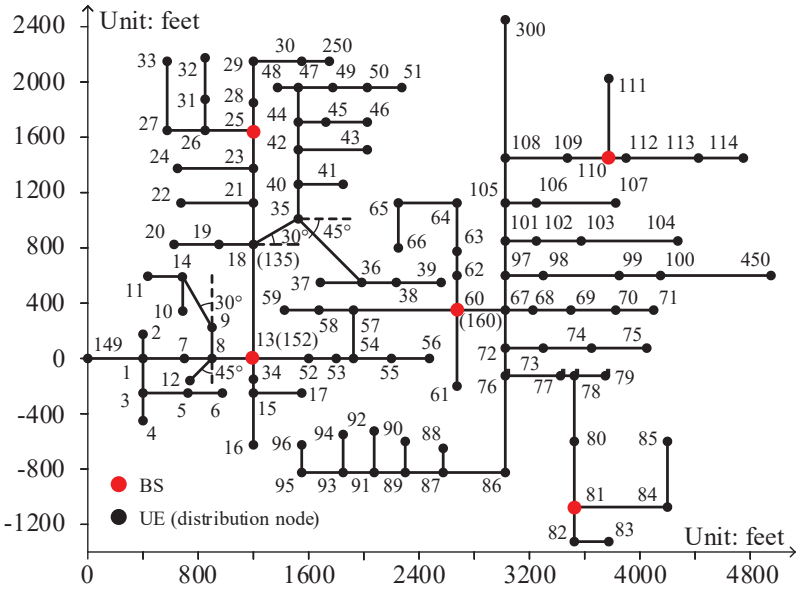

Fig. 2. Configuration of the LTE network for the IEEE 123-node test feeder.

Simulation Results:

The simulation results demonstrate the efficacy of the setup for a controller-in-the-loop system that models system dynamics and allows algorithms to be developed and tested with realistic communication links considered in a laboratory environment. The one-minute distribution of the nodal voltage without control and with the centralized volt-var control (CVVC) from 12:00 to 22:00 is summarized in Fig. 3. Both cases have a perfect communication link without any interruption and a control voltage margin (0.014 p.u.). As shown in Fig. 4, if no voltage margin is used, nodal voltage will drop below the desired voltage lower limit. While setting up a large voltage margins (e.g., 0.02 p.u.) can remove all voltage violations, it leads to frequent control actions, causing higher wear-and-tear and higher control cost. Fig. 5 demonstrates the impact of both missing and corrupted data caused by interrupted communication links on CVVC performance using the same settings as Case 3 and Case 4. The missing rate and corrupted rate are all set as 10%. The total number of voltage violations (TNVV), the max voltage violation magnitude (MVVM), and the average execution time (AET) are used as the evaluation metrics.

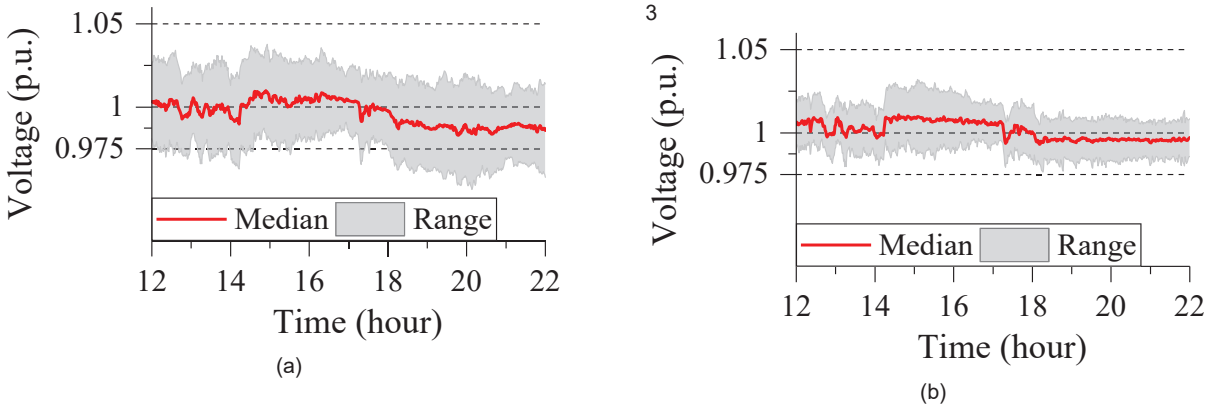

Fig. 3. Nodal voltage profiles: (a) no-control baseline case and (b) controlled case with perfect communication link.

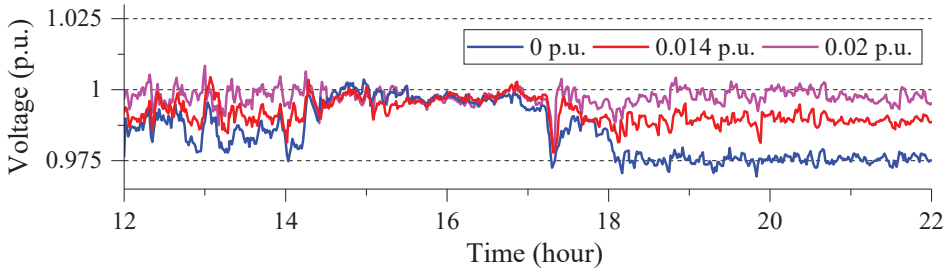

Fig. 4. Phase *a* voltage at Node 50 when using different voltage control margins.

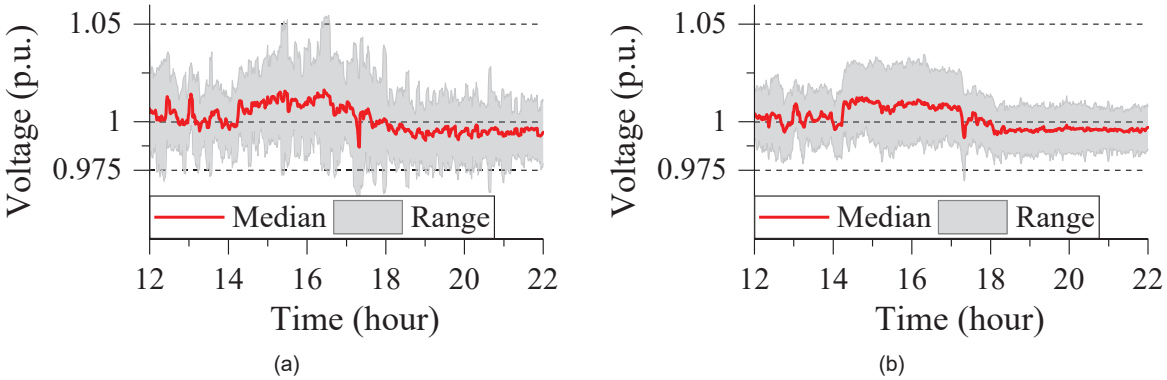

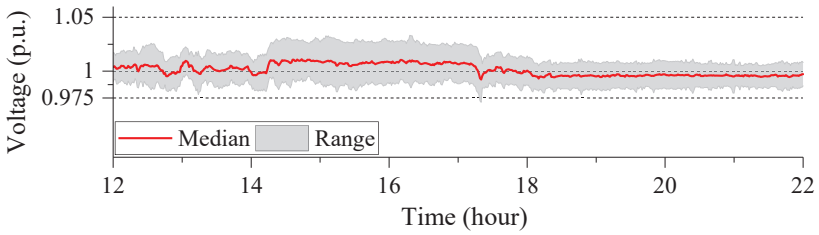

(c)

Fig. 5. Nodal voltage profiles when there are missing and corrupted data sets: (a) no data recovery, (b) recovery using SVT, and (c) recovery using EALM-EDR.

TABLE II: Summary of Simulation Results

Method	TNVV	MVVM (p.u.)	AET (second)
Unrecovered	799	0.0185	\
SVT []	32	0.0029	0.9973
Proposed	23	0.0027	0.2688

References

[1] Liu, Hao Jan, Wei Shi, and Hao Zhu. "Hybrid voltage control in distribution networks under limited communication rates." IEEE Transactions on Smart Grid 10.3 (2018): 2416-2427.
[2] Johnson, Jay, et al. "Design and evaluation of SunSpec-compliant smart grid controller with an automated hardware-in-the-loop testbed." Technology and Economics of Smart Grids and Sustainable Energy 2.1 (2017): 16.
[3] Barbierato, Luca, et al. "A Distributed Multi-Model Co-simulation Platform to Assess General Purpose Services in Smart Grids." IEEE Transactions on Industry Applications (2020).
[4] Hematian, Amirshahram, et al. "Performance assessment of smart meter traffic over lte network using sdr testbed." 2019 International Conference on Computing, Networking and Communications (ICNC). IEEE, 2019.
[5] Tong, Heqin, et al. "Flexible hardware-in-the-loop testbed for cyber physical power system simulation." IET Cyber-Physical Systems: Theory & Applications 4.4 (2019): 374-381.
[6] Pandakov, Konstantin, et al. "Experimental validation of a new impedance based protection for networks with distributed generation using co-simulation test platform." IEEE Transactions on Power Delivery (2019).
[7] Anwar, Adnan, et al. "HPC-based intelligent volt/VAr control of unbalanced distribution smart grid in the presence of noise." IEEE Transactions on Smart Grid 8.3 (2017): 1446-1459.
[8] Xie, Fuhong, et al. "Development of an encoding method on a co-simulation platform for mitigating the impact of unreliable communication." IEEE Transactions on Smart Grid 12.3 (2020): 2496-2507.
[9] Cai, Jian-Feng, Emmanuel J. Candès, and Zuowei Shen. "A singular value thresholding algorithm for matrix completion." SIAM Journal on optimization 20.4 (2010): 1956-1982.

9.15 Task D.8 Real-Time Parameterization for a PV-farm Digital Twin using a Two-Stage Optimization Approach

Background: This task delves into the escalating relevance of Power System Digital Twins (PSDTs), propelled by the global shift towards decarbonization and electrification of power grids. PSDTs, serving as virtual counterparts to physical systems, are progressively utilized in the innovation and evaluation of new technologies within power systems. Contrasting with traditional power system simulation test beds, which are generally either hypothetical or static imitations, PSDTs offer dynamic simulation that mirrors real-time system changes. This document introduces an innovative technique for the real-time parameterization of a photovoltaic digital twin (PV-DT) employing high-resolution field data. This approach marks a significant departure from conventional practices, emphasizing the distinctive requirements in PSDT development. The benefits and limitations of existing PV-DT methods, in relation to our proposed methodology, are comprehensively analyzed and summarized in Table I.

TABLE I: State-of-the-art comparison of parameterization methods

		Model Input	Model Output	Description	Advantage	Disadvantage
Model free based	[16], [23], [24]	5 min resolution	Irradiance, PV power output	Estimates variables, including tilt angle, azimuth angles, and albedo, which are related to irradiance.	Parameterize and simulate PV systems without the use of electrical model analysis.	1) Considers only the power, not the output voltage and current of the PV 2) Performance varies greatly depending on weather conditions.
MD model based	[12]-[15]	Manufactural data sheet	PV model parameters	Model the PV system equivalently using the MD model to estimate its parameters.	Accurate electrical modeling of PV becomes possible.	Increased model complexity longer computation times
SD model based	[17], [29] (Benchmark method)	5 min resolution	Irradiance	Estimate irradiance by employing an optimization-based approach derived from the equations of the SD model	1) Information such as tilt angle and albedo are not required. 2) Can consider the uncertainty of irradiance measurement.	Real-time parameterization of the SD model's model parameter was not conducted.
	[18]-[21], [25],[26],	Manufactural data sheet	PV model parameters	Estimate model parameter using the SD model's equations and the Lambert W function. However, the uncertainty of the irradiance sensor was not considered.	Can estimate model parameters that correspond to the V-I curve and V-P curve in the manufacturer's datasheet.	1) Some papers do not consider the time-variability of parameters. 2) If the measured irradiance is inaccurate, the estimated parameters cannot be deemed accurate either.
	[22] (Benchmark method)	5 min resolution	PV model parameters			
	Our method	1 sec resolution	Irradiance & PV model parameters	1) Considers the uncertainty of the irradiance measurement. 2) Estimates model parameters using the SD model's equations and the Lambert W function.	Can maximize the parameterization performance in utility-scale PV data at one-second intervals that are greatly affected by partial shading.	The computation time increases because of co-optimization

Task Objectives:

- Implement a two-stage optimization process for real-time PV-DT parameterization
- Improve the steady-state and transient performance of the PV-DT

Methodology Overview: The PV-DT framework is depicted in Fig. 1. Real-time measurement of voltage, current, and temperature (V_{PV}^{meas}, I_{PV}^{meas}, and T_{PV}^{meas}) are used to estimate the irradiance assuming the five model parameters are known. If the modeling error exceeds pre-determined thresholds, or the estimated parameters deviates the parameters in use, the parameters will be

updated using the two-stage optimization algorithm. The PV-DT is developed on the PARS OPAL-RT platform and verified using two-week, second-by-second PV farm measurements.

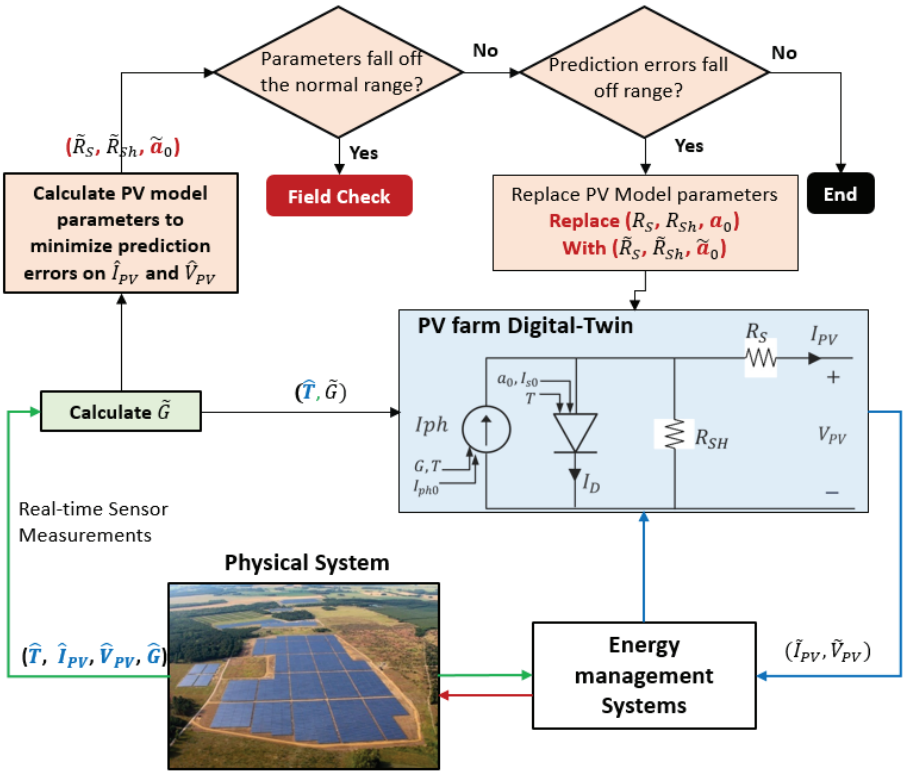

Fig. 1. Configuration of a utility-scale PV farm

Simulation Results: Tables II and III presents the anticipated errors in comparison to actual PV farm operations in the Estimation stage and during Simulation, respectively.

TABLE II: Comparison of Results across Three Optimization Methods

Estimation Level	Real-time parameterization	Irradiance Estimation	Mean Absolute Percentage Error (MAPE)			Root Mean Square Error (RMSE)		
			Δ Current (%)	Δ Voltage (%)	Δ Power (%)	Δ Current (A)	Δ Voltage (V)	Δ Power (kW)
Base Case	No	No	34.83	2.21	36.19	286.37	26.56	305.89
Method 1 [9]	No	Yes	1.58	1.25	0.33	11.15	14.65	2.41
Method 2 [16]	Applied	No	0.62	0.05	0.65	41.73	0.75	43.34
Our Method [17]	Applied	Applied	0.17	0.04	0.20	1.50	0.66	1.86

TABLE III: Comparison of Results across Three Optimization Methods

Simulink Level	Real-time parameterization	Irradiance Estimation	Mean Absolute Percentage Error (MAPE)			Root Mean Square Error (RMSE)		
			Δ Current (%)	Δ Voltage (%)	Δ Power (%)	Δ Current (A)	Δ Voltage (V)	Δ Power (kW)
Base Case	No	No	34.96	2.11	36.25	288.2	26.36	306.87
Method 1 [9]	No	Yes	1.31	1.06	0.25	7.73	13.38	1.49
Method 2 [16]	Applied	No	1.19	0.39	0.90	42.69	5.72	43.67
Our Method [17]	Applied	Applied	0.29	0.22	0.13	2.76	2.79	0.89

The baseline PV-DT, using a fixed set of model parameters and relying on irradiance sensor measurements as inputs, demonstrated the least favorable performance. Method 1, utilizing a fixed set of model parameters but with calculated equivalent irradiance, showed improved performance compared to the baseline PV-DT. Method 2, incorporating real-time parameterization while still using irradiance sensor measurements as inputs, outperformed Method 1. The proposed model, which calculates equivalent irradiance and is enhanced by real-time parameterization algorithms, achieved the best performance among the four approaches. As shown in the table, the proposed method outperformed other methodologies in terms of current, voltage, and power, demonstrating MAPE improvements of 0.9%, 0.17%, and 0.87%, respectively, when compared with the second-best model.

References

[1] D. E. G. Razo, B. Müller, H. Madsen, and C. Wittwer, "A Genetic Algorithm Approach as a Self-Learning and Optimization Tool for PV Power Simulation and Digital Twinning," Energies, vol. 13, no. 24, pp. 1-20, Dec. 2020.
[2] Y. M. Saint-Drenan, S. Bofinger, R. Fritz, S. Vogt, G. H Good, J. Dobschinski, "An empirical approach to parameterizing photovoltaic plants for power forecasting and simulation," Solar Energy, vol. 120, pp. 479-93, Oct. 2015.
[3] S. Killinger, N. Engerer, B. Müller, "QCPV: A quality control algorithm for distributed photovoltaic array power output," Solar Energy, vol. 143, pp. 120-131, Feb. 2017.
[4] S. R. Fahim, H. M. Hasanien, R. A. Turky, S. H. E. A. Aleem, and M. Calasan, "A Comprehensive Review of Photovoltaic Modules Models and Algorithms Used in Parameter Extraction," Energies, no. 23, vol. 15, pp. 1-56, Nov. 2022.
[5] H. S. Moreira, J. L. S. Silva, M. V. G. Reis, D. B. Mesquita, B. H. K. Paula, and M. G. Villalva, "Experimental comparative study of photovoltaic models for uniform and partially shading conditions," Renewable Energy, vol. 164, pp. 58-73, Feb. 2021.
[6] M. H. Qais, H. M. Hasanien, and S. Alghuwainem, "Identification of electrical parameters for three-diode photovoltaic model using analytical and sunflower optimization algorithm," Applied Energy, vol. 250, pp. 109-17, Sep. 2019.
[7] J. J. Soon, K. Low, "Optimizing Photovoltaic Model for Different Cell Technologies Using a Generalized Multidimension Diode Model," IEEE Transactions on Industrial Electronics, vol. 62, no. 10, pp. 6371-80, Oct. 2015.
[8] V. D. Paduani, H. Yu, B. Xu, N. Lu, "A Unified Power-Setpoint Tracking Algorithm for Utility-Scale PV Systems With Power Reserves and Fast Frequency Response Capabilities," IEEE Transactions on Sustainable Energy, vol. 13, no. 1, pp.479-90, Jan. 2022.
[9] X. Li, H. Wen, Y. Zhu, L. Jiang, Y. Hu, and W. Xiao, "A Novel Sensorless Photovoltaic Power Reserve Control With Simple Real-Time MPP Estimation," IEEE Transactions on Power Electronics, vol. 34, no. 8, pp. 7521-31, Aug. 2019.
[10] M. Ćalasan, S. H. E. A. Aleem, and A. F. Zobaa, "On the root mean square error (RMSE) calculation for parameter estimation of photovoltaic models: A novel exact analytical solution based on Lambert W function," Energy Conversion and Management, vol. 210, no. 112716, pp. 1-16, Apr. 2020.
[11] S. Pindado et al., "Simplified Lambert W-Function Math Equations When Applied to Photovoltaic Systems Modeling," IEEE Transactions on Industry Applications, vol. 57, no. 2, pp. 1779-88, Jan. 2021.
[12] M. H. Qais, and S. M. Muyeen, "A Novel Adaptive Filtering Algorithm Based Parameter Estimation Technique for Photovoltaic System,"IEEE Transactions on Energy Conversion," vol. 37, no. 1, pp. 286-94, Mar. 2022.
[13] S. Duman, H. T. Kahraman, Y. Sonmez, U. Guvenc, M. Kati, S. Aras, "A powerful meta-heuristic search algorithm for solving global optimization and real-world solar photovoltaic parameter estimation problems," Engineering Applications of Artificial Intelligence, vol. 111, no. 104763, pp. 1-31, May. 2022.
[14] D. H. Muhsen, A. B. Ghazali, T. Khatib, I. A. Abed, "A comparative study of evolutionary algorithms and adapting control parameters for estimating the parameters of a single-diode photovoltaic module's model," Renewable Energy, vol. 96, pp. 377-89, Oct. 2016.
[15] J. D. Bastidas-Rodriguez, G. Petrone, C. A. Ramos-Paja, and G. Spagnuolo, "A genetic algorithm for identifying the single diode model parameters of a photovoltaic panel," Mathematics and Computers in Simulation, vol. 131, pp. 38-54, Jan. 2017.
[16] J. Xu, C. Zhou, and W. Li, "Photovoltaic single diode model parameter extraction by dI/dV-assisted deterministic method," Solar Energy, vol. 251, pp. 30-38, Feb. 2023.
[17] Jongha Woo, et al. “Real-Time Parameterization for a PV-farm Digital Twin using a Two-Stage Optimization Approach”, to submit to IEEE transactions on smart grid.

9.16 Task E.1 A Meta-learning Based Distribution System Load Forecasting Model Selection Framework

Background: This task presents an automated, extendable and robust load forecasting model selection framework to solve the heterogeneous load forecasting tasks with different forecasting requirements and data availabilities in power distribution systems. In general, there are two types of methods achieving model selection: knowledge-based expert system (KES) and machine-learning based methods. Table I summarizes the advantages and disadvantages of the state-of-the-art methods. We can see that the KES methods are less flexible because the system needs to be updated manually whenever new forecasting models are introduced or new forecasting scenarios are considered. Meanwhile, there lacks a rigorous problem formulation as well as a generalized test case for the current machine-learning based methods.

TABLE I: Comparison of STATE-OF-THE-ART load forecasting model selection methods

	Description	Advantages	Disadvantages
Knowledge-based Expert System **Error! Reference source not found.-Error! Reference source not found.**	Construct a rule-based model selection mechanism to determine which model to use under what forecasting scenarios, based on experts' knowledge.	Explainable and friendly to system operators, since the model selection rules are built based on human knowledge.	Inflexible because the system needs to be updated manually whenever new models or scenarios are introduced.
Machine-learning based methods **Error! Reference source not found.-Error! Reference source not found.**	Construct a mapping from forecasting task features to the optimal forecasting models to achieve model selection.	Automated and easy to update when new models or forecasting tasks are considered.	Less explainable, and currently there lacks are rigorous problem formulation for the model selection system.

Task Objectives:

- Provide a rigorous problem formulation for the machine-learning based model selection.
- Develop a meta-learning based model selection framework to solve the heterogeneous load forecasting tasks in power distribution systems, which is automated, extendable and flexible.

Methodology Overview: The meta-learning based load forecasting model selection framework is illustrated in Fig. 1. In the base-learning layer, all candidate forecasting model will be tested on each forecasting task to find out the best-performed model on each task. In the meta-learning layer, the features of forecasting tasks will be calculated as the input to train the meta-learner, the nature of which is a classifier, to construct the mapping from task features to the best-performed models. In the online application layer, the trained meta-learner will provide the forecasting model recommendation among candidate models for the new forecasting task, given the task features as the input.

Simulation Results: As shown in Table II, the proposed model selection framework has 46% chance to identify the best-performed load forecasting model among 10 candidate forecasting models for a given load forecasting task, and 76% chance to provide a top-3 forecasting model. Consequently, the average forecasting error on 170 testing tasks is reduced: compared with the best-performed single forecasting model, the proposed model selection framework can reduce the Mean Absolute Percentage Error (MAPE) from **0.188** to **0.143**, and reduce the System Error Ratio (SER) from **1.40** to **1.14**.

As shown in Table III, when data granularity is 5-min and 15-min, Load-PIN outperforms all other models and shows 15-30% improvement compared with the second-best model. This shows that Load-PIN can extract information hidden inside the high-resolution data for forecasting the missing data segments. However, if the data resolution is too low, the Load-PIN does not show significant performance improvements. This is because in those cases, forecasting average values outweigh uncovering load shape details.

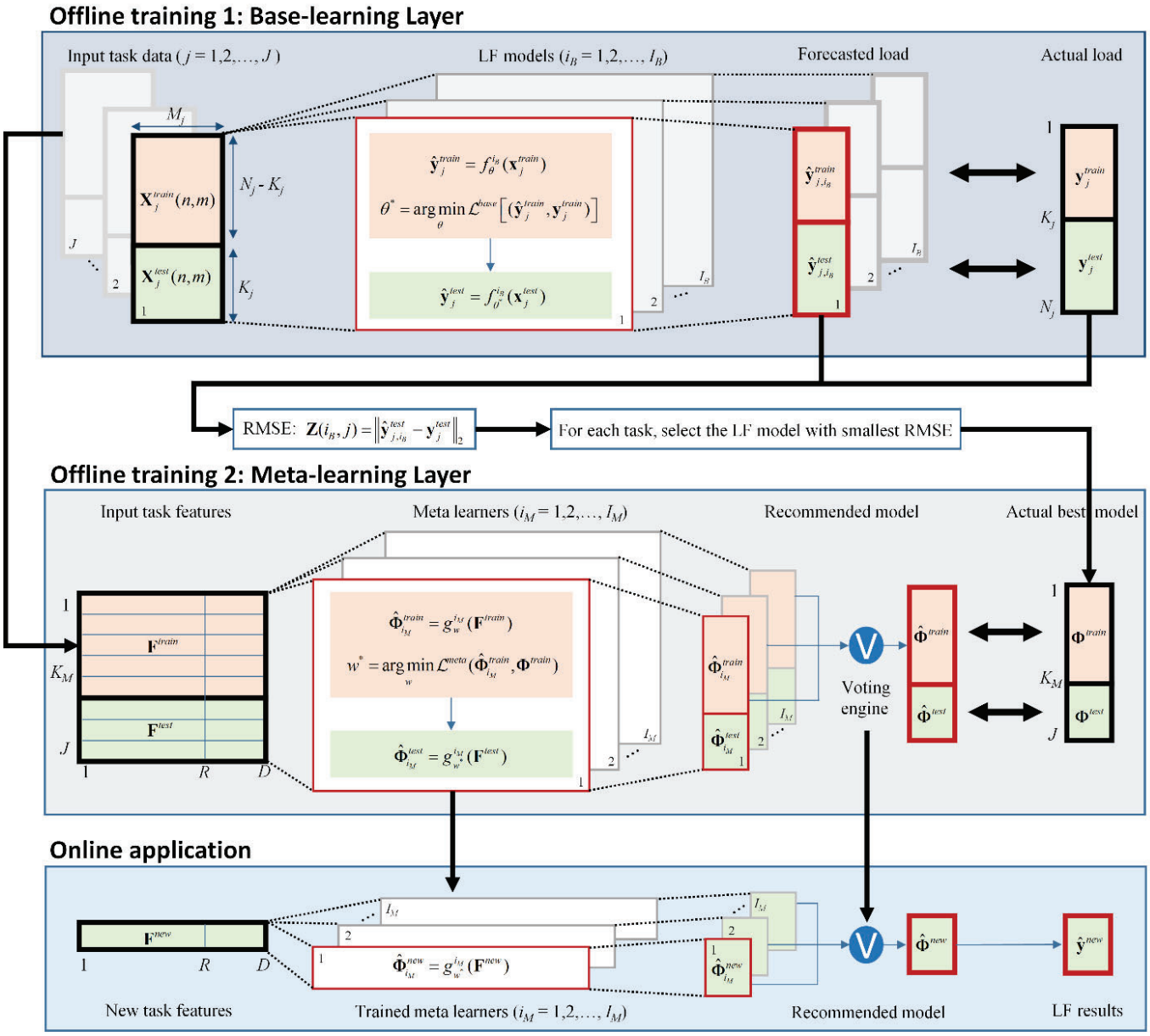

Figure 1. The proposed meta-learning based load forecasting model selection framework, including base-learning layer, meta-learning layer and online application layer.

TABLE II: Model performance on different rankings

Ranking	1	2	3	4	5	6	7	8	9	10
Classification accuracy	46%	17%	13%	6%	4%	3%	3%	3%	2%	3%
SER	1.14	1.27	1.34	1.46	4.18	2.89	4.48	3.61	2.61	3.09
Failure count	0	0	2	10	10	12	12	17	14	11

TABLE III: Error comparison between our method and the best-performed single model

	Average SER	Average MAPE	Failure Count
Proposed meta-learning mechanism	**1.14**	**0.143**	0
Best-performed single LF model	1.40	0.188	0

References

[1] Kandil MS, El-Debeiky SM, Hasanien NE. Long-term load forecasting for fast developing utility using a knowledge-based expert system. IEEE Trans on Power Syst 2002;17(2):Aug.
[2] Kandil MS, El-Debeiky SM, Hasanien NE. The implementation of long-term forecasting strategies using a knowledge-based expert system: part-II. Electr Power Syst Res May 2001;58(1):19–25.
[3] Kazemi SMR, Seied Hoseini MM, Abbasian-Naghneh S, Rahmati SHA. An evolutionary-based adaptive neuro-fuzzy inference system for intelligent short term load forecasting. Int Trans Operational Res 2014;21(2):Mar.
[4] Liao SH. Expert system methodologies and applications—a decade review from 1995 to 2004. Expert Syst Appl Jan. 2005;28(1):93–103.
[5] Thrun S, Pratt L. “Learning to learn: Introduction and overview”, in Learning to learn. Boston, MA Springer 1998:3–17.
[6] Finn C, Abbeel P, Levine S. Model-agnostic meta-learning for fast adaptation of deep networks. arXiv preprint, arXiv:1703.03400; 2017.
[7] Cui C, Wu T, Hu M, Weir JD, Li X. Short-term building energy model recommendation system: A meta-learning approach. Appl Energy Jun. 2016;172: 251–63.
[8] Feurer M, Springenberg JT, Hutter F. Initializing bayesian hyperparameter optimization via meta-learning. In: Twenty-Ninth AAAI Conference on Artificial Intelligence, Feb. 2015.
[9] Lemke C, Budka M, Gabrys B. Metalearning: a survey of trends and technologies. Artif Intell Rev Jun. 2015;44(1):117–30.
[10] Li Y, Zhang S, Hu R, et al. A meta-learning based distribution system load forecasting model selection framework[J]. Applied Energy, 2021, 294: 116991.

9.17 Task E.2 A TCN-based Hybrid Forecasting Framework for Hours-ahead Utility-scale PV Forecasting

Background: This task presents a hybrid forecasting framework for utility-scale PV farms to achieve hours-ahead PV forecasting, based on the Temporal Convolutional Network (TCN). In general, there are two types of PV forecasting models: physics-based model and data-driven model, as summarized in Table I. As can be seen, both physics-based model and data-driven model have advantages and disadvantages. There still lacks a deep fusion approach for integrating their advantages to further improve the forecasting accuracy. Besides, recent studies start to leverage the spatial-temporal correlations between the target site and its neighboring sites to improve the forecasting accuracy. However, how to automatically identify the most efficient neighboring network is still unsolved.

TABLE I: Comparison of STATE-OF-THE-ART PV forecasting models

	Description	Advantages	Disadvantages
Physics-based model [11]-[13]	An analytical model to describe the internal physical process of an actual PV system, therefore achieving PV forecasting by converting the Numerical Weather Prediction (NWP) results to PV forecasts.	Do not rely on historical data, and the forecasting error only comes from NWP when the model is well-calibrated.	Only available to the PV sites whose physical parameters are known, and the forecasting resolution and accuracy are limited by the NWP sources.
Data-driven model [14]-[19]	Use statistical or machine learning methods to construct the mapping from historical data or exogenous variables to the future PV output to achieve forecasting.	Flexible to be implemented in any PV systems that has enough data.	Rely heavily on the quality and quantity of the data of the target PV system, and the forecasting performance can be unstable if the model is not well-trained.

Task Objectives:

- Develop a hybrid PV forecasting framework that combines the advantages of both physics-based model and data-driven model.
- Develop a neighboring site selection method that can automatically identify the most effective neighboring networks to help improve the forecasting accuracy for the target site.

Methodology Overview: The proposed hybrid PV forecasting framework is in Fig. 1, including trend forecasting, fluctuation forecasting, and forecasting results reconciliation. In the trend forecasting stage, the physics-based model of the target site is built to forecast the hourly PV output by converting the hourly NWP to power. To enhance the trend forecasting, a TCN network is introduced to blend multiple NWP sources. In the fluctuation forecasting stage, another TCN network is used to extract the spatial-temporal correlations among the target site and its neighbors to achieve intra-hour forecasting. A neighboring site selection algorithm is proposed to automatically identify the most effective neighbors. Finally, the two forecasting results with different granularities will be reconciled by a third TCN network to generate the final forecasting results.

Simulation Results: The proposed method is tested on 95 PV farms in North Carolina. As shown in Table II, our data-driven model equipped with the neighbor site selection algorithm can achieve 10% accuracy improvement while remaining the lowest model training time, compared with another 3 benchmarking models. As shown in Table III, our hybrid forecasting method can achieve 30% overall accuracy improvement for 6-hour ahead PV forecasting.

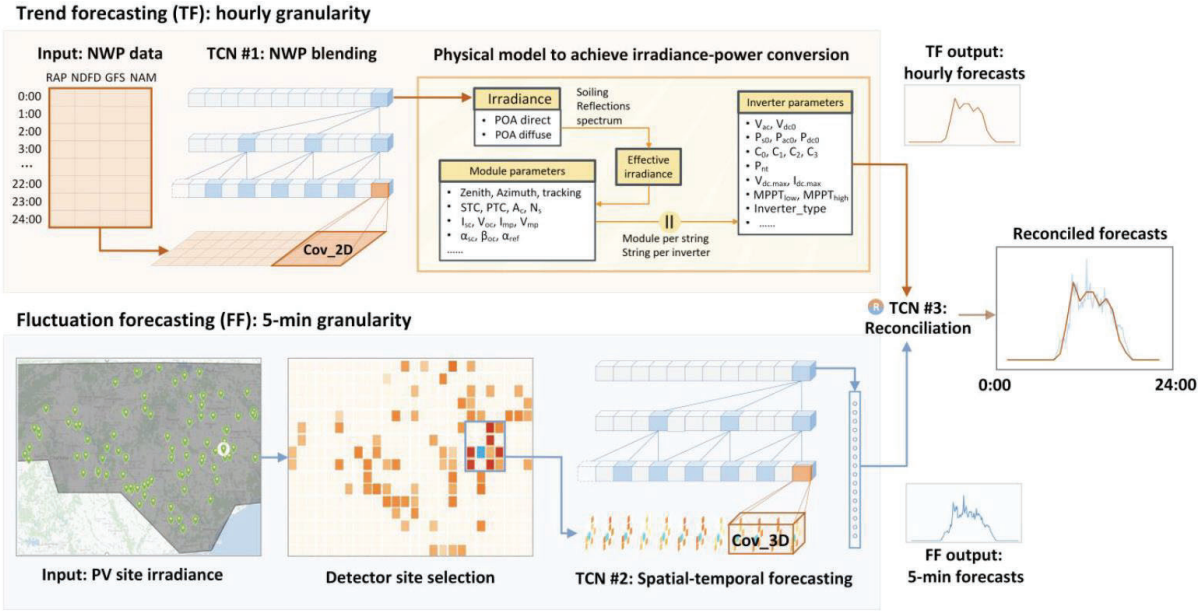

Fig. 1. The proposed hybrid PV forecasting framework, including trend forecasting, fluctuation forecasting and forecasting results reconciliation.

TABLE II: Forecasting performance evaluation (averaged on 95 sites)

Scenarios	Evaluation Metrics	TCN	CNN-LSTM	VGG-8	GARNN
Selected neighbors	RMSE	**39.80**	51.88	48.52	43.81
	CI-90%	**10.37**	15.81	16.25	10.89
Single site	RMSE	**52.86**	55.80	61.77	56.71
	CI-90%	**11.67**	18.00	15.03	12.66
All sites	RMSE	49.92	57.74	54.30	**42.15**
	CI-90%	17.84	23.33	25.69	**14.52**
Random neighbors	RMSE	54.60	52.26	58.11	**49.77**
	CI-90%	13.96	16.07	15.22	**11.33**
Average computation time		**≈ 6min**	≈ 22min	≈ 31min	≈ 164min

TABLE III: AVERAGE FORECASTING RMSE BEFORE AND AFTER RECONCILIATION UNDER DIFFERENT WEATHER CONDITIONS

		5min	30min	2h	4h	6h	Average
Before reconciliation	Sunny	13.70	15.09	20.40	23.62	28.01	20.16
	Cloudy	26.37	37.70	68.80	106.02	142.70	76.32
	Rainy	19.90	26.84	36.44	59.33	91.80	46.86
After reconciliation	Sunny	11.31	13.70	14.44	16.20	17.68	14.67
	Cloudy	28.66	40.68	56.71	60.64	64.00	50.14
	Rainy	21.07	27.55	34.70	37.11	43.17	32.72

Improvement	Sunny	**17.45%**	**9.21%**	**29.22%**	**31.41%**	**36.88%**	**27.27%**
	Cloudy	-8.68%	-7.90%	**17.57%**	**42.80%**	**55.15%**	**34.30%**
	Rainy	-5.88%	-2.65%	**4.77%**	**37.45%**	**52.97%**	**30.18%**

References

[11] Antonanzas, Javier, et al. "Review of photovoltaic power forecasting." Solar energy 136 (2016): 78-111.
[12] Ahmed, Razin, et al. "A review and evaluation of the state-of-the-art in PV solar power forecasting: Techniques and optimization." Renewable and Sustainable Energy Reviews, 124 (2020): 109792.
[13] Das, Utpal Kumar, et al. "Forecasting of photovoltaic power generation and model optimization: A review." Renewable and Sustainable Energy Reviews, 81 (2018): 912-928.
[14] Yang, Dazhi, et al. "Solar irradiance forecasting using spatial-temporal covariance structures and time-forward kriging." Renewable Energy, 60 (2013): 235-245. [9] Kim, Hyeonjin, and Duehee Lee. "Probabilistic Solar Power Forecasting Based on Bivariate Conditional Solar Irradiation Distributions." IEEE Transactions on Sustainable Energy 12.4 (2021): 2031-2041.
[15] Tascikaraoglu, Akin, et al. "Compressive spatio-temporal forecasting of meteorological quantities and photovoltaic power." IEEE Transactions on Sustainable Energy. 7.3 (2016): 1295-1305.
[16] Zhang, Ruiyuan, et al. "Data-driven photovoltaic generation forecasting based on a Bayesian network with spatial–temporal correlation analysis." IEEE Transactions on Industrial Informatics, 16.3 (2019): 1635-1644.
[17] Liu, Yongqi, et al. "Ensemble spatiotemporal forecasting of solar irradiation using variational Bayesian convolutional gate recurrent unit network." Applied Energy 253 (2019): 113596.
[18] Wang, Kejun, Xiaoxia Qi, and Hongda Liu. "A comparison of day-ahead photovoltaic power forecasting models based on deep learning neural network." Applied Energy 251 (2019): 113315.
[19] Jeong, Jaeik, and Hongseok Kim. "Multi-site photovoltaic forecasting exploiting space-time convolutional neural network." Energies 12.23 (2019): 4490.
[20] Li Y, Song L, Zhang S, et al. A TCN-based hybrid forecasting framework for hours-ahead utility-scale PV forecasting[J]. IEEE Transactions on Smart Grid, 2023.

9.18 Task E.3 A GAN based Super-Resolution Method for Generating High-Resolution Load Profiles

Background: In the realm of data-driven applications, the significance of high-resolution load data has grown exponentially. Addressing this imperative, this task presents a a two-stage load profile super-resolution (LPSR) framework, ProfileSR-GAN[9]. In the first stage, a GAN-based model is adopted to restore high-frequency components from the low-resolution load profiles (LRLPs). The trdaditional LPSR methods mainly have two catagory: model-based and deep learning-based, which are based on Mean Square Error (MSE) loss. However, the current algorithms can introduce unrealistic details and cause over-smoothing in the reconstructed HR data. Table I summarizes the advantages and disadvantages of the state-of-the-art methods.

TABLE I: Comparison of STATE-OF-THE-ART missing data restoration methods

	Description	Advantages	Disadvantages
Interpolation-based methods [1]-[4]	Populate high-resolution data points based on prior knowledge and interpolation algorithms.	A large amount of training data is not required, and the model's prediction process is explainable	Need prior knowledge and rule-based prediction is complex, which needs to be manually fine-tune for different scenarios. Low accuracy.
Deep learning-based methods [5]-[8]	End-to-end models based on deep neural networks, which are trained on a large amount of real data complete super-resolution tasks to minimie MSE error.	No prior knowledge modeling is required through manual work. Easy to train and deploy.	Need a large amount of training data. Prediction is lack of high-frequecy component and over-smoothed.

Task Objectives:

- Develop ProfileSR-GAN model for restoring realistic high-resolution load profile from low resolution ones.

Methodology Overview: The ProfileSR-GAN framework is illustrated in Fig. 1. In the first stage, LR profiles and their corresponding weather data are used as inputs of the GAN-based model to generate HR profiles through adversarial training. In the second stage, a polishing network will remove unrealistic power fluctuations from the GAN generated HR profiles. The network comprises a generator with deep convolution layers for high-level feature extraction and transpose convolution layers for profile recovery. Residual blocks and batch normalization address gradient issues. The discriminator utilize LeakyReLU activation, with four convolutional layers and a fully connected layer for real/fake classification. The polishing network is similar to the generator but with fewer layers and no up-sampling transpose convolution layers. Three shape similarity metrics, Peak Load Error (PLE), Frequency Component Error (FCE), and Critical Point Error (CPE), are proposed to comprehensivly eavluate the realiticness compared with state of the art method.

Simulation Results: As shown in Table II, the proposed ProfileSR-GAN model has significant improvement regarding realiticness. This shows that ProfileSR-GAN achieved 36%-62% improvements in shape-related evaluation metrics compared with the baseline methods. Table III is presented NILM as a case study to demonstrate that applying ProfileSR-GAN on upsampling can benefit downstream tasks that require the use of high-resolution load profiles. Simulation

results show that when using ProfileSR-GAN to upsample the low resolution profiles before conducting NILM, appliance-level activities can be better recognized by the NILM algorithms.

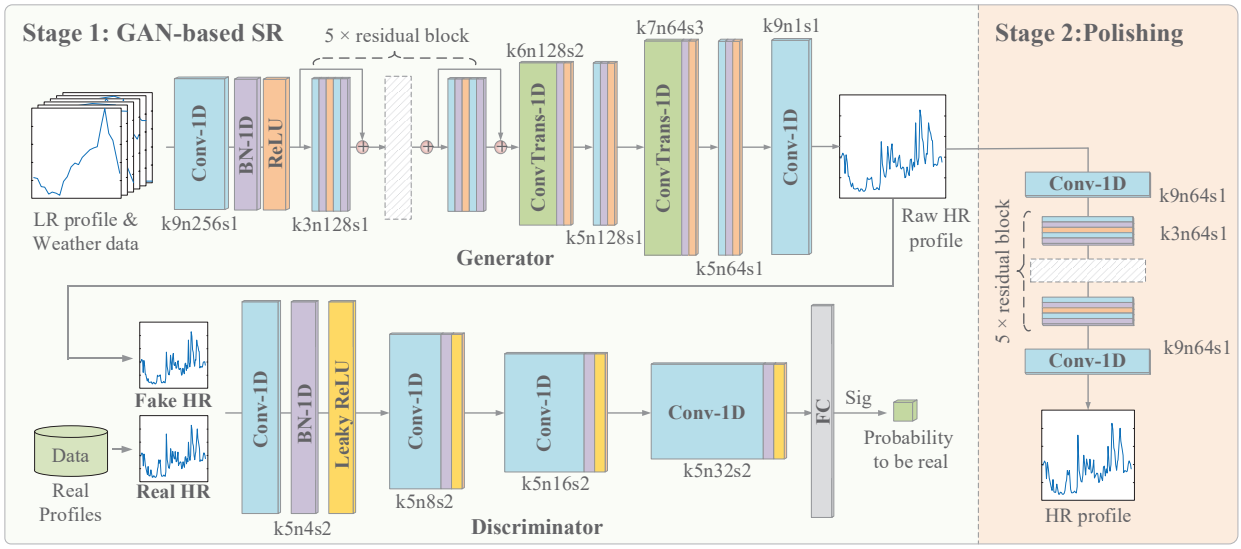

Figure 1. The two-stage ProfileSR-GAN architecture with corresponding kernel size (k), number of feature maps (n), and stride (s) indicated for each convolution layer.

TABLE II: Model performances on the Pecan Street Test Case

SR method		LERP	ASR	SRP	CNN	ProfileSR GAN- (unpolished)	ProfileSR GAN (polished)
MSE	mean	0.55	0.44	0.42	**0.41**	0.61	0.51
	Gain	/	20%	24%	25%	-11%	7%
PLE	mean	1.38	0.99	0.92	0.91	0.86	**0.73**
	Gain	/	28%	33%	34%	38%	47%
FCE	mean	7.22	5.83	5.36	5.38	4.81	**4.65**
	Gain	/	19%	26%	25%	33%	36%
CPE	mean	0.65	0.41	0.29	0.31	0.26	**0.25**
	Gain	/	37%	55%	52%	60%	62%

TABLE III: Performance Comparison of Different NILM Algorithms

Appliance	Metrics	Root mean square error (kW)					Overall error (10^{-1})				
	Houses	LERP	ASR	SRP	CNN	ProfileSR-GAN	LERP	ASR	SRP	CNN	ProfileSR-GAN
Air-conditioner	1	1.063	1.049	1.024	1.016	0.969	0.780	0.883	0.403	0.430	0.346
	2	1.216	1.201	1.071	1.103	1.048	2.417	2.303	1.587	1.917	0.758
	3	1.348	1.350	1.134	1.199	0.922	4.949	4.925	2.620	3.004	1.102
	4	0.793	0.809	0.710	0.727	0.679	0.713	0.790	0.404	0.453	0.104
	mean	1.105	1.102	0.985	1.011	**0.905**	2.215	2.225	1.253	1.451	**0.578**
Fridge	1	0.105	0.106	0.105	0.105	0.106	0.145	0.155	0.128	0.144	0.040
	2	0.071	0.074	0.074	0.078	0.067	0.325	0.285	0.233	0.261	0.160
	3	0.102	0.104	0.089	0.088	0.084	2.703	2.712	1.258	1.539	0.482
	4	0.078	0.079	0.078	0.079	0.078	0.278	0.335	0.138	0.153	0.236
	mean	0.089	0.091	0.087	0.087	**0.084**	0.863	0.872	0.439	0.524	**0.230**
Electric furnace	1	0.118	0.116	0.106	0.106	0.090	0.329	0.362	0.162	0.138	0.130
	2	0.063	0.064	0.057	0.058	0.056	0.687	0.634	0.501	0.644	0.474
	3	0.299	0.299	0.220	0.243	0.201	0.571	0.569	0.689	0.654	0.349
	4	0.071	0.073	0.066	0.067	0.064	0.055	0.057	0.049	0.064	0.021
	mean	0.138	0.138	0.112	0.119	**0.103**	0.410	0.405	0.350	0.375	**0.244**
Dish washer	1	0.127	0.135	0.100	0.114	0.075	0.453	0.495	0.293	0.329	0.051
	2	0.364	0.365	0.321	0.333	0.224	1.378	1.362	0.832	0.990	0.151
	3	0.128	0.123	0.102	0.106	0.073	1.434	1.351	0.636	0.755	0.248
	4	0.089	0.086	0.105	0.095	0.087	0.065	0.049	0.163	0.123	0.025
	mean	0.177	0.177	0.157	0.162	**0.115**	0.832	0.814	0.481	0.549	**0.119**
Microwave	1	0.085	0.084	0.083	0.084	0.083	0.114	0.124	0.130	0.138	0.156
	2	0.023	0.022	0.022	0.022	0.021	0.023	0.018	0.018	0.020	0.010
	3	0.028	0.028	0.013	0.014	0.013	0.468	0.453	0.037	0.055	0.023
	4	0.123	0.122	0.121	0.122	0.120	0.489	0.492	0.433	0.458	0.160
	mean	0.065	0.064	0.060	0.060	**0.059**	0.273	0.272	0.154	0.168	**0.087**

References

[1] Zhang, Yunfeng, et al. "Single-image super-resolution based on rational fractal interpolation." IEEE Transactions on Image Processing 27.8 (2018): 3782-3797.
[2] Ding, Na, et al. "Single image super-resolution via dynamic lightweight database with local-feature based interpolation." Journal of Computer Science and Technology 34 (2019): 537-549.
[3] Cheng, Dong, and Kit Ian Kou. "FFT multichannel interpolation and application to image super-resolution." Signal Processing 162 (2019): 21-34.
[4] Yao, Xunxiang, et al. "Adaptive rational fractal interpolation function for image super-resolution via local fractal analysis." Image and Vision Computing 82 (2019): 39-49.
[5] V. Kuleshov, S. Z. Enam, and S. Ermon, "Audio super resolution using neural networks," arXiv preprint arXiv:.00853, 2017.
[6] G. Liu, J. Gu, J. Zhao, F. Wen, and G. Liang, "Super Resolution Perception for Smart Meter Data," Information Sciences, 2020
[7] Su, Hua, et al. "Super-resolution of subsurface temperature field from remote sensing observations based on machine learning." International Journal of Applied Earth Observation and Geoinformation 102 (2021): 102440.
[8] Wang, Zhisheng, et al. "Temporal graph super resolution on power distribution network measurements." IEEE Access 9 (2021): 70628-70638.
[9] Song, Lidong, Yiyan Li, and Ning Lu. "ProfileSR-GAN: A gan based super-resolution method for generating high-resolution load profiles." IEEE Transactions on Smart Grid 13.4 (2022): 3278-3289.

9.19 Task E.4 Synthetic load profile generation

Background: This task presents a deep-learning framework, Multi-load Generative Adversarial Network (MultiLoad-GAN), for generating a group of synthetic load profiles (SLPs) simultaneously, considering the spatial-temporal correlations among a group of loads that are served by the same distribution transformer. SLPs are generated load profiles bearing similar characteristics as the real ones. In general, there are two approaches for generating SLPs: simulation-based and data-driven. Table X.I summarizes the advantages and disadvantages of the state-of-the-art SLP generation methods and compares our algorithm with the existing ones. As can be seen in the table, up till now, all existing generative methods generate SLPs one at a time. There is no generative method proposed for generating a group of SLPs served by the same distribution transformer or the same feeder, where the SLPs have strong spatial-temporal correlations.

Task Objectives

- Enable the generation of correlated realistic SLPs in large quantity for meeting the emerging need in microgrid and distribution system planning.
- Evaluate the realisticness of generated load profiles.
- Develop an iterative data augmentation mechanism is to tackle data scarcity.

Methodology Overview: The configuration of MultiLoad-GAN is shown in Fig. 1, it generates N load profiles simultaneously. It is a GAN-based model and consists of two components: a generator network (G) and a discriminator network (D).

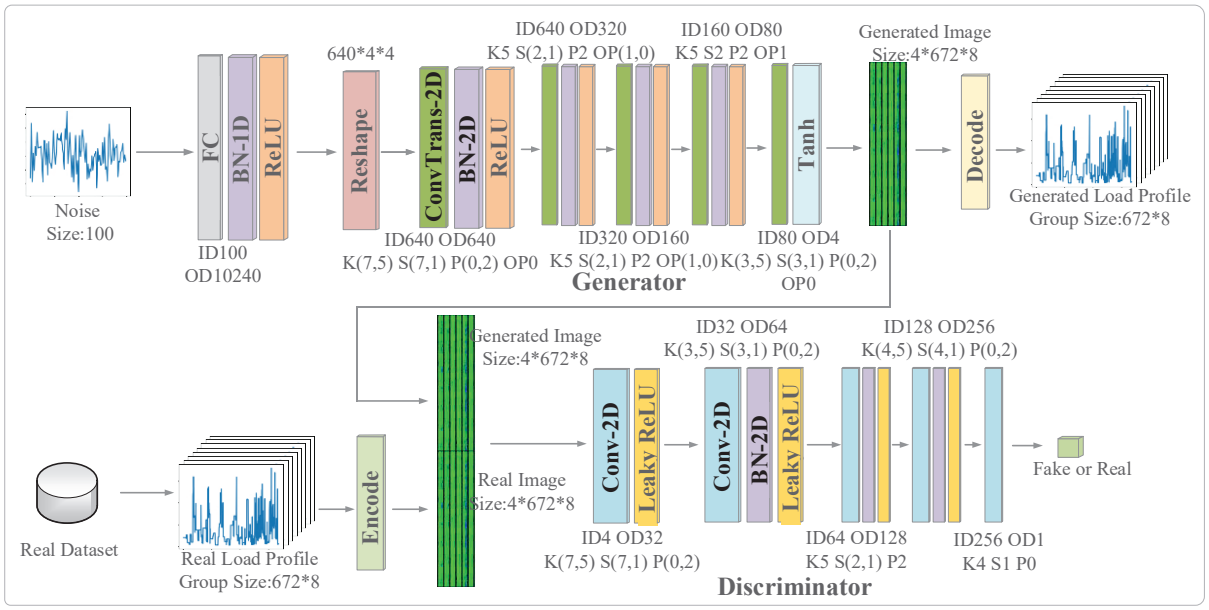

Fig. 1. MultiLoad-GAN architecture with corresponding input dimension (ID), output dimension (OD), kernel size (K), stride (S), padding (P), output padding (OP) for each convolutional layer. The parameter is an example for generating weekly 15-min load group with 8 households

Simulation Results: The realisticness of the generated load groups is evaluated by comparing the generated load groups with the "original positive samples" using two different kinds of realisticness metrics: statistics metrics based on domain knowledge and a deep-learning classifier for comparing high-level features. The performance indices are summarized in Table II and Fig. 2.

The results show that MultiLoad-GAN captures group-level characteristics better than benchmark methods, and the Automatic Data Augmentation (ADA) process significantly shorten the distance between MultiLoad-GAN generated data set and the real data set. This shows that the ADA process avoids MultiLoad-GAN to be over-trained so that it only generates load groups strongly resemble the “original positive samples”.

TABLE I: Comparison of our Multiload-GAN model with the state-of-the-art generative methods

		Description	Advantages	Disadvantages	Model output
Model-based methods [10][11]		Use physical models, such as building thermodynamics and customer behavioral models, to simulate electricity consumption profiles.	Explainable as the models reflect the laws of physics when describing the behavior behind field measurements	Require detailed physics-based models with many inputs and require parameter tuning.	**Single load profile** (When generating a load profile, the methods do not consider the spatial-temporal correlations among a group of generated load profiles)
Data-driven methods	Clustering based [12][13]	Cluster existing load profiles into different categories so that by combining the load profiles across different categories, SLPs are generated.	Easy to implement and can represent some realistic load profile characteristics.	Lack of diversity when using combinations of a limited number of existing profiles.	
	Forecasting based [14]-[17] (the benchmark method)	Generate SLPs based on publicly available load or weather data.	Easy to implement and flexible to generate load profiles with different lengths and granularities.	Depend heavily on historical data. The generated load profiles have similar patterns with historical data, therefore, lack of diversity.	
	SingleLoad-GAN-based [19]-[21] (the benchmark method)	GAN-based generative methods to generate the SLP for one customer at a time.	Learn from the real data distribution to generate diversified load profiles with high-frequency details.	Hard to train.	
	MultiLoad-GAN (the proposed method)	GAN-based generative methods to generate a group of spatial-temporal correlated load profiles simultaneously. Such load profiles can be loads served by the same transformer or feeder.	Learn from the distribution of real data to generate diversified load profiles with high-frequency details. Preserve the spatial-temporal correlations between loads.	Hard to train.	**Multiple spatial-temporal correlated load profiles**

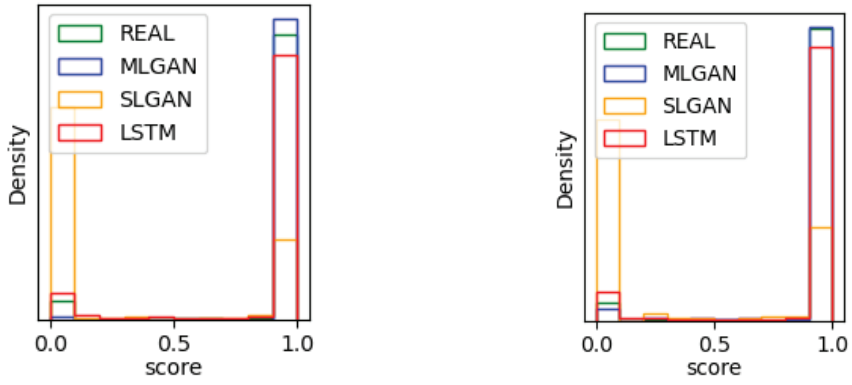

Figure 2. Distribution of DLC scores (a) without ADA and (b) with ADA.

TABLE II: Results of DLC-based evaluation

Indices	Real data	SingleLoad-GAN	LSTM	MultiLoad-GAN	MultiLoad-GAN (with ADA)
Percent of Real	94.38%	19.69%	84.83%	99.06%	**94.99%**
Mean Confidence Level	0.9371	0.1913	0.8919	0.9899	**0.9491**
Fréchet inception distance with the *Real* load group	N/A	0.5173	0.00706	0.01106	**0.000055**

References

[10] J. Dickert and P. Schegner, "A time series probabilistic synthetic load curve model for residential customers," *2011 IEEE Trondheim PowerTech*, Trondheim, Norway, pp. 1-6, 2011, doi: 10.1109/PTC.2011.6019365.
[11] J. K. Gruber and M. Prodanovic, "Residential Energy Load Profile Generation Using a Probabilistic Approach," *2012 Sixth UKSim/AMSS European Symposium on Computer Modeling and Simulation*, Malta, pp. 317-322, 2012, doi: 10.1109/EMS.2012.30.
[12] Y. -I. Kim, S. -J. Kang, J. -M. Ko and S. -H. Choi, "A study for clustering method to generate Typical Load Profiles for Smart Grid," *8th International Conference on Power Electronics - ECCE Asia*, Jeju, Korea (South), pp. 1102-1109, 2011, doi: 10.1109/ICPE.2011.5944675.
[13] A. Pinceti, O. Kosut and L. Sankar, "Data-Driven Generation of Synthetic Load Datasets Preserving Spatio-Temporal Features," *2019 IEEE Power & Energy Society General Meeting (PESGM)*, Atlanta, GA, USA, 2019, pp. 1-5, doi: 10.1109/PESGM40551.2019.8973532.
[14] X. Liu, N. Iftikhar, H. Huo, R. Li, and P. Sieverts Nielsen, "Two approaches for synthesizing scalable residential energy consumption data." *Future Generation Computer Systems,* vol. 95, pp. 586-600, 2019.
[15] N. Iftikhar, X. Liu, F. E. Nordbjerg and S. Danalachi, "A Prediction-Based Smart Meter Data Generator," *2016 19th International Conference on Network-Based Information Systems (NBiS)*, Ostrava, Czech Republic, 2016, pp. 173-180, doi: 10.1109/NBiS.2016.15.
[16] J. Sarochar, I. Acharya, H. Riggs, A. Sundararajan, L. Wei, T. Olowu, A. I. Sarwat, "Synthesizing Energy Consumption Data Using a Mixture Density Network Integrated with Long Short Term Memory," *2019 IEEE Green Technologies Conference(GreenTech)*, Lafayette, LA, USA, 2019, pp. 1-4, doi: 10.1109/GreenTech.2019.8767148.
[17] G. -G. Pillai, G. -A. Putrus, N. -M. Pearsall. "Generation of synthetic benchmark electrical load profiles using publicly available load and weather data." *International Journal of Electrical Power & Energy Systems*, vol. 61, pp. 1-10, 2014.
[18] I. Goodfellow, J. Pouget-Abadie, M. Mirza, B. Xu, D. Warde-Farley, S. Ozair, A. Courville, and Y. Bengio. "Generative adversarial nets." *Communications of the ACM*, vol. 63, no. 11, pp. 139-144, 2020.
[19] Y. Gu, Q. Chen, K. Liu, L. Xie and C. Kang, "GAN-based Model for Residential Load Generation Considering Typical Consumption Patterns," *2019 IEEE Power & Energy Society Innovative Smart Grid Technologies Conference (ISGT)*, Washington, DC, USA, 2019, pp. 1-5, doi: 10.1109/ISGT.2019.8791575.
[20] Z. Wang and T. Hong, “Generating realistic building electrical load profiles through the Generative Adversarial Network (GAN),” *Energy and Buildings*, vol. 224, pp. 0378-7788, Oct. 2020, doi: 10.1016/j.enbuild.2020.110299.
[21] C. Zhang, S. R. Kuppannagari, R. Kannan and V. K. Prasanna, "Generative Adversarial Network for Synthetic Time Series Data Generation in Smart Grids," *2018 IEEE International Conference on Communications, Control, and Computing Technologies for Smart Grids (SmartGridComm)*, Aalborg, Denmark, 2018, pp. 1-6, doi: 10.1109/SmartGridComm.2018.8587464.
[22] Yi Hu, Yiyan Li, Lidong Song, Han Pyo Lee, PJ Rehm, Mattew Makdad, Edmond Miller, and Ning Lu, "MultiLoad-GAN: A GAN-Based Synthetic Load Group Generation Method Considering Spatial-Temporal Correlations," *in IEEE Transactions on Smart Grid*, doi: 10.1109/TSG.2023.3302192.

9.20 Task E.5 Power-Band based Data Segmentation (PBDS) Method for Enhancing Meter Phase and Transformer-Meter Pairing Identification

Background: We applied power-band-based data segmentation (PBDS) in two meter topology identification algorithms: customer phase identification and transformer-meter pairing identification. Through simulation on thirteen real feeders, our proposed algorithm outperformed existing approaches, significantly improving the accuracy of meter topology identification without introduction significant computational complexity.

Table 1 presents a comprehensive overview of existing methods for addressing phase and transformer-meter pairing identification problems, along with a comparison of their strengths and weaknesses in relation to the proposed approach.

TABLE I: A Review of Existing Methods and Our Contributions

Category	Methodology	Descriptions	Strength	Weakness
Phase Identification	Signal injection [1]	Detect a signal injected into a specific phase	Extremely accurate	Additional equipment required
	PMU [2]	Measure the voltage phase angle		PMU data required
	Real Power-based [3-4]	Customer loads on the same phase should match substation power measurements	Simplicity	Degradation depending on the AMI penetration
	Voltage-based [6-7]	Customers on the same phase exhibit stronger voltage correlations than those on different phases	Easily-interpretable Require only voltage from AMI	Inefficient use of data
	ML-based [812]	Unsupervised learning algorithms that solve the clustering problem	High accuracy Identify phases without labels	Uninterpretable and unexplainable Manual verification and retraining required if applied to other feeders
	PBDS (Proposed) [13-14]	**Power-band based data segmentation algorithm to extract highly correlated voltage segments on the same phase**	**Easily-interpretable Identify phases without labels Require only real power and voltage from AMI Efficient use of data through data segmentation**	**Parameter tuning required**
Transformer-Meter Pairing Identification	Load summing [5], [15]	Customer loads under the same DT should match DT power measurements	Simplicity	DT metering required
	Voltage-based [16-19]	Analyze voltage correlation coefficient between all customers labeled on the same transformer	Easily-interpretable Require only AMI data and customer DT labels	Inefficient use of data Not provide a complete DT grouping result No solution provided for incorrect DT labeling
	Regression-based [20-22]	Estimate line impedance using linear regression and build up a secondary circuit	Mathematical simplicity	Requires reactive power from AMI
	PBDS (Proposed) [14]	**A two-stage algorithm based on PBDS to distinguish between a group of meters under the same DT and a group of meters under different DTs**	**Present a method to correct abnormal DT-meter pairs Required only AMI data and customer DT labels Efficient use of data through data segmentation**	**Cannot identify a transformer that serves only one customer**

Task Objectives

- Automated identification of smart meter phase and transformer-meter pairing relationships.

Methodology Overview: The configuration of the proposed phase identification algorithm is shown in Fig. 1(a). The PBDS steps are highlighted in the two shaded boxes. Two cases, known and unknown phase labels, are considered. The configuration of the proposed transformer-meter pairing identification algorithm is shown in Fig. 1(b). The PBDS is used to eliminate false positives.

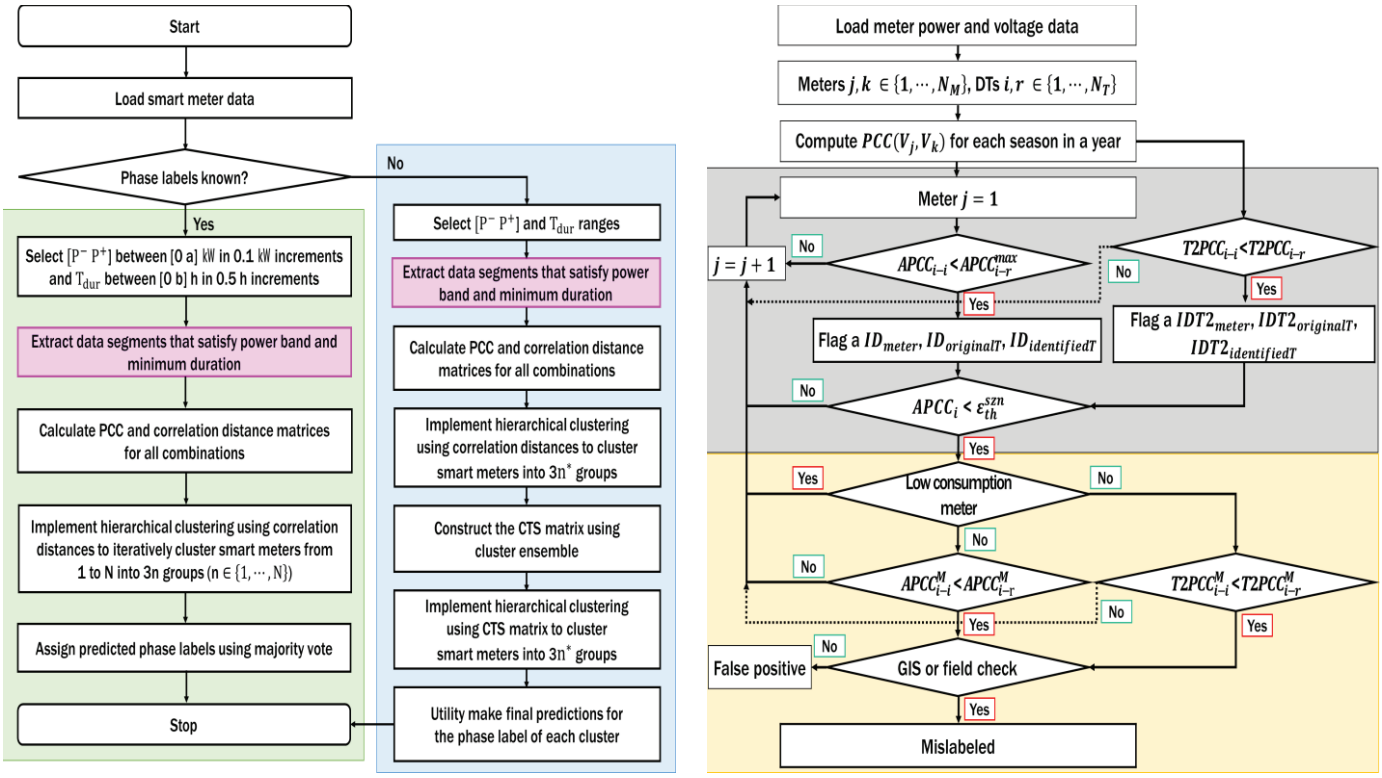

(a) (b)

Figure 1. Flowchart of the PBDS based, (a) meter phase identification methodology, (b) the two-stage transformer-meter pairing identification algorithm.

Simulation Results: The proposed method is tested on 13 real feeders in North Carolina. As shown in Tables II and III, the proposed phase identification algorithm achieves a 1.1% and 1.9% improvement in accuracy compared to benchmarking methods (i.e., Spectral Clustering and Co-association Matrix Ensemble Clustering), respectively. As indicated in Table IV, our transformer-meter pairing identification algorithm achieves an 84.6% reduction in the false positive rate.

TABLE II. Case 1: Phase Identification Results and Performance Comparison.

Feeder No.	Phases in the utility records				Predicted phases				Round 1				Round 2			
	A	B	C	A+B+C (N_{RT})	A	B	C	A+B+C (N_{PT})	Detected as correct (N_{C1})	Detected as incorrect ($N_{RT}-N_{C1}$)	Validated (N_{V1})	Accuracy $((N_{C1}+N_{V1})/N_{RT})$	Detected as correct (N_{C2})	Detected as incorrect ($N_{RT}-N_{C2}$)	Validated (N_{V2})	Accuracy $((N_{C2}+N_{V2})/N_{RT})$
PBDS																
1 BR	7	24	2	33	5	25	3	33	31	2	-	**93.9%**	31	2	-	**93.9%**
2 DB	146	159	145	450	139	152	159	450	415	35	35	**100%**	447	3	-	**99.3%**
3 DF	11	26	36	73	11	26	36	73	73	-	-	**100%**	73	-	-	**100%**
4 EB	147	91	178	416	144	94	178	416	399	17	10	**98.3%**	411	5	-	**98.8%**
5 H1	192	214	231	637	210	218	209	637	605	32	24	**98.7%**	629	8	-	**98.7%**
6 H4	344	249	306	899	363	262	274	899	803	96	80	**98.2%**	898	1	-	**99.9%**
7 HD	113	102	109	324	115	104	105	324	313	11	5	**98.1%**	318	6	-	**98.1%**
8 IR	51	51	71	173	49	53	71	173	169	4	2	**98.8%**	171	2	-	**98.8%**
9 PV	62	193	301	556	57	194	305	556	505	51	35	**97.1%**	543	13		**97.7%**
10 PG	22	42	67	131	22	42	67	131	131	-	-	**100%**	131	-	-	**100%**
11 SL	3	10	11	24	3	10	11	24	24	-	-	**100%**	24	-	-	**100%**
12 SF	39	37	32	108	39	37	32	108	108	-	-	**100%**	108	-	-	**100%**
13 VF	55	56	26	137	55	56	26	137	137	-	-	**100%**	137	-	-	**100%**
Total	**1192**	**1254**	**1515**	**3961**	**1212**	**1273**	**1476**	**3961**	**3713**	**248**	**191**	**98.6%**	**3921**	**40**	**-**	**99.0%**
SC [13]																
1 BR	7	24	2	33	9	24	-	33	29	4	1	**90.9%**	30	3	-	**90.9%**
2 DB	146	159	145	450	158	155	137	450	435	15	8	**98.4%**	441	9	-	**98.0%**
3 DF	11	26	36	73	11	24	38	73	70	3	-	**95.9%**	70	3	-	**95.9%**
4 EB	147	91	178	416	164	80	172	416	397	19	12	**98.3%**	408	8	-	**98.1%**
5 H1	192	214	231	637	204	221	212	637	606	31	16	**97.6%**	619	18	-	**97.2%**
6 H4	344	249	306	899	347	250	302	899	831	68	60	**99.1%**	893	6	1	**99.4%**
7 HD	113	102	109	324	115	103	106	324	312	12	5	**97.8%**	318	6	-	**98.1%**
8 IR	51	51	71	173	49	50	74	173	167	6	-	**96.5%**	167	6	-	**96.5%**
9 PV	62	193	301	556	50	183	323	556	527	29	14	**97.3%**	532	24	2	**96.0%**
10 PG	22	42	67	131	21	42	68	131	130	1	-	**99.2%**	130	1	-	**99.2%**
11 SL	3	10	11	24	4	10	10	24	23	1	-	**95.8%**	23	1	-	**95.8%**
12 SF	39	37	32	108	39	37	32	108	108	-	-	**100%**	108	-	-	**100%**
13 VF	55	56	26	137	55	56	26	137	135	2	-	**98.5%**	135	2	-	**98.5%**
Total	**1192**	**1254**	**1515**	**3961**	**1226**	**1235**	**1500**	**3961**	**3770**	**191**	**116**	**98.1%**	**3874**	**87**	**3**	**97.9%**

TABLE III. Case 2: Phase Identification Results and Performance Comparison.

Feeder No.		Phases in the utility records				Predicted phases				Round 1				Round 2			
		A	B	C	A+B+C (N_{RT})	A	B	C	A+B+C (N_{PT})	Detected as correct (N_{C1})	Detected as incorrect ($N_{RT}-N_{C1}$)	Validated (N_{V1})	Accuracy $((N_{C1}+N_{V1})/N_{RT})$	Detected as correct (N_{C2})	Detected as incorrect ($N_{RT}-N_{C2}$)	Validated (N_{V2})	Accuracy $((N_{C2}+N_{V2})/N_{RT})$
PBDS																	
1	BR	7	24	2	33	7	25	1	33	31	2	-	**93.9%**	31	2	-	**93.9%**
2	DB	146	159	145	450	133	153	164	450	412	38	37	**99.8%**	444	6	4	**99.6%**
3	DF	11	26	36	73	11	26	36	73	73	-	-	**100%**	73	-	-	**100%**
4	EB	147	91	178	416	152	90	174	416	407	9	6	**99.3%**	402	14	4	**97.6%**
5	H1	192	214	231	637	213	218	206	637	606	31	25	**99.1%**	630	7	-	**98.9%**
6	H4	344	249	306	899	330	253	316	899	796	103	103	**100%**	898	1	-	**99.9%**
7	HD	113	102	109	324	114	104	106	324	314	10	4	**98.1%**	315	9	1	**97.5%**
8	IR	51	51	71	173	49	54	70	173	170	3	-	**98.3%**	170	3	-	**98.3%**
9	PV	62	193	301	556	36	174	346	556	505	51	40	**98.0%**	548	8	-	**98.6%**
10	PG	22	42	67	131	22	42	67	131	131	-	-	**100%**	131	-	-	**100%**
11	SL	3	10	11	24	3	10	11	24	24	-	-	**100%**	24	-	-	**100%**
12	SF	39	37	32	108	39	37	32	108	108	-	-	**100%**	108	-	-	**100%**
13	VF	55	56	26	137	55	56	26	137	137	-	-	**100%**	137	-	-	**100%**
Total		**1192**	**1254**	**1515**	**3961**	**1164**	**1242**	**1555**	**3961**	**3714**	**247**	**215**	**99.2%**	**3911**	**50**	**9**	**99.0%**
CAM-EC [14]																	
1	BR	7	24	2	33	6	24	3	33	27	6	1	**84.8%**	28	5	-	**84.8%**
2	DB	146	159	145	450	155	159	136	450	435	15	8	**98.4%**	441	9	-	**98.0%**
3	DF	11	26	36	73	18	20	35	73	65	8	-	**89.0%**	65	8	-	**89.0%**
4	EB	147	91	178	416	165	77	174	416	394	22	12	**97.6%**	400	16	-	**96.2%**
5	H1	192	214	231	637	205	218	214	637	606	31	16	**97.6%**	619	18	-	**97.2%**
6	H4	344	249	306	899	322	248	329	899	803	96	88	**99.1%**	895	4	-	**99.6%**
7	HD	113	102	109	324	115	104	105	324	313	11	5	**98.1%**	318	6	-	**98.1%**
8	IR	51	51	71	173	49	46	78	173	165	8	-	**95.4%**	165	8	-	**95.4%**
9	PV	62	193	301	556	58	182	316	556	526	30	16	**97.5%**	521	35	-	**93.7%**
10	PG	22	42	67	131	21	42	68	131	130	1	-	**99.2%**	130	1	-	**99.2%**
11	SL	3	10	11	24	4	10	10	24	23	1	-	**95.8%**	23	1	-	**95.8%**
12	SF	39	37	32	108	37	39	32	108	106	2	-	**98.1%**	106	2	-	**98.1%**
13	VF	55	56	26	137	55	56	26	137	135	2	-	**98.5%**	135	2	-	**98.5%**
Total		**1192**	**1254**	**1515**	**3961**	**1210**	**1225**	**1526**	**3961**	**3728**	**233**	**146**	**97.8%**	**3846**	**115**	**-**	**97.1%**

TABLE IV. Transformer-Meter Pairing Identification Results (ID: Average PCC; IDT2: Top-2 PCC).

Feeder No.		No. of DTs	No. of meters	Stage 1							Stage 2					Reduced false positive rate $(N_{T1} - N_{T2})/N_{T1}$
				ID	*IDT2*	ID_{szn}	$IDT2_{szn}$	*Total* (N_{T1})	*Validated* (N_{V1})	N_{V1}/N_{T1}	*ID*	*IDT2*	*Total* (N_{T2})	*Validated* (N_{V2})	N_{V2}/N_{T2}	
1	BR	9	33	2	1	1	1	1	-	-	-	-	-	-	-	100
2	DB	66	450	25	13	21	12	21	3	14.3	4	6	6	3	50.0	71.4
3	DF	16	73	3	3	3	3	3	-	-	-	-	-	-	-	100
4	EB	78	416	7	2	7	2	7	-	-	-	-	-	-	-	100
5	H1	143	637	28	14	26	13	28	2	7.1	2	3	3	2	66.7	89.3
6	H4	155	899	15	15	12	12	14	3	21.4	3	3	3	3	100	78.6
7	HD	78	324	5	1	5	1	5	-	-	-	-	-	-	-	100
8	IR	24	173	-	-	-	-	-	-	-	-	-	-	-	-	-
9	PV	118	556	39	10	30	9	32	4	12.5	3	2	4	-	-	87.5
10	PG	54	131	6	2	6	2	6	1	16.7	1	2	2	1	50.0	66.7
11	SL	8	24	-	-	-	-	-	-	-	-	-	-	-	-	-
12	SF	40	108	1	-	1	-	1	-	-	-	-	-	-	-	100
13	VF	37	137	5	3	5	3	5	1	20.0	1	1	1	1	100	80.0
Total		**826**	**3961**	**136**	**64**	**117**	**58**	**123**	**14**	**11.4**	**14**	**17**	**19**	**10**	**52.6**	**84.6**

Reference

[1] Shen, Zhiyu, et al. "Three-phase AC system impedance measurement unit (IMU) using chirp signal injection." 2013 Twenty-Eighth Annual IEEE Applied Power Electronics Conference and Exposition (APEC). IEEE, 2013.
[2] Wen, Miles HF, et al. "Phase identification in distribution networks with micro-synchrophasors." 2015 IEEE Power & Energy Society General Meeting. IEEE, 2015.
[3] Arya, Vijay, et al. "Phase identification in smart grids." 2011 IEEE International Conference on Smart Grid Communications (SmartGridComm). IEEE, 2011.
[4] Arya, Vijay, et al. "Inferring connectivity model from meter measurements in distribution networks." Proceedings of the fourth international conference on Future energy systems. 2013.
[5] Pezeshki, Houman, and Peter J. Wolfs. "Consumer phase identification in a three phase unbalanced LV distribution network." 2012 3rd IEEE PES Innovative Smart Grid Technologies Europe (ISGT Europe). IEEE, 2012.
[6] Olivier, Frederic, et al. "Phase identification of smart meters by clustering voltage measurements." 2018 Power Systems Computation Conference (PSCC). IEEE, 2018.
[7] Mitra, Rajendu, et al. "Voltage correlations in smart meter data." Proceedings of the 21th ACM SIGKDD International Conference on Knowledge Discovery and Data Mining. 2015.
[8] Wang, Wenyu, et al. "Phase identification in electric power distribution systems by clustering of smart meter data." 2016 15th IEEE International Conference on Machine Learning and Applications (ICMLA). IEEE, 2016.
[9] Hosseini, Zohreh S., Amin Khodaei, and Aleksi Paaso. "Machine learning-enabled distribution network phase identification." IEEE Transactions on Power Systems 36.2 (2020): 842-850.
[10] Foggo, Brandon, and Nanpeng Yu. "Improving supervised phase identification through the theory of information losses." IEEE Transactions on Smart Grid 11.3 (2019): 2337-2346.
[11] Blakely, Logan, Matthew J. Reno, and Wu-chi Feng. "Spectral clustering for customer phase identification using AMI voltage timeseries." 2019 IEEE Power and Energy Conference at Illinois (PECI). IEEE, 2019.
[12] Blakely, Logan, and Matthew J. Reno. "Phase identification using co-association matrix ensemble clustering." IET Smart Grid 3.4 (2020): 490-499.
[13] Lee, Han Pyo, et al. "A novel data segmentation method for data-driven phase identification." 2022 IEEE Power & Energy Society General Meeting (PESGM). IEEE, 2022. Available online at: https://ieeexplore.ieee.org/
[14] Lee, Han Pyo, et al. "A Novel Power-Band based Data Segmentation Method for Enhancing Meter Phase and Transformer-Meter Pairing Identification." Submitted to IEEE Transactions on Power Delivery. Review. 2023. Available online at: https://arxiv.org/abs/2210.00155
[15] Pappu, Satya Jayadev, et al. "Identifying topology of low voltage distribution networks based on smart meter data." IEEE Transactions on Smart Grid 9.5 (2017): 5113-5122.
[16] Luan, Wenpeng, et al. "Smart meter data analytics for distribution network connectivity verification." IEEE Transactions on Smart Grid 6.4 (2015): 1964-1971.
[17] Watson, Jeremy Donald, John Welch, and Neville R. Watson. "Use of smart-meter data to determine distribution system topology." The Journal of Engineering 2016.5 (2016): 94-101.
[18] Weng, Yang, Yizheng Liao, and Ram Rajagopal. "Distributed energy resources topology identification via graphical modeling." IEEE Transactions on Power Systems 32.4 (2016): 2682-2694.
[19] Blakely, Logan, and Matthew J. Reno. "Identifying errors in service transformer connections." 2020 IEEE Power & Energy Society General Meeting (PESGM). IEEE, 2020.
[20] Short, Tom A. "Advanced metering for phase identification, transformer identification, and secondary modeling." IEEE Transactions on Smart Grid 4.2 (2012): 651-658.
[21] Ye, C. H. E. N., et al. "Two-stage topology identification method for distribution network via clustering correction." 2019 IEEE Innovative Smart Grid Technologies-Asia (ISGT Asia). IEEE, 2019.
[22] Blakely, Logan, and Matthew J. Reno. "Identification and correction of errors in pairing AMI meters and transformers." 2021 IEEE Power and Energy Conference at Illinois (PECI). IEEE, 2021.

9.21 Task F.1 An Iterative Bidirectional Gradient Boosting Approach for Conservation Voltage Reduction (CVR) Baseline Estimation

Background: In this subtask, we developed IBi-GBM, a novel iterative, bidirectional gradient boosting CVR baseline estimation algorithm designed to assess the efficacy of CVR in load reduction. Our approach introduces a hybrid methodology, incorporating a bi-directional framework and a hybrid similar day selection method. The proposed algorithm exhibits robust performance across different data resolutions (ranging from 5- to 60-minute intervals), various data types (including aggregated smart meter and SCADA data), and seasonal changes (specifically, summer and winter). Our findings reveal substantial variability in CVR performance across different feeders and seasons.

In general, there are four main approaches for CVR baseline estimation: comparison-based, synthesis-based, load modeling-based, regression-based, and machine learning (ML)-based techniques. In Table 1, we offer a thorough literature review of current CVR baseline estimation approaches, highlighting their strengths and weaknesses in comparison to the proposed approach

Table 1: A Review of Existing Methods and Our Contributions

Category	Methodology	Descriptions	Strength	Weakness
Comparison -based	Field experiments [1]	Compare performance between test and control groups	Simplicity	Dependent on control group
Synthesis -based	LTV [2]	Aggregate LTV behaviors to estimate the CVR effects of a circuit	Quick estimation	Difficult to collect load share information for a feeder Requires LTV response of all existing electrical appliances
Load Modeling -based	LTV sensitivity [3], [4]	Represent load consumption as a function of voltages, and calculate CVR factors from the identified LTV sensitivities	Can estimate time varying CVR factors	Cannot represent different load compositions depending on the load model used
Regression -based	Linear regression [5], [6] Multivariate regression [7]-[9]	Loads are modeled as a function of several impact factors to calculate the CVR factor	Interpretable Mathematical simplicity	The margin of error may be larger than CVR effect Inability to capture the characteristics of nonlinear loads
ML -based	MSVR [10]	MSVR-based model	Interpretable Can approximate nonlinear behaviors of load	Noniterative and uni-directional Accuracy relies on the existence of similar profiles Results may not always be attainable for each test day
	MLP, LSTM, TCN [11]-[13]	Uni-directional DL model	Can capture complex and nonlinear relationships	Uni-directional Fixed prediction length Demands a substantial volume of training data
	Load-PIN [14]	GAN-based generative method	Bi-directional Variable prediction length Can capture complex and nonlinear relationships	Mathematically complex Lack of interpretability Computationally expensive for training Demands a substantial volume of training data
Iterative bidirectional	**IBi-GBM IBi-LightGBM (Proposed) [15]**	**Iterative, bidirectional GB-based algorithm**	**Interpretable, capture nonlinear behaviors of load and bi-directional information for variable-duration events and require very few training data**	**Accuracy relies on the existence of available similar profiles**

Task Objectives: Identify the baseline of CVR to enable performance evaluation of CVR based load reduction.

Methodology Overview: Accurate baseline estimation is crucial for utilities to assess the effectiveness of demand response (DR) programs. The baseline of a DR event is essentially the load profile that would exist if a DR action had not been implemented. Thus, to estimate the DR baseline, it's essential to reconstruct the electricity consumption as it would be during the DR period, assuming that not DR actions are implemented. This process can be conceptualized as a missing data segments (MSDs) recovery problem.

As illustrated in Fig. 1, the proposed Iterative, Bidirectional Gradient Boosting Model (IBi-GBM)-based CVR baseline estimation methodology involves three essential processes: the selection of similar days, the training of the GB model, and the iterative generation of baseline data points.

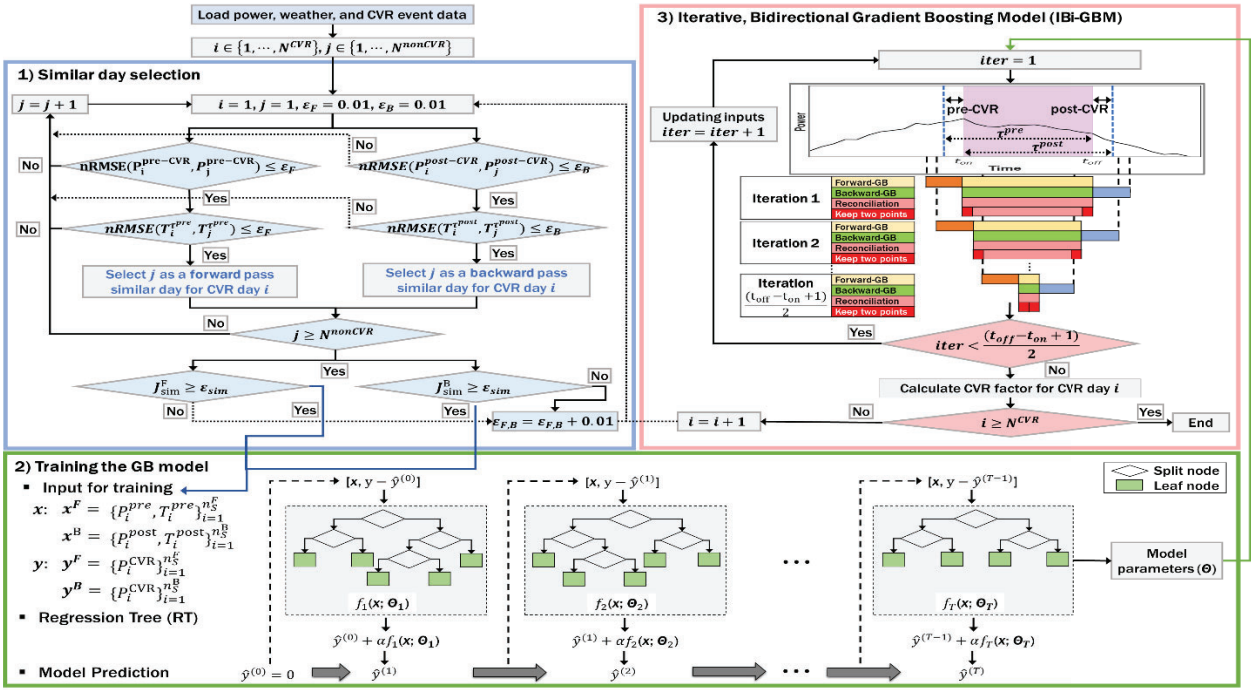

Fig. 1. A three-stage framework proposed for CVR baseline estimation, involving: 1) selecting similar days, 2) training the GB model, and 3) implementing IBi-GBM.

Simulation Results: Two real-world datasets (i.e., 15-min smart meter data and 5-min SCADA data) are used to develop and validate the performance of the two iterative bidirectional-GB based CVR baseline estimation algorithms. Tables II and III demonstrate that the proposed IBi-GBM exhibits robust performance across various data resolutions and in different seasons for virtual-CVR days, and outperforms existing methods by achieving a 1-2% reduction in normalized Root Mean Square Error (nRMSE). Figure 2 shows the examples of the proposed IBi-GBM generated CVR baseline for the actual CVR days. After estimating the CVR baseline, CVR performance can be evaluated using the CVR factor in (1). The CVR factor for each time step is shown in Fig. 3.

$$CVR_f = \frac{\Delta\bar{P}\%}{\Delta\bar{V}\%} = \frac{(\bar{P}_{baseline} - \bar{P}_{CVR})/\bar{P}_{baseline}}{(\bar{V}_{baseline} - \bar{V}_{CVR})/\bar{V}_{baseline}} \quad (1)$$

TABLE II. Average Estimation Errors of Virtual-CVR Days at Feeder Level.

Feeder	Data Rez.	nRMSE (%)				ϵ_e (%)				MPE			
		MSVR	Load-PIN	IBi-LightGBM	IBi-GBM	MSVR	Load-PIN	IBi-LightGBM	IBi-GBM	MSVR	Load-PIN	IBi-LightGBM	IBi-GBM
BR	15-min	5.33	2.50	1.75	0.81	3.81	1.13	1.11	0.41	3.44	0.03	-1.12	-0.38
	30-min	5.07	2.98	2.47	0.97	3.79	1.92	1.79	0.70	3.32	0.06	-1.68	-0.70
	60-min	4.99	2.64	3.15	0.86	3.85	1.46	2.58	0.53	3.57	0.04	-2.57	-0.49
DF	15-min	8.59	2.86	2.78	0.64	5.43	1.98	1.15	0.24	3.66	0.22	-0.50	0.01
	30-min	8.65	1.55	3.43	0.35	5.67	1.24	1.82	0.15	4.09	0.15	-0.10	0.05
	60-min	8.48	2.70	4.33	0.94	5.54	1.15	2.85	0.58	4.46	0.11	-2.57	0.51
SL	15-min	6.72	3.02	2.52	1.16	5.04	1.40	2.03	0.79	4.37	0.05	-2.06	-0.80
	30-min	6.58	1.75	2.40	0.67	5.06	0.47	1.17	0.27	4.56	0.01	0.14	-0.15
	60-min	6.62	1.51	2.31	0.58	5.11	0.46	1.27	0.26	4.75	0.01	-0.13	-0.22

TABLE III. Average Estimation Errors of Virtual-CVR Days at Substation Level.

SS		Data Rez.	nRMSE (%)				ϵ_e(%)				MPE			
			MSVR	Load-PIN	IBi-LightGBM	IBi-GBM	MSVR	Load-PIN	IBi-LightGBM	IBi-GBM	MSVR	Load-PIN	IBi-LightGBM	IBi-GBM
Summer	CL	5-min	6.25	2.17	0.47	0.83	4.94	1.09	0.18	0.32	4.75	0.48	0.07	-0.01
		15-min	5.63	0.69	1.51	0.26	5.45	0.41	0.89	0.12	5.44	0.55	0.21	0.04
		30-min	5.42	0.60	3.51	0.23	4.42	0.48	2.55	0.14	4.21	0.43	-1.90	0.05
		60-min	4.88	1.45	5.74	0.56	4.88	1.43	4.91	0.42	4.88	0.49	-4.78	-0.26
	RF	5-min	2.72	1.92	0.59	0.85	1.78	1.12	0.24	0.33	1.55	0.33	-0.11	0.10
		15-min	2.66	1.68	1.76	0.74	1.96	1.21	1.06	0.36	1.73	0.37	-0.16	-0.29
		30-min	2.47	0.45	3.78	0.20	1.98	0.37	3.19	0.11	1.78	0.38	-2.74	0.01
		60-min	1.59	0.74	4.13	0.33	1.19	0.81	3.90	0.24	0.71	0.15	-3.17	0.04
	RR	5-min	2.17	2.20	0.64	0.70	1.33	0.97	0.20	0.21	1.30	0.26	0.06	-0.04
		15-min	1.69	1.67	1.51	0.53	0.87	1.03	0.83	0.23	0.61	0.12	0.02	0.16
		30-min	1.74	0.65	2.57	0.20	1.22	0.55	1.72	0.12	1.14	0.23	-0.12	0.07
		60-min	1.95	2.25	3.06	0.71	1.67	2.37	2.61	0.53	1.09	0.22	-1.76	-0.21
Winter	CL	5-min	4.45	2.82	1.11	0.71	4.29	1.44	0.60	0.41	4.28	0.39	0.49	0.40
		15-min	3.94	2.49	3.31	1.10	3.50	0.83	2.43	0.88	3.48	0.32	-1.60	0.88
		30-min	3.71	2.35	3.51	0.93	3.63	1.08	3.18	0.74	3.63	0.33	-2.24	0.73
		60-min	2.65	1.68	3.03	1.89	2.65	0.16	3.03	1.89	2.28	0.21	-1.23	1.89
	RF	5-min	3.06	2.41	1.62	1.54	1.44	1.05	1.11	1.22	1.43	-0.31	-1.10	-1.21
		15-min	2.51	1.98	6.35	0.85	2.19	1.60	5.94	0.65	-2.22	0.47	-5.95	-0.64
		30-min	2.33	1.84	10.76	0.99	2.14	1.56	9.99	0.85	-2.15	0.46	-10.05	-0.84
		60-min	2.77	2.18	14.05	0.12	2.77	2.02	14.05	0.12	2.69	-0.57	-14.05	0.01
	RR	5-min	3.59	2.91	2.39	2.34	3.05	1.21	2.17	2.03	2.89	-0.58	-2.18	-2.03
		15-min	2.53	2.05	3.38	1.81	2.14	0.85	2.56	1.69	1.97	-0.39	-2.30	-1.70
		30-min	2.48	2.01	7.16	1.47	2.39	0.95	5.84	1.42	0.76	-0.15	-5.81	-1.42
		60-min	2.48	2.01	9.43	1.75	2.48	0.98	9.43	1.75	2.17	-0.43	-9.43	-1.74

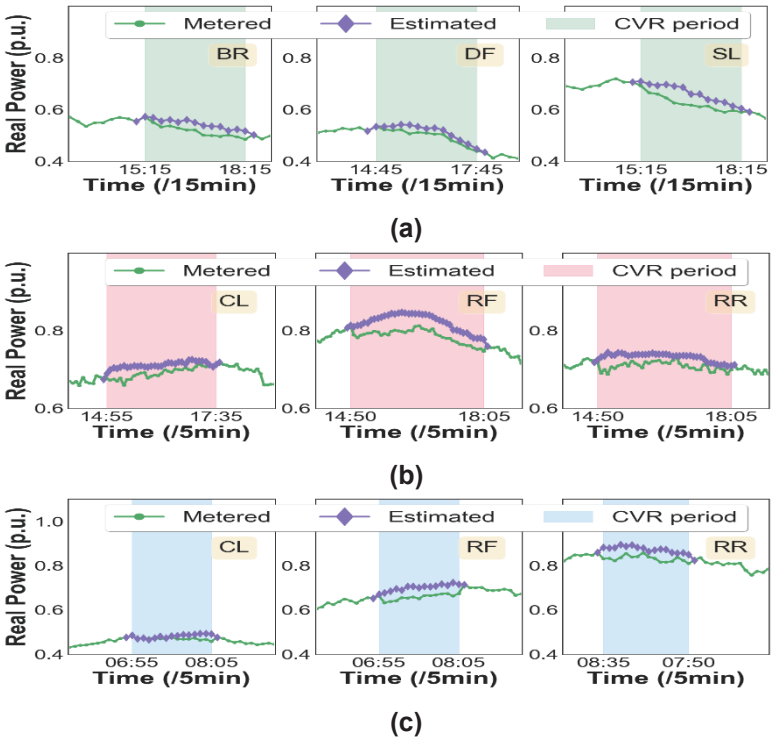

Figure. 2. Examples of the IBi-GBM generated CVR baseline for (a) three feeders with 15-min smart meter data, (b) three substations with 5-min SCADA data in summer, and (c) three substations with 5-min SCADA data in winter.

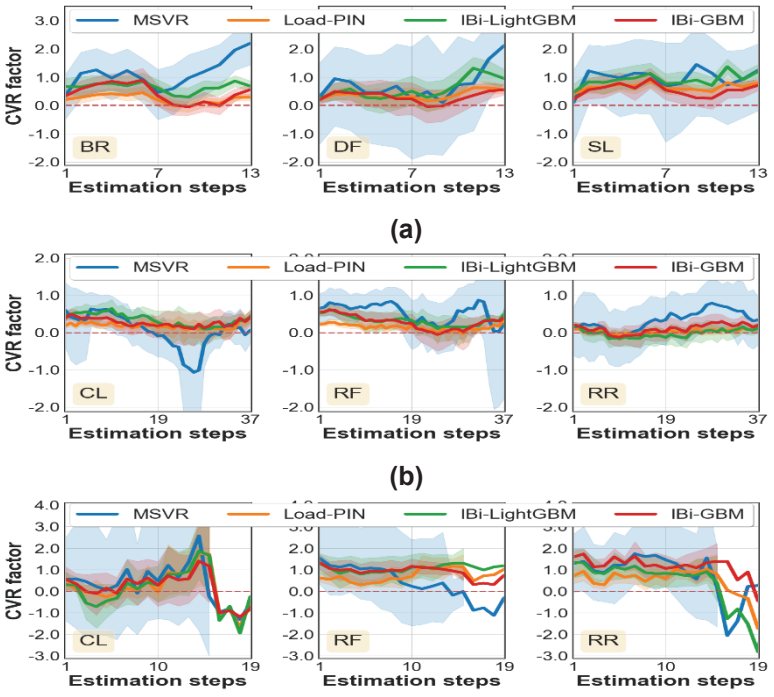

Figure. 3. Average step-by-step CVR factors and 95% confidence intervals for (a) three feeders with 15-min smart meter data, (b) three substations with 5-min SCADA data in summer, and (c) three substations with 5-min SCADA data in winter.

Reference

[23] Kennedy, B. W., and R. H. Fletcher. "Conservation voltage reduction (CVR) at Snohomish County PUD." IEEE Transactions on Power Systems 6.3 (1991): 986-998.
[24] Kirshner, Daniel. "Implementation of conservation voltage reduction at Commonwealth Edison." IEEE Transactions on Power Systems 5.4 (1990): 1178-1182.
[25] Wang, Zhaoyu, and Jianhui Wang. "Time-varying stochastic assessment of conservation voltage reduction based on load modeling." IEEE Transactions on Power Systems 29.5 (2014): 2321-2328.
[26] Zhao, Junbo, Zhaoyu Wang, and Jianhui Wang. "Robust time-varying load modeling for conservation voltage reduction assessment." IEEE Transactions on Smart Grid 9.4 (2016): 3304-3312.
[27] Wilson, Thomas L. "Measurement and verification of distribution voltage optimization results for the IEEE power & energy society." IEEE PES General Meeting. IEEE, 2010.
[28] Dwyer, Alf, et al. "Load to voltage dependency tests at BC Hydro." IEEE Transactions on Power Systems 10.2 (1995): 709-715.
[29] Papalexopoulos, Alex D., and Timothy C. Hesterberg. "A regression-based approach to short-term system load forecasting." IEEE Transactions on power systems 5.4 (1990): 1535-1547.
[30] Hong, Tao, Pu Wang, and H. Lee Willis. "A naïve multiple linear regression benchmark for short term load forecasting." 2011 IEEE power and energy society general meeting. IEEE, 2011.
[31] Hong, Tao, and Pu Wang. "On the impact of demand response: Load shedding, energy conservation, and further implications to load forecasting." 2012 IEEE Power and Energy Society General Meeting. IEEE, 2012.
[32] Wang, Zhaoyu, Miroslav Begovic, and Jianhui Wang. "Analysis of conservation voltage reduction effects based on multistage SVR and stochastic process." IEEE Transactions on Smart Grid 5.1 (2013): 431-439.
[33] Dudek, Grzegorz. "Multilayer perceptron for short-term load forecasting: from global to local approach." Neural Computing and Applications 32.8 (2020): 3695-3707.
[34] Zheng, Jian, et al. "Electric load forecasting in smart grids using long-short-term-memory based recurrent neural network." 2017 51st Annual conference on information sciences and systems (CISS). IEEE, 2017.
[35] Bai, Shaojie, J. Zico Kolter, and Vladlen Koltun. "An empirical evaluation of generic convolutional and recurrent networks for sequence modeling." arXiv preprint arXiv:1803.01271 (2018).
[36] Li, Yiyan, et al. "Load Profile Inpainting for Missing Load Data Restoration and Baseline Estimation." IEEE Transactions on Smart Grid (2023).
[37] Lee, Han Pyo, et al. "An iterative bidirectional gradient boosting algorithm for CVR baseline estimation." 2023 IEEE Power & Energy Society General Meeting (PESGM). IEEE, 2023. Available online at: https://ieeexplore.ieee.org/

9.22 Task F.2 Load Profile Inpainting for Missing Load Data Restoration

Background: This task presents a Generative Adversarial Nets (GAN) based, Load Profile Inpainting Network (Load-PIN) for restoring missing load data segments and estimating the baseline for a demand response event. In general, there are two categories of missing data restoration methods for load profile inpainting: model-based and data-driven. Table X.I summarizes the advantages and disadvantages of the state-of-the-art methods. As can be seen in the table, up till now, all existing generative methods require the format of the input and output to be fixed. However, in practice, the duration of missing data (model output) varies from minutes to several hours, and the length and number of available measurements (model input) also vary case by case. To cope with the varying-length cases, traditional methods need either increase the output window to cover the longest event or train separate models for different scenarios.

TABLE I : Comparison of STATE-OF-THE-ART missing data restoration methods

		Description	Advantages	Disadvantages
Model-based methods [1]-[5]		Use physical system models to simulate responses to external disturbances in hope of restoring missing data segments.	Explainable as the models reflect the laws of physics when describing the behavior behind field measurements	Require accurate distribution system models.
Data-driven methods	**similarity-based [5]-[7]**	Groups load profiles by day type, weather conditions, and shape characteristics of load profiles. The missing data segments are restored by referencing to the data on the load profiles having the best similarity match.	Straightforward, easy to implement and explainable	Defined by human analysts, making the accuracy of the method dependent on subjective selections of similarity metrics and weights.
	regression-based [11]-[11]	Include linear regression, Long Short Term Memory (LSTM), Stacked Autoencoder (SAE), Gaussian Regression, Support Vector Regression (SVR)	Achieve higher estimation accuracy compared to the similar day approach because of their nonlinear learning capabilities, especially when using deep-learning models	Compared with similarity-based methods, the deep-learning based methods are less explainable and having higher computing costs the data format of the input and output is required to be fixed.

Task Objectives

- Develop Load-PIN model for missing data restoration and baseline estimation.
- The most distinct feature of the Load-PIN model is its flexibility in restoring variable-length data segments and its superior accuracy compared with the state-of-the-art methods.

Methodology Overview: The Load-PIN framework is illustrated in Fig. 1. The model input z has three parts: 24-hour load and temperature profiles, and a Boolean mask indicating the event period as one and the normal period as zero. The load data resolution varies from 1-minute to 15-minute and the missing data duration, T_{event}, is less than 4 hours. The generator contains two stages: a coarse network for initial estimation and a fine-tuning network for polishing. The discriminator is a deep convolutional network with specially designed loss functions.

Simulation Results: As shown in Table II, when data granularity is 5-min and 15-min, Load-PIN outperforms all other models and shows 15-30% improvement compared with the second-best model. This shows that Load-PIN can extract information hidden inside the high-resolution data for forecasting the missing data segments. However, if the data resolution is too low, the Load-PIN does not show significant performance improvements. This is because in those cases, forecasting average values outweigh uncovering load shape details.

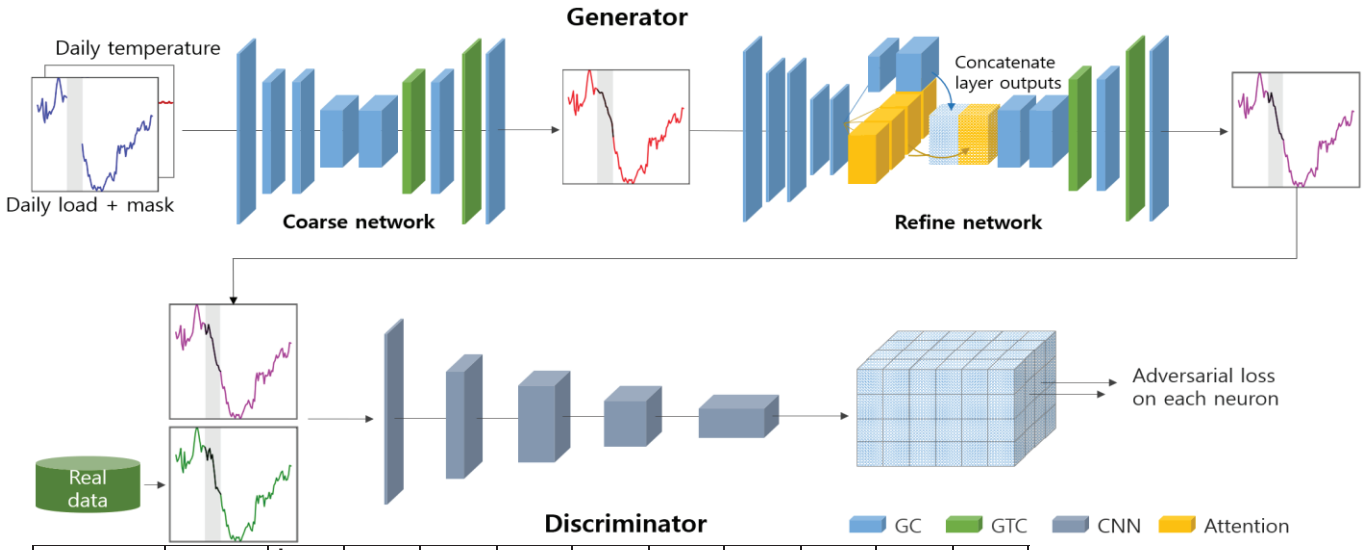

Generator	Coarse	Layer	gc	gc	gc	gc	gc	gtc	gc	gtc	gc			
		ks	5	4	3	4	3	3	3	3	3			
		kn	64	128	128	256	256	128	128	64	1			
		st	1	2	1	2	1	2	1	2	1			
	Refine	Layer	gc	gc	gc	gc	gc	gc	gcn	attn*4	gcn*2	gtcn	gcn	gtcn	gcn
		ks	5	4	3	4	3	3	3	3	3	3	3	3	3
		kn	64	64	64	64	64	128	256	64	1	2	128	2	128
		st	1	2	1	2	1	1	1	1	256	128	1	128	1
Discriminator		Layer	cnn	cnn	cnn	cnn	cnn								
		ks	4	4	4	4	4								
		kn	16	32	64	128	256								
		st	2	2	2	2	2								

Figure 1. The proposed Load-PIN framework. "GC" refers to a gated convolution block, "GTC" refers to a gated transpose convolution block, "CNN" refers to a convolutional block, and "Attention" refers to a self-attention block. "ks" means kernel size, "kn" means number of kernels, and "st" means stride.

TABLE II: Model performances on the Pecan Street Test Case (Mask length is set to be 3 hours)

data Resolution	aggregation level	nRMSE								EE							
		LSTM	TCN	MLP	SAE	Bi-LSTM	Vanilla-GAN	Load-PIN	Improve-ment	LSTM	TCN	MLP	SAE	Bi-LSTM	Vanilla-GAN	Load-PIN	Improve-ment
1-min	10users	0.46	0.43	0.39	0.35	0.57	0.54	0.35	-0.85%	0.22	0.21	0.16	0.15	0.26	0.32	0.15	-1.99%
	50users	0.25	0.21	0.19	0.15	0.22	0.26	0.12	18.90%	0.17	0.13	0.11	0.08	0.13	0.19	0.06	23.35%
	100users	0.19	0.17	0.15	0.11	0.16	0.25	0.10	7.79%	0.13	0.10	0.09	0.06	0.10	0.19	0.06	4.48%
	200users	0.16	0.15	0.12	0.08	0.12	0.23	0.07	15.74%	0.12	0.10	0.06	0.05	0.09	0.17	0.05	4.14%
	300users	0.15	0.13	0.10	0.07	0.11	0.22	0.09	-25.30%	0.12	0.09	0.06	0.05	0.08	0.17	0.05	-12.78%
	mean	0.24	0.22	0.19	0.15	0.24	0.30	0.15	3.26%	0.15	0.13	0.10	0.08	0.13	0.21	0.08	3.44%
5-min	10users	0.39	0.34	0.35	0.32	0.38	0.40	0.19	39.76%	0.20	0.13	0.15	0.15	0.17	0.15	0.08	38.46%
	50users	0.20	0.15	0.15	0.14	0.15	0.20	0.10	26.63%	0.14	0.08	0.08	0.08	0.08	0.12	0.07	9.76%
	100users	0.15	0.11	0.12	0.10	0.11	0.16	0.11	-7.36%	0.10	0.06	0.07	0.06	0.06	0.11	0.05	11.79%
	200users	0.15	0.09	0.12	0.08	0.08	0.13	0.07	17.36%	0.11	0.05	0.09	0.05	0.05	0.10	0.05	3.40%
	300users	0.08	0.08	0.10	0.07	0.07	0.12	0.06	13.73%	0.05	0.05	0.07	0.05	0.05	0.10	0.04	24.77%
	mean	0.19	0.15	0.17	0.14	0.16	0.20	0.11	18.02%	0.12	0.07	0.09	0.08	0.08	0.12	0.06	17.64%
15-min	10users	0.30	0.30	0.30	0.27	0.28	0.27	0.21	21.20%	0.15	0.15	0.15	0.14	0.15	0.12	0.09	26.74%
	50users	0.14	0.14	0.15	0.12	0.12	0.12	0.09	24.88%	0.09	0.10	0.09	0.08	0.07	0.07	0.05	25.60%
	100users	0.11	0.11	0.12	0.09	0.09	0.09	0.08	8.68%	0.07	0.07	0.09	0.06	0.06	0.05	0.05	7.59%
	200users	0.10	0.10	0.09	0.07	0.07	0.07	0.05	31.02%	0.07	0.07	0.06	0.05	0.05	0.04	0.04	5.32%
	300users	0.08	0.08	0.09	0.06	0.06	0.06	0.05	15.70%	0.06	0.05	0.07	0.05	0.05	0.04	0.03	21.10%
	mean	0.15	0.15	0.15	0.12	0.13	0.12	0.10	20.30%	0.09	0.09	0.09	0.08	0.07	0.06	0.05	22.94%
30-min	10users	0.27	0.27	0.28	0.23	0.23	0.21	0.22	-5.73%	0.15	0.15	0.19	0.15	0.14	0.12	0.11	5.41%
	50users	0.15	0.14	0.15	0.11	0.11	0.10	0.09	10.41%	0.12	0.09	0.09	0.08	0.07	0.06	0.07	-16.13%
	100users	0.11	0.12	0.12	0.08	0.08	0.07	0.08	-7.18%	0.08	0.09	0.08	0.06	0.06	0.05	0.05	-9.32%
	200users	0.10	0.10	0.10	0.07	0.07	0.06	0.06	-5.11%	0.07	0.06	0.07	0.05	0.05	0.04	0.04	-4.05%
	300users	0.09	0.10	0.10	0.06	0.06	0.05	0.05	-2.46%	0.06	0.06	0.07	0.05	0.05	0.03	0.04	-25.85%
	mean	0.14	0.15	0.15	0.11	0.11	0.10	0.10	-2.24%	0.10	0.09	0.10	0.08	0.07	0.06	0.06	-2.55%
1-h	10users	0.29	0.28	0.27	0.19	0.19	0.18	0.19	-3.45%	0.19	0.23	0.18	0.15	0.15	0.11	0.12	-5.79%
	50users	0.14	0.14	0.15	0.09	0.09	0.09	0.10	-12.00%	0.11	0.10	0.11	0.07	0.07	0.06	0.08	-31.52%
	100users	0.13	0.13	0.11	0.07	0.07	0.06	0.07	-8.64%	0.10	0.09	0.08	0.06	0.06	0.04	0.05	-11.12%
	200users	0.12	0.11	0.11	0.06	0.06	0.05	0.06	-16.91%	0.10	0.07	0.08	0.05	0.05	0.04	0.05	-36.27%
	300users	0.11	0.09	0.09	0.05	0.06	0.04	0.04	4.50%	0.09	0.06	0.07	0.04	0.05	0.03	0.04	-26.57%
	mean	0.16	0.15	0.15	0.09	0.09	0.09	0.09	-4.51%	0.12	0.11	0.10	0.07	0.08	0.06	0.07	-21.72%

References

[1] Visconti, Igor F., Delberis A. Lima, and Jovica V. Milanović. "Comprehensive analysis of conservation voltage reduction: A real case study." 2019 IEEE Milan PowerTech. IEEE, 2019.
[2] Zhang, Yongxi, et al. "Optimal placement of battery energy storage in distribution networks considering conservation voltage reduction and stochastic load composition." IET Generation, Transmission & Distribution 11.15 (2017): 3862-3870.
[3] Wang, Zhaoyu, and Jianhui Wang. "Time-varying stochastic assessment of conservation voltage reduction based on load modeling." IEEE Transactions on Power Systems 29.5 (2014): 2321-2328.
[4] Diaz-Aguiló, Marc, et al. "Field-validated load model for the analysis of CVR in distribution secondary networks: Energy conservation." IEEE Transactions on Power Delivery 28.4 (2013): 2428-2436.
[5] Schneider, Kevin P., et al. Evaluation of conservation voltage reduction (CVR) on a national level. No. PNNL-19596. Pacific Northwest National Lab.(PNNL), Richland, WA (United States), 2010.
[6] Coughlin, Katie, et al. Estimating demand response load impacts: Evaluation of baselineload models for non-residential buildings in california. No. LBNL-63728. Lawrence Berkeley National Lab.(LBNL), Berkeley, CA (United States), 2008.
[7] Xiang, Biao, et al. "Smart Households' Available Aggregated Capacity Day-ahead Forecast Model for Load Aggregators under Incentive-based Demand Response Program." 2019 IEEE Industry Applications Society Annual Meeting. IEEE, 2019.
[8] Wijaya, Tri Kurniawan, Matteo Vasirani, and Karl Aberer. "When bias matters: An economic assessment of demand response baselines for residential customers." IEEE Transactions on Smart Grid 5.4 (2014): 1755-1763.
[9] Han Pyo Lee, Lidong Song, Yiyan Li, Ning Lu, Di Wu, PJ Rehm, Matthew Makdad, Edmond Miller, "An Iterative Bidirectional Gradient Boosting Algorithm for CVR Baseline Estimation" 23PESGM0022, submitted to 2023 IEEE PES General Meeting, Available online at: http://arxiv.org/abs/2211.03733. . (An alternative approach: Conference publication from another subtask)
[10] Matsukawa, Shun, et al. "Stable segment method for multiple linear regression on baseline estimation for smart grid fast automated demand response." 2019 IEEE Innovative Smart Grid Technologies-Asia (ISGT Asia). IEEE, 2019
[11] Oyedokun, James, et al. "Customer baseline load estimation for incentive-based demand response using long short-term memory recurrent neural network." 2019 IEEE PES Innovative Smart Grid Technologies Europe (ISGT-Europe). IEEE, 2019.
[12] Chen, Yang, et al. "Privacy-Preserving Baseline Load Reconstruction for Residential Demand Response Considering Distributed Energy Resources." IEEE Transactions on Industrial Informatics (2021).
[13] Weng, Yang, Jiafan Yu, and Ram Rajagopal. "Probabilistic baseline estimation based on load patterns for better residential customer rewards." International Journal of Electrical Power & Energy Systems 100 (2018): 508-516.
[14] Chen, Yongbao, et al. "Short-term electrical load forecasting using the Support Vector Regression (SVR) model to calculate the demand response baseline for office buildings." Applied Energy 195 (2017): 659-670.
[15] Wang, Zhaoyu, Miroslav Begovic, and Jianhui Wang. "Analysis of conservation voltage reduction effects based on multistage SVR and stochastic process." IEEE Transactions on Smart Grid 5.1 (2013): 431-439.
[16] Yiyan Li, Lidong Song, Yi Hu, Hanpyo Lee, Di Wu, PJ Rehm, Ning Lu, "Load Profile Inpainting for Missing Load Data Restoration and Baseline Estimation," in IEEE Transactions on Smart Grid, doi: 10.1109/TSG.2023.3293188. (Journal publication from this subtask)

9.23 Task F.3 HVAC Load Disaggregation Method 1

Background: Load disaggregation is an important technique in distribution system analysis. Its results can be used in many downstream tasks, for example, customer segmentation, resource identification, and rate recommendation. When the sampling rate of available data sets is less than 1 minute, non-intrusive load monitoring (NILM) methods are often used to disaggregate the electricity consumption curves of different appliances. However, in practice, inputs to many load disaggregation algorithms are 15-minute smart meter data and hourly weather data. This makes those NILM methods relying on second-level meter data inapplicable. The goal of the proposed HVAC disaggregation algorithm is to filter out hidden portions of HVAC usage lying in total metering, using the row resolution smart meter profile and outdoor temperature profile, which are applicable for customer-level and aggregated-level load profiles.

TABLE 1: A Review of Existing Methods and Our Contribution

Methodology	Description	Disadvantage	Advantage
HMM-based method [1]	HMM-based methods assume that appliances operate in distinct states, represented as hidden states within the HMM model.	Exponential increases in complexity as the number of appliances rises. Requiring metering data with a sampling rate of 1 minute.	Interpretability.
Deep learning-based method [2]	State-of-the-art supervised learning methods	Heavy reliance on large labeled sub-metered datasets.	High Accuracy.
Optimization-based method [3]	Steady-state-based and dictionary-learning-based approaches using appliance signature matrices	Low transferability.	Requiring less training data and model complexity.
Our method [4][5]	Optimization-based approach and applicable to various smart meter data resolution with low dependency on labeled data set		

Task Objectives: Develop a HVAC load disaggregation model that is transferable and generalizable to diverse customers and customers with limited training data and no sub-metered information.

Methodology Overview: As shown in Fig. 1, there are three different steps in the proposed HVAC disaggregation algorithm. The inputs of the optimization algorithm include daily temperature and load profiles, base load dictionary, and HVAC electricity consumption references calculated by minimizing the mutual information (MI) between the ambient temperature profile and the temperature-insensitive load (i.e., total load minus the HVAC loads). In the end, a fine-tuning process is used to detect and remove the anomalies in the estimated HVAC load based on predetermined criteria extracted from the statistical characteristics of the HVAC loads.

Simulation Results: The data sets used in this study were collected by Pecan Street Inc. from 1070 residential users in New York, Colorado, California, and Texas. The data sets include 1-minute electricity consumption of the total household and appliances (e.g., HVAC, water heater, and dryer). The 1-minute data is down-sampled to 1 hour to match the typical smart grid data. 230 users with only one HVAC unit and 90 days in Summer 2019 are selected to illustrate the algorithm performance on cooling load disaggregation.

To measure the aggregated-level results, we randomly pick 10 to 500 customers and use the aggregated profiles.

As represented in Table 2, when compared to all three benchmark models, our model demonstrates substantially higher accuracy and the lowest standard deviation in nMAE, indicating the superior performance and consistency of our model in accurately disaggregating HVAC load from smart meter data, even when dealing with varying data resolutions. The model exhibits satisfactory performances as shown in Table 3 where results are compared across different aggregation levels.

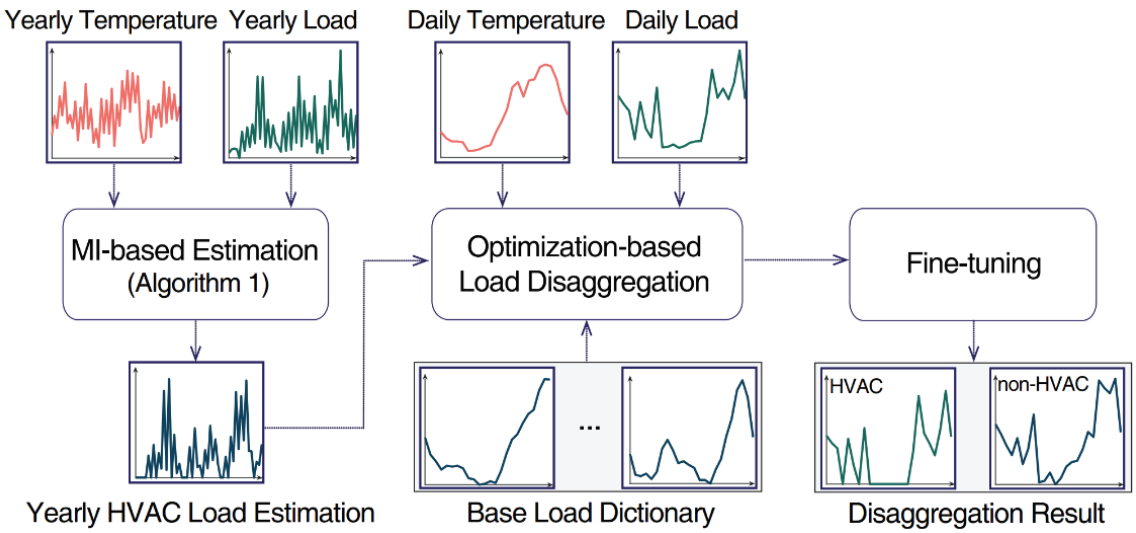

Figure 1. Workflow of the proposed load disaggregation algorithm.

TABLE 2. Customer-level HVAC Load Disaggregation Performance Comparison

Data Resol.	*n*MAE (%)				EE (kWh)				std (*n*MAE)			
	Proposed	**BM1**	**BM2**	**BM3**	**Proposed**	**BM1**	**BM2**	**BM3**	**Proposed**	**BM1**	**BM2**	**BM3**
5-min	9.02	16.80	12.76	19.76	3.44	7.13	8.52	9.72	1.93	6.24	4.91	7.20
15-min	8.10	14.32	11.95	20.47	2.78	8.84	7.98	9.40	2.53	6.37	4.64	8.34
30-min	8.48	14.85	10.55	18.12	3.20	6.12	5.30	8.72	2.68	6.72	4.37	7.49
60-min	8.70	12.65	9.62	18.70	3.54	6.71	4.69	7.95	2.71	6.02	4.21	8.27

TABLE 3. Aggregated-level HVAC Load Disaggregation Performance Comparison

Data Resol.	*n*MAE (%)					EE (kWh)				
	10 users	**50 users**	**100 users**	**300 users**	**500 users**	**10 users**	**50 users**	**100 users**	**300 users**	**500 users**
5-min	4.96	4.75	3.61	3.76	3.76	1.17	2.18	1.14	1.09	1.10
15-min	6.05	5.18	3.75	3.76	3.72	1.91	2.46	1.22	1.16	1.16
30-min	6.09	5.23	3.70	3.70	3.77	2.11	2.51	1.23	1.17	1.17
60-min	5.75	4.90	4.24	4.48	4.18	1.83	1.54	1.33	1.43	1.21

References

[1] Roberto Bonfigli, et al. “Non-intrusive Load monitoring by using active and reactive power in additive factorial hidden Markov models.” Applied Energy, vol. 208, pp. 1590–1607, 2017.

[2] Michele D'Incecco, et al. " Transfer learning for non-intrusive load monitoring." IEEE Transactions on Smart Grid, vol. 11, no. 2, pp.1419-1429, 2019.
[3] Alireza Rahimpour, et al. " Non-intrusive energy disaggregation using non-negative matrix factorization with sum-to-k constraint." IEEE Transactions on Power Systems, vol. 32, no. 6, pp 4430-4441, 2017.
[4] Hyeonjin Kim, et al. "An ICA-based HVAC load disaggregation method using smart meter data." 2023 IEEE Power and Energy Society Innovative Smart Grid Technologies Conference (ISGT). IEEE, 2023
[5] Hyeonjin Kim, et al. "A Contextually Supervised Optimization-based HVAC Load Disaggregation Methodology", submitted to IEEE Transactions on Smart Grid

9.24 Task F.4 Load Disaggregation Method 2

Background: HVAC loads are widely used demand response (DR) resources nowadays, which takes 30% of residential and 40% of commercial building electricity consumption. However, in practice, only the total building electricity consumption is metered. Thus, load service providers and utility engineers mainly rely on HVAC load disaggregation algorithms for conducting DR potential studies. The existing methods are reviewed and listed in Table I in comparison to our proposed method.

TABLE I: A Review of Existing Methods and Our Contribution

		Description	Advantages	Disadvantages
Edge-detection algorithm [17]		Use edge-detection to directly identify on and off events of HVAC.	Straightforward, interpretable, and easy to implement,	Require high-resolution (1-min/5-min) data, sub-optimal accuracy.
Average Value Subtraction Algorithm [18]		Sequentially separate the HVAC load with average values by considering the day types.	Explainable. Mathematical simplicity.	Require the classification of day types and not generalizable to all sites.
Data-driven methods	MLP and LSTM [19]	Use MLP and LSTM as the classifier to detect on and off event of HVAC and the regressor to get the HVAC profile.	Easy to implement and can capture complex and nonlinear relationships.	Require the training of site-specific machine-learning (ML) models. Requires high-resolution data.
	Random forest [20]	Use random forest to aggregate and deploy extra trees to select the best feature.	Increased interpretability and accuracy with manual feature extraction.	The accuracy of the method is dependent on the feature selection.
	S2P CNN [21]	Use sequence-to point convolutional neural network (S2P-CNN) and sliding window to separate HVAC profile.	Quick estimation with the pre-trained model, higher accuracy, and better generalizability.	The deep-learning based methods are less explainable and having higher computing costs.

Task Objectives: Develop a modified S2P algorithm to use low resolution smart meter data as inputs for HVAC load disaggregation with great generalizability.

Methodology Overview: As shown in Fig. 1, the modified S2P algorithm is conducted in three steps: data augmentation, training and testing the model on one location, transfer learning (port the pre-trained model to other locations) with fine-tuning. First, the infrequently used loads (i.e., water heater and dryer loads) are removed from the total load profile. Then, the sub-metered HVAC data is removed from the residual load profile to obtain the base-load profiles. Next, the augmented load profiles are generated by shuffling the HVAC profiles against each base load profile. After data augmentation, the original N yearly 1-minute load profiles are expanded to N × N yearly 1-minute load profiles. Then, the model is trained using the augmented load profiles and their corresponding ambient temperature profiles. The trained S2P model is first tested for the same location. Then, it is ported to two other locations, and we further improve the pretrained model by fine-tuning.

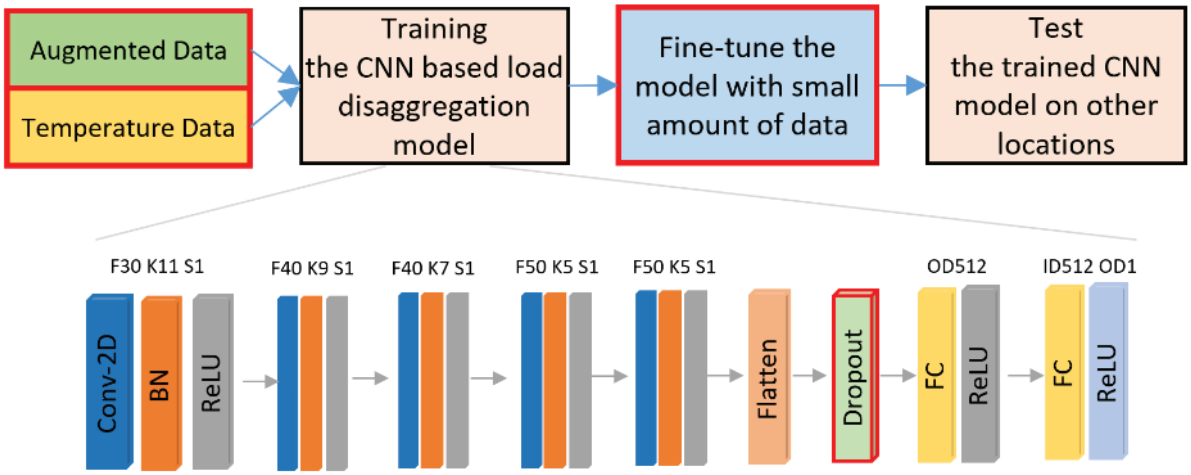

Figure 1. Architecture of the modified S2P HVAC load disaggregation algorithm.

Simulation Results: We compared the proposed model with two benchmark models using data collected in Austin, Texas: Support Vector Machine (SVM) and the original S2P-CNN. We set up three cases to compare the performance improvements brought by data augmentation and adding temperature to the input: 1) using data sets collected from the 150 users for training, 2) using augmented data (150 × 150 users) for training, and 3) using augmented data for training and using both load and temperature data as model inputs. The trained model is tested on the remaining 50 Austin users. As shown in Table II, augmentation significantly reduces error variances (i.e., improved model consistency) and adding temperature to the inputs reduces the errors (i.e., improved accuracy).

For new sites with limited amounts of sub-metered data, we can fine-tune the model for each household using the transfer learning algorithm. We use one weeks' labelled data to demonstrate the efficacy of fine-tuning. As shown in Table III, the pre-trained model has shown satisfactory accuracy when directly used on new sites. And fine-tuning can considerably reduce the disaggregation errors and error variances. As shown in Fig. 2, fine-tuning achieves noticeable improvements in HVAC disaggregation accuracy because it can identify some distinct user characteristics (e.g., the HVAC rated power).

The modified model shows significant improvement in disaggregation accuracy and consistency compared to previous methods in an area with labelled data sets. The model generalizability is also improved because the pre-trained model achieves satisfactory performance in other locations where there is no sub-metered HVAC load data for training. The proposed transfer learning technique using a small amount of labelled data at the new location to fine-tune the pre-trained model can also significantly improve the model performance.

Table II: Performance Comparison for Different Load Disaggregation Method

	Benchmark Models		Proposed Model		
	SVM	S2P-CNN	Case 1	Case 2	Case 3
nMAE (%)	13.09	9.54	8.54	8.44	**7.17**
nEE (%)	11.36	6.47	4.37	4.54	**3.51**
std(nMAE)	8.47	4.25	3.89	2.28	**2.85**
std(nEE)	7.42	3.72	2.39	2.47	**1.86**

Table III: Performance Comparison for Different Locations (Boulder, CO & San Diego, CA)

Area	Metrics	Benchmark Models		Modified S2P	
		SVM	S2P-CNN	NoFT	WithFT
CO	nMAE (%)	23.78	11.26	9.28	7.90
	std(nMAE)	17.12	7.61	6.54	3.73
CA	nMAE (%)	19.82	6.71	4.40	4.52
	std(nMAE)	9.62	3.55	1.82	0.86

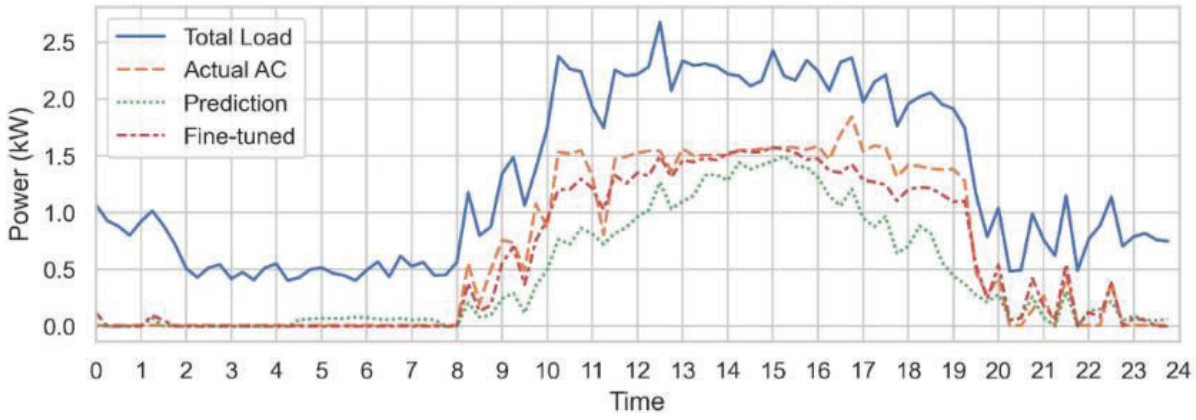

Figure 2. An example of load disaggregation results for one user located at Boulder, CO.

References

[1] K. X. Perez, W. J. Cole, J. D. Rhodes, A. Ondeck, M. Webber, M. Baldea, and T. F. Edgar, “Nonintrusive disaggregation of residential air-conditioning loads from sub-hourly smart meter data,” Energy and Buildings, vol. 81. Elsevier BV, 2014, pp. 316–325.
[2] M. Liang, Y. Meng, N. Lu, D. Lubkeman, and A. Kling, “HVAC load disaggregation using low-resolution smart meter data,” in 2019 IEEE Power & Energy Society Innovative Smart Grid Technologies Conference.
[3] J. Cho, Z. Hu, and M. Sartipi, “Non-intrusive a/c load disaggregation using deep learning,” in 2018 IEEE/PES Transmission and Distribution Conference and Exposition (T&D). IEEE, 2018, pp. 1–5.
[4] B. Najafi, L. Di Narzo, F. Rinaldi, and R. Arghandeh, “Machine learning based disaggregation of air-conditioning loads using smart meter data,” IET Generation, Transmission & Distribution, vol. 14, no. 21. Institution of Engineering and Technology (IET), 2020, pp. 4755–4762.
[5] K. Ye, H. Kim, Y. Hu, N. Lu, D. Wu, and P. Rehm, “A Modified Sequence-to-point HVAC Load Disaggregation Algorithm,” 2023 IEEE Power & Energy Society General Meeting (PESGM). IEEE, 2023. (Conference publication from this subtask